Determining the role of NAD biosynthetic pathways in chemosensitivity in glioblastoma

Richard Adrian Perryman

MRes, BSc (Hons)

Division of Brain Sciences

Department of Medicine

Imperial College London

r.perryman13@imperial.ac.uk

Thesis submitted in fulfilment of the requirements

for the degree of Doctor of Philosophy

2nd July, 2018

Copyright © 2018 Richard Adrian Perryman.

The copyright of this thesis rests with the author and is made available under a Creative Commons Attribution Non-Commercial No Derivatives licence. Researchers are free to copy, distribute or transmit the thesis on the condition that they attribute it, that they do not use it for commercial purposes and that they do not alter, transform or build upon it. For any reuse or redistribution, researchers must make clear to others the licence terms of this work.

This is to certify that to the best of my knowledge, the content of this thesis is my own work. This thesis has not been submitted for any other degree or other purposes. I certify that the intellectual content of this thesis is the product of my own work and that all the assistance received in preparing this thesis and sources have been acknowledged.

Acknowledgements

I would first like to thank my primary supervisor, Dr Nelofer Syed, head of the John-Fulcher Neuro-Oncology Research Group, for her continued support throughout my PhD. She has always encouraged me to pursue novel ideas and practice new techniques to improve the quality and diversity in my research. I would also like to thank my secondary supervisor, Dr Hector Keun, for providing with the opportunity to work in his lab, allowing me to plant the seed of my research career in cancer metabolism. I would also like to thank the other members of the John-Fulcher Neuro-Oncology Research Group for their support both in and out of the lab, particularly Dr Alexander Renziehausen, Dr Tzouliana Stylianou, Dr Combiz Khozoie, Mr John DeFelice and Miss Qingyu Zeng. I specifically want to thank Tsz Wing Chau for carrying out the FASTClear protocol and confocal imaging on my tissue sections. I also want to thank the clinical team based at Charing Cross hospital for their input and clinical expertise, including Mr Kevin O'Neill, Mr Barbar Vaqas and Mr Giulio Anichini.

I would also like to acknowledge the funding bodies that have supported my research. I thank the Medical Research Council for awarding me the DTP Studentship, which has supported me through both my research Masters and my PhD. I would also like to thank Mrs Wendy Fulcher and the Brain Tumour Research Campaign for funding the lab and providing me with the equipment necessary to carry out my work. I would also like to thank Brain Tumour Research for supporting my research during the final months of my PhD.

Finally, I would like to express my profound gratitude to my family for their continued support throughout my early career. I would like to thank my partner, Miss Emily Price, for her help editing and proof reading my thesis. This could not have been possible without her unfailing support and constant encouragement throughout both the research and writing stages of my PhD. Thank you.

Richard A. Perryman

Abstract

Glioblastoma (GBM) is an aggressive form of brain cancer with a median survival time of only one year. Since the turn of the 21st century, the only major advancement in the treatment of GBM has been the discovery of the DNA damaging agent temozolomide (TMZ), but this only offers a small increase in survival time. Attempts to target dysregulated signalling pathways in GBM have offered very little clinical benefit. Cancers, including GBM, adapt their metabolism by increasing their consumption of glucose and glutamine, and activating metabolic pathways to promote cell growth, including nucleotide, amino acid and fatty acid biosynthesis. Cancer cells have also been shown to require rapid synthesis of nicotinamide adenine dinucleotide (NAD) to support metabolic reactions, regulation of the cell cycle by sirtuins (SIRTs), and repair of DNA damage by poly (ADP-ribose) polymerase (PARP). This allows them to maintain high rates of proliferation. Inhibition of a key enzyme in NAD biosynthsis, nicotinamide phosphoribosyltransferase (NAMPT), has demonstrated significant anti-neoplastic activity *in vitro*. However, translation to the clinic has been poor. This is largely due to the lack of patient stratification and understanding of resistance mechanisms. I hypothesised that there is a subset of GBM tumours that lack alternative NAD biosynthetic pathways, rendering them sensitive to NAMPT inhibitors and unable to survive even in the presence of NAD precursors. I show that a proportion of GBM tumours lack key enzymes involved in salvage and *de novo* NAD biosynthetic pathways, including nicotinate phosphoribosyltransferase (NAPRT), ecto-5'-nucleotidase (NT5E) and quinolinate phosphoribosyltransferase (QPRT). This renders them sensitive to the NAMPT inhibitor FK866, and prevents rescue from FK866-induced growth arrest by different NAD precursors. Inhibition of NAMPT disrupts different aspects of cell cycle regulation in FK866-sensitive and FK866-resistant GBM cells lines. Finally, the combination of FK866 and TMZ limits the proliferation of GBM cells both *in vitro*, and in a murine orthotopic xenograft model, by initiating a G_2/M cell cycle arrest. Combining NAMPT inhibitors with standard therapy may be an effective treatment for patients with GBM.

Contents

List of Figures **vii**

List of Tables **x**

List of Abbreviations **xi**

1 Introduction **1**
1.1 Glioblastoma . . . 1
1.1.1 Incidence, clinical presentation and diagnosis . . . 1
1.1.2 Histological and molecular classification . . . 2
1.1.3 Standard therapy . . . 3
1.1.4 Recurrence . . . 7
1.2 Cancer metabolism . . . 9
1.2.1 Metabolic adaptations of cancer cells . . . 9
1.2.2 Targeting metabolic changes in cancer . . . 14
1.2.3 Pathways that regulate cancer metabolism . . . 19
1.3 NAD metabolism and biosynthesis in cancer . . . 30
1.3.1 NAD metabolism . . . 31
1.3.2 Sirtuins . . . 37
1.3.3 PARPs . . . 41
1.3.4 Targeting NAD biosynthesis in cancer . . . 45
1.4 Hypothesis and aims . . . 59
1.4.1 Hypothesis . . . 59
1.4.2 Aims . . . 59

2 Materials and Methods **60**
2.1 Cell lines and culture conditions . . . 60
2.2 Proliferation assays . . . 61
2.3 Cell cycle, apoptosis and cell death . . . 62
2.4 NAD/NADH quantification . . . 64
2.5 Bacterial transformation and plasmid purification . . . 64
2.6 Genetic knockdowns . . . 65
2.7 RNA extraction, cDNA synthesis and qPCR . . . 65
2.7.1 RNA extraction using TRI reagent . . . 65
2.7.2 cDNA synthesis using M-MLV . . . 66
2.7.3 Quantitative PCR . . . 66
2.8 Protein extraction and western blotting . . . 67
2.8.1 Protein extraction . . . 67

2.8.2 Protein quantification using the Bradford assay and dilution in loading buffer . . . 67
2.8.3 Western blotting using the Invitrogen mini gel tank system . . . 68
2.9 RNA sequencing . . . 69
2.9.1 RNA extraction using the Qiagen kit . . . 69
2.9.2 RNA sequencing . . . 69
2.9.3 Data analysis . . . 70
2.10 *In vivo* modelling of intracranial tumours . . . 70
2.10.1 Surgical implantation of human GBM cells into nude mice . . . 70
2.10.2 *In vivo* imaging using the IVIS . . . 71
2.10.3 Treatment of tumour-bearing mice with TMZ and/or FK866 . . . 71
2.10.4 FASTClear . . . 72
2.11 *In silico* analysis of TCGA data . . . 72
2.12 Statistics and data analysis . . . 73

3 Characterisation of GBM tumours and cell lines and the effects of NAMPT inhibition 74
3.1 Variability in the expression of genes involved in NAD biosynthesis in GBM samples from TCGA . . . 75
3.2 The expression of key genes involved in NAD biosynthesis varies between GBM cell lines . . . 79
3.3 Proliferation assays show variability in the sensitivity of GBM cell lines to NAMPT inhibition . . . 82
3.4 NAMPT inhibition does not affect apoptosis or cell death in GBM cell lines . . . 85
3.5 NAMPT inhibition causes a G_2/M cell cycle block in GBM cell lines . . . 87
3.6 Discussion . . . 87

4 The role of alternative NAD biosynthetic pathways in resistance to NAMPT inhibition 90
4.1 GBM cells expressing NAPRT utilise NA as an alternative source of NAD during treatment with a NAMPT inhibitor . . . 91
4.2 NT5E activity is required in GBM to fuel NAD biosynthesis from NMN in the presence of NAMPT inhibitors . . . 96
4.3 QA promotes proliferation in GBM cells treated with a NAMPT inhibitor . . . 101
4.4 shRNA mediated knockdown of genes involved in NAD biosynthesis in LN229 cells is insufficient to replicate results seen with molecular inhibitors . . . 107
4.5 Discussion . . . 111

5 RNA sequencing of FK866-resistant and FK866-sensitive GBM cell lines 116
5.1 NAMPT inhibition significantly alters gene expression profiles in both FK866-sensitive and FK866-resistant GBM cell lines . . . 116
5.2 NAMPT inhibition disrupts the cell cycle and the unfolded protein response in FK866-sensitive 42MG cells . . . 118
5.3 NAMPT inhibition specifically alters the G_1/S phase of the cell cycle and HIF signalling in FK866-resistant DBTRG cells . . . 122
5.4 Changes to E2F/RB, CDK and HSP cell signalling events occur in both FK866-sensitive and FK866-resistant GBM cells . . . 126
5.5 Discussion . . . 129
5.5.1 FK866-sensitive 42MG cells . . . 129

5.5.2 FK866-resistant DBTRG cells . . . 133
5.5.3 Consistent effects on both cell lines . . . 136

6 The effects of combined TMZ and FK866 treatment on GBM cell lines 139
6.1 Proliferation assays show variability in the sensitivity of GBM cell lines to TMZ, correlated with MGMT expression . . . 139
6.2 The combination of TMZ and FK866 significantly limits the proliferation of GBM cells compared to either alone . . . 143
6.3 FK866 increases the G_2/M cell cycle block caused by TMZ treatment in GBM cells . . . 145
6.4 The combination of TMZ and FK866 significantly alters the expression of genes involved in NAD biosynthesis, energy production and regulation of the cell cycle 150
6.5 Discussion . . . 155

7 The effects of combined TMZ and FK866 therapy *in vivo* 158
7.1 NAMPT inhibition synergises with TMZ to reduce tumour burden in mice . . . 158
7.2 FK866 inhibits proliferation and stabilises GBM tumours *in vivo* . . . 161
7.3 Discussion . . . 163

8 General discussion 164
8.1 Conclusion and future work . . . 169

Bibliography 172

Appendices 216

A Supplementary methods 216
A.1 qPCR primers . . . 216
A.2 ENRICHR databases . . . 218
A.3 Reagents . . . 219
A.3.1 Composition of buffers and gels used in western blotting . . . 219
A.4 Antibodies used in western blotting . . . 221
A.4.1 Primary antibodies . . . 221
A.4.2 Secondary antibodies . . . 222
A.5 Staining reagents used in histology . . . 222

B Supplementary results 223
B.1 RNAseq . . . 223
B.2 *In vivo* data . . . 228

List of Figures

1.1 Diagram showing the mechanism of action of TMZ in cancer cells 7
1.2 Diagram showing major metabolic changes in cancer, and some of the therapies that target them 14
1.3 Diagram showing major regulators of cancer cell metabolism 30
1.4 Diagram showing NAD biosynthetic pathways and its uses in cells 33
1.5 Diagram showing the chemical structures of different NAD metabolites, and inhibitors of some of the enzymes involved in NAD biosynthesis 34

2.1 Scatter graphs and histograms showing the gating strategies for Annexin V and PI staining in LN229 cells treated with TMZ 63

3.1 Key genes involved in NAD biosynthesis are upregulated in GBM tumours compared to healthy tissue 76
3.2 Elevated expression of key genes involved in NAD biosynthesis leads to poorer overall survival in patients with GBM 77
3.3 GBM tumours cluster on mutation status for their expression of genes involved in NAD biosynthesis 79
3.4 Expression of genes involved in NAD biosynthesis is highly variable across GBM cell lines 81
3.5 Protein levels of genes involved in NAD biosynthesis are highly variable between GBM cell lines 82
3.6 FK866 has time and dose dependent effects on established GBM cell lines 83
3.7 FK866 has time and dose dependent effects on primary GBM cell lines 84
3.8 nicotinamide phosphoribosyltransferase (NAMPT) inhibition reduces proliferation in GBM cell lines 84
3.9 FK866 does not activate apoptosis or initiate cell death in GBM cell lines 86
3.10 FK866 causes a G_2/M cell cycle arrest in GBM cells 87

4.1 NA rescues proliferation in GBM cells treated with FK866 92
4.2 NA maintains NAD and NADH levels in LN229 cells treated with FK866 93
4.3 NA does not affect apoptosis or cell viability when added to FK866 in LN229 cells 94
4.4 NA restores a normal cell cycle in LN229 cells treated with FK866 95
4.5 NMN rescues proliferation in GBM cells treated with FK866 97
4.6 NMN partially maintains NAD and NADH levels in LN229 cells treated with FK866 98
4.7 NMN does not affect apoptosis or cell viability when added to FK866 in LN229 cells 100
4.8 NMN restores a normal cell cycle in LN229 cells treated with FK866 101
4.9 QA rescues proliferation in GBM cells treated with FK866 103

4.10 Increased concentrations of PA does not lead to inhibition of QA mediated recovery in FK866 treated cells . . . 104
4.11 QA does not maintain NAD and NADH levels in LN229 cells treated with FK866 105
4.12 QA does not affect apoptosis or cell viability when added to FK866 in LN229 cells 106
4.13 QA restores a normal cell cycle in LN229 cells treated with FK866 . . . 107
4.14 shRNA-mediated knockdown of genes involved in NAD biosythesis in LN229 cells 109
4.15 shRNA mediated knockdowns of genes involved in NAD biosynthesis in LN229 cells do not replicate results seen with molecular inhibitors . . . 110

5.1 FK866 treatment in 42MG and DBTRG cells causes significant changes in gene expression . . . 117
5.2 Bar charts showing the top hits from gene set enrichment analysis for GO and cellular pathways in 42MG cells treated with FK866 . . . 119
5.3 Bar charts showing the top hits from gene set enrichment analysis for TF, PPI and metabolites in 42MG cells treated with FK866 . . . 120
5.4 Bar charts showing the top hits from gene set enrichment analysis for GO and cellular pathways in DBTRG cells treated with FK866 . . . 123
5.5 Bar charts showing the top hits from gene set enrichment analysis for TF, PPI and metabolites in DBTRG cells treated with FK866 . . . 124

6.1 TMZ has time and doses dependent effects on established GBM cell lines . . . 140
6.2 TMZ has time and doses dependent effects on primary GBM cell lines . . . 141
6.3 Sensitivity to TMZ is highly variable across GBM cell lines . . . 141
6.4 The expression of MGMT is highly variable across established and primary GBM cell lines . . . 142
6.5 TMZ and FK866 have time and dose dependent effects on LN229 and U87 cell lines . . . 144
6.6 FK866 yields additive effects when combined with TMZ in GBM cells . . . 145
6.7 TMZ decreases the proportions of live GBM cells . . . 147
6.8 TMZ activates apoptosis in GBM cells . . . 148
6.9 TMZ and FK866 lead to a G_2/M cell cycle block . . . 149
6.10 The expression of genes involved in NAD biosynthesis are altered upon treatment of LN229 cells with TMZ and FK866 . . . 151
6.11 The expression of genes related to cell cycle control and bioenergetics are altered upon treatment of LN229 cells with TMZ and FK866 . . . 152
6.12 Changes in the expression of other genes involved in NAD biosynthesis/consumption and bioenergetics in LN229 cells treated with TMZ and FK866 . . . 153
6.13 Changes in the expression of genes involved in NAD biosynthesis/consumption and bioenergetics in U87 cells treated with TMZ and FK866 . . . 154

7.1 Images of the tumours in all mice taken from the final round of imaging on the IVIS . . . 159
7.2 Dot and line plot showing the average weight of the animals in each treatment group over the course of the study . . . 160
7.3 Dot and line graphs showing the change in tumour size over time in the four treatment groups . . . 161
7.4 Confocal microscope images of mouse brain sections stained with Ki-67 and tomato lectin . . . 162

B.1 Images of the mouse brains used for FASTClear 228

List of Tables

1.1 Table summarising the different sirtuins and their roles in cellular function . . . 40

2.1 Established and primary GBM cell lines used for this project 61
2.2 qPCR reaction conditions 67

3.1 Table showing the IC_{50} values for FK866 in different GBM cell lines 85

4.1 Table summarising GBM cell lines, their responses to FK866, and their rescue with different NAD precursors 114

5.1 Table showing the top 10 differentially expressed genes in 42MG cells treated with FK866 121
5.2 Table showing the top 10 differentially expressed genes in DBTRG cells treated with FK866 125
5.3 Table showing differentially expressed genes with FK866 treatment in 42MG and DBTRG cell lines 128

6.1 Table showing the IC_{50} values for TMZ and MGMT status in different GBM cell lines 142

A.1 Primer sequences used for qPCR 218
A.2 Summary of the datasets used from the Enrichr analysis 219
A.3 Primary antibodies used in western blotting 221
A.4 Secondary antibodies used in western blotting 222
A.5 Table showing staining reagents used in FASTClear 222

B.1 Table showing other differentially expressed genes in 42MG cells treated with FK866 that also have an effect on survival in GBM 225
B.2 Table showing other differentially expressed genes in DBTRG cells treated with FK866 that also have an effect on survival in GBM 227

List of Abbreviations

E. coli *Escherichia coli*.
H. influenzae *Haemophilus influenzae*.
1MT 1-methyl-L-tryptophan.
2-HNA 2-hydroxinicotinic acid.
2DG 2-deoxy-D-glucose.
2HG *R*-2-hydroxyglutarate.
4E-BP eukaryotic translation initiation factor 4E-binding protein.
5FU 5-fluorouracil.
6PGD 6-phosphogluconate dehydrogenase.

ABC ATP-binding cassette.
ACC acetyl-CoA carboxylase.
ACLY ATP citrate lyase.
ACoA acetyl coenzyme A.
ADAMTS ADAM metallopeptidase with thrombospondin type 1 motif.
ADI arginine deiminase.
ADI-PEG20 pegylated ADI.
AHR aryl hydrocarbon receptor.
AIC 5-aminoimidazole-4-carboxamide.
AICAR 5-aminoimidazole-4-carboxamide ribonucleotide.
AIF apoptosis-inducing factor.
Akt AKT serine/threonine kinase.
AKTS1 AKT1 substrate 1.
ALKBH AlkB homolog.
ALL acute lymphoblastic leukaemia.
AMBRA1 autophagy and beclin 1 regulator 1.
AMPK AMP-activated protein kinase.
APC/C anaphase-promoting complex/cyclosome.
APCP adenosine 5-(α,β-methylene)diphosphate.
APE1 apurinic/apyrimidinic endodeoxyribonuclease.
APLF aprataxin and PNKP like factor.
APS ammonium persulfate.
APTX aprataxin.
ASL arginosuccinate lyase.
ASNS asparagine synthetase.
ASS1 argininosuccinate synthase 1.
ATCC American Type Culture Collection.
ATF6 activating transcription factor 6.
ATM ATM serine/threonine kinase.

ATP adenosine triphosphate.
ATR ATR serine/threonine kinase.
ATRX ATRX, chromatin remodeler.
AURK aurora kinase.

BAD BCL2-associated agonist of cell death.
BAX BCL2-associated X, apoptosis regulator.
BBB blood-brain barrier.
BCL2 BCL2, apoptosis regulator.
BCP 1-bromo-3-chloropropane.
BCR B cell receptor.
BER base excision repair.
BMF BCL2-modifying factor.
BNIP3 BCL2-interacting protein 3.
BRC Biomedical Research Centre.
BRCA BRCA, DNA repair associated.
BSA bovine serum albumin.

CAB39 calcium-binding protein 39.
CAT catalase.
CCND1 cyclin D1.
CCO cytochrome *c* oxidase.
CDC cell division cycle.
CDK cyclin-dependent kinase.
CDKN cyclin-dependent kinase inhibitor.
CENP centromere protein.
CHI3L1 chitinase 3 like 1.
CHX Charing Cross Hospital.
CLL chronic lymphocytic leukaemia.
CML chronic myeloid leukaemia.
CNS central nervous system.
CPS1 carbamoyl-phosphate synthase 1.
CQ-CCR coenzyme Q-cytochrome *c* reductase.
CTCF CCCTC-binding factor.
CTLA4 cytotoxic T-lymphocyte-associated protein 4.
CYP1A cytochrome P450 family 1 subfamily A.

DHF dihydrofolate.
DHFR dihydrofolate reductase.
DHRS3 dehydrogenase/reductase 3.
DMEM Dulbecco's Modified Eagle's medium.
DMSO dimethyl sulfoxide.
DNA-PKcs DNA-dependent protein kinase, catalytic subunit.
DSB double-strand break.
DSMZ The Leibniz Institute DSMZ - German Collection of Microorganisms and Cell Cultures.
DTAB dodecyltrimethylammonium bromide.
dTMP thymidine monophosphate.
DTT dithiothreitol.

E2F E2F transcription factor.

EGFR epidermal growth factor receptor.
EHMT2 euchromatic histone lysine methyltransferase 2.
EMT epithelial-mesenchymal transition.
ENT equilibrative nucleoside transporter.
ERCC ERCC excision repair, endonuclease non-catalytic subunit.
ETC electron transport chain.

FABP fatty acid-binding proteins.
$FADH_2$ reduced flavin adenine dinucleotide.
FASN fatty acid synthase.
FASTClear Free-of-Acrylamide SDS-based Tissue Clearing.
FBS foetal bovine serum.
FC fold change.
FMN flavin mononucleotide.
FOX forkhead box.
FRMD5 FERM domain containing 5.
FZR1 fizzy and cell division cycle 20 related 1.

G6PC glucose-6-phosphatase.
G6PD glucose-6-phosphate dehydrogenase.
GABRA1 gamma-aminobutyric acid type A receptor alpha 1 subunit.
GAPDH glyceraldehyde-3-phosphate dehydrogenase.
GBM glioblastoma.
GDH glutamate dehydrogenase.
GFP green fluorescent protein.
GINS3 GINS complex subunit 3.
GLI1 GLI family zinc finger 1.
GLRX glutaredoxin.
GLS glutaminase.
GLUL glutamate-ammonia ligase.
GLUT glucose transporter.
GO gene ontology.
GP glutathione peroxidase.
GR glutathione reductase.
GS glutamine synthetase.
GSCs glioblastoma stem cells.
GSEA gene set enrichment analysis.
GSK3 glycogen synthase kinase 3.
GST glutathione S-transferases.

H2AFZ H2A histone family member Z.
HAAO 3-hydroxyanthranilate 3,4-dioxygenase.
HDAC histone deacetylase.
HDIs histone deacetylase inhibitors.
HER2 Erb-B2 receptor tyrosine kinase 2.
HIF hypoxia-inducible factor.
HJURP holliday junction recognition protein.
HK hexokinase.
HMDB Human Metabolome Database.

HMGN2 high mobility group nucleosomal-binding domain 2.
HOXB5 homeobox B5.
HR homologous recombination.
HRP horseradish peroxidase.
HSP heat shock protein.

IC_{50} relative half maximal inhibitory concentration.
IDH isocitrate dehydrogenase.
IDO indoleamine 2,3-dioxygenase.
IGF2BP2 insulin-like growth factor 2 mRNA-binding protein 2.
IQR interquartile range.
IVIS In Vivo Imaging System.

JAK janus kinase.
JNK c-Jun N-terminal kinase.

KAT2 lysine acetyltransferase 2.
KDM4A lysine demethylase 4A.
Ki-67 Ki-67 protein.
KM plots Kaplan-Meir plots.
KMO kynurenine 3-monooxygenase.
KRAB Kruppel-associated box repressor domain.
KYNU kynureninase.

LB Luria broth.
LDHA lactate dehydrogenase A.
LDLR low-density lipoprotein receptor.
LIG3 DNA ligase 3.
LKB1 serine/threonine kinase 11.
LSM3 LSM3 homolog, U6 small nuclear RNA and mRNA degradation-associated.
LXR liver X receptor.

MAPK mitogen-activated protein kinase.
MAPKAP1 mitogen-activated protein kinase associated protein 1.
MDH malate dehydrogenase.
MDM2 MDM2 proto-oncogene.
MDM4 MDM4, p53 regulator.
ME malic enzyme.
MET MET proto-oncogene, receptor tyrosine kinase.
MGMT O-6-methylguanine-DNA methyltransferase.
miRNA microRNA.
MLST8 mTOR associated protein, LST8 homolog.
MMP matrix metallopeptidase.
MMR mismatch repair.
MRI magnetic resonance imaging.
MRN MRE11-RAD50-NBM.
MSH6 mutS homolog 6.
MTIC 5-(3-methyltriazen-1-yl)-imidazole-4-carboxamide.
mTOR mechanistic target of rapamycin.
MYC MYC proto-oncogene, BHLH transcription factor.

MYCN MYCN proto-Oncogene, BHLH transcription factor.

NA nicotinic acid.
NaAD nicotinic acid adenine dinucleotide.
NAD nicotinamide adenine dinucleotide.
NADH reduced nicotinamide adenine dinucleotide.
NADK NAD kinase.
NADP nicotinamide adenine dinucleotide phosphate.
NADPH reduced nicotinamide adenine dinucleotide phosphate.
NADSYN1 NAD synthetase 1.
Nam nicotinamide.
NaMN nicotinic acid mononucleotide.
NAMPT nicotinamide phosphoribosyltransferase.
NANOG nanog homeobox.
NAPRT nicotinate phosphoribosyltransferase.
NDU NADH dehydrogenase (ubiquinone).
NEB New England Biolabs.
NEFL neurofilament light.
NER nucleotide excision repair.
NF-$\varkappa$B nuclear factor kappa B.
NF1 neurofibromin 1.
NFYA nuclear transcription factor Y subunit alpha.
NHEJ non-homologous end joining.
NMN nicotinamide mononucleotide.
NMNAT nicotinamide nucleotide adenylyltransferase.
NMRK nicotinamide riboside kinase.
NNT nicotinamide nucleotide transhydrogenase.
NOTCH1 notch 1.
NQO1 NADPH: quinone oxidoreductase 1.
NR nicotinamide riboside.
NSCLC non-small cell lung cancer.
NT5E ecto-5'-nucleotidase.

OD optical density.
OGDH oxoglutarate dehydrogenase.
OTC ornithine carbamoyltransferase.
OXPHOS oxidative phosphorylation.

p14$^{\mathbf{ARF}}$ p14, CDKN2A alternate reading frame.
PA phthalic acid.
PAGE polyacrylamide gel electrophoresis.
PAK4 P21 (RAC1)-activated kinase 4.
PAR poly (ADP-ribose).
PARG poly (ADP-ribose) glycohydrolase.
PARP poly (ADP-ribose) polymerase.
PARylation poly-ADP-ribosylation.
PBS phosphate-buffered saline.
PBS-T PBS with with 0.1% TWEEN 20.
PCNA proliferating cell nuclear antigen.

PD1 programmed cell death protein 1.
PDGFRA platelet-derived growth factor receptor alpha.
PDH pyruvate dehydrogenase.
PDK pyruvate dehydrogenase kinase.
PEPCK phosphoenolpyruvate carboxykinase.
PET positron emission tomography.
PFA paraformaldehyde.
PFS progression-free survival.
PGC1α PPARG coactivator 1 alpha.
PGD phosphogluconate dehydrogenase.
PHD prolyl hydroxylase.
PI propidium iodide.
PI3K phosphatidylinositol-4,5-bisphosphate 3-kinase.
PKM2 pyruvate kinase M2.
PLK1 polo-like kinase 1.
PNKP polynucleotide kinase 3'-phosphatase.
PPARGC1 PPARG coactivator 1.
PPI protein-protein interactions.
PPP pentose phosphate pathway.
PROM1 prominin 1.
PS phosphatidylserine.
PTEN phosphatase and tensin homolog.

QA quinolinic acid.
qPCR quantitative polymerase chain reaction.
QPRT quinolinate phosphoribosyltransferase.

Raptor regulatory associated protein of mTOR complex 1.
RB RB transcriptional corepressor.
RBBP8 RB-binding protein 8, endonuclease.
RELA RELA proto-Oncogene, NF-κB subunit.
Rictor Raptor independent companion of mTOR complex 2.
RIPA radioimmunoprecipitation assay.
RISCs recurrence-initiating stem cells.
RNAseq RNA sequencing.
ROS reactive oxygen species.
RRM2 ribonucleotide reductase regulatory subunit M2.

S6K1 ribosomal protein S6 kinase beta-1.
SCO2 synthesis of cytochrome *c* oxidase 2.
SDH succinate dehydrogenase.
SDS sodium dodecyl sulfate.
SEM standard error of the mean.
shRNA short hairpin RNA.
siRNA small interfering RNA.
SIRT sirtuin.
SLC solute carrier family.
SLC12A5 SLC 12 member 5.
SLC1A5 SLC 1 member 5.

SNAI snail family transcriptional repressor.
SNP single nucleotide polymorphism.
SOC Super Optimal broth with Catabolite repression.
SOD superoxide dismutase.
SOX2 SRY-box 2.
SRB sulforhodamine B.
SREBF1 sterol regulatory element-binding transcription factor 1.
SSB single-strand break.
STAT signal transducer and activator of transcription.
STRAD STE20-related kinase adaptor.
SYT1 synaptotagmin 1.

TCA trichloroacetic acid.
TCGA The Cancer Genome Atlas.
TDO tryptophan 2,3-dioxygenase.
TEMED tetramethylethylenediamine.
TERT telomerase reverse transcriptase.
TF transcription factor.
TGFβ transforming growth factor beta.
THF tetrahydrofolate.
TIGAR TP53-induced glycolysis regulatory phosphatase.
TIPARP TCDD inducible PARP.
TKT transketolase.
TLR toll-like receptor.
TMZ temozolomide.
TNF tumour necrosis factor.
TNKS tankyrase.
TP53 tumour protein P53.
TP63 tumour protein P63.
TP73 tumour protein P73.
TPI triosephosphate isomerase.
TRAIL TNF-related apoptosis-inducing ligand.
TRF2 telomeric repeat-binding factor 2.
TSC TSC complex subunit.
TYMS thymidylate synthetase.

UCSC University of California, Santa Cruz.

VAD Vacor adenine dinucleotide.
VEGF vascular endothelial growth factor.
VHL von Hippel-Lindau.
VP64 VP16 tetramer activation domain.

WHO World Health Organisation.

XRCC X-ray repair cross complementing.

Chapter 1

Introduction

1.1 Glioblastoma

1.1.1 Incidence, clinical presentation and diagnosis

There are more than 10,000 new cases of brain tumours diagnosed every year in the UK alone (CRUK, 2016). Whilst cancers of the brain are comparatively rare, they tend to have a much lower five year survival rate than other cancers, and are also far more common in young people (CRUK, 2016). Gliomas account for approximately 81% of all malignant brain tumours (Ostrom et al., 2014). High grade gliomas (grade IV) are the most aggressive form of brain cancer, and most cases of high grade gliomas are glioblastoma (GBM). The majority (∼90%) of GBM tumours are primary or *de novo* GBM, but those that progress from low grade astrocytomas (grade II/III) are known as secondary GBM (Louis et al., 2016). Primary GBM tumours are generally considered to be spontaneous events, as there is little evidence to suggest a familial component (Urbanska et al., 2014). Even with the current standard of care, primary GBM has a poor median survival time of only 14.2 months with standard therapy (Johnson and O'Neill, 2012).

Patients with GBM tumours often present with classic signs of impaired brain function that normally appear over the course of a few weeks or months (Demir et al., 1987), including, but not limited to:

- Ataxia (lack of coordination of muscle movements)

- Blurred vision
- Headaches
- Syncope (fainting)
- Seizures
- Nausea/vomiting

Diagnosis depends first and foremost on imaging, generally via high contrast magnetic resonance imaging (MRI), followed by histopathology of tumour tissue either during surgical debulking, or by fine needle biopsy (Urbanska et al., 2014).

1.1.2 Histological and molecular classification

GBM tumours normally exhibit diffuse behaviour with clear invasion of local brain tissue. They are characterised by hypercellularity, nuclear atypia, a high degree of mitotic activity, and microvascular proliferation (Wesseling et al., 2015). GBM tumours normally show extensive vascularisation, but as the tumours grow, the blood supply to the centre is insufficient to maintain cell viability, resulting in a large, necrotic core (Urbanska et al., 2014). GBM tumours are highly heterogeneous; not only do tumours from individual patients show significant differences between them (inter-tumour heterogeneity), but there are also many distinct sub-clones present in any given tumour (intra-tumour heterogeneity) (Patel et al., 2014).

The molecular characteristics of GBM are specific to the different sub-types. Primary GBM tumours often possess mutations in phosphatase and tensin homolog (PTEN) and the telomerase reverse transcriptase (TERT) promotor region, as well as epidermal growth factor receptor (EGFR) amplification (Wesseling et al., 2015). On the other hand, secondary GBM tumours normally have mutations in tumour protein P53 (TP53), ATRX, chromatin remodeler (ATRX) and isocitrate dehydrogenase (IDH)1 (Ichimura et al., 2009; Wesseling et al., 2015). Mutations in IDH1 have been incorporated into the 2016 World Health Organisation (WHO) classification of tumours of the central nervous system (Louis et al., 2016), and it is generally thought that IDH1 mutations are very early events in secondary GBM (Wesseling et al., 2015). Secondary GBM is normally found in younger patients, and is associated with longer survival times (Williams Parsons et al., 2008). Other molecular markers of GBM include amplifications

of cyclin-dependent kinase (CDK)4, platelet-derived growth factor receptor alpha (PDGFRA) and MDM2 proto-oncogene (MDM2), and homozygous deletions in cyclin-dependent kinase inhibitor (CDKN)2, RB transcriptional corepressor (RB)1 and neurofibromin 1 (NF1), as well as phosphatidylinositol-4,5-bisphosphate 3-kinase (PI3K) mutations (TCGA, 2008). These specific mutations have resulted in GBM being further divided into four sub-categories (Verhaak et al., 2010):

- Proneural - defined by frequent TP53 and IDH1 mutations, as well as PDGFRA copy number alterations. Most secondary GBM belong to this group, which partially explains the lower median age, and the link to increased survival time
- Neural - defined by expression of neurofilament light (NEFL), gamma-aminobutyric acid type A receptor alpha 1 subunit (GABRA1), synaptotagmin 1 (SYT1), and the solute carrier family (SLC) protein SLC 12 member 5 (SLC12A5) markers
- Classical - defined by high level EGFR amplifications without TP53 mutations, as well as focal 9p21.3 homozygous deletion targeting CDKN2
- Mesenchymal - defined by NF1 deletions as well as expression of mesenchymal markers, including chitinase 3 like 1 (CHI3L1) and MET proto-oncogene, receptor tyrosine kinase (MET) and a clear display of markers indicating epithelial-mesenchymal transition (EMT)

Aggressive therapy in the classical and mesenchymal subtypes significantly improves survival (Verhaak et al., 2010). Interestingly, single-cell RNA sequencing has indicated that individual tumours can actually have populations representing multiple different GBM subtypes (Patel et al., 2014). Patients whose tumours exhibit high levels of intra-tumour heterogeneity have poorer survival times. Bioinformatic models have been used to show that GBM tumours may have anything up to 16 distinct sub-populations at the time of initial surgical resection (Andor et al., 2014).

1.1.3 Standard therapy

GBM is normally treated with surgical debulking followed by radiotherapy and chemotherapy in the form of temozolomide (TMZ). This aggressive treatment regimen, known as the "Stupp

protocol", has been proven to significantly increase survival in patients with GBM with minimal side effects, compared to surgery and radiotherapy alone (Stupp et al., 2005). Prior to surgery, patients are often given corticosteroids, often in the form of dexamethasone (Kostaras et al., 2014), to suppress tumour-induced oedema and therefore reduce brain swelling, in an attempt to control symptoms (Dietrich et al., 2011). Gadolinium contrast-enhanced MRI images are used to determine the location and size of the tumour before and after surgery. The optimal surgical outcome is gross total resection, defined as the absence of contrast-enhancing tissue on post-operative T1-weighted MRI images (Sanai et al., 2008). Surgical resection is guided by the use of intraoperative stimulation-induced speech tests. This allows surgeons to determine critical areas for speech function, to ensure that normal neurological functions are not damaged during resection (Sanai et al., 2008).

TMZ is the primary chemotherapeutic option for patients with GBM. It is a prodrug that is stable in acidic conditions such as those found in the stomach, which allows it to be administered orally (Zhang et al., 2012a). Most importantly, due to its small size and lipophilic properties, TMZ is able to cross the blood-brain barrier (BBB) (Agarwala and Kirkwood, 2000). A diagram showing the mechanisms of action of TMZ can be seen in Fig. 1.1. Pharmacokinetic reactions in the body lead to the decomposition of TMZ to5-(3-methyltriazen-1-yl)-imidazole-4-carboxamide (MTIC), followed by hydrolysis to generate 5-aminoimidazole-4-carboxamide (AIC) and the active compound, a highly reactive methyldiazonium cation (Newlands et al., 1997). In cells, this compound reacts with DNA to preferentially produce methylated groups at N7 positions on guanine residues (*N7*-MeG), but also at O6 positions and N3 positions on guanine (*O6*-MeG) and adenine (*N3*-MeA) residues, respectively (Tisdale, 1987; Denny et al., 1994). It is the *O6*-MeG damage that gives TMZ its primary anti-tumour properties. These groups cause the guanine residues to mismatch with thymine instead of cytosine during DNA replication. This damage is easily recognised by the DNA mismatch repair (MMR) machinery, but instead of removing the *O6*-MeG group, it removes the thymine group on the opposite strand, whilst the *O6*-MeG group remains on the template strand (Zhang et al., 2012a). This happens repeatedly, causing single- and double-stranded DNA breaks to occur (Mojas et al., 2007), which eventually leads to G_2/M cell cycle arrest (Cejka et al., 2003) and TP53-mediated

apoptosis (D'Atri et al., 1998).

The primary resistance mechanism for TMZ is through the action of O-6-methylguanine-DNA methyltransferase (MGMT). As shown in Fig. 1.1, MGMT is a suicide protein that is able to bind to the methyl groups of *O6*-MeG residues and remove them (Zhang et al., 2012a). MGMT is then degraded by the ubiquitin proteolytic pathway (Srivenugopal et al., 1996). MGMT promoter methylation is observed in ∼34% of patients with glioma, and results in a lack of MGMT protein (Esteller and Herman, 2004). Patients whose tumours exhibit MGMT-promoter methylation treated with TMZ have far greater survival times (Hegi et al., 2008). Furthermore, MGMT expression also affects the efficacy of other alkylating drugs (Paz et al., 2004). However, MGMT expression can be induced in GBM cells upon exposure to TMZ both *in vitro* and *in vivo* (Kitange et al., 2009; Zhang et al., 2010a). MGMT-promoter methylation is also associated with a unique hypermutated phenotype, and both TP53 and MMR dysfunction (TCGA, 2008). MGMT inhibitors such as lomeguatrib have shown promising results *in vitro* (Taspinar et al., 2013), and have been proven to be relatively well tolerated *in vivo*, with myelosuppression being the major dose-limiting toxicity (Ranson et al., 2006). However, MGMT levels rapidly return to normal following lomeguatrib treatment (Ranson et al., 2007; Watson et al., 2010), and it is yet to show clinical efficacy in any cancer (Tawbi et al., 2011). As seen in Fig. 1.1, cancer cells with MGMT-promoter methylation may also be resistant to TMZ through deficiencies in MMR. Cells lacking normal MMR machinery do not recognise the *O6*-MeG DNA bases, therefore no attempt is made to correct them, and they are tolerated without initiating apoptosis (Karran, 2001). Indeed, mutations in the MMR machinery can be selected for during TMZ treatment, and directly lead to TMZ resistance (Yip et al., 2009).

Whilst *O6*-MeG and the action of MGMT are generally considered to be the most important aspects of TMZ therapy in GBM, the other types of DNA damage induced by TMZ can also have an effect on the cells. As shown in Fig. 1.1, *N7*-MeG and *N3*-MeA bases are repaired through the action of the base excision repair (BER) machinery. These damaged bases are removed and replaced with normal bases either one at a time, or in batches of 2-10 (Zhang et al., 2012a). Removal of the damaged base is carried out by DNA glycosylases, and apurinic/apyrimidinic

endodeoxyribonuclease (APE1) prepares the single-strand break (SSB) for repair (Caldecott, 2008). The SSB is then bound by poly (ADP-ribose) polymerase (PARP), which catalyses the cleavage of nicotinamide adenine dinucleotide (NAD) into nicotinamide (Nam) and ADP-ribose. Multiple ADP-ribose groups are attached to both PARP itself, and to other targets such as histones H1 and H2B, forming long poly (ADP-ribose) (PAR) chains (Ciccia and Elledge, 2010). This process, known as poly-ADP-ribosylation (PARylation), allows relaxing of the DNA for access by the DNA repair machinery (Jagtap and Szabo, 2005). The DNA repair machinery, consisting of X-ray repair cross complementing (XRCC)1 and DNA ligase 3 (LIG3), is then able to access the DNA and repair the damage (Malanga and Althaus, 2005). PARP inhibition can sensitise cells to TMZ, including in situations where the MGMT promotor is unmethylated (Cheng, 2005; Donawho et al., 2007; Barazzuol et al., 2013). In addition to MGMT- and BER-related resistance to TMZ, there are a number of other mechanisms thought to lead to TMZ resistance. These include drug efflux pumps, such as ATP-binding cassette (ABC)B1 (Schaich et al., 2009; Munoz et al., 2015), and resistance mechanisms linked to oxidative stress caused by TMZ, such as increased glutathione production (Rocha et al., 2016).

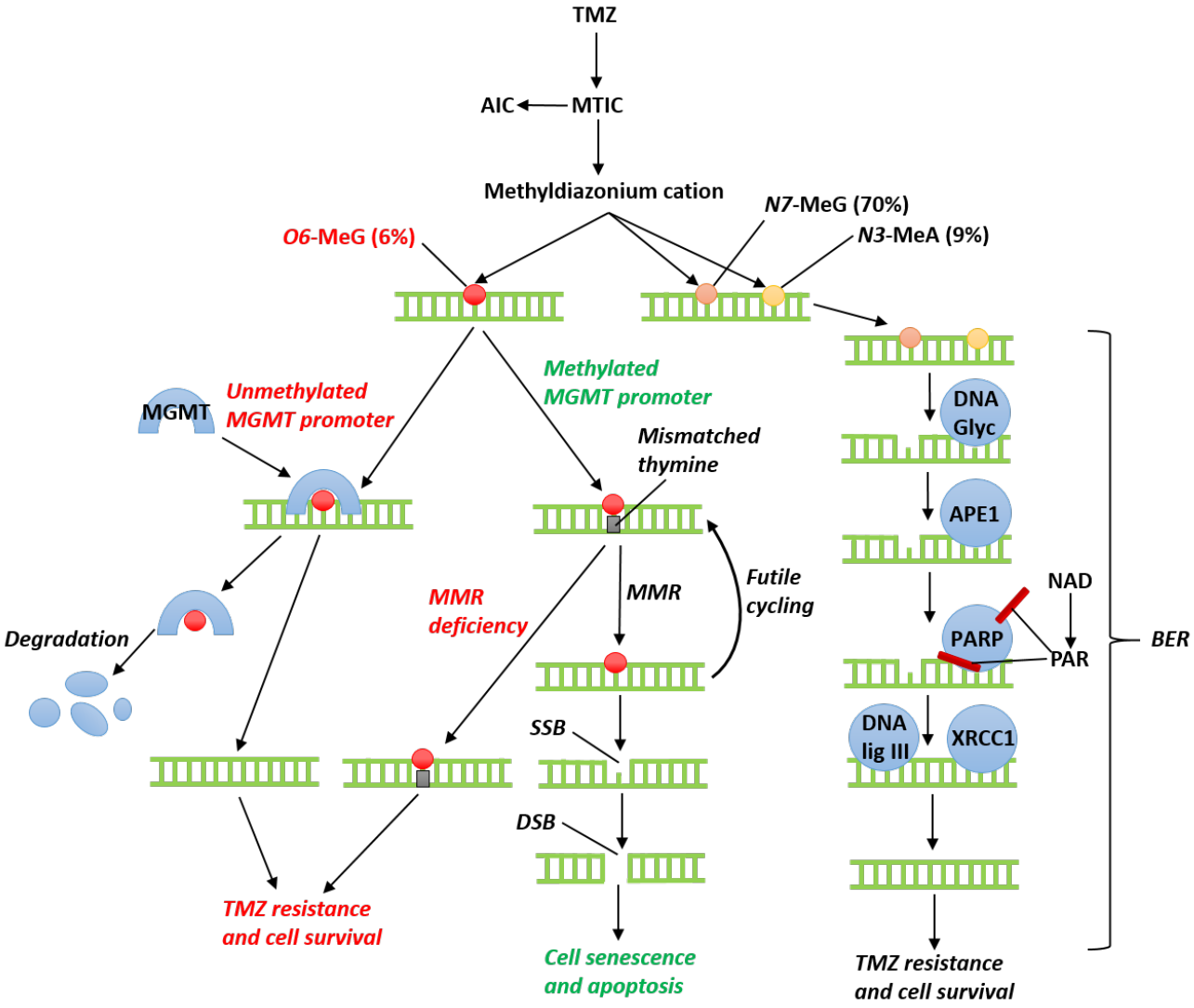


Figure 1.1: **Diagram showing the mechanism of action of TMZ in cancer cells.** The diagram shows the different damage caused by TMZ, as well as the effects of MGMT promoter methylation and PARP activity. Chemicals/metabolites seen in black writing. Italicised writing indicates a cellular process. The green ladder represents double stranded DNA. Blue molecules are proteins. The small, coloured circles represent the different types of DNA damage caused by TMZ. Unmethylated *MGMT* promoter leads to expression of MGMT. Proportions of DNA damage caused by TMZ taken from Zhang et al., 2012a. Figure adapted from Ruiz, 2014.

1.1.4 Recurrence

Despite the availability of an aggressive treatment regimen of surgery, radiation and chemotherapy, almost every patient diagnosed with GBM will eventually experience recurrence (Stupp et al., 2005). Residual cancer cells that have already infiltrated local healthy tissue escape initial surgical resection, and develop resistance to both radiation and chemotherapy (Osuka and Meir, 2017). Tumour recurrence usually appears on post-operative MRI scans ∼8 months after

initial treatment, and often presents as a local recurrence within 2 cm of the original tumour boundary (De Bonis et al., 2013). Local recurrence normally exhibits a relatively high degree of genetic similarity to the original tumour. However, recurrent tumours contain sub-populations that are enriched for from the original tumour after treatment (Andor et al., 2014). Furthermore, some sub-populations found in the recurrent tumour are completely unique, indicating the presence of divergent evolution. This is especially true in distal recurrence, i.e. recurrence found more than 2 cm away from the initial tumour boundary, which only shares ∼30% of the mutations found in the original tumour (Kim et al., 2015).

Recurrent tumours are thought to occur through the survival of GBM cells with stem cell-like properties, known as glioblastoma stem cells (GSCs) (Jackson et al., 2014) or, more recently, recurrence-initiating stem cells (RISCs) (Osuka and Meir, 2017). These cells are thought to be resistant to chemotherapy and radiation because of their decreased rates of proliferation, increased expression of DNA repair machinery and other drug resistance mechanisms (Jackson et al., 2014). The existence of a hypoxic niche is also likely to promote the survival of these cells (Li et al., 2009b). Currently, the only reliable marker for GSCs is CD133, a cell surface molecule linked to increased chemoresistance, greater tumourigenic potential and patient survival (Campos et al., 2016). These cells are thought to continue divergent evolution, creating a heterogeneous, therapy-resistant recurrent tumour for which there are few treatment options (Osuka and Meir, 2017).

The invasive nature of the recurrence means that only a very small subset of patients are eligible for further surgery and/or radiation. Most patients are given further chemotherapy in the form of TMZ, nitrosoureas or bevacizumab, but these only offer very small benefits (Weller et al., 2012). Much of the treatment for recurrent GBM is palliative, aimed at minimising neurological deficits and preventing other complications. Novel, targeted therapies such as EGFR inhibitors have proven to be ineffective in GBM (Artene et al., 2018). Other chemotherapeutic drugs, particularly those focused on promoting the response of the immune system to tumours, are still in clinical trials,. This includes the immune checkpoint inhibitors Nivolumab and Ipilimumab, directed against programmed cell death protein 1 (PD1) and cytotoxic T-lymphocyte-associated protein 4 (CTLA4), respectively (Osuka and Meir, 2017). Clearly, there

is a desperate need for novel therapeutic options to either treat GBM at its recurrence, or eliminate residual cancer cells to prevent recurrence in the first instance.

1.2 Cancer metabolism

1.2.1 Metabolic adaptations of cancer cells

Cancer cells are known to have a distinct metabolic profile. A summary of the major metabolic changes in cancer cells and their relationship with NAD metabolism can be seen in Fig. 1.2. Normal cells utilise oxygen to metabolise glucose, producing energy in the form of adenosine triphosphate (ATP) and releasing CO_2 and H_2O in a process known as oxidative phosphorylation (OXPHOS) (Campbell et al., 2008). This process is critically dependent on the presence of NAD. Multiple reactions during glycolysis and the trichloroacetic acid (TCA) cycle utilise NAD to generate NADH. The NADH is used by the electron transport chain to generate ATP. In normal cells, most ATP is generated by this way. In contrast, seminal work by Otto Warburg in the 1920's showed that cancer cells consume large amounts of glucose to produce lactate, even in the presence of sufficient oxygen to fuel OXPHOS (Warburg et al., 1927). This phenomenon, known as aerobic glycolysis or the "Warburg effect", allows cancer cells to produce biosynthetic intermediates such as nucleotides, amino acids and lipids required for cell growth and proliferation (Heiden et al., 2009). The conversion of glyceraldehyde-3-phosphate to 1,3-bisphosphoglycerate by glyceraldehyde-3-phosphate dehydrogenase (GAPDH) utilises NAD to generate NADH. As highly proliferative cells, cancer cells require large amounts of nucleotides to repair DNA damage and synthesise DNA during mitosis. Precursors for nucleotides are obtained primarily through glycolytic intermediates via the pentose phosphate pathway (PPP), and from folate metabolism (Kohnken et al., 2015). Two key reactions in the oxidative branch of the PPP depend on the presence of NADP to properly function. Entry of glucose-6-phosphate into the PPP is catalysed by glucose-6-phosphate dehydrogenase (G6PD), which utilises NADP to generate NADPH (Stincone et al., 2015). In addition, the conversion of 6-phosphogluconate to ribulose 5-phosphate is catalysed by 6-phosphogluconate dehydrogenase (6PGD), and is also NADP-dependent. Finally, the conversion of pyruvate in to acetyl coenzyme A (ACoA) and its

entry in to the TCA cycle is catalysed by pyruvate dehydrogenase (PDH), which utilises NAD to generate another molecule of NADH.

GBM cells show clear evidence of increased rates of glycolysis, which is correlated with to increases in hexokinase (HK)2 expression (Warburg, 1956; Kirsch and Leitner, 1967; Oudard et al., 1996; Wolf et al., 2011). Comprehensive analysis of genes involved in glycolysis showed that multiple enzymes are important in GBM growth, including HK2 and pyruvate dehydrogenase kinase (PDK)1 (Sanzey et al., 2015). Furthermore, a glycolytic signature for GBM has been shown to predict a poor prognosis and poor response to chemotherapy, and is even associated with IDH1 status in GBM (Chen et al., 2017). Glucose-6-phosphatase (G6PC) is an important regulator of glycolysis in GBM, and also promotes proliferation, migration and invasion (Abbadi et al., 2014). There is some evidence to suggest that GSCs display a very prominent Warburg phenotype. GBM cells exhibiting very high rates of glycolysis with little OXPHOS show stem-like properties, and have increased tumour initiating capacity, as well as a preference for hypoxic conditions (Zhou et al., 2011). This likely reflects their slower growth, with glycolysis being used to fuel ATP production instead. Inducing GBM cells to undergo differentiation in to astroglia using cAMP derivatives has been shown to reverse the "Warburg effect" and promote OXPHOS via PPARG coactivator 1 alpha (PGC1α) (Xing et al., 2017).

Even though many cancers exhibit the "Warburg effect", proper mitochondrial function is also important in cancer pathophysiology. The TCA cycle takes place in the mitochondria, which is important in the utilisation of glutamine, and the production of certain biosynthetic intermediates to support cancer cell growth (Dang, 2012). A functional TCA cycle also allows utilisation of fatty acids via β-oxidation (Carracedo et al., 2013). The major uses of NAD in the mitochondria, and metabolic adaptations in cancer cells, can be seen in Fig. 1.2. Studies have demonstrated that some GBM cell lines rely on OXPHOS to generate ATP (Kennedy et al., 2013). This effect is mediated by insulin-like growth factor 2 mRNA-binding protein 2 (IGF2BP2), which upregulates the expression of numerous mitochondrial respiratory chain complex subunits (Janiszewska et al., 2012). This suggests that both glycolysis and OXPHOS coexist to support growth in GBM. To maintain OXPHOS, cells must maintain a large NAD pool to generate the NADH required for the electron transport chain. Multiple reactions in the

TCA cycle utilise NAD to generate NADH, including those catalysed by IDH, oxoglutarate dehydrogenase (OGDH) and malate dehydrogenase (MDH) (Campbell et al., 2008). In addition, IDH can utilise NADP to generate NADPH,. This contributes to antioxidative mechanisms that help to prevent the build-up of reactive oxygen species (ROS).

Cancer cells are known to produce large amounts of ROS, which can themselves regulate cell metabolism, but also need to be eliminated if the cancer cells are to survive. ROS can alter mitochondrial permeability and cause DNA damage, both of which can trigger apoptosis (Solaini et al., 2011).ROS are also able to inhibit the major glycolytic enzyme pyruvate kinase M2 (PKM2), which diverts glucose in to the PPP, generating reduced nicotinamide adenine dinucleotide phosphate (NADPH) from nicotinamide adenine dinucleotide phosphate (NADP) (Anastasiou et al., 2011). This allows reduced glutathione levels to be maintained to combat ROS, as well as producing metabolic intermediates to synthesise nucleotides. In the brain, astrocytes are known to produce large amount of ROS due to their high metabolic activity, which predisposes them to ROS mediated DNA damage and therefore tumourigenesis (Salazar-Ramiro et al., 2016). In GBM, tumour necrosis factor (TNF) induced production of ROS causes phosphorylation and therefore activation of AKT serine/threonine kinase (Akt), leading to a decrease in superoxide dismutase (SOD)1 levels and altered cytoskeletal organisation (Ghosh et al., 2010). Furthermore, inhibition of TERT, a gene frequently mutated and overexpressed in GBM, has been reported to decrease the expression of the key PPP enzymes G6PD and transketolase (TKT), leading to increased apoptosis in a ROS dependent manner (Ahmad et al., 2016). Interestingly, others have reported that glycloysis and the PPP have divergent roles in GBM. Whilst rapidly proliferating GBM cells have high expression of genes involved in the PPP, migrating cells preferentially express genes involved in glycolysis (Kathagen-Buhmann et al., 2016).

Cancer cells also exhibit altered amino acid metabolism, in particular through elevated consumption of glutamine. In cancer cells, glutamine is used as a nitrogen donor for amino acid production to support protein synthesis, as well as fuelling the TCA cycle, and promoting glutathione production to combat oxidative stress (Deberardinis and Cheng, 2010). However, in GBM, very little circulating glutamine is taken up by the cells. Instead, GBM cells synthesise

glutamine from glutamate through the action of glutamine synthetase (GS) to fuel *de novo* purine synthesis (Tardito et al., 2015). However, recent metabolomic work has demonstrated that there are two distinct populations of GBM cells; one that relies on glutamine (GLN^{High}), and another that does not (GLN^{Low}) (Oizel et al., 2017). GLN^{High} cells appear to be normal GBM cells, whereas GLN^{Low} cells are $CD133^{+}$ and thought to represent a subpopulation of GSCs. This subpopulation is more dependent on glucose metabolism. Furthermore, studies have reported that glucose deprivation can lead to a switch to increased glutamine consumption in GBM. Low glucose levels lead to an increase in glutamate dehydrogenase (GDH) activity to support glutamine utilisation by the TCA cycle (Chendong et al., 2009). In addition to the role of glutamine in cancer metabolism, there is also evidence to suggest that some cancer cells exhibit specific amino acid dependencies. Studies have demonstrated that certain cancers rely on an exogenous supply of the non-essential amino acids asparagine or arginine. This is because they lack the necessary enzymes to synthesise them *de novo*, namely asparagine synthetase (ASNS) and argininosuccinate synthase 1 (ASS1), respectively (Lukey et al., 2017).

Lipid metabolism is now also regarded as an important part of the cancer metabolome. Observations of increased *de novo* fatty acid synthesis in cancer were described as far back as 1951 (Olson, 1951; Zamecnik et al., 1951). To support their rapid growth, cancer cells need to either consume or produce large amounts of fatty acids and cholesterol, particularly to support membrane synthesis. As cancer cells consume large amounts of glucose and glutamine, both of these molecules can be used to fuel the TCA cycle, which results in the generation of citrate (Röhrig and Schulze, 2016). As the citrate moves from the mitochondria to the cytosol, it can be converted into ACoA by ATP citrate lyase (ACLY). ACoA is then converted into malonyl-CoA by acetyl-CoA carboxylase (ACC), followed by the conversion into palmitate by fatty acid synthase (FASN). Palmitate contributes significantly to the overall fatty acid pool, which fuels lipid and cholesterol synthesis. Cancer cells increase lipid and cholesterol synthesis specifically through the upregulation of this pathway (Beloribi-Djefaflia et al., 2016). In addition, some cancers have been demonstrated to increase fatty acid uptake in response to particular stressors, further contributing to the fatty acid pool (Röhrig and Schulze, 2016).

Whilst it is generally accepted that fatty acid synthesis is the primary metabolic pathway

in cancer, others have suggested that some cancer types utilise β-oxidation of fatty acids to supplement energy production. Triglycerides are broken down in to fatty acids by hydrolases, and the fatty acids are then transported in to the mitochondria (Carracedo et al., 2013). β-oxidation produces reduced nicotinamide adenine dinucleotide (NADH) and reduced flavin adenine dinucleotide ($FADH_2$) to be used in OXPHOS, and ACoA, which can enter the TCA cycle to generate further reducing agents. This phenotype has been observed in most clearly in breast cancer (Carracedo et al., 2012). The composition of lipids in GBM have been reported to be significantly altered compared to normal healthy tissue (Guo et al., 2013a). In addition, studies have reported that EGFR signalling, which is frequently upregulated in GBM, leads to the activation and nuclear translocation of sterol regulatory element-binding transcription factor 1 (SREBF1), a master regulator of fatty acid synthesis (Guo et al., 2009b).

Clearly, cancer cells, including GBM, show a vast array of metabolic adaptations compared to their normal, healthy counterparts. These changes allow them to maintain energy production whilst consuming and synthesising the molecular intermediates required to grow and proliferate.

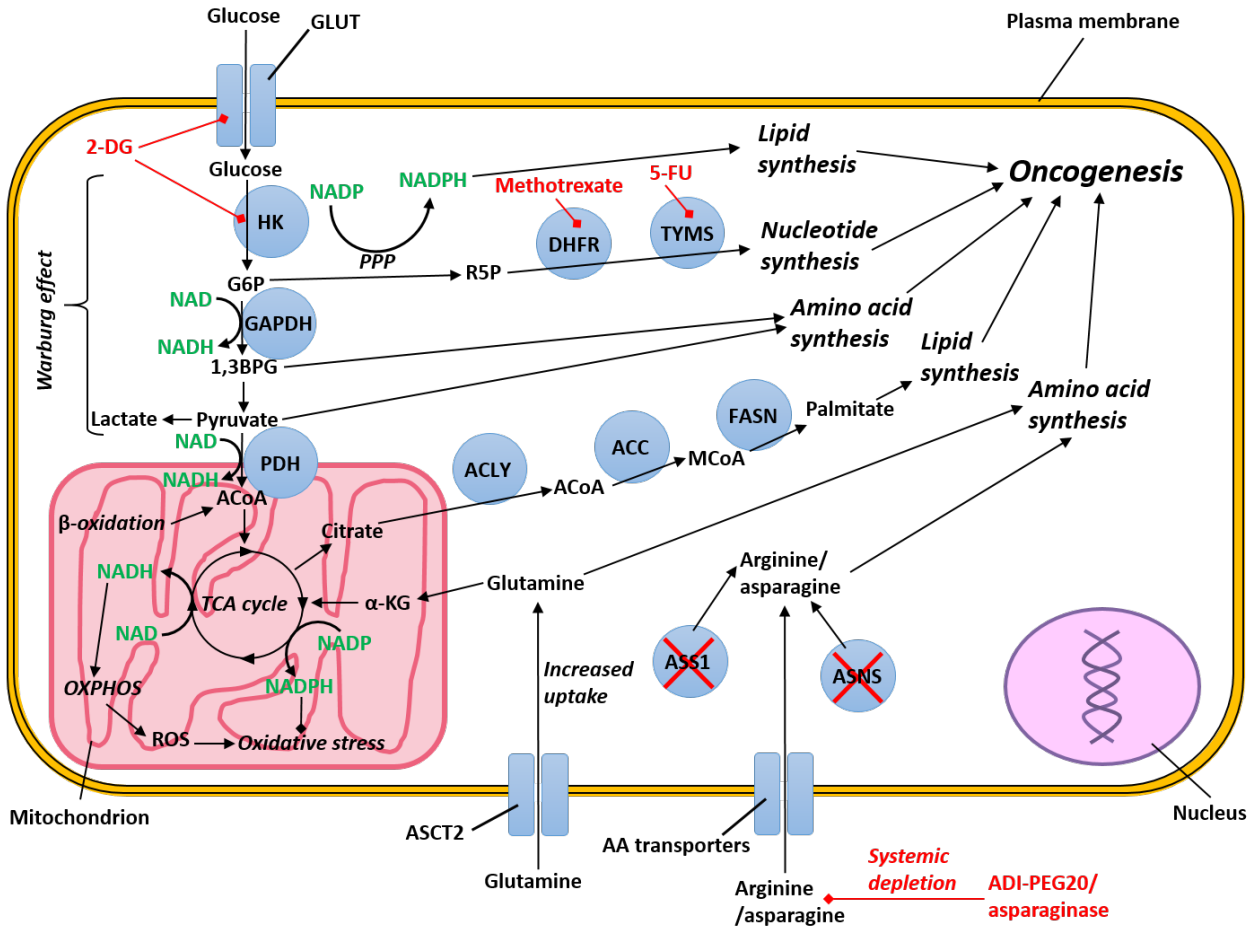


Figure 1.2: **Diagram showing major metabolic changes in cancer, and some of the therapies that target them.** NAD and NADH shown in green. Metabolites seen in black writing. Italicised writing indicates a cellular process. Chemotherapeutics shown in red writing. Blue molecules are proteins.

1.2.2 Targeting metabolic changes in cancer

The diverse range of alterations to cellular metabolism in cancer opens up hundreds of avenues for therapeutic intervention. Targeting cancer metabolism with chemotherapy is not a new concept. Indeed, some of the first chemotherapeutics used clinically were derivatives of normal metabolic substrates, which were able to act as inhibitors of proliferation in cancer cells.

The first metabolic targeted chemotherapeutics were aimed at nucleotide metabolism. Seminal work by Sydney Farber, often cited as the father of modern chemotherapy (Miller, 2006), showed that antifolates such as aminopterin and methotrexate were effective in childhood leukaemia (Farber et al., 1948; Djerassi et al., 1967). As shown in Fig. 1.2, methotrexate inhibits the enzyme dihydrofolate reductase (DHFR), which catalyses the conversion of dihy-

drofolate (DHF) to tetrahydrofolate (THF) (Khan et al., 2012). This leads to a depletion of THF, which is required by thymidylate synthetase (TYMS) to synthesise thymidine monophosphate (dTMP). Loss of the dTMP pool prevents the cell from initiating both DNA repair and synthesis, leading to senescence and cell death. Methotrexate is still used today to treat numerous types of cancer, including lung, bladder, acute lymphoblastic leukaemia (ALL), chronic myeloid leukaemia (CML), primary central nervous system (CNS) lymphoma and medulloblastoma (Abolmaali et al., 2013). Not long after the first use of methotrexate, another drug targeting nucleotide metabolism in cancers was discovered; 5-fluorouracil (5FU). 5FU was proven to have anti-proliferative effects that could be reversed by the addition of thymidine or its metabolic derivatives (Rich et al., 1958). 5FU works in a very similar way to methotrexate, by directly inhibiting TYMS, as shown in Fig. 1.2 (Longley et al., 2003). In addition, 5FU has a secondary mode of action, whereby its direct incorporation into RNA during transcription leads to disruptions in RNA processing. 5FU has been used to treat breast, stomach, pancreatic, and head and neck cancers to some degree, but it is best known as a first line treatment option for colorectal cancer (Longley et al., 2003). However, even for colorectal cancer, the response rates are very low, at only 10-15%. This is because only a small subset of colorectal cancers exhibit the necessary DNA MMR deficiency required for 5FU to work (Bracht et al., 2010). Unfortunately, both methotrexate and 5FU have failed in GBM, primarily due to a lack of BBB penetration (Decker et al., 1987; Shapiro et al., 1992; Stewart et al., 1995; Herrlinger et al., 2005). Recent work using novel methods to permeabilise the BBB or deliver methotrexate using lipid nanoparticles have shown promising results (Cooper et al., 2015; Battaglia et al., 2017). However, this work is still in very early, pre-clinical development, and some concerns have been raised about its immunosuppressive effects preventing the immune system from attacking GBM cells (Figueiro et al., 2016).

Not long after the antimetabolites were tested in cancer, attempts were made to target the "Warburg effect" itself using glycolytic inhibitors. The first of these was the glucose analogue 2-deoxy-D-glucose (2DG), which was quickly proven to have anti-tumour effects *in vivo* (Ely, 1954). As shown in Fig. 1.2, 2DG competitively inhibits glucose uptake by glucose transporter (GLUT), and blocks the entry of glucose into glycolysis by inhibiting HK (Zhang et al., 2014a).

Inhibition of glycolysis leads to changes in AMP-activated protein kinase (AMPK) and Akt signalling, increased oxidative stress, disruption of post-translational modifications to proteins and the induction of autophagy (Shutt et al., 2010; Xi et al., 2011; Ahadova et al., 2015). Despite promising findings *in vitro*, the translation of 2DG to clinical use has been very slow. This is in part due to the discovery that chronic, high-dose 2DG leads to cardiotoxicity and shorter survival in rats (Minor et al., 2010). However, numerous attempts have been made to combine short term, low dose 2DG with other therapies, particularly in GBM. Administration of 2DG with radiation is safe in patients with glioma (Mohanti et al., 1996; Singh et al., 2005). 2DG combined with both 6-aminonicotinamide and irradiation leads to increased production of ROS, and inhibition of growth in numerous cancer cell lines, including GBM (Bhardwaj et al., 2012). The combination of 2DG and histone deacetylase inhibitors (HDIs) also induces apoptosis in GBM (Egler et al., 2008). Furthermore, 2DG with metformin decreases the viability of GBM tumour spheres both *in vitro* and *in vivo*, whilst simultaneously downregulating the expression of genes related to EMT and stemness (Kim et al., 2017).

Mitochondria are known to play a role in the activity of numerous anti-cancer compounds, primarily through the activation of mitochondrial-mediated apoptosis, the production of DNA-damaging ROS, and the induction of autophagy (Dickerson et al., 2017). Disruption of mitochondria in GBM cells using dichloroacetate reverses their hyperpolarised phenotype, leading to depolarisation, increased production of ROS and activation of apoptosis (Michelakis et al., 2010). This has also been demonstrated using other mitochondrial toxins (Shen et al., 2015a). Furthermore, inhibition of TERT, a gene frequently mutated and overexpressed in GBM, decreases the expression of the key PPP enzymes G6PD and TKT, leading to increased apoptosis in a ROS-dependent manner (Ahmad et al., 2016).

Given that cancer cells consume large amounts of glutamine to fuel their metabolism, inhibition of glutamine metabolic pathways is a promising therapeutic strategy. To this end, drugs targeting glutamine import, conversion to glutamate and subsequent metabolism to produce α-ketoglutarate have shown promise in treating specific cancers *in vivo*, particularly neuroblastoma (Hensley et al., 2013). However, toxicity is often a major problem with compounds targeting glutamine metabolism, and so efforts are required to generate novel compounds with

better toxicity profiles. As previously described, GBM cells synthesise glutamine from glutamate through the action of GS to fuel *de novo* purine synthesis (Tardito et al., 2015). This renders them mostly insensitive to systemic depletion of glutamine and inhibitors of glutaminolysis. However, it is possible to treat cancers showing arginine or asparagine auxotrophy by systemically depleting these non-essential amino acids, as shown in Fig. 1.2. This is the case for ALL, whereby asparagine auxotrophy means that systemic depletion of asparagine using asparaginase starves the cells, eventually leading to cell death (Egler et al., 2016). In GBM, asparagine depletion potentiates the effects of TMZ *in vivo*, although some GBM cell lines are resistant due to upregulation of ASNS (Panosyan et al., 2014). Systemic depletion of arginine can be achieved through the use of the enzyme arginine deiminase (ADI). ADI catalyses the conversion of arginine to citrulline and ammonia (Takaku et al., 1992). Early work demonstrated that a stabilised form of the enzyme, pegylated ADI (ADI-PEG20), could potently inhibit hepatocellular carcinoma and melanoma growth both *in vitro* and *in vivo* (Ensor et al., 2002). In GBM, methylation of ASS1 and arginosuccinate lyase (ASL) confers hypersensitivity to arginine depletion through the use of ADI-PEG20 (Syed et al., 2013). Treatment of GBM cells with ADI limits cell growth both *in vitro* and *in vivo* (Fiedler et al., 2015), as well as impairing cell motility, invasion and adhesion through alterations in β-actin organisation (Pavlyk et al., 2015). Clinical trials have indicated that ADI-PEG20 is well tolerated and effective in treating melanoma (Ascierto et al., 2005; Ott et al., 2013), hepatocellular carcinoma (Izzo et al., 2004; Glazer et al., 2010; Thongkum et al., 2017), and mesothelioma (Szlosarek et al., 2017). Furthermore, a clinical trial combining ADI-PEG20 with docetaxel has shown promising clinical efficacy in patients with advanced malignant solid tumours, including those of the lung, prostate, gastrointenstinal tract, head and neck (Tomlinson et al., 2015). It remains to be seen whether or not this could be of therapeutic benefit in GBM.

Attempts have also been made to target lipid metabolism in cancer. Inhibition of ACLY blocks cancer cell proliferation both *in vitro* and *in vivo* (Hatzivassiliou et al., 2005). This effect is mediated by increases in ROS, leading to DNA damage and AMPK activation (Migita et al., 2013). In GBM, inhibition of ACLY leads to decreases in clonogenicity, migration and invasion, and potentiates the effects of Met kinase inhibitors (Beckner et al., 2010). Inhibition

of ACC blocks proliferation and induces cell death in numerous types of cancer (Wang et al., 2015a). Recent work has indicated that inhibition of ACC also leads to a block in fatty acid synthesis and proliferation in EGFR mutant GBM cells (Jones et al., 2017). Early inhibitors of FASN showed promising anti-neoplastic activity, but had potentially dangerous side effects, including appetite suppression and concomitant weight loss (Flavin et al., 2010). However, novel FASN inhibitors have shown more promising results, with better specificity and fewer side effects (Menendez and Lupu, 2017). In GBM, overexpression of FASN is associated with glioma tumour grades, and inhibition of FASN using orlistat initiates apoptosis in GBM cells (Grube et al., 2014). Furthermore, FASN induced lipogenesis is greater in GSCs, and inhibition of FASN using cerulenin suppresses proliferation and migration in these cells (Yasumoto et al., 2016).

There is also evidence to suggest that targeting cholesterol metabolism could be of clinical benefit in cancer, particularly through the liver X receptor (LXR)/low-density lipoprotein receptor (LDLR) pathway. Cholesterol is required for the maintenance of cell surface signalling molecules in lipid rafts, as well as regulating endoplasmic reticulum stress (Beloribi-Djefaflia et al., 2016). LXR agonists inhibit cancer cell growth by decreasing the expression of LDLR, thereby suppressing cholesterol uptake (Lin and Gustafsson, 2015). In GBM, activation of LXR leads to LDLR degradation and cell death *in vivo* (Guo et al., 2011; Villa et al., 2016). In addition, TMZ sensitivity in GBM cells is associated with a reduction in intracellular cholesterol levels, and soluble cholesterol can increase sensitivity to TMZ through a death receptor 5/caspase-8 dependent mechanism (Yamamoto et al., 2018). However, despite promising preclinical results, psychiatric side effects stemming from LXR agonist treatment has prevented their use in the clinic (Lin and Gustafsson, 2015). It appears that cholesterol metabolism is another vital part of cancer biology, including in GBM. However, more work is required to fully elucidate the mechanisms by which these pathways affect cancer initiation and growth before effective therapies can be applied in the clinic.

1.2.3 Pathways that regulate cancer metabolism

Clearly, cancer cells show a vast array of metabolic adaptations compared to their normal, healthy counterparts. These changes allow cancer cells, including GBM, to consume large amounts of metabolites, maintain the production of ATP and synthesise the biosynthetic intermediates required to survive and proliferate. Therapies targeting some of these metabolic adaptations, particularly nucleotide metabolism, have had great success in treating cancer. There are a few major metabolic pathways that control cancer cell metabolism. The first is the PI3K/Akt pathway, and the second is the serine/threonine kinase 11 (LKB1)/AMPK pathway. Both of these converge on mechanistic target of rapamycin (mTOR), which is a major regulator of cell metabolism. In addition, other major cancer pathways are able to affect cancer cell metabolism, including TP53, MYC proto-oncogene, BHLH transcription factor (MYC) and hypoxia-inducible factor (HIF)1. A summary of the major signalling pathways that control cancer cell metabolism can be seen in Fig. 1.3.

PI3K/Akt

In GBM, the PI3K/Akt pathway is activated in up to 90% of cases (Langhans et al., 2017). As shown in Fig. 1.3, this is often due to EGFR amplications or activating mutations, but these genetic alterations also occur in PI3K as well (TCGA, 2008). PI3K is amplified or mutated in a variety of cancers, leading to an increase in PI3K/Akt signalling that promotes a cancerous phenotype (Tu et al., 2009). PTEN, a major negative regulator of PI3K, is one of the most frequently mutated tumour suppressor genes across all cancers. Indeed, in primary GBM, PTEN is mutated in 30% of cases, and is associated with shorter survival times (TCGA, 2008; Lino and Merlo, 2011). Loss of PTEN activity leads to a constitutively activated PI3K/Akt signalling pathway and aberrant metabolism (Chalhoub and Baker, 2009).

Akt influences a range of different pathways involved in cancer survival and proliferation. Akt activates HK2 to promote glycolysis in numerous cancer types (Zhuo et al., 2015; Li et al., 2016). Upregulation of HK2 is critical in maintaining the "Warburg effect" in GBM, allowing the cells to proliferate and even promoting resistance to radiation and chemotherapy (Wolf et al., 2011). Akt also promotes glycolysis by increasing phosphofructokinase activity in cancer

(Novellasdemunt et al., 2013; Simon-Molas et al., 2016). In addition, Akt stimulates *de novo* fatty acid synthesis through its interaction with ACLY (Bauer et al., 2005; Hanai et al., 2012). In GBM, constitutive activation of Akt leads to activation of MDM2, which suppresses TP53 activity (Daniele et al., 2015). Furthermore, Akt inhibits glycogen synthase kinase 3 (GSK3), leading to block in apoptotic signalling and upregulation of β-catenin activity (Majewska and Szeliga, 2017). Finally, activation of the PI3K/Akt pathway leads to translocation of GLUT1 to the plasma membrane, to allow glucose uptake, thus promoting glycolysis (Hong et al., 2016).

PI3K/Akt inhibitors are in the relatively early stages of clinical development, but have shown some promise. PI3K inhibitors are effective in treating chronic lymphocytic leukaemia (CLL), as well as some solid tumours such as breast cancer (Khan et al., 2014; Mateo et al., 2017; Morgillo et al., 2017). In GBM, pan PI3K inhibitors such as wortmannin suppress EGFR-mediated cell signalling and limit proliferation (Klingler-Hoffmann et al., 2003). Furthermore, inhibition of PI3K can sensitise GBM cells to radiation and chemotherapy (Kao et al., 2007; Opel et al., 2008; Shi et al., 2017). Development of PI3K inhibitors has led to the synthesis of compounds that can more easily cross the BBB, such as GNE-317. GNE-317 inhibits tumour growth in orthotopic models of GBM (Salphati et al., 2012). Despite this progress, translation to a clinical setting has been slow. In a recent phase II clinical trial, the PI3K inhibitor PX-866 was reported to be relatively well tolerated but demonstrated poor efficacy in recurrent GBM (Pitz et al., 2015). Furthermore, in phase I/II clinical trials, the Akt inhibitor perifosine showed a good toxicity profile, but poor efficacy as monotherapy in head, neck and prostate cancer, as well as neuroblastoma (Argiris et al., 2006; Chee et al., 2007; Becher et al., 2017; Kushner et al., 2017). Perifosine has not been tested in a clinical setting in GBM, but has been reported to synergise with bevacizumab, yielding increases in apoptosis and longer survival in a pre-clinical model (Ramezani et al., 2017). However, clinical trials using the pan-Akt inhibitor MK-2206 have been more successful. MK-2206 was demonstrated to synergise with various anti-cancer agents both *in vitro* and *in vivo*, leading to increased suppression of proliferation across multiple cancer types (Hirai et al., 2010). Phase I clinical trials showed that MK-2206 was well tolerated and yielded partial responses in patients with pancreatic cancer (Yap et al., 2011). Phase II clinical trials took this further, demonstrating that MK-2206 has modest activity in

patients with lymphoma and CLL (Larsen et al., 2017). In GBM, MK-2206 synergises with the EGFR inhibitor gefitinib, leading to a significant increase in apoptosis both *in vitro* and *in vivo* (Cheng et al., 2012). Furthermore, MK-2206 synergises with radiation and TMZ *in vitro* (Narayan et al., 2017). Other Akt inhibitors, including GSK690693 and PBI-05204, have shown anti-cancerous activity *in vitro* (Levy et al., 2009; Hong et al., 2014a; Pan et al., 2015; Korkola et al., 2015); however, more work is required to fully assess their safety and efficacy, and their potential application in GBM.

LKB1/AMPK

LKB1 is a tumour suppressor gene that is frequently mutated in cancer (Momcilovic and Shackelford, 2015). LKB1 phosphorylates AMPK leading to its activation (Woods et al., 2003; Shaw et al., 2004). As shown in Fig. 1.3, mutations in LKB1 result in a loss of function, leading to a lack of AMPK activity (Momcilovic and Shackelford, 2015). AMPK is a critical regulator of cell metabolism. It functions as an energy sensor, monitoring the AMP/ADP/ATP ratio, and responding accordingly. Under conditions in which ATP is being used rapidly, such as in response to low glucose levels or through the actions of specific signalling pathways, ADP and AMP are released. These can bind to the γ-subunit of AMPK, leading to a conformational change that allows phosphorylation by LKB1, and inhibits dephosphorylation (Mihaylova and Shaw, 2011). This activates AMPK, which is then able to stimulate energy production through the upregulation of glycolysis, OXPHOS and β-oxidation of fatty acids, as well as illiciting changes to pathways that control cell growth, proliferation, autophagy and even cell polarity (Mihaylova and Shaw, 2011). Whilst LKB1 mutations are rare in GBM, studies have demonstrated that high levels of microRNA (miRNA)-451 can inhibit LKB1 activity in glioma cells. miRNA-451 suppresses the expression of the LKB1 binding protein, calcium-binding protein 39 (CAB39), which stabilises the interaction between LKB1 and STE20-related kinase adaptor (STRAD) (Godlewski et al., 2010). This leads to a reduction in AMPK activity and activation of mTOR.

Despite its diverse range of roles in cellular metabolism, AMPK is generally considered to act as a tumour suppressor. It helps to counteract the "Warburg effect" by upregulating

OXPHOS (Zadra et al., 2015). Furthermore, it suppresses lipid and protein synthesis through its inhibition of ACC/FASN and mTOR, respectively (Zadra et al., 2015). Therefore, AMPK activators present a unique therapeutic opportunity. The most widely studied AMPK activator is metformin. Metformin activates AMPK indirectly by stimulating ATP consumption and therefore increasing intracellular AMP (Kasznicki et al., 2014). It has been demonstrated to have anti-neoplastic effects in numerous types of cancer, including lung, breast, colon, ovarian and melanoma (Li et al., 2015b). There have been numerous phase I, II and III clinical trials on metformin in cancer. Whilst many are still in progress, some have indicated promising results, with reductions in tumour markers such as Ki-67 protein (Ki-67), but few have reported any clinical efficacy (Chae et al., 2016). In GBM, metformin is able to synergise with TMZ and induce apoptosis both *in vitro* and *in vivo* (Yu et al., 2015b; Ho Yang et al., 2016; Valtorta et al., 2017). The AMPK agonist, 5-aminoimidazole-4-carboxamide ribonucleotide (AICAR), has been demonstrated to have anti-neoplastic activity in numerous cancers both *in vitro* and *in vivo* (Sun et al., 2007; Theodoropoulou et al., 2012; Montraveta et al., 2014; Wu et al., 2016). In GBM, AICAR inhibits the growth of EGFR-mutated GBM cells *in vitro* by blocking lipogenesis, and inhibits tumour growth *in vivo* (Guo et al., 2009a). This inhibition of *de novo* fatty acid synthesis makes GBM cells dependent on extracellular lipids, and leads to an increase in the expression of lipoprotein receptors (Ríos et al., 2014). Studies have also reported that TMZ induces AMPK expression leading to apoptosis, likely due to TP53 activation and inhibition of mTOR signalling (Zhang et al., 2010b).

mTOR

Both the PI3K/Akt and LKB1/AMPK pathways converge on arguably the most important regulator of cell metabolism, mTOR. There are two mTOR complexes: mTORC1 and mTORC2. mTORC1 is composed of mTOR, regulatory associated protein of mTOR complex 1 (Raptor), mTOR associated protein, LST8 homolog (MLST8) and AKT1 substrate 1 (AKTS1), and is relatively well characterised (Porta et al., 2014). On the other hand, mTORC2 is composed of mTOR, Raptor independent companion of mTOR complex 2 (Rictor), mitogen-activated protein kinase associated protein 1 (MAPKAP1) and MLST8, but its exact functions are still

relatively poorly understood (Porta et al., 2014). Here, I will focus on the roles of mTORC1 in cancer.

The PI3K/Akt pathway regulates mTORC1 primarily through TSC complex subunit (TSC)2. Phosphorylation of TSC2 by Akt removes its inhibitory effect on mTORC1 (Porta et al., 2014). On the other hand, AMPK inhibits mTORC1 function both by activating TSC2 and by phosphorylating raptor, a major component of the mTORC1 (Shaw, 2009). Somatic mutations in TSC1 can lead to its inactivation, causing increased mTORC1 activity and promoting a cancerous phenotype. However, the role of TSC1/2 in cancer is normally attributed to mutations in signalling molecules upstream, such as PTEN and LKB1, both of which lead to their inactivation and constitutive activation of mTORC1 (Ben-Sahra and Manning, 2017). This is especially true of GBM, where increases in EGFR signalling, coupled with PTEN mutations, lead to a constitutively activated PI3K/Akt pathway and therefore high mTORC1 activity (Akhavan et al., 2010). mTORC1 acts as a convergence point for many different pathways related to cell survival and proliferation, including numerous growth factors, oxygen concentrations and amino acid levels (Sami and Karsy, 2013). mTORC1 primarily activates anabolic pathways to encourage cell growth and proliferation. Activation of mTORC1 leads to increased protein synthesis through the phosphorylation and activation of eukaryotic translation initiation factor 4E-binding protein (4E-BP) and ribosomal protein S6 kinase beta-1 (S6K1) (Ben-Sahra and Manning, 2017). In addition, mTORC1 upregulates MYC to increase nucleotide biosynthesis, glycolysis and glutaminolysis. mTORC1 also regulates lipid metabolism by suppressing fatty acid oxidation (Ben-Sahra and Manning, 2017). Furthermore, mTORC1 forms part of a positive feedback loop by activating Akt to maintain PI3K/Akt signalling (Yang et al., 2015a).

In GBM, mTORC1 is upregulated in IDH1 wild type tumours, and is a marker of poor prognosis (Machado et al., 2018). mTORC1 controls glycolysis through its regulation of MYC. mTORC1 phosphorylates and therefore inactivates the class IIa histone deacetylases histone deacetylase (HDAC)4 and HDAC5. This results in acetylation and inactivation of forkhead box (FOX)O1/3, removing the suppressive effects of these proteins on MYC, and promoting a glycolytic phenotype (Masui et al., 2013). Because this pathway is PI3K/Akt-independent, it confers resistance to PI3K and Akt inhibitors. mTORC1 also promotes OXPHOS and sup-

presses HK2 activity under irradiation (Lu et al., 2015). Finally, whilst inhibition of mTORC1 decreases GBM cell growth both *in vitro* and *in vivo*, resistance occurs through the upregulation of glutamine metabolism (Tanaka et al., 2015).

Whilst drugs targeting PI3K or Akt have shown some promise in recent years, inhibitors of mTORC1 were proven to have anti-neoplastic activity decades ago. The drug for which mTORC1 is named, rapamycin (also known as sirolimus), was demonstrated to inhibit the growth of numerous cancer cell lines, but was not used clinically due to its poor pharmacokinetic properties (Porta et al., 2014). However, derivatives of sirolumus, such as temsirolimus and everolimus, are used to treat renal cell carcinoma (Zanardi et al., 2015; Buti et al., 2016) and breast cancer (Royce and Osman, 2015), but have shown little clinical value in treating GBM (Chang et al., 2005; Kreisl et al., 2009; Lassen et al., 2013; Ma et al., 2015; Chinnaiyan et al., 2017; Schiff et al., 2018).

One area of clinical research that has received particular interest is that of dual PI3K/mTOR inhibitors. This approach is facilitated by that fact that the catalytic subunits in PI3K and mTOR have a high degree of sequence homology (Porta et al., 2014). Most data on the effects of dual PI3K/mTOR inhibition has been collected on dactolisib (NVP-BEZ235). Initial experiments showed that dactolisib was more effective at inhibiting proliferation than everolimus in a range of different cancer cell lines (Maira et al., 2008; Serra et al., 2008). Furthermore, high doses of dactolisib can suppress the reactivation of Akt often seen with standard mTOR inhibitors, and attributed to resistance to this class of compounds. In GBM, dactolisib inhibits double-strand break (DSB) repair in irradiated cells, leading to reduced tumour growth and a significant increase in survival *in vivo* (Gil Del Alcazar et al., 2014). Dactolisib can also sensitise GBM cells to TMZ both *in vitro* and *in vivo* (Yu et al., 2015a), although its safety and efficacy in preclinical models has been questioned (Netland et al., 2016). Multiple phase II clinical trials have indicated that dactolisib is poorly tolerated, and clinical benefits have not been observed in advanced or everolimus-resistant cancers (Seront et al., 2016; Fazio et al., 2016; Wise-Draper et al., 2017). Given the wide range of responses to different inhibitors of the PI3K/Akt/mTORC1 pathway, it is likely that the greatest benefits will be seen in patients whose cancers display oncogene-addiction.

TP53

TP53 is arguably the single most important gene in the history of cancer. It is well established as a tumour suppressor gene, regulating proliferation through control of the cell cycle, DNA repair, apoptosis and a vast array of other mechanisms (Bieging et al., 2014). TP53 mutations are found in almost every single type of cancer, albeit at highly variable proportions (Rivlin et al., 2011). In GBM, TP53 mutations are present in ∼40% of cases (TCGA, 2008). In addition, other components of the TP53 pathway are altered in GBM, including deletions in p14, CDKN2A alternate reading frame ($p14^{ARF}$) and amplifications of MDM2 and MDM4, p53 regulator (MDM4) (TCGA, 2008). These mutations are highlighted in Fig. 1.3; the TP53 pathway is dysregulated in 87% of GBM cases (TCGA, 2008). Most mutations in TP53 lead to loss of its DNA-binding functions, which prevent it from activating its targets, thereby allowing proliferation to continue unhindered, leading to cancer (Rivlin et al., 2011). This occurs through the loss of proper cell cycle regulation to allow DNA repair at G_1, loss of vital apoptotic signalling pathways and alterations to a myriad of other pathways related to cell growth, proliferation and survival (Nozaki et al., 1999). However, some mutations in TP53 result in gain-of-function. These lead to inhibition of other TP53 family proteins such as tumour protein P63 (TP63) and tumour protein P73 (TP73), as well as direct activation of genes that promote cancer cell survival, such as those involved in chemoresistance, proliferation and apoptosis (Weisz et al., 2007).

Early studies indicated that TP53 mutations were linked to chemoresistance in glioma (Iwadate et al., 1996). Both mutant TP53 and high expression of TP53 are linked to poorer survival in GBM, and knockdown of mutant TP53 in GBM cells increases their sensitivity to TMZ (Wang et al., 2014). Mouse models have demonstrated that combined TP53 and PTEN deletions are enough to initiate a GBM-like phenotype, as this combination leads to MYC activation, thus enhancing tumourigenesis (Zheng et al., 2008). In addition, mutant TP53 regulates PPARG coactivator 1 (PPARGC1)A, which is an important regulator of energy metabolism, and FERM domain containing 5 (FRMD5), thought to play a role in cell motility (Brázdová et al., 2009). Furthermore, whilst concurrent alterations in TP53 and EGFR are rare, they are predictive of poorer survival in patients with GBM (Ruano et al., 2009). Finally,

despite the clear role of mutant PTEN in initiating GBM, there is some evidence to suggest that normal PTEN can actually support cancer growth. In GBM cases with gain-of-function mutant TP53, PTEN acts as a pro-cancer molecule by inhibiting the degradation of mutant TP53 by MDM2 (Li et al., 2008).

TP53 also has a diverse range of roles in cell metabolism. Expression of TP53 is able to counteract the "Warburg effect" by downregulating the expression of the glucose transporters GLUT1/4 (Schwartzenberg-Bar-Yoseph et al., 2004). This was further reinforced by the discovery of TP53-induced glycolysis regulatory phosphatase (TIGAR). TIGAR is a TP53 responsive gene that inhibits glycolysis through reduction of fructose-2,6-bisphosphate levels (Bensaad et al., 2006). In addition to this, TP53 also promotes OXPHOS through the induction of synthesis of cytochrome *c* oxidase 2 (SCO2), which stabilises the cytochrome C oxidase complex in mitochondria (Matoba et al., 2006). TP53 expression is modulated through a number of major metabolic signalling pathways, including the PI3K/Akt pathway. TP53 can also be activated by AMPK in response to low glucose levels, leading to cell senescence (Jones et al., 2005). Furthermore, there is a positive feedback mechanism in place, whereby TP53 is able to activate AMPK signalling (Feng et al., 2007).

In GBM, suppression of wild type TP53, or induction of mutant TP53 leads to increases in glucose consumption and lactate production, as well as decreased oxygen consumption and increased sensitivity to hypoxia-induced cell death; this is in part due to the downregulation of SCO2 (Wanka et al., 2012a). TP53 also protects GBM cells from apoptosis under low glucose and oxygen conditions by upregulation of TIGAR, leading to increased glutathione production and therefore protection from oxidative stress (Wanka et al., 2012b). Furthermore, stabilisation of normal TP53 allows the activation of apoptosis when combined with inhibition of EGFR-driven glycolysis (Mai et al., 2017).

MYC

MYC is a transcription factor that is well established as an oncogene frequently dysregulated in cancer (Stine et al., 2015). It is highly expressed in GBM tissue, and the expression levels of MYC are correlated with cell cycle progression (Engelhard et al., 1989). MYC mediates

apoptosis in TMZ-treated cells expressing MGMT through the Akt/GSK3 pathway (De Salvo et al., 2011). In a mouse model of *de novo* GBM, deletion of both PTEN and TP53 leads to MYC activation, promoting a cancerous phenotype in neural stem cells (Zheng et al., 2008). MYC also negatively regulates PTEN through upregulation of miRNA-26a (Guo et al., 2013b). MYC activity is regulated by mTORC1 through the action of S6K1 and autophagy and beclin 1 regulator 1 (AMBRA1) (Csibi et al., 2014; Cianfanelli et al., 2015). In addition, MYC is regulated by the PI3K/Akt pathway through its interaction with FOXO proteins (Peck et al., 2013), and hypoxia is known to downregulate MYC expression and protein stability (Okuyama et al., 2010).

MYC promotes glycolysis through the upregulation of the glucose transporter GLUT1 and other key glycolytic genes (Osthus et al., 2000). MYC also promotes glutaminolysis by upregulating the glutamine transporter SLC 1 member 5 (SLC1A5), and the enzyme glutaminase (GLS), which catalyses the first step in glutamine metabolism, converting glutamine into glutamte to be used in the TCA cycle (Wise et al., 2008). Recent work has indicated that MYC can also induce the expression of glutamate-ammonia ligase (GLUL) under low glutamine conditions to promote *de novo* glutamine synthesis (Bott et al., 2015). In addition, MYC promotes glutathione synthesis, through glutamine and glycine metabolism, to combat oxidative stress (Gao et al., 2009). Furthermore, MYC directly binds and initiates the transcription of a vast array of genes involved in both purine and pyrimidine biosynthesis (Liu et al., 2008), leading to an increase in the shunting of glucose into the PPP and increased TCA cycling (Morrish et al., 2009).

Using ^{13}C-labelled glucose, it has been demonstrated that MYC overexpression increases glycolytic flux in GBM through the increased expression of genes involved in glycolysis (Tateishi et al., 2016). GSK3 is a key regulator of metabolism dependent on MYC signalling. Downregulation of GSK3 results in the dissociation of HK2 from the mitochondrial membrane and mitochondrial destabilisation, as well as increases in MYC expression, both of which lead to apoptosis (Kotliarova et al., 2008). Inhibition of GSK3 sensitises GBM cells to TMZ by promoting MYC-mediated methylation of the MGMT promoter (Pyko et al., 2013). Clearly, MYC has a diverse range of functions in GBM, some of which are distinctly oncogenic, but others that

indicate a role as a tumour suppressor. More work is required to fully elucidate the mechanisms and situations in which MYC plays these different roles.

HIF1

The HIF1 pathway is activated in response to low oxygen conditions, which are often observed in solid tumours, particularly in GBM (Bar, 2011). HIF1 activity is regulated by the prolyl hydroxylase (PHD) family. HIF1 is constitutively expressed, but in the presence of oxygen, PHD proteins are able to hydroxylate proline residues on HIF1 (Bruick and McKnight, 2001). This allows von Hippel-Lindau (VHL) to bind, tagging HIF1 for degradation by the E3-ubiquitin ligase system (Koh et al., 2008). The interaction of HIF1 with PKM2 and PHD3 forms part of a positive feedback loop to promote a hypoxic phenotype (Semenza, 2011). HIF1 acts as a transcription factor that upregulates numerous genes involved in glycolysis, including GLUT1, lactate dehydrogenase A (LDHA) and PDK1 (Semenza et al., 1996; Kim et al., 2006a; Pore et al., 2006). HIF1 also promotes mitochondrial autophagy to prevent excessive ROS production through the action of BCL2-interacting protein 3 (BNIP3) (Zhang et al., 2008). These conditions allow cancer cells to maintain ATP levels and protect themselves from hypoxia-associated production of ROS, thereby preventing the activation of apoptosis (Kim et al., 2006a).

In GBM, loss of PTEN leads to increased Akt activity, which in turn stimulates HIF1 expression under hypoxic conditions (Zundel et al., 2000), thus leading to increased expression of the HIF1 targets GLUT1 and vascular endothelial growth factor (VEGF) (Pore et al., 2006). HIF1 degradation can be induced by MDM2, providing further evidence for the importance of this molecule in GBM pathopysiology, independent of its effects on TP53 (Joshi et al., 2014). Global metabolic profiling of GBM showed that hypoxia induces increases in glycolysis, the PPP and production of *R*-2-hydroxyglutarate (2HG), as well as downregulation of the TCA cycle, impaired cholesterol, glycerolipid and sphingolipid metabolism and enhanced catabolism of proteins and amino acids (Kucharzewska et al., 2015). Hypoxia also induces fatty acid uptake and lipid storage in a HIF1-dependent manner through the action of fatty acid-binding proteins (FABP) (Bensaad et al., 2014). Inhibition of the HIF1 target gene PDK1 using dichloroacetate

is able to force GBM cells into a more oxidative phenotype, leading to a G_2/M cell cycle block (Shen et al., 2015b). Dichloroacetate also synergises with radiation by blocking the radiotherapy-induced glycolytic shift, and increasing oxidative stress and DNA damage. PDK1 may induce EGFR activation, and combined inhibition of both proteins is able to block the "Warburg effect" and shift tumour metabolism to OXPHOS, inhibiting proliferation in GBM (Velpula et al., 2013).

IDH1

It is now known that metabolic enzymes themselves can also act as oncogenes and tumour suppressors. The best known example of this is that of IDH1. As shown in Fig. 1.3. mutations in IDH1, which are common in secondary GBM, lead to a gain of function whereby the enzyme produces 2HG from α-ketoglutarate (Dang et al., 2009). Accumulation of this "oncometabolite" leads to activation of mTORC1 through the direct inhibition of lysine demethylase 4A (KDM4A) (Carbonneau et al., 2016). 2HG also increases the contribution of glutamine to lipid synthesis, specifically palmitate, under hypoxic conditions (Reitman et al., 2014). 2HG can also increase the sensitivity of cancer cells to alkylating chemotherapy through the inhibition of the AlkB homolog (ALKBH) family (Wang et al., 2015b). In addition to this, IDH1 mutations in GBM lead to the downregulation of numerous HIF1 target genes, including LDHA, which affects their glycolytic capacity (Chesnelong et al., 2014). IDH1 mutations have also been linked to increased expression of genes involved in the TCA cycle and increased levels of OXPHOS, demonstrating an anti-Warburg phenotype (Khurshed et al., 2017).

Efforts have been made to utilise the production of 2HG in cancer for both imaging and disease monitoring. Early studies indicated that whilst serum 2HG was a useful marker for IDH-mutated leukaemias, it could not be used as a marker for disease monitoring in glioma (Capper et al., 2012). However, further studies have indicated that 2HG levels in urine can be indicative of IDH status (Lombardi et al., 2015; Fathi et al., 2016). There has also been great success in the detection of 2HG using MRI in patients with glioma, highlighting its potential clinical use (Elkhaled et al., 2012; Kalinina et al., 2012). Recent work has demonstrated that 2HG production can even be tracked from labelled glutamine *in vivo* (Salamanca-Cardona et

al., 2017).

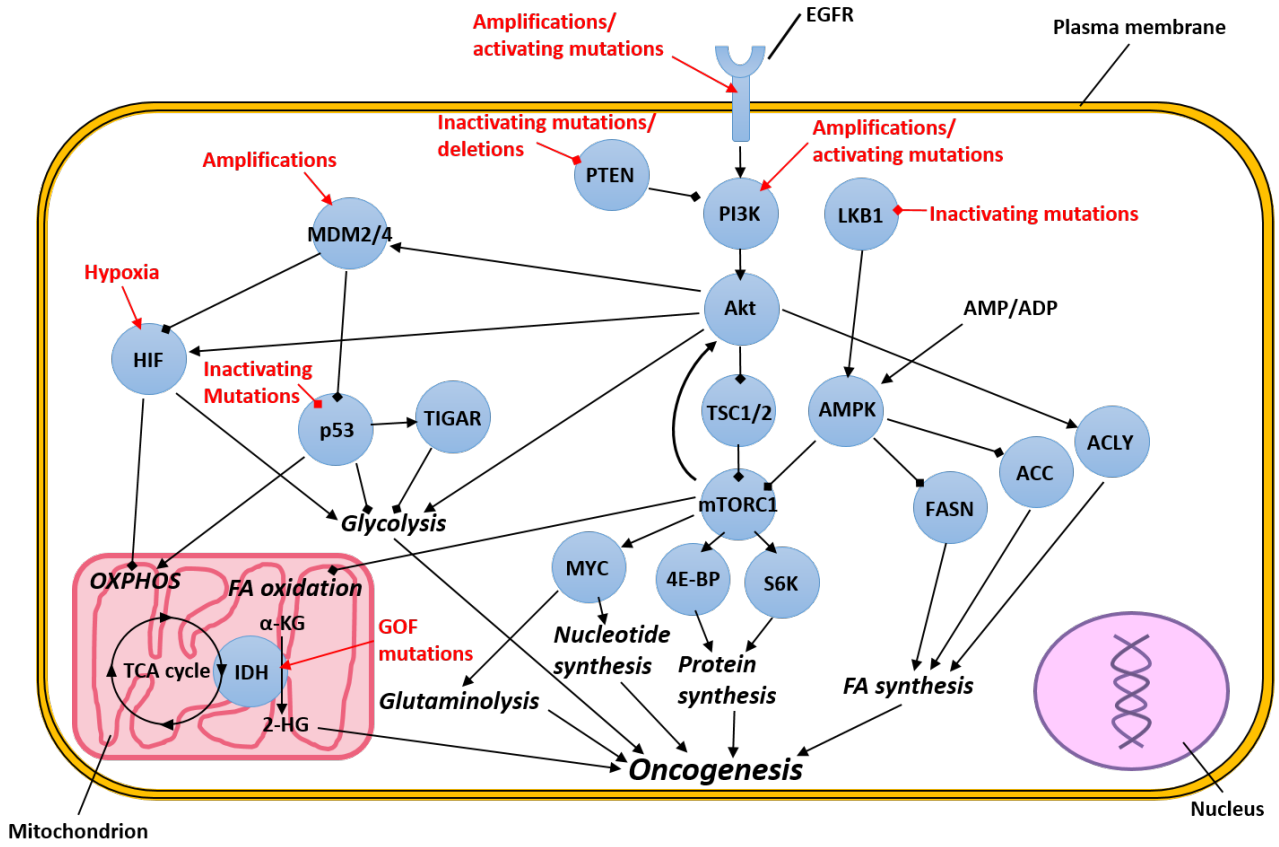


Figure 1.3: **Diagram showing major regulators of cancer cell metabolism.** Italicised writing indicates a cellular process. Molecular changes such as gain of function (GOF)/inactivating mutations, amplifications and deletions shown in red writing. Blue molecules are proteins.

1.3 NAD metabolism and biosynthesis in cancer

Drugs targeting major regulators of cancer metabolism have been proven to be effective, and are currently in use for some cancers and in clinical trials for many others. However, much of this is thought to be due to the disruption of cell signalling pathways that maintain proliferation and inhibit apoptosis; few are attributed solely to their effects on cell metabolism alone. Targeting NAD metabolism is a relatively novel concept in the field of cancer therapy. NAD acts as a cofactor in numerous metabolic reactions, and plays a major role in the regulation of the cell cycle and DNA repair. All of these are features that affect cancer survival, which makes it an attractive therapeutic target. However, there are of course reservations about interfering with such a critical metabolic pathway with regards to potential side effects. Here I will summarise

the roles of NAD in both normal and cancer cell biology, and the therapeutic potential in treating GBM.

1.3.1 NAD metabolism

NAD biosynthesis

There are a huge range of different cellular activities that are NAD-dependent. It can be used as an electron carrier to generate energy, it helps to regulate proliferation, DNA repair and cell death, and it can be adapted by phosphorylation to help combat oxidative stress. Therefore, cells must actively maintain a sufficient pool of NAD at all times. They do this through a number of different metabolic pathways. A summary of these pathways, as well as the major uses of NAD discussed previously, can be seen in Fig. 1.4. The chemical structures of the different NAD biosynthetic intermediates can be seen in Fig. 1.5.

It is generally accepted that the most important enzyme in NAD biosynthesis is NAMPT, historically referred to as PBEF or visfatin (Wang et al., 2006b). Enzymes that consume NAD, such as the aforementioned sirtuin (SIRT)s and PARPs, release Nam. As shown in Fig. 1.4, NAMPT catalyses the conversion of Nam to nicotinamide mononucleotide (NMN), which is the rate-limiting step in NAD biosynthesis (Garten et al., 2015). NAMPT is found in the cytoplasm, the nucleus and extracellularly as eNAMPT (Garten et al., 2015). It is expressed in almost every single tissue in the body, highlighting its importance in cellular homeostasis (Garten et al., 2015). The NMN generated by NAMPT can in turn be used by the nicotinamide nucleotide adenylyltransferase (NMNAT) family to synthesise NAD (Brazill et al., 2017). There are three members of the NMNAT family; NMNAT1, NMNAT2 and NMNAT3, which are located in the nucleus, the golgi apparatus and mitochondria, respectively (Ying, 2008). They facilitate the rapid regeneration of NAD in compartments known to consume it at very high rates. The constant recycling of Nam, to NMN, to NAD allows cells to maintain NAD pools to be used in metabolism, proliferation and DNA repair. In addition, the NAD generated can be converted in to NADP through the action of NAD kinase (NADK), which can the be used in other reactions, such as the PPP and fatty acid metabolism.

Whilst NAMPT and the NMNAT family are the key components of the canonical NAD

biosynthetic pathway, there are a number of other pathways that contribute to the overall NAD pool. The first of these is the nicotinate phosphoribosyltransferase (NAPRT) pathway. As shown in Fig. 1.4, NAPRT catalyses the conversion of nicotinic acid (NA) to nicotinic acid mononucleotide (NaMN) (Hara et al., 2007). NA, also known as niacin or vitamin B3, is found in numerous parts of a normal diet, including meat, fish, eggs, dairy products, certain vegetables and whole wheat (Bogan and Brenner, 2008); therefore, it is considered an important dietary source of NAD. Like NMN, NaMN can be converted to nicotinic acid adenine dinucleotide (NaAD) by members of the NMNAT family (Zhang et al., 2003). The NaAD must then undergo a final metabolic step to convert the NA group to Nam, which is catalysed by the enzyme NAD synthetase 1 (NADSYN1) (Yamaguchi et al., 2007). The conversion of NaMN to NAD via these series of reactions is known as the Preiss-Handler pathway (De Figueiredo et al., 2011).

The next pathway that feeds into NAD biosynthesis is relatively novel. It is an extracellular Nam salvage pathway that relies on the activity of the enzyme ecto-5'-nucleotidase (NT5E). NT5E, also known as CD73, is a well characterised membrane-bound enzyme that catalyses the breakdown of ATP, ADP and AMP to release adenosine, which plays a major role in immunological signalling (Allard et al., 2016b). Recent work showed that NT5E could also catalyse the breakdown of NAD to NMN, releasing AMP, and further catalyse the breakdown of NMN to nicotinamide riboside (NR) (Garavaglia et al., 2012). It is thought that extracellular NR can enter cells through equilibrative nucleoside transporter (ENT) channels (Ratajczak et al., 2016). Once in the cytoplasm, NR can be converted into NMN by members of the nicotinamide riboside kinase (NMRK) family (Sasiak and Saunders, 1996). This can be seen in Fig. 1.4. The NMN then follows the same route as the canonical NAD biosynthetic pathway, being used by the NMNAT family to synthesise NAD.

There is another NAD biosynthetic pathway that is able to feed into the Preiss-Handler pathway. This is the *de novo* NAD biosynthesis pathway, which occurs through kynurenine metabolism. This system is also reliant on a dietary precursor to NAD, the essential amino acid tryptophan (Badawy, 2017). Through a series of reactions, tryptophan is converted into quinolinic acid (QA) via kynurenine intermediates. As shown in Fig. 1.4, QA is then converted

into NaMN by the enzyme quinolinate phosphoribosyltransferase (QPRT), which enters the Preiss-Handler pathway to be used in NAD biosynthesis (De Figueiredo et al., 2011). The existence of these different NAD biosynthetic pathways shows not only how important NAD is in cellular homeostasis, but also how much redundancy there is in the system. NAD is a vital component of numerous cellular activities.

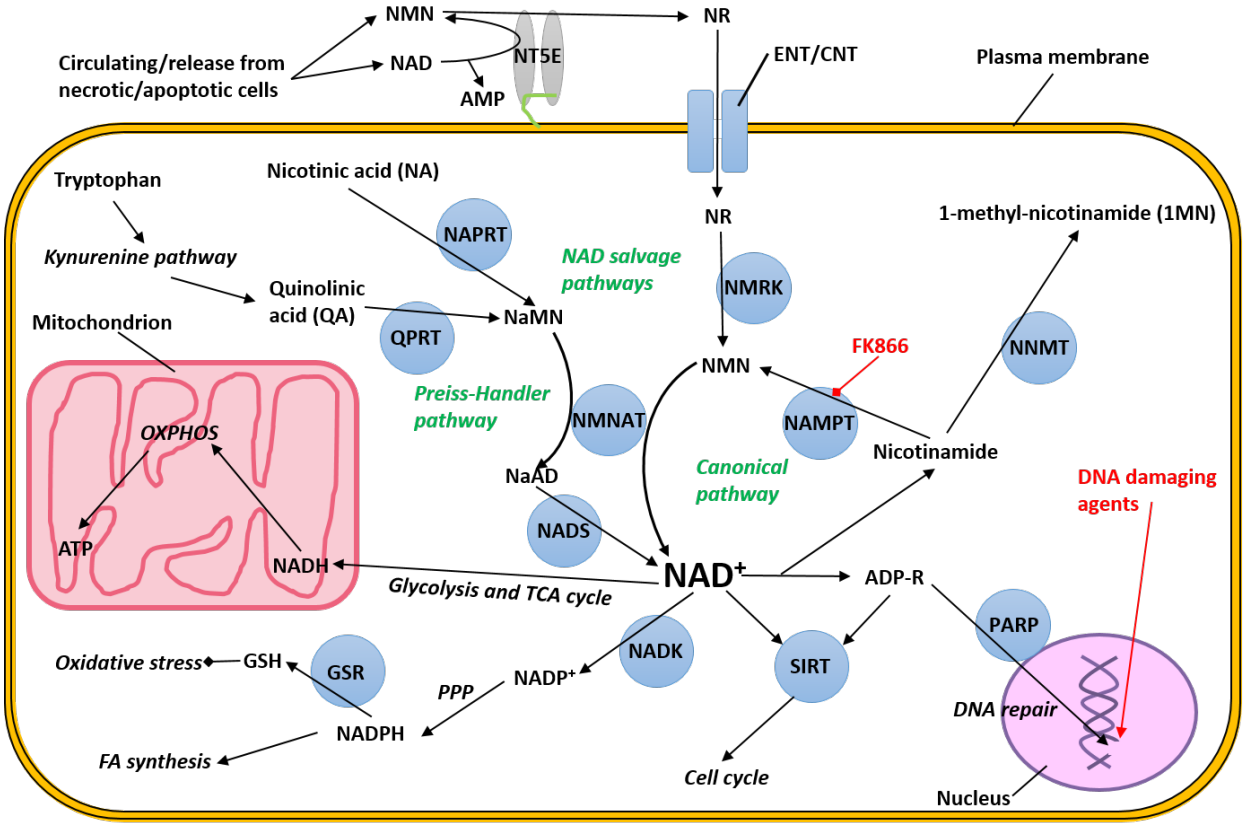


Figure 1.4: **Diagram showing NAD biosynthetic pathways and its uses in cells.** Includes the major uses of NAD in oxidative metabolism, cell cycle and DNA repair, as well as all of the unique biosynthetic pathways of NAD. Metabolites seen in black writing. Italicised green writing highlights the different NAD biosynthetic pathways. Italicised black writing indicates a cellular process. Chemotherapeutics shown in red writing. Blue molecules are proteins.

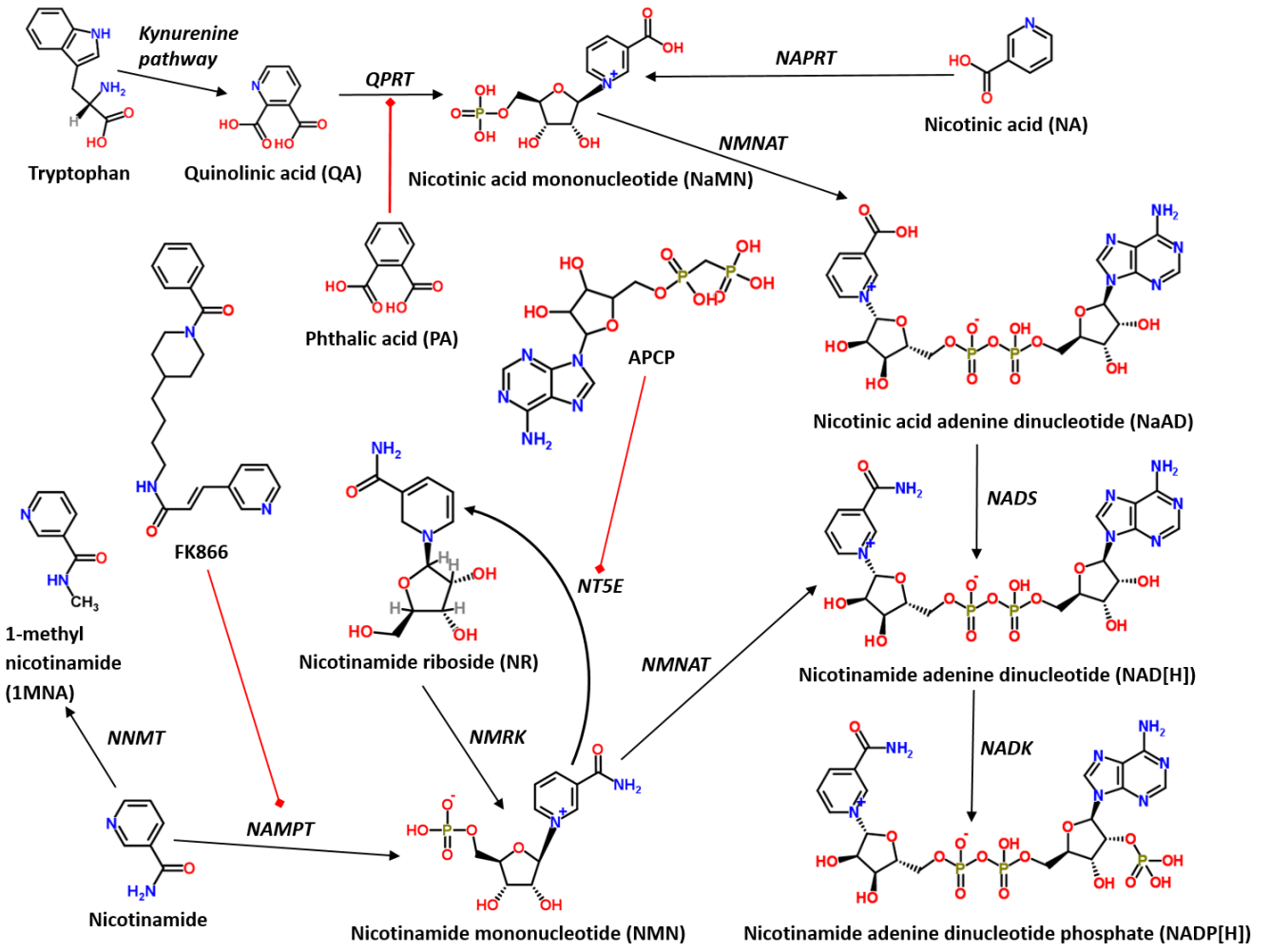


Figure 1.5: **Diagram showing the chemical structures of different NAD metabolites, and inhibitors of some of the enzymes involved in NAD biosynthesis.** Includes metabolites in all of the NAD biosynthetic pathways, as well as the inhibitors of NAMPT, NT5E and QPRT. Chemical structures obtained from Royal Society of Chemistry, 2018.

NAD in glycolysis, OXPHOS and fatty acid metabolism

NAD and its phosphorylated counterpart NADP are important cofactors in a huge range of different metabolic reactions, including glycolysis, the TCA cycle, the PPP and of course, OXPHOS. It is well established that the total conversion of one molecule of glucose into energy yields 36 molecules of ATP (Campbell et al., 2008). NAD plays a key role in the translation of the series of reactions required to generate this energy. The breakdown of fructose-1,6,bisphosphate generates two molecules of glyceraldehyde-3-phosphate, through the actions of aldolase and triosephosphate isomerase (TPI) (Campbell et al., 2008). NAD acts as a cofactor in the conversion of each of these molecules of glyceraldehyde-3-phosphate into 1,3-

bisphosphoglycerate, producing two molecules of NADH (Campbell et al., 2008). Subsequent metabolic reactions result in the production of four molecules of ATP, and the release of two molecules of pyruvate (Campbell et al., 2008). In normal cells, the pyruvate is then converted into ACoA by PDH and is transported into the mitochondrial matrix to be used in the TCA cycle (Campbell et al., 2008). As each molecule of pyruvate passes through the TCA cycle, four more molecules of NADH are generated, as well as one molecule of $FADH_2$ (Campbell et al., 2008). Whilst the NADH generated by glycolysis can pass through the outer mitochondrial membrane into the intermembrane space, it cannot cross the inner mitochondrial membrane directly (Houtkooper et al., 2010). A series of reactions involving the malate/aspartate shuttle system allows the NADH in the mitochondrial intermembrane space to be converted into NADH in the mitochondrial matrix, to be used in OXPHOS (Kane, 2014).

Whilst it is generally accepted that fatty acid synthesis is the primary metabolic pathway in cancer, studies have indicated that some cancer types utilise β-oxidation of fatty acids to supplement energy production. Triglycerides are broken down into fatty acids by hydrolases, and the fatty acids are then transported into the mitochondria (Carracedo et al., 2013). β-oxidation produces NADH and $FADH_2$ to be used in OXPHOS, and ACoA, which can enter the TCA cycle to generate further reducing agents. This phenotype has been observed most clearly in breast cancer (Carracedo et al., 2012).

The accumulation of NADH in the mitochondrial matrix is used to fuel the primary energy-producing system in normal cells, OXPHOS. NADH dehydrogenase (ubiquinone) (NDU), also known as complex I, passes electrons from NADH to flavin mononucleotide (FMN), releasing NAD (Campbell et al., 2008). Electrons are passed along the electron transport chain (ETC) from both NDU and succinate dehydrogenase (SDH) (complex II) through coenzyme Q-cytochrome *c* reductase (CQ-CCR) (complex III) to cytochrome *c* oxidase (CCO) (complex IV) (Campbell et al., 2008). They use this energy to transport protons out of the mitochondrial matrix and into the intermembrane space, and the resulting proton gradient drives ATP production as protons move back through ATP synthase (Campbell et al., 2008). This system is the basis of energy production in all eukaryotes, but it could not function without NAD acting as a carrier molecule from one set of reactions to the next.

NADP in redox balance and nucleotide synthesis

Whilst NAD is a vital part of aerobic respiration, it's phosphorylated form, NADP, and its corresponding reduced form NADPH, are required in different metabolic pathways. NADP is generated from NAD by the action of NADK (Nikiforov et al., 2015). NADPH is generated in the mitochondria through a few major metabolic reactions. The transhydrogenase reaction allows the production of NADPH from NADH by nicotinamide nucleotide transhydrogenase (NNT) (Rydström, 2006). Certain enzymes of the TCA cycle can utilise NADP to produce NADPH, including IDH and malic enzyme (ME) (Smolková and Ježek, 2012). These reactions contribute to the accumulation of NADPH in the mitochondria, which is particularly important in combating oxidative stress. The enzyme glutathione reductase (GR) uses NADPH to synthesise glutathione from glutathione disulfide (Ying, 2008). The glutathione can then be used by enzymes such as glutathione peroxidase (GP) and glutathione S-transferases (GST) to combat oxidative stress. Furthermore, NADPH is used as an oxidising agent in the thioredoxin system, which detoxifies hydrogen peroxide into water, and it can even bind and activate catalase (CAT) directly, another enzyme that detoxifies hydrogen peroxide (Ying, 2008). This makes NADPH a major factor in combating oxidative stress, which is particularly important in highly proliferative cells.

NADP also plays a major role in nucleotide synthesis through the PPP. The enzyme G6PD catalyses the conversion of glucose-6-phosphate to 6-phosphogluconate, and simultaneously uses NADP to generate NADPH (Wamelink et al., 2008). In a second reaction, phosphogluconate dehydrogenase (PGD) catalyses the conversion of 6-phosphogluconate to ribulose-5-phosphate, generating another molecule of NADPH (Wamelink et al., 2008). The ribulose-5-phosphate can be converted into ribose-5-phosphate to be used in nucleotide synthesis, but the NADPH feeds other major metabolic pathways in the cytosol, particularly fatty acid synthesis (Wamelink et al., 2008). Numerous enzymes involved in the synthesis of different fatty acids require either NADH or NADPH to function. Some enzymes, including the β-ketoacyl and enoyl reductases, show a high degree of specificity for NADPH, reinforcing the importance of this molecule in fatty acid synthesis (Wakil et al., 1983).

As described previously, all of these metabolic pathways are able to support cancer growth

in some way. Furthermore, NAD is required for proper mitochondrial function, which allows cancer cells to utilise glutamine and fatty acids to fuel the TCA cycle, maintain glycolysis through HK2 expression, and maintain proper redox balance to prevent DNA damage and apoptosis (Solaini et al., 2011).

1.3.2 Sirtuins

In addition to its roles in metabolism, NAD also acts as a substrate for reactions that control numerous cellular activities, particularly with regards to the cell cycle. It does this through its interaction with the SIRT family of proteins. SIRTs are thought to play a major role in longevity, and are often dysregulated in cancer (Wątroba et al., 2017). They are HDAC enzymes that regulate gene transcription by removing acetyl groups from lysine amino acids on histones bound to DNA (Yamamoto et al., 2007). There are seven SIRTs, each of which has been shown to have unique, distinct roles (Table 1.1). Generally speaking, the removal of acetyl groups from histones results in them more tightly binding DNA, and prevent the access of the DNA transcription machinery (Yamamoto et al., 2007). This effectively suppresses gene expression at that specific point. However, whilst histones are generally considered to be the primary targets of SIRTs, there is also evidence to suggest that some act directly on other proteins. These include major transcriptional regulators with known roles in cancer, such as TP53, nuclear factor kappa B (NF-$\varkappa$B), PGC1α and the FOXO family, as well as metabolic enzymes such as PDH (Yamamoto et al., 2007). In addition to their well established deacetylase activity, two SIRTs have ADP-ribosylation activity; these are SIRT4 and SIRT6 (Yamamoto et al., 2007). Indeed, SIRT4 exclusively exhibits ADP-ribosylation activity. These SIRTs catalyse the attachment of ADP-ribose to proteins, which can either activate or inhibit them depending on the target in question (Yamamoto et al., 2007). Both the deacetylase and ADP-ribosylation activities of SIRTs depend on NAD. During the removal of acetyl groups from histones or other proteins, NAD undergoes hydrolysis to produce O-acetyl-ADP-ribose (Yamamoto et al., 2007). SIRT4/6 catalyse the removal of the ADP-ribose motif on NAD and facilitate its binding to proteins, normally on to lysine residues (Dang, 2014). Both of these reactions release Nam, which can be recycled to form NAD again. SIRTs have a huge range of activities, and can

function as either oncogenes or tumour suppressor genes.

SIRT1 deacetylates multiple histone residues (Table 1.1), many of which are related to genomic stability and cellular longevity (Wątroba et al., 2017). SIRT1 also regulates TP53 activity through its interactions with HDAC1 (Vaziri et al., 2001; Yang et al., 2015b). Deacetylation of the mitochondrial regulator PGC1α by SIRT1 increases its activity and leads to increased oxygen consumption (Nemoto et al., 2005). Activation of AMPK enhances SIRT1 activity by increasing NAD availability, leading to deacetylation of PGC1α and activation of genes involved in energy production (Cantó et al., 2013). The oncogenic roles of SIRT1 are linked to its established inhibitory effects on the tumour suppressor genes TP53 and E2F transcription factor (E2F)1 (Luo et al., 2001; Wang et al., 2006a). In glioma cells, knockdown of SIRT1 inhibits proliferation and induces apoptosis via the PI3K/Akt pathway, supporting its role as an oncogene (Qu et al., 2012). SIRT2 has many similar targets to SIRT1, such as PGC1α, NF-ϰB and FOXO1 (Dang, 2014). Both SIRT1 and SIRT2 have been shown to deacetylate S6K1, which promotes mTORC1-dependent phosphorylation of S6K1 and activation of downstream genes involved in protein synthesis and cell survival (Hong et al., 2014b). SIRT2 is important in the regulation of the cell cycle, with its activity peaking in G_2/M (Dryden et al., 2003; Vaquero et al., 2006). SIRT2 regulates the activity of the anaphase-promoting complex/cyclosome (APC/C) through deacetylation of fizzy and cell division cycle 20 related 1 (FZR1) and cell division cycle (CDC)20, coordinating normal cell cycle progression (Kim et al., 2011). SIRT2 is significantly upregulated in GBM compared to normal healthy brain tissue, and nuclear staining of SIRT2 positively correlates with tumour grade (Imaoka et al., 2012). In C6 glioma cells, inhibition or knockdown of SIRT2 leads to caspase-mediated apoptosis and necrosis (He et al., 2012). SIRT3 is particularly important in the regulation of cell metabolism, as it regulates numerous enzymes involved in glycolysis, the TCA cycle, and redox balance (Table 1.1). SIRT3 also regulates the urea cycle and fatty acid oxidation through its deacetylation and activation of ornithine carbamoyltransferase (OTC) (Hallows et al., 2011). SIRT4 is the only SIRT that solely displays ADP-ribosylation activity. SIRT4 suppresses PDH through its lipoamidase activity, also reducing the flux of pyruvate into the TCA cycle (Mathias et al., 2014). In addition, SIRT4 suppresses GDH, which blocks the entry of glutamine in to the TCA

cycle (Haigis et al., 2006). SIRT5 is able to act not only as a deacetylase, but also as a demalonylase and desuccinylase (Mei et al., 2016). The first major target of SIRT5 was reported to be carbamoyl-phosphate synthase 1 (CPS1), which is a major component of the urea cycle relating to arginine metabolism (Nakagawa et al., 2009). The desuccinylation activity of SIRT5 has been implicated in a variety of metabolic pathways, including the TCA cycle, mitochondrial metabolism, and both amino acid and fatty acid metabolism (Park et al., 2013). Some studies have also demonstrated that SIRT5 can regulate glycolysis through demalonylation and suppression of of GAPDH activity (Nishida et al., 2015). SIRT6 is the only SIRT that displays both deacetylase and ADP-ribosylation activities. Loss of SIRT6 promotes glycolysis, MYC activation and a tumourigenic phenotype in cancer cells (Sebastián et al., 2012). In GBM, SIRT6 suppresses proliferation and induces apoptosis via nuclear translocation of apoptosis-inducing factor (AIF), whilst simultaneously inhibiting the janus kinase (JAK)2/signal transducer and activator of transcription (STAT)3 signalling pathway and reducing oxidative stress (Feng et al., 2016b). Finally, SIRT7 is poorly understood, but studies have indicated that its most important activity lies in its positive regulation of RNA polymerase I (Ford et al., 2006).

Sirtuin (location)	**Activity**	**Histone modifications**	**Other targets**	**Functions affected**
SIRT1 (Nucleus)	Deacetylase	H4K16dac, H3K9dac, H1K26dac, H3K14dac, HK16dac, H3K56dac, H3K79me3a, H3K27me3	HDAC1, TP53, PGC1α, MYC, NF-ϰB, RB, FOXO1, FOXO3, FOXO4, PI3K, AKT, HIF1α, E2F1, PPARα, PPARγ, SREBF1, SREBF2, LXR, S6K1, PARP1	Cell cycle, proliferation, apoptosis, mitochondrial regulation, metabolism
SIRT2 (Cytoplasm)	Deacetylase	H3K56dac, H4K16dac, H4K20me1	PGC1α, NF-ϰB, FOXO1, FOXO3, α-tubulin, G6PD, ACLY, HIF1α, S6K1, FZR1, CDC20, CDK9	Mitosis, OXPHOS, DNA repair
SIRT3 (Mitochondria)	Deacetylase	H4K16dac	ACSS2, IDH2, SOD2, PDH, FOXO3, OTC, ACADL	TCA cycle, OXPHOS, oxidative stress, fatty acid oxidation
SIRT4 (Mitochondria)	ADP-ribosylation	N/A	PDH, GDH, SLC25A5, MCD	TCA cycle, fatty acid oxidation
SIRT5 (Mitochondria)	Deacetylase, deacylase	N/A	CPS1, PDH, SDH, PKM2, GAPDH, SOD1	Urea cycle, glycolysis, gluconeogenesis
SIRT6 (Nucleus)	Deacetylase, deacylase, ADP-ribosylation	H3K9dac, H3K56dac	NF-ϰB, TNF, MYC, FOXO3, SREBP2, PARP1	Proliferation, DNA repair
SIRT7 (Nucleolus)	Deacetylase	H3K18dac	RNApolI, TP53, MYC, HIF1α, HIF2α,	rDNA transcription

Table 1.1: **Table summarising the different sirtuins and their roles in cellular function**. Table adapted from (Yamamoto et al., 2007; Dang, 2014; Chalkiadaki and Guarente, 2015; Wątroba et al., 2017; Blank and Grummt, 2017)

.

1.3.3 PARPs

Last, but by no means least, are the roles of NAD in DNA repair. Over the course of a lifetime, DNA damage can occur in any cells in the human body, from either endogenous or exogenous sources (Ciccia and Elledge, 2010). Without sufficient DNA repair, this damage would either lead to cell death and consequent organ failure, or mutations and the beginning of tumourigenesis. However, cells have a vast array of different mechanisms to deal with DNA damage. The area I want to focus on is PARP-mediated DNA repair. The PARP family consists of 18 members, but only three of them are involved in DNA repair; PARP1, PARP2 and PARP3 (Morales et al., 2014). Many of the other members of the PARP family are poorly characterised ($<$ 20 articles, (NCBI, 2018), and will not be discussed here. PARP1 and PARP2 show a high degree of similarity, and both are activated by SSB and DSB in DNA. However, most of the work carried out regarding the roles of PARPs in DNA repair concern PARP1.

PARP1

As previously described, upon recognition of DNA damage, PARP1 catalyses PARylation of itself and other targets such as histones H1 and H2B, resulting in chromatin remodelling to allow access for the DNA repair machinery (Ciccia and Elledge, 2010). For SSB, this leads to the recruitment of the DNA repair protein XRCC1, a critical component of the BER repair machinery (Morales et al., 2014). XRCC1 recruits APE1, polynucleotide kinase 3'-phosphatase (PNKP), aprataxin (APTX) and LIG3, and the coordinated response of these enzymes results in the repair of the SSB (Caldecott, 2008). When XRCC1 binds to the SSB, PARP1 is released, and PAR chains are rapidly removed by poly (ADP-ribose) glycohydrolase (PARG) (Caldecott, 2008). This reactivates PARP1, and allows it to recognise further DNA damage. PARP1 is also able to recognise DSBs in DNA. Whilst these are rare in comparison to SSBs, they are far more damaging, and mammalian cells have a highly complex network of repair mechanisms in place to ensure their rapid and efficient repair (Ciccia and Elledge, 2010). One of these mechanisms is non-homologous end joining (NHEJ). This is initiated by XRCC5, which recruits DNA-dependent protein kinase, catalytic subunit (DNA-PKcs), and in turn recruits other proteins that catalyse the ligation of DSBs (Ciccia and Elledge, 2010). Whilst PARP1 is not directly

involved in this mechanism, it can initiate an alternative version of NHEJ. PARP1 can bind to DSBs and recruit the MRE11-RAD50-NBM (MRN) complex, a vital component of many DSB repair pathways (Ciccia and Elledge, 2010). This leads to the recruitment of XRCC1, which initiates something akin to SSB repair (Beck et al., 2014b). PARP1 is also important in the initiation of another form of DSB repair, homologous recombination (HR). This occurs during the S/G_2 phase of the cell cycle, where the sister chromatids can be used to mediate DNA repair (Ciccia and Elledge, 2010). HR is also initiated by the recruitment of the MRN complex, but results in a different cascade of DNA repair events. MRN recruits and activates ATM serine/threonine kinase (ATM), which coordinates the interaction of BRCA, DNA repair associated (BRCA)1 and RB-binding protein 8, endonuclease (RBBP8) with one of the many different available repair pathways (Beck et al., 2014b). HR is particularly important in instances where unrepaired SSBs lead to stalled or collapsed replication forks and result in DSBs (Beck et al., 2014b). PARP1 is known to interact with other NAD-consuming enzymes, including members of the SIRT family. PARP1 and SIRT1 share many targets, including histones, components of the DNA damage response network, cell death proteins, and key transcription factors, such as TP53, MYC and NF-$\varkappa$B (Luna et al., 2013). In addition, c-Jun N-terminal kinase (JNK) phosphorylates SIRT6, which in turn activates PARP1 to stimulate the repair of DNA damage (Mao et al., 2011; Van Meter et al., 2016). This highlights the interplay between different molecules and systems that require NAD to function.

PARP2

In addition to the well-established roles of PARP1 in DNA repair, there is clear evidence for the role of PARP2. PARP2 is also able to bind damaged DNA and initiate BER (Kutuzov et al., 2015). In addition, recent work has demonstrated that, like PARP1, PARP2 is able to initiate the recruitment of XRCC1 in the repair of SSBs (Hanzlikova et al., 2017). PARP2 is also important in recognition of gaps and flap structures in DNA, which require more advanced repair intermediates (Kutuzov et al., 2013). Early work indicated that PARP2 interacts with kinetochore proteins, including centromere protein (CENP)A/B to maintain proper kinetochore function and chromatid separation during mitosis (Saxena et al., 2002). In addition, PARP2

has been shown to interact with telomeric repeat-binding factor 2 (TRF2), a key regulator of telomere integrity (Dantzer et al., 2004). The DNA binding and enzymatic activity of PARP2 is suppressed by the histone acetyltransferases lysine acetyltransferase 2 (KAT2)A/B (Haenni et al., 2008). Furthermore, PARP2 has been shown to suppress SIRT1 expression through interaction with the SIRT1 gene promoter (Bai et al., 2011), reinforcing the roles of these two classes of NAD-consuming enzymes in the regulation of cellular activity. Interestingly, PARP2 has been implicated in the regulation of genes involved in the cell cycle, independent of its PARylation activity (Liang et al., 2013). It does this by recruitment of HDAC5, HDAC7 and euchromatic histone lysine methyltransferase 2 (EHMT2) to the promoters of genes such as MYC, RB and E2F1.

PARP3

The last PARP with a clear role in DNA repair is PARP3. Early work demonstrated that PARP3 localised preferentially to the daughter centriole during mitosis, and it was shown to interfere with the progression from G_1 to S phase during the cell cycle (Augustin, 2003). PARP3 associates with polycomb group bodies, as well as many other proteins involved in the DNA damage response, including PARP1 (Rouleau et al., 2007). In addition, PARP3 is able to activate PARP1 in the absence of DNA damage (Loseva et al., 2010). PARP3 is also activated by DSBs, and facilitates the accumulation of aprataxin and PNKP like factor (APLF) to promote the recruitment of the XRCC4/DNA ligase IV complex and initiate NHEJ (Rulten et al., 2011). Furthermore, activation of APLF by ATM is dependent on PARP3 (Fenton et al., 2013). PARP3 may play a role in regulating the balance between different mechanisms of DSB repair, including NHEJ and HR (Beck et al., 2014a).

PARPs and DNA repair in cancer

Proper DNA repair is required not only to maintain cancer cell viability, but also to repair DNA damage caused by treatments meant to kill them, including chemotherapy and radiation. Multiple studies have indicated that genetic polymorphisms in PARP1 can increase susceptibility to GBM (Liu et al., 2009a; McKean-Cowdin et al., 2009; Yosunkaya et al., 2010; Wang

et al., 2016b; Liu and Jiang, 2017). The expression of PARP1 is higher in GBM compared to control samples (Galia et al., 2012). Further studies have shown that PARP1 expression is associated with the classical subtype of GBM, and in this group high expression of PARP1 is associated with shorter survival times (Murnyák et al., 2017). Whilst there has been little work on the role of PARP2 in GBM, it has been demonstrated that PARP3 promotes proliferation and radioresistance through activation of FOXM1 (Quan et al., 2015). PARP inhibitors are approved for use in BRCA-deficient cancers, which show unique hypersensitivity to this class of chemotherapy, particularly ovarian cancer (Ohmoto and Yachida, 2017). Inhibition of PARP using NU1025 has been reported to sensitise GBM cells with high levels of EGFR activity to radiation (Nitta et al., 2010). The combination of the PARP inhibitor PJ34 and the EGFR inhibitor erlotinib more effectively block tumour growth *in vivo* when compared to either treatment alone (Majuelos-Melguizo et al., 2015). Furthermore, in PTEN-mutated GBM cells, PARP inhibition leads to severe genomic instability, mitotic collapse and cell death. In GSCs, DNA damage response genes such as PARP1 are upregulated, and the combined inhibition of PARP and ATR serine/threonine kinase (ATR) sensitises cells to radiation (Ahmed et al., 2015). Alkylating agents such as TMZ cause DNA damage that must be repaired for a cell to survive, otherwise they will enter apoptosis and die. The addition of the pan-PARP inhibitor 3-aminobenzamide to TMZ further increases its growth inhibitory effects in GBM cells in a TP53-independent manner, but with a greater effect in MMR-deficient cells (Tentori et al., 2002). These results were replicated *in vivo* using the PARP inhibitor INO-1001 (Cheng, 2005). The PARP inhibitor ABT-888 (also known as veliparib) sensitises GBM cells to combined TMZ and radiation in both $MGMT^-$ and $MGMT^+$ cell lines (Barazzuol et al., 2013). However, the results with combined TMZ/PARP inhibitor therapy could not be replicated in TMZ-resistant GBM cell lines *in vivo* (Gupta et al., 2014). More recently, it was reported that IDH1 mutant GBM cells are highly sensitive to PARP inhibitors. Due to their low levels of NAD, likely as a consequence of NAPRT suppression by 2HG, treatment of IDH1-mutated cells with olaparib sensitises them to TMZ (Lu et al., 2017).

1.3.4 Targeting NAD biosynthesis in cancer

NAMPT

To target NAD metabolism therapeutically, the most logical place to start is at the rate-limiting step in NAD biosynthesis, the enzyme NAMPT. NAMPT was relatively poorly studied in cancer, but came to light at the turn of the 21st century, with the discovery of the highly specific NAMPT inhibitor FK866 (also known as APO866 and daporinad) (Hasmann and Schemainda, 2003). FK866 is a highly specific, non-competitive inhibitor of NAMPT. It binds across the NA/NMN binding site, but also interacts with other parts of NAMPT, resulting in the inhibition of its enzymatic activities (Kim et al., 2006b). The structure of FK866 can be seen in Fig. 1.5. Inhibition of NAMPT using FK866 leads to a gradual reduction in NAD levels and eventually apoptosis in cancer cells. Whilst it does not affect mitochondrial respiration, it specifically affects cancer cells because of their high rate of NAD consumption by enzymes such as the SIRTs and PARPs. After the initial discovery of FK866, other papers began to emerge on the effects of NAMPT inhibitors in cancer. FK866 was demonstrated to limit tumour growth and increase radiosensitivity in a mouse model of breast cancer (Muruganandham et al., 2005). FK866 was also reported to synergise with antimetabolites and intercalating agents in leukaemia cells (Pogrebniak et al., 2006), as well as inducing autophagy in neuroblastoma cells (Billington et al., 2008). FK866 was reported to be highly effective in a panel of hematological cancer cell lines, but showed little to no effect on normal hematopoietic progenitor cells (Nahimana et al., 2009). It was shown to cause NAD depletion leading to a loss of ATP levels linked to mitochondrial dysfunction, caspase-mediated apoptosis, autophagy and eventually cell death. Furthermore, FK866 was able to limit tumour growth *in vivo*. FK866 was shown to synergise with TNF-related apoptosis-inducing ligand (TRAIL) targeted therapy by triggering autophagy-mediated cell death in leukaemia (Zoppoli et al., 2010). It has been demonstrated that FK866 specifically depletes cytosolic NAD, but not mitochondrial NAD, indicating that its effects are not dependent on changes in OXPHOS (Pittelli et al., 2010). Furthermore, depletion of NAD following treatment with FK866 was shown to be dependent on the activity of PARP2 rather than SIRTs. In parallel to the work on NAMPT inhibitors in cancer, more work on NAMPT itself began to emerge. Hypoxia was shown to induce the expression of NAMPT

in breast cancer cells through the action of HIF1 (Bae et al., 2006). Furthermore, knockdown of either NAMPT or NMNAT1 alters the HDAC activity of SIRT1 at specific promoter regions (Zhang et al., 2009).

Another NAMPT inhibitor, GMX1778 (also known as CHS828), was first shown to have anti-tumour activity both *in vitro* and *in vivo* in 1999 (Hjarnaa et al., 1999). Further studies went on to demonstrate its effectiveness as a chemotherapeutic agent (Martinsson et al., 2001b; Martinsson et al., 2001a; Martinsson et al., 2002; Hovstadius et al., 2002; Svensson et al., 2002), and even went so far as phase I clinical trials (Hovstadius et al., 2002; Ravaud et al., 2005). It has been reported that GMX1778 achieves this through suppression of NF-κB activity (Olsen et al., 2004; Hassan et al., 2006). However, its function as a NAMPT inhibitor was not revealed until 2008. GMX1778 has been demonstrated to deplete both NAD and NADH levels by inhibiting NAMPT, which may be reversed with the addition of Nam, in small cell lung cancer cells (Olesen et al., 2008). Further development of GMX1778 led to the discovery of a soluble prodrug version with better pharmacokinetic properties, GMX1777 (Binderup et al., 2005). Administration of GMX1777 showed that whilst individual injections of the drug did not suppress tumour growth, continuous infusion effectively reduced tumour burden in mouse models of lymphoma, lung and colon cancer (Beauparlant et al., 2009). Combination therapy using GMX1777 and radiation in head and neck cancer showed considerable synergism, linked to a loss of PARP activity (Kato et al., 2010).

By 2010, a huge amount of interest was developing in NAD metabolism, NAMPT and its inhibitors in cancer. It is now known that NAMPT is overexpressed in numerous cancers, including GBM, ovarian, prostate, gastric, breast, leukaemia, colorectal, thyroid, pancreatic and melanoma (Reddy et al., 2008; Shackelford et al., 2010; Patel et al., 2010; Wang et al., 2011; Bi et al., 2011; Lee et al., 2011; Dan et al., 2012; Zhang et al., 2013; Shackelford et al., 2013; Maldi et al., 2013; Sawicka-Gutaj et al., 2015; Ju et al., 2016). Elevated NAMPT is associated with poor prognosis in GBM, melanoma, breast and lung cancer (Reddy et al., 2008; Lee et al., 2011; Zhou et al., 2014; Hung et al., 2016; Zhu et al., 2016; Zhao et al., 2017b). In addition, studies have reported that genetic variants in NAMPT are associated with increased risk of bladder and oesophageal cancer, although the exact mechanism is unknown (Zhang et al., 2014b; Zhang et

al., 2015). Mutations in NAMPT also lead to resistance to inhibitors of the enzyme, although there is little evidence to suggest that this is a common occurence in cancer (Olesen et al., 2010a). NAMPT has even been proposed to be used as a circulating biomarker for prognosis in cancer. Serum NAMPT is linked to higher grades in brain tumours, with the greatest amounts seen in patients with GBM (Reddy et al., 2008). In patients with endometrial cancer, NAMPT in serum is much higher compared to healthy controls, and is significantly correlated with tissue levels (Tian et al., 2013). Furthermore, NAMPT-negative patients have significantly longer survival times. NAMPT is also higher in the serum of patients with CLL compared to healthy controls, and its release from CLL cells is triggered by stimulation of B cell receptor (BCR), toll-like receptor (TLR)9, CD38 and CD40 (Audrito et al., 2015). Furthermore, serum NAMPT is associated with poor prognosis, including shorter survival times, in patients with hepatocellular carcinoma (Sun et al., 2017; Tsai et al., 2017). However, despite clear evidence of upregulation of NAMPT in colorectal cancer tissue and a possible link to tumour stage (Lv et al., 2015; Yang et al., 2016), serum levels have been reported to either be the same or even lower than healthy controls, suggesting that serum NAMPT can only be used as a biomarker in some types of cancer (Neubauer et al., 2015; Fazeli et al., 2016). Testing the tumour tissue itself is the only way to be sure of an accurate measurement of NAMPT status.

NAMPT affects a huge range of activities in different types of cancer, most of which are directly related to NAD biosynthesis. In prostate cancer, NAMPT increases proliferation through activation of mitogen-activated protein kinase (MAPK) pathways, such as MAPK14 (Patel et al., 2010). FK866 inhibits migration and invasion in prostate cancer cells, as well as blocking tumour growth *in vivo* (Wang et al., 2011). Furthermore, FK866 sensitises cells to oxidative stress by suppressing the expression of FOXO3, leading to a reduction in the expression of antioxidative genes CAT and SOD2 (Wang et al., 2011). In addition to the suppression of CAT expression, FK866 suppresses the expression of another antioxidant enzyme, glutaredoxin (GLRX), as well as the DNA damage-associated proteins proliferating cell nuclear antigen (PCNA) and PARP1 (Xu et al., 2017). FK866 also reduces fatty acid synthesis by activating AMPK leading to phosphorylation and therefore inhibition of ACC (Bowlby et al., 2012). This is specifically linked to the loss of SIRT1 and SIRT3 activity. In addition, NAMPT is

coexpressed with SIRT2, and inhibition of either limits proliferation and induces apoptosis, potentially through a block in Akt/β-catenin signalling (Dan et al., 2012). In pancreatic cancer, both FK866 and small interfering RNA (siRNA)-mediated inhibition of NAMPT block cell growth and survival by limiting the "Warburg effect" and disrupting mitochondrial function, leading to a loss of ATP production (Chini et al., 2014). This effect was also linked to increased AMPK activation, but completely independent of SIRT1 or PARP1 activity. The combination of FK866 and irradiation is more effective than either alone when applied to prostate cancer cells both *in vitro* and *in vivo* (Zerp et al., 2014).

Combined treatment with FK866 and the PARP inhibitor olaparib more effectively inhibits the growth of breast cancer and Ewing sarcoma cells compared to either agent alone (Bajrami et al., 2012; Heske et al., 2017). NAMPT stimulates the expression of notch 1 (NOTCH1) in breast cancer cells, leading to activation of NF-ϰB signalling, and inhibition of either NAMPT or NOTCH1 causes a decrease in cell growth both *in vitro* and *in vivo* (Park et al., 2014). Knockdown of NAMPT in breast cancer cells leads to increases in integrin expression and interactions with extracellular matrix proteins, indicating an increase in metastatic capabilities (Santidrian et al., 2014). Exposure of breast and colorectal cancer cells to eNAMPT leads to EMT, independent of its enzymatic activity, but dependent on transforming growth factor beta (TGFβ) signalling and PI3K/Akt-mediated nuclear translocation of snail family transcriptional repressor (SNAI)1 (Soncini et al., 2014; Yang et al., 2016). Introduction of eNAMPT to breast cancer cells has also been shown to increase cell viability and metastatic capabilities both *in vitro* and *in vivo* (Hung et al., 2016). Further to this, eNAMPT can promote proliferation in breast cancer cells by increasing intracellular SIRT1 activity, leading to the deacetylation and inactivation of TP53 (Behrouzfar et al., 2017). NAD levels are much higher in BRCA-mutated breast cancers, and NAMPT expression increases NAD levels and can promote PARP1 activity (Li et al., 2014a). This link between BRCA activity and NAD metabolism has also been established in ovarian cancer (Li et al., 2014b). The expression of NAMPT in breast cancer cells promotes resistance to glucose deprivation by increasing the production of NADPH, maintaining glutathione-mediated detoxification of mitochondrial ROS (Hong et al., 2015b). Increases in the activity of both the PI3K/Akt and MAPK pathways determine this response (Gholinejad

et al., 2017). This has also been demonstrated in endometrial cancer cells, where it leads to the upregulation of MYC and cyclin D1 (CCND1) (Wang et al., 2016d). In multiple myeloma, FK866 induces autophagy-mediated cell death via both PI3K/Akt/mTORC1-dependent and -independent mechanisms (Cea et al., 2012). NAMPT is part of a unique postitive feedback loop, whereby MYC activation leads to increased NAMPT and SIRT1 expression, significantly increasing SIRT1 activity, which in turn increases MYC activation (Menssen et al., 2012). Inhibition of NAMPT may induce autophagy and cell death via TP73, and a combination of high NAMPT expression and low TP73 expression are prognostic in breast cancer (Sharif et al., 2016). It was recently demonstrated that both NAMPT and NMNAT1 play a role in the interaction of PARP1 with CCCTC-binding factor (CTCF) in breast cancer cells (Henderson et al., 2017). Loss of PAR on CTCF results in the inhibition of tumour suppressor genes, such as TP53.

In leukaemia, FK866 acts synergistically with HDAC inhibitors through the upregulation of BCL2-associated X, apoptosis regulator (BAX), dependent on a loss of SIRT activity (Cea et al., 2011). Some studies have indicated that functional TP53 is required for the activity of FK866 in cancer cells. FK866 leads to increased acetylation of TP53, likely due to reduced NAD availability for SIRTs, leading to increased expression of the pro-apoptotic proteins CDKN1A and BAX (Thakur et al., 2012a; Thakur et al., 2012b; Alaee et al., 2017). Treatment of CLL cells with FK866 results in a drop in ATP levels followed by apoptosis (Gehrke et al., 2014). FK866 can induce AMPK expression, leading to a block in the mTORC1/4E-BP pathway and suppression of protein synthesis in both leukaemia and hepatocellular carcinoma cells (Zucal et al., 2015; Schuster et al., 2015). FK866 also acts synergisitcally with cyclosporin-A in leukaemia cells, disrupting mitochondrial membrane potential, depleting ATP levels and increasing endoplasmic reticulum stress (Cagnetta et al., 2015). Furthermore, exposure of normal monocytes to eNAMPT produced by CLL cells leads to their differentiation into tumour-supporting M2 macrophages independent of enzymatic NAMPT activity (Audrito et al., 2015).

In EGFR-mutated lung cancer cells, either FK866 or suppression of NAMPT expression using siRNA limits their growth by reducing the phosphorylation of EGFR targets, such as Akt and the MAPK family (Okumura et al., 2012). In both lung and ovarian cancer cells,

FK866 causes a block in glycolysis at GAPDH, because of its dependence on NAD as a cofactor, reducing the flow of glucose into the TCA cycle and serine biosynthesis, shunting glucose into the PPP, and significantly disrupting carbohydrate metabolism (Tan et al., 2013; Tan et al., 2015). These results were confirmed in another study, where they also showed that FK866 significantly disrupts amino acid and nucleotide metabolism (Tolstikov et al., 2014). Despite this, the metabolic response to NAD depletion varies even in different cancer cell lines of the same type. In one study, four different lung cancer cell lines treated with the NAMPT inhibitor GNE-617 showed significant differences in their utilisation of the PPP, as well as the ability to cope with oxidative stress, and divergent responses based on AMPK activity (Xiao et al., 2016). The combination of GMX1777 and pemetrexed in non-small cell lung cancer (NSCLC) showed a significant synergistic effect both *in vitro* and *in vivo* (Chan et al., 2014). This effect could be further enhanced by the addition of the BER inhibitor methoxyamine, and was dependent on the rapid depletion of NAD by PARPs. Furthermore, NAMPT promotes resistance of non-small lung cancer cells to the topoisomerase inhibitor doxorubicin through upregulation of ABCC1 in an Akt-dependent manner (Cao et al., 2017b). This effect is also seen in colorectal cancer cells, but is dependent on the RELA proto-Oncogene, NF-κB subunit (RELA)-mediated upregulation of ABCB1 (Yan et al., 2017). In both lung and pancreatic cancer, the combination of FK866 and β-lapachone induced PARP-mediated cell death through activation of NADPH: quinone oxidoreductase 1 (NQO1), resulting in a glycolytic block and rapid decrease in ATP levels (Moore et al., 2015; Liu et al., 2016).

In GBM, FK866 blocked proliferation in C6 (rat) glioma cells by inhibiting MAPK signalling, leading to G_2/M cell cycle arrest (Zhang et al., 2012b). The combination of FK866 and methoxyamine was able to sensitise GBM cells to TMZ, even in those with elevated expression of MGMT or impaired MMR machinery (Goellner et al., 2011). This was later shown to be dependent on the activation of autophagy (Yang et al., 2015c). FK866 also induces autophagy in neuroblastoma cells, and potentiates the effects of the DNA-damaging agent, cisplatin, and the topoisomerase inhibitor, etoposide (Travelli et al., 2011). Both FK866 and GMX1778 enhanced the activity of TMZ in GBM cells by increasing caspase activity, inducing the production of ROS and inhibiting antioxidative mechanisms such as SOD, possibly

through phosphorylation and therefore activation of JNK, triggering cell death (Feng et al., 2016a). FK866- or short hairpin RNA (shRNA)-mediated knockdown of NAMPT limited the motility and invasive properties of GBM cells, linked to the need of NAD for the conversion of pyruvate to lactate by LDHA (Van Horssen et al., 2013). It has been reported that hypoxia, often seen at the core of GBM tumours, can significantly alter NAD metabolism in GBM cells. Hypoxia induces increases in NAD, NADH and NaAD levels, but lowers NADP levels, which is linked to a decrease in NADK activity (Kucharzewska et al., 2015). This indicates that hypoxia induces increases in *de novo* biosynthesis of NAD. MYC/MYCN proto-Oncogene, BHLH transcription factor (MYCN)-driven GBM tumourspheres were shown to be uniquely sensitive to FK866, rapidly undergoing apoptosis *in vitro*, and significantly increasing survival time in mouse orthotopic xenograft models of GBM (Tateishi et al., 2016).

Recent work on GSCs has indicated a role for NAMPT. FK866- or shRNA-mediated knockdown of NAMPT decreased self-renewal capacity of GSCs and limited their growth *in vivo*, whilst increasing radioresistance (Gujar et al., 2016). Expression of NAMPT is consistent with the classical/mesenchymal sub-types, but also correlates with well-established stem cell markers, such as nanog homeobox (NANOG) and prominin 1 (PROM1) (Lucena-Cacace et al., 2017). Overexpression of NAMPT in GBM cells promotes stem cell pathways and increases tumour-initiating capacity. In addition, the combination of FK866 and TMZ is slightly more effective than either drug alone in cell monolayers and tumourspheres.

In initial clinical trials, FK866 was shown to be very well tolerated in humans, with the only dose-limiting toxicity being thrombocytopenia (Holen et al., 2008); this was also confirmed for GMX1778 (Von Heideman et al., 2010). In one phase II clinical trial, FK866 was given as a monotherapy to patients with refractory or relapsed cutaneous T-cell lymphoma, with 7 of the 12 patients having either a partial response or stable disease (Goldinger et al., 2016). However, the vast majority of the patients did not complete the full three cycles of treatment, and FK866 not only induced thrombocytopenia, but some patients also presented with severe lymphocytopenia. Two other clinical trials for FK866 as a monotherapy, one for melanoma and one for B-cell lymphoma, were completed in 2009, but results for these trials have not been published, indicating a lack of responses in these patients (ClinicalTrials.gov, 2018). Three

clinical trials for GMX1777, in metastatic melanoma, solid tumours and lymphomas, were either terminated or withdrawn before completion (ClinicalTrials.gov, 2018).

It seems that NAMPT inhibitors have not yet been given the opportunity to prove their efficacy in a clinical setting. It has been proposed that the failure of NAMPT inhibitors could be due to the use of low concentrations, which are necessary due to dose-limiting thrombocytopenia. In rats, toxicity could be partially limited by supplementation with NA (Tarrant et al., 2015). Despite this, concerns were raised regarding the prolonged use of FK866 leading to retinal toxicity, which could not be limited by the addition of NA (Zabka et al., 2015). However, recent efforts have produced novel NAMPT inhibitors such as LSN3154567, which has demonstrated potent anti-neoplastic activity *in vivo*, and does not lead to thrombocytopoenia or retinal damage when administered with NA (Zhao et al., 2017a). Another novel NAMPT inhibitor, STF-118804, has been demonstrated to limit proliferation in pancreatic cancer cells, triggering the upregulation of AMPK and corresponding suppression of mTORC1 signalling (Espindola-Netto et al., 2017). STF-118804 was also effective *in vivo*, and showed an additive effect when combined with chemotherapy, including paclitaxel, gemcitabine, and etoposide.

There have also been efforts to develop dual-targeting agents that block NAMPT and other molecules, such as P21 (RAC1)-activated kinase 4 (PAK4). KPT-9274 is a dual NAMPT/PAK4 inhibitor, which has been demonstrated to limit proliferation and induce apoptosis in renal cancer cells by blocking the Wnt/β-catenin and MYC pathways, as well as effectively limiting tumour growth *in vivo* (Abu Aboud et al., 2016). In pancreatic cancer, KPT-9274 inhibits proliferation through downregulation of BCL2-associated agonist of cell death (BAD) and upregulation of tumour suppressive miRNAs, and also showed efficacy *in vivo* (Mohammad et al., 2017; Aboukameel et al., 2017). KPT-9274 is also effective in B-cell acute lymphoblastic leukemia cells, primarily due to its inhibitory effects on NAMPT (Takao et al., 2017). Conversely, KPT-9274 was able to limit the growth of triple-negative breast cancers both *in vitro* and *in vivo* by reducing the levels of PAK4 and triggering apoptosis (Rane et al., 2017). In addition, KPT-9274 effectively limits proliferation through the induction of apoptosis in multiple myeloma cells, both *in vitro* and *in vivo* (Fulciniti et al., 2017). A phase I clinical trial testing KPT-9274 as a single agent in solid tumours of lymphoma is currently recruiting, and is due to

complete in November 2019 (ClinicalTrials.gov, 2018). Finally, there have even been efforts to create dual NAMPT/HDAC inhibitors, although these are currently still in development, and are yet to show significant benefits versus the use of individual inhibitors (Dong et al., 2017; Chen et al., 2017).

Whilst NAMPT inhibitors have demonstrated great success both *in vitro* and *in vivo*, their translation into clinical practice has been poor. This could be due to the presence of other NAD biosynthetic pathways, which can compensate for a lack of NAMPT activity. Nam, NA, NMN, NR and tryptophan can all enter the cell to be used to fuel NAD biosynthesis through different pathways (Nikiforov et al., 2011). But questions still remain as to how these pathways are regulated, and how they might affect the sensitivity of cancer cells to NAMPT inhibitors.

NAPRT

As previously described, NAPRT catalyses the conversion of NA to NaMN, which fuels NAD biosynthesis through the actions of the NMNAT family, and NADSYN1 (Fig. 1.4). The effects of NAMPT inhibitors can be reversed by the addition of NA, but only in cells expressing NAPRT (Watson et al., 2009). In mouse models of different types of cancer, supplementing FK866 with NA limited thrombocytopenia, whilst maintaining anti-tumour activity in tumours that lacked NAPRT (Olesen et al., 2010b), thus allowing for safe administration of FK866 at concentrations four times the standard maximum tolerated dose. In lymphoma, whilst NAMPT expression appeared to be higher in more aggressive cancers, NAPRT expression was expressed at low levels in up to 50% of samples, indicating that these patients could respond to coadministration of NAMPT inhibitors and NA (Olesen et al., 2011). This effect has also been reported for other cancer cell lines, including GBM, neuroblastoma and sarcoma (Cerna et al., 2012). This mechanism was expanded to a panel of 400 cancer cell lines, which demonstrated that NAPRT promoter methylation correlated with gene expression, and could be used to predict the response of cancer cell lines to rescue with NA (Shames et al., 2013). Furthermore, genetic variants in NAPRT are far more common than those found in NAMPT, and modelling of the protein indicated that it may affect its enzymatic function and therefore alter NA-mediated rescue from NAMPT inhibitors (Duarte-Pereira et al., 2014). NAPRT deficiency is necessary for

the effects of the novel NAMPT inhibitor LSN3154567 (Zhao et al., 2017a). However, despite a clear link between NAMPT inhibition, NAPRT expression and rescue with NA *in vitro*, there has been some evidence to suggest that this may not always be the case *in vivo*. In mouse models of gastric cancer and sarcoma, the addition of NA protected NAPRT-deficient cells from the effects of NAMPT inhibitors, without triggering upregulation of NAPRT (O'Brien et al., 2013).

A link between IDH mutations and NAD metabolism has been identified, which is particularly important in secondary GBM. Early work demonstrated that IDH mutations reduce the ability of the enzyme to utilise NADP without affecting NAD-dependent activity in GBM cells (Bleeker et al., 2010). IDH1-mutated cancers are particularly sensitive to NAMPT inhibition (Tateishi et al., 2015). The mutant IDH1 leads to the production of 2HG, which inhibits the activity of NAPRT. This renders the cells highly sensitive to NAMPT inhibitors, leading to the induction of AMPK, autophagy and cell death. Building on this, treatment of IDH1-mutated cells with TMZ resulted in rapid consumption of NAD by PARP, and increased sensitivity of the cells to FK866 and GMX1778 regardless of MGMT or MMR status (Tateishi et al., 2017). The combination of TMZ and FK866 also limited subcutaneous tumour growth *in vivo*. In chondrosarcoma, another cancer where IDH mutations are common, FK866 and GMX1778 reduced cell viability, colony formation and invasive properties, dependent on NAPRT status (Peterse et al., 2017). Alterations to the expression of NAMPT and NAPRT have been well established across multiple cancer types (Duarte-Pereira et al., 2016). Furthermore, a highly specific monoclonal antibody developed against NAPRT has shown that ∼70% of GBM tumours do not express the protein, and would likely benefit from combined NAMPT inhibitor/NA treatment (Cole et al., 2017). In addition, NAPRT is overexpressed in some subsets of ovarian cancer, where it promotes DNA repair, and regulates mitochondrial metabolism (Piacente et al., 2017). Finally, work with the dual NAMPT/PAK4 inhibitor KPT-9274 has demonstrated that a loss of NAPRT expression sensitises renal cancer cells to this compound, and NA supplementation can rescue cancer cells from the effects of KPT-9274 in the same manner as standard NAMPT inhibitors (Abu Aboud et al., 2016; Takao et al., 2017).

NT5E

The next pathway of NAD biosynthesis is relatively novel. It is an extracellular salvage pathway that is dependent on the expression of NT5E, also known as CD73. NT5E is well established as an important molecule in cancer pathophysiology. It is best characterised as a regulator of extracellular adenosine metabolism. NT5E catalyses the conversion of AMP to adenosine, which can either enter the cell through adenosine transporters, or act directly on extracellular adenosine receptors (Gao et al., 2014). In cancer, this adenosine has a profound immunosuppressive effect, preventing the cells of the immune system from killing tumour cells (Allard et al., 2016a). However, the adenosine can also affect the tumour directly. Adenosine receptors are G-protein coupled, and the binding of adenosine can either activate or inhibit the activity of adenylyl cyclase, increasing or decreasing the production of cAMP respectively (Antonioli et al., 2013). This can alter the activity of numerous cellular pathways, but particularly those involving JNK and the MAPK family. These pathways control cancer cell proliferation, apoptosis, angiogenesis and migration, so play a major role in regulating cancer cell homeostasis. The entry of adenosine into cells through nucleotide transporters promotes its conversion to AMP, which activates AMPK and can alter numerous pathways involved in metabolism, proliferation and apoptosis (Antonioli et al., 2013). Finally, rapid conversion of AMP to adenosine by NT5E promotes the activity of CD39, which degrades ATP and ADP to AMP. The removal of ATP in the extracellular environment prevents activation of of the P2 family receptors, further altering pathways involved in proliferation and apoptosis (Burnstock and Di Virgilio, 2013).

In U138MG cells, the production of adenosine by NT5E increases their proliferation and adhesion, both of which can be blocked by inhibition of NT5E or the adenosine transport inhibitor dipyridamole (Bavaresco et al., 2008; Cappellari and Vasques, 2012). NT5E also promotes the resistance of GBM cells to chemotherapeutics, such as vincristine, by increasing the expression of the multi-drug resistance protein ABCC1 (Quezada et al., 2013). Expression of both CD39 and NT5E has been linked to immune tolerance in GBM, through their sequential metabolism of ATP/ADP to adenosine (Kmiecik et al., 2013; Xu et al., 2013). Expression of CD39 on $CD4^+$ T_{reg} cells provides AMP for tumour-bound NT5E to generate adenosine, which suppresses the activity of cytotoxic $CD4^+$ cells, and prevents tumour killing. These results

were confirmed with the immunosuppressive chemotherapeutic compound methotrexate, which suppressed the invasion of GBM tumours by all T cell populations *in vivo* (Figueiro et al., 2016). Further to this, NT5E is used as a marker of glioma-resident mesenchymal stem cells, which are thought to support glioma growth through multiple paracrine signals (Shahar et al., 2017). The presence of these cells at greater proportions is linked to shorter survival times in patients with GBM. Inhibition of NT5E with the monastrol-derived compound, LaSOM 63, in GBM cell lines induces apoptosis (Figueiró et al., 2014). Interestingly, NT5E is expressed at lower levels on blood vessels surrounding glioma cells compared to normal healthy tissue, and low levels of expression reduce the integrity of the BBB (Wang et al., 2016a).

Multiple studies have demonstrated that NMN can rescue cancer cells from the effects of NAMPT inhibitors (Billington et al., 2008; Watson et al., 2009; Nikiforov et al., 2011; Zhang et al., 2012b; Xiao et al., 2013; Van Horssen et al., 2013; Tateishi et al., 2015). Analysis of the structure of *Haemophilus influenzae* (*H. influenzae*) NAD nucleotidase revealed a high degree of similarity to human NT5E (Garavaglia et al., 2012). Further work demonstrated that NT5E could support NAD biosynthesis in FK866-treated U87 cells, but only when the correct NAD precursor was available (Grozio et al., 2013). As described previously, NT5E catalyses the breakdown of NAD/NMN to NR, which is able to enter the cells and fuel NAD biosynthesis (Fig. 1.4). Knockdown of NT5E, or blocking its activity using adenosine 5-(α,β-methylene)diphosphate (APCP), inhibits NAD- or NMN-mediated rescue from FK866 treatment, but has no effect on rescue by NR (Grozio et al., 2013). The structure of the NT5E inhibitor APCP can be seen in Fig. 1.5. In ovarian cancer cells, combined inhibition of NAMPT and NT5E decreases NAD and ATP levels, and prevents rescue with exogenous NMN, resulting in decreased cell viability (Sociali et al., 2015). *In vivo*, combination therapy reduces the proportion of Ki-67-positive cells, increases tumour necrosis and extends the survival of tumour bearing mice.

QPRT

The final pathway for NAD biosynthesis is the kynurenine pathway, which uses tryptophan as its substrate and ends with the conversion of QA to NaMN by QPRT (Fig. 1.4). QPRT is

expressed in both glial cells and astrocytes in the brain (Du et al., 1991). Both astrocytes and neurons utilise the kynurenine pathway to produce NAD (Braidy et al., 2011). Kynurenine itself can rescue HeLa cells from NAD depletion induced by FK866 (Pittelli et al., 2010). However, deficiency in some enzymes of the kynurenine pathway in different cancer cells prevents rescue from FK866 treatment with tryptophan or QA (Xiao et al., 2013). Specifically, cancer cells deficient in indoleamine 2,3-dioxygenase (IDO)1 or kynureninase (KYNU) could not be rescued with tryptophan, and cells deficient in QPRT could not be rescued with either. However, long term exposure of fibrosarcoma cells to GMX1778 leads to specific upregulation of QPRT, allowing NAD biosynthesis through the kynurenine pathway (Guo et al., 2017). Inhibition of IDO1 using 1-methyl-L-tryptophan (1MT) limits the activity of the kynurenine pathway, and synergistically inhibits the growth of LN229 cells treated with the DNA-damaging agents carmustine and cisplatin, but not TMZ or etoposide (Miyazaki et al., 2009). Kynurenic acid is able to suppress both migration and invasion of T98G cells, and shows a moderate additive effect when combined with TMZ (Walczak et al., 2014). Dexamethasone downregulates the expression and activity of tryptophan 2,3-dioxygenase (TDO), an enzyme with similar functions to IDO, both *in vitro* and *in vivo* (Ott et al., 2015). This indicates that GBM tumours may already be sensitised to NAMPT inhibitors through other pharmacological intervention. Furthermore, tryptophan metabolism has been utilised to improve positron emission tomography (PET) imaging of GBM tumours, demonstrating a non-invasive method to determine the activity of the kynurenine pathway (Guastella et al., 2016).

Downregulation of the expression of IDO1 was linked to increased sensitivity not only to FK866, but also to other chemotherapeutic agents, including pemetrexed, gemcitabine, and methoxyamine, all of which cause DNA damage in some way (Vareki et al., 2015). Further work showed that in glioma, QPRT levels were correlated with brain tumour grade, and were highest in GBM (Sahm et al., 2013). QA, but not NA, was able to rescue glioma cells from FK866 treatment under conditions of oxidative stress, whereas the opposite was true for normal astrocytes. Interestingly, whilst glioma cells themselves were unable to synthesise QA, they could utilise the QA produced by proximal microglia to support their growth. Elevated QPRT in glioma has further been established, as well as alterations to the expression of numerous

other enzymes involved in the kynurenine pathway (Adams et al., 2014). Furthermore, the concentrations of some of the metabolites in the kynurenine pathway were demonstrated to be lower in patients with GBM compared to controls, indicating a possible role for them as biomarkers of kynurenine pathway activity.

Summary

It is clear that NAD metabolism plays a significant role in the proliferation and survival of cancer cells, including GBM. However, whilst the last decade has seen an increase in our understanding of GBM biology, this has yet to be translated into a significant therapeutic advancement. A recent paper studying the introduction of novel cancer drugs in Europe demonstrated that very few actually improved survival or even quality of life (Davis et al., 2017). Targeted therapies have not been the "magic bullets" that they were originally promised to be. Many novel therapies are only effective in a small subset of patients with cancers that exhibit specific molecular features, for example PARP inhibitors in BRCA-mutated cancers. More work is required to develop novel therapeutic options across cancer, but particularly in devastating forms of the disease such as GBM. Targeting NAD metabolism, specifically using NAMPT inhibitors, has been proven to be effective both *in vitro* and in preclinical studies. However, in the few phase I and II clinical trials that have been completed, responses have been poor. This is likely due to two main reasons. First of all, NAMPT inhibitors have been tested on patients with multi-drug resistant forms of the disease for which most other treatment options have failed. These cancers are inherently difficult to treat because they will likely have multiple adaptations that promote resistance to chemotherapy, such as drug efflux pumps or detoxification systems. Secondly, these studies have failed to stratify patients based on known redundant NAD biosynthetic pathways, which promote resistance to NAMPT inhibitors. This thesis aims to elucidate the mechanisms by which GBM cells resist treatment with NAMPT inhibitors, in an attempt to identify a subpopulation of patients that are likely to derive significant benefits from treatment with this class of compounds. Furthermore, I aim to determine the efficacy of combined TMZ and NAMPT inhibitor treatment both *in vitro* and *in vivo*.

1.4 Hypothesis and aims

1.4.1 Hypothesis

Multiple NAD biosynthetic pathways contribute to the resistance of GBM cells to inhibitors of NAMPT, but a subpopulation of GBM patients are highly sensitive to NAMPT targeted therapy, both alone and in combination with TMZ

1.4.2 Aims

1. Characterise GBM cells for their expression of genes involved in NAD biosynthesis
2. Determine the sensitivity of multiple GBM cell lines to NAMPT inhibition *in vitro*
3. Identify the pathways by which GBM cells are able to synthesise NAD in the presence of NAMPT inhibitors
4. Determine whether or not treatment of GBM with NAMPT inhibitors can improve responses to TMZ both *in vitro* and *in vivo*

Chapter 2

Materials and Methods

2.1 Cell lines and culture conditions

Details of all the cell lines used in this work, including their source and growth media, can be seen in Table 2.1. Established cell lines were obtained from either the American Type Culture Collection (ATCC) or The Leibniz Institute DSMZ - German Collection of Microorganisms and Cell Cultures (DSMZ), and maintained in Dulbecco's Modified Eagle's medium (DMEM) supplemented with 10% foetal bovine serum (FBS). Primary cell lines were derived from patient tumour tissue received from Charing Cross Hospital (CHX) and maintained in DMEM supplemented with F-12 nutrient mixture and 10% FBS. All cells were maintained in incubators at 37°C with 5% CO_2 and 95% relative humidity. Cells were passaged once every 3-4 days and plated to achieve a maximum of 90% confluence.

Cell Line	Type	Origin	Culture Condition
LN229	Established GBM	ATCC	DMEM + 10% FBS
SNB19	Established GBM	DSMZ	DMEM + 10% FBS
T98G	Established GBM	ATCC	DMEM + 10% FBS
U87	Established GBM	ATCC	DMEM + 10% FBS
U118	Established GBM	ATCC	DMEM + 10% FBS
DBTRG	Established GBM	DSMZ	DMEM + 10% FBS
8MG	Established GBM	DSMZ	DMEM + 10% FBS
42MG	Established GBM	DSMZ	DMEM + 10% FBS
GBM31	Primary GBM	CHX	DMEM + F12 + 10% FBS
GBM59	Primary GBM	CHX	DMEM + F12 + 10% FBS
GBM96	Primary GBM	CHX	DMEM + F12 + 10% FBS
TB26	Primary GBM	CHX	DMEM + F12 + 10% FBS
TB43	Primary GBM	CHX	DMEM + F12 + 10% FBS
TB48	Primary GBM	CHX	DMEM + F12 + 10% FBS
TB70	Primary GBM	CHX	DMEM + F12 + 10% FBS
TB77	Primary GBM	CHX	DMEM + F12 + 10% FBS

Table 2.1: **Established and primary GBM cell lines used for this project**. Both established and primary GBM cell lines were used from different sources. FBS and growth media were all purchased from Thermo Fisher Scientific, Inc., USA. American Type Culture Collection (ATCC), The Leibniz Institute DSMZ - German Collection of Microorganisms and Cell Cultures (DSMZ), Charing Cross Hospital (CHX), Dulbecco's Modified Eagle's medium (DMEM), foetal bovine serum (FBS).

2.2 Proliferation assays

Proliferation assays were carried out using the sulforhodamine B (SRB) method. GBM cells were plated at 500-10,000 cells/well in 96 well plates in 100 µl growth medium. The cells were left for 24 h to adhere, at which point the medium was supplemented with a further 100 µl growth medium containing various concentrations of chemotherapeutics, such as TMZ and FK866, as well as other compounds of interest. Cells were allowed to proliferate for the desired amount of time, at which point they were fixed using cold (4°C) 10% TCA for 1 h. The plates

were washed gently with running water and left to dry overnight, then stained with 50 µl 0.4% SRB in 1% acetic acid at room temperature for 1 h. Unbound SRB stain was washed away using 1% acetic acid and the plates were left to dry overnight. Finally, 150 µl 10 mM Tris (pH 10.5) was added to each well to solubilise the bound SRB dye, and the absorbance was measured at 490 nm on a BioTek EL800 microplate reader. Data were normalised to vehicle control for each experiment. For individual timepoints, proliferation was plotted against the dose and S-shaped dose response curves were fitted to allow calculation of relative half maximal inhibitory concentration (IC_{50}) values.

2.3 Cell cycle, apoptosis and cell death

Cell death, apoptosis and the cell cycle were measured using trypan blue staining, the Muse Annexin V and Dead Cell reagent and propidium iodide (PI) staining, respectively. Cells were plated into 6 well plates at 50,000-1,000,000 cells/well in 1 ml of growth medium. The cells were left to adhere and start growing for 24 h, then the medium was replaced with 2 ml media containing chemotherapeutics and other compounds of interest. After the desired amount of time, the medium was collected to ensure retention of dead cells, and the remaining cells were trypsinised and washed off with fresh media, at which point the samples were combined. Some of the sample was stained with trypan blue, and both the live and dead cell populations were recorded to assess cell death. The samples were then resuspended to 500,000 cells/ml, and 100 µl of cell solution was added to 100 µl of Annexin V staining solution and mixed. The cells were incubated at room temperature for 20 min in the dark, then run on a Muse Cell Analyzer. Healthy, early apoptotic, late apoptotic/dead and necrotic populations were recorded using the gating strategy shown in Fig. 2.1A/B. The remaining cells were resuspended in 200 µl phosphate-buffered saline (PBS) and then fixed by adding 1 ml of cold (4°C) 90% methanol to yield a 70% methanol solution. Samples were stored at 4°C for $\geq$ 1 h, then washed with PBS twice to remove the methanol. Samples were then resuspended in 200-500µl of PI staining solution containing 50 µg/ml of PI and 100 µg/ml of RNase A, transferred to a flow cytometry tube and incubated at 4°C for 1 h in the dark. The cells were then analysed on a BD Biosciences FACScalibur flow cytometer using BD CellQuest Pro software (ver. 4.0.2). Cells in different

stages of the cell cycle were recorded using the gating strategy shown in Fig. 2.1C.

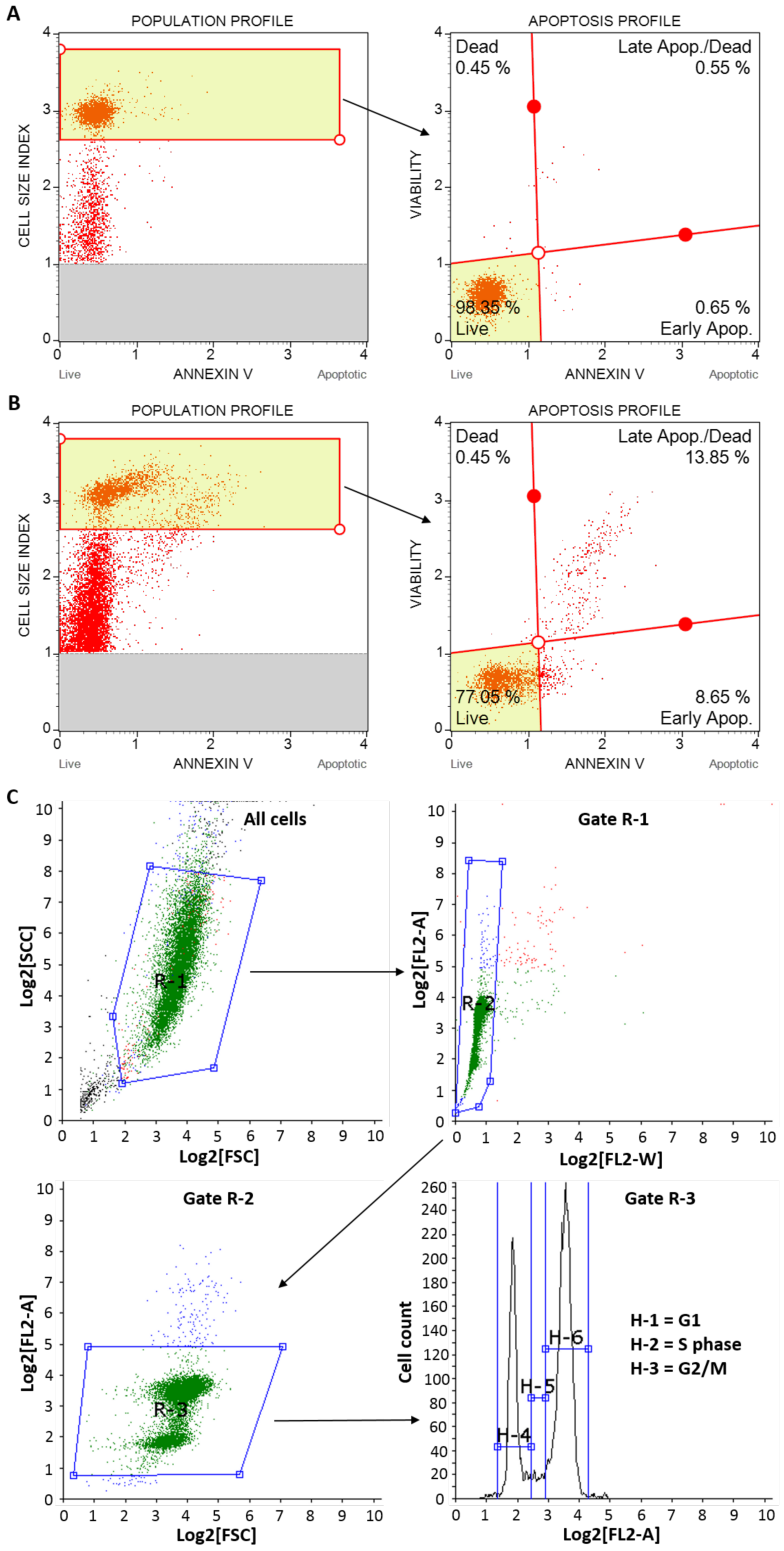


Figure 2.1: **Scatter graphs and histograms showing the gating strategies for Annexin V and PI staining in GBM cells treated with TMZ.** Gating for live cells and the four different quadrants representing live cells, early apoptotic cells, late apoptotic cells and dead cells in (A) healthy LN229 cells and (B) LN229 cells treated with TMZ (20 µM). (C) Gating for the different stages of the cell cycle in LN229 cells treated with TMZ (20 µM).

2.4 NAD/NADH quantification

Total NAD and NADH were quantified using the Promega NAD/NADH-Glo Assay. Cells were plated into 96 well plates at 1,000-10,000 cells/well in 100 µl of growth medium. The cells were left to adhere and start growing for 24 h, after which 100 µl medium containing chemotherapeutics and other compounds of interest was added. Parallel SRB plates were set up to allow normalisation of the data to proliferation. After the desired amount of time (0, 12, 24, 48 or 72 h) both the NAD/NADH assay plates and the SRB assay plates were removed from the incubator. Whilst the NAD/NADH plate equilibrated to room temperature, the SRB plate was fixed as described previously. The medium was removed from the NAD/NADH plate and 50 µl of PBS at room temperature was added to each well. Subsequently, 50 µl of 0.2 N NaOH solution containing 1% dodecyltrimethylammonium bromide (DTAB) was added to each well and the plate was transferred to a plate shaker to lyse the cells whilst preserving NAD and NADH. A total of 50 µl of the solution was then transferred to the adjacent well to allow measurement of both NAD and NADH individually. 25 µl of 0.4 N HCl was then added to the second well (NAD measurements), and the plate was incubated at 60°C for 15 min. The plate was then equilibrated to room temperature for 10 min, and 25 µl of 0.5 M Trizma base was added to the second well to neutralise the acid. 50 µl of 0.4 N HCl/0.5 M Trizma 1:1 solution was added to the first well only (NADH measurements). Then, 25 µl of each was then transferred to a white-walled 96 well plate, and 25 µl of NAD/NADH-Glo Detection Reagent was added to each well and mixed gently. The plate was incubated at room temperature for 30 min, then the bioluminescence was measured at 10 min intervals on a Promega GloMax luminometer with 0.3 second integration time up to a total of 60 min incubation.

2.5 Bacterial transformation and plasmid purification

Plasmids were transformed into competent DH5α TOP10 *Escherichia coli* (*E. coli*). To start, 1 µl of each plasmid was added to 15 µl of bacteria in individual 1.5 ml eppendorf tubes and incubated at 4°C for 30 min. Heat shock transformation was carried out by placing the bacteria in a water bath at 42°C for 30 seconds, followed by a further 2 min at 4°C. Subsequently, 300 µl

of Super Optimal broth with Catabolite repression (SOC) medium was added to each tube and they were incubated at 37°C for 45 min on a shaking incubator. Afterwards, 150 µl of each was then spread on to individual Luria broth (LB)-agar plates containing 100 µg/ml of ampicillin. Plates were inverted and incubated at 37°C overnight. Individual colonies were picked and added to centrifuge tubes containing 5 ml of LB also containing 100 µg/ml of ampicillin. The tubes were incubated at 37°C overnight on a shaking incubator. Plasmid purification was achieved using the QIAprep Spin Miniprep Kit from Qiagen as per the manufacturer's instructions.

2.6 Genetic knockdowns

Genetic knockdowns were achieved using Metafectene PRO reagent. Cells were plated into 6 well plates at 250,000 cells/well in 2 ml of growth medium and left to adhere and start growing for 24 h. Subsequently, 2 µg of each plasmid was resuspended in 100 µl of PBS, which was then added to 6 µl of metafectene diluted in 94 µl of PBS and mixed once. The solution was incubated at room temperature for 20 min, then each was added to individual wells of 6 well plates containing GBM cells. After 24 h, the medium was replaced with 2 ml growth medium containing puromycin at 0.5 µg/ml. Cells were passaged in medium containing puromycin for at least 2 weeks to generate stable cells lines, at which point the protein and RNA were extracted to allow measurement of gene knockdown levels.

2.7 RNA extraction, cDNA synthesis and qPCR

2.7.1 RNA extraction using TRI reagent

RNA extractions were carried out using TRI reagent. Cells were plated into 12 well plates in 1 ml of growth medium to achieve ∼90% confluence on the day of extraction. The medium was removed from each well and 300 µl of TRI reagent was added per well. The plate was incubated at room temperature for 5 min on a plate shaker to lyse the cells, then the solutions were transferred to individual 1.5 ml eppendorf tubes. Subsequently, 30 µl of 1-bromo-3-chloropropane

(BCP) was added to each tube and the samples were mixed using a vortex for 10 seconds to create an emulsion, which was incubated at room temperature for 3 min. Samples were centrifuged at 12,000 g for 15 min at 4°C to separate the phases; 75 µl of the clear, aqueous, upper phase was then added to 150 µl of 2-propanol, mixed thoroughly using a pipette and then incubated at room temperature for 10 min. Samples were centrifuged at 12,000 g for 30 min at 4°C to sediment the precipitated RNA, and the excess solution was poured off. RNA pellets were washed twice with cold (4°C) 75% ethanol, then resuspended in 15 µl of preheated (65°C) sterile RNase-free water. RNA concentration and purity were measured on a NanoVue Plus.

2.7.2 cDNA synthesis using M-MLV

cDNA synthesis was carried out using M-MLV reverse transcriptase. To start, 1-2 µg of RNA was diluted in water containing 0.5-1 µg of random primers to a total volume of 15 µl. Samples were heated to 70°C for 5 min to melt the secondary structure within the RNA and allow the random primers to bind, and were then placed on ice to cool. Subsequently, 10 µl of master mix containing M-MLV reverse transcriptase enzyme (20 U/µl), RNaseOUT Recombinant Ribonuclease Inhibitor (2 U/µl) and 2 mM dNTP mix was added to each tube, and they were incubated at 37°C for 60 min to allow synthesis of cDNA.

2.7.3 Quantitative PCR

Quantitative polymerase chain reaction (qPCR) was carried out using SYBR Select reagent, as directed by the manufacturer. Briefly, 50 ng of cDNA in 5 µl of water was added to 5 µl of water containing 0.5 µM of the forward and reverse primers for a specific gene as well as 10 µl of SYBR Select reagent in a Bio-Rad qPCR plate. Gene names and their forward and reverse primer sequences can be seen in the appendices (Table A.1). Plates were sealed using adhesive films and run on a Bio-Rad C1000 Thermal Cycler with CFX96 Real Time System running CFX Manager software (ver. 3.1). The qPCR thermocycling conditions can be seen in Table 2.2.

Step	Sub-step	Temperature (°C)	Time (sec)
1	N/A	50	120
2	N/A	95	120
3 (45 cycles)	a	95	15
	b	60	60
4 (melt curve)	a	65	5
	b	95	120

Table 2.2: **qPCR reaction conditions.** Temperatures and times run on the Bio-Rad C1000 Thermal Cycler.

2.8 Protein extraction and western blotting

2.8.1 Protein extraction

Protein extraction was carried out using radioimmunoprecipitation assay (RIPA) buffer. Cells were plated into 6 well plates in 2 ml of growth medium to achieve ∼90% confluence on the day of extraction. The medium was removed from each well and the cells were washed twice with cold (4°C) PBS. 150 µl of RIPA buffer was added to each well and the cells were scraped immediately and transferred to 1.5 ml eppendorf tubes. The samples were kept on ice for 30 min and were then centrifuged at 14,000 g for 30 min at 4°C to sediment the cell debris. The supernatant containing the protein was then transferred to fresh 1.5 ml eppendorf tubes, and protein concentration was quantified using the Bradford assay.

2.8.2 Protein quantification using the Bradford assay and dilution in loading buffer

Fresh protein samples were diluted 1:10 in a 96 well plate also containing eight bovine serum albumin (BSA) standards at 0, 0.025, 0.05, 0.1, 0.25, 0.5, 0.75 and 1 mg/ml, all to a total volume of 10 µl. Bio-Rad protein assay reagent was diluted 1:5 and 200 µl was added to each well. The plate was incubated at room temperature for 5 min, then absorbance was measured at 595 nm on a BioTek EL800 microplate reader. A standard curve was generated from the

BSA standards in Microsoft Excel, then protein concentrations in the samples were calculated. Protein was diluted in 6X western blot loading buffer containing dithiothreitol (DTT), the composition of which can be seen in appendix A.3.1.

2.8.3 Western blotting using the Invitrogen mini gel tank system

Western blotting was carried out using sodium dodecyl sulfate (SDS)-polyacrylamide gel electrophoresis (PAGE) in an Invitrogen Mini Gel Tank system. Briefly, 10% acrylamide/bis-acrylamide gels were made in Invitrogen gel cassettes and allowed to set (see appendix A.3.1). Protein samples in DTT loading buffer were boiled for 5 min at 100°C, and were then placed on ice prior to gel loading. Gels were placed into the western blot tank filled with running buffer (see appendix A.3.1), then the samples were loaded into individual wells in the gel alongside a New England Biolabs (NEB) broad range protein ladder. Samples were separated by SDS-PAGE at 100V for 90 min, or until they had run to the end of the gel. The gels were removed from the cassettes and placed into transfer modules with nitrocellulose blotting membrane. The modules were then placed into the western blot tank filled with transfer buffer (see appendix A.3.1). Protein was transferred to the membrane at 10V for 1 h. The blotting paper was removed and stained with Ponceau S solution to confirm the presence of protein and to aid in cutting of the membrane. Individual segments were cut with a scalpel and then washed with PBS with with 0.1% TWEEN 20 (PBS-T). Blots were blocked by incubating in 20 ml blocking buffer (5% skimmed milk powder in PBS-T) at room temperature for 1 h on a plate shaker. Blots were washed with PBS-T, then placed into 50 ml centrifuge tubes containing 10 ml of PBS-T with the appropriate primary antibody (Table A.4). The blots were incubated at 4°C overnight on a tube roller, then removed and washed with PBS-T. They were then placed into fresh 50 ml centrifuge tubes containing 10 ml of PBS-T with the appropriate secondary antibody (Table A.4) conjugated to horseradish peroxidase (HRP), and incubated at room temperature for 1 h on a tube roller, then removed and washed with PBS-T. Blots were exposed to LI-COR chemiluminescent substrate for 5 min, then scanned on a LI-COR C-Digit blot scanner. Where necessary, blots were then stripped using stripping buffer (see appendix A.3.1). The blots were washed with PBS-T, then incubated in warm (37°C) stripping buffer for 10 min. They were

then washed in PBS-T, then blocked again in blocking buffer at room temperature for 1 h on a plate shaker. The blots were washed again with PBS-T, then probed using a different primary antibody following the same procedures as described previously. Images were analysed semi-quantitatively using the built in gel analysis function in ImageJ (ver. 1.48).

2.9 RNA sequencing

2.9.1 RNA extraction using the Qiagen kit

Either 42MG or DBTRG GBM cells were plated into 6 well plates in triplicate in 2 ml of growth medium to achieve ∼90% confluence on the day of extraction. The cells were left to adhere and start growing for 24 h, then the medium was replaced with fresh growth medium containing either FK866 at 20 nM or vehicle control (PBS). After 24 h, the medium was removed and RNA was extracted using the Qiagen RNeasy Mini Kit with optional on column DNase treatment, as directed by the manufacturer. RNA concentration and purity were measured on an 2100 Bioanalyzer system (Agilent Technologies, USA).

2.9.2 RNA sequencing

The mRNA library preparation and sequencing was performed on an Illumina HiSeq 4000 system with 75 base paired-end reads, by the Imperial Biomedical Research Centre (BRC) Genomics Facility. FASTQ sequencing data were mapped to a reference genome using TopHat2 (Kim and He, 2013) to generate aligned BAM files, which were further processed using HTseq (Anders et al., 2015) to generate count matrices. Finally, data analysis was carried out using DESeq2 (Love et al., 2014) to generate quality control plots and lists of differentially expressed genes between the following groups:

- 42MG control versus 42MG FK866-treated
- DBTRG control versus DBTRG FK866-treated
- 42MG control versus DBTRG control
- 42MG FK866-treated versus DBTRG FK866-treated

2.9.3 Data analysis

Differentically expressed genes ($P < 0.1$, appendix B.1) from the RNA sequencing (RNAseq) data were subject to gene set enrichment analysis (GSEA) using EnrichR (Chen et al., 2013; Kuleshov et al., 2016). Datasets used included those predicting transcription factor (TF) regulation, protein-protein interactions (PPI), gene ontology (GO) terms and cell signalling pathways. A list of the datasets interrogated can be seen below:

- BioPlex 2017
- ChEA 2016
- ENCODE TF Chip-Seq 2015
- GO Biological Process 2017b
- GO Cellular Component 2017b
- GO Molecular Function 2017b
- HMDB Metabolites
- KEA 2015
- KEGG 2016
- NCI-Nature 2016
- PANTHER 2016
- PPI Hub Proteins
- Reactome 2016
- Transcription Factor PPI's
- TRANSFAC and JASPAR PWM's
- WikiPathways 2016

Full details of each database can be seen in the appendices (Table A.2).

2.10 *In vivo* modelling of intracranial tumours

2.10.1 Surgical implantation of human GBM cells into nude mice

In vivo modelling of GBM tumours was achieved using U87 GBM cells labelled with a green fluorescent protein (GFP)/luciferase reporter and nude CD1-*Fox1*$^{nu/nu}$ mice. Mice were anaes-

thetised with a mixture of ketamine (100 mg/kg) and xylazine (8 mg/kg) administered intraperitoneally, with the analgesic buprenorphine (20 µg/kg) administered subcutaneously. The head of each mouse was fixed into a stereotactic frame and the scalp was cut along the cranial midline. The coordinates for injection were determined from the bregma as follows:

- Anteroposterior: +0.1 cm
- Mediolateral: -0.2 cm
- Dorsoventral: -0.3 cm

Once the anteroposterior and mediolateral coordinates were located, a small hole was drilled into the skull and underlying bone fragments were removed to expose the meninges. A glass needle was then inserted through the meninges to the correct dorsoventral coordinates, and 2 µl of cell solution containing 2×10^5 U87-GFP/luciferase cells were injected into the right cerebral cortex of the mouse. The needle was carefully removed and the scalp was sutured. Sedation was then reversed using atipamezole (0.5 mg/kg). The mice were left to allow tumours to establish for at least one week before being imaged using the In Vivo Imaging System (IVIS).

2.10.2 *In vivo* imaging using the IVIS

To monitor tumour growth, the mice were imaged using the IVIS once or twice a week. Animals were anaesthetised using 2% isoflurane, then given luciferin (15 mg/ml) via subcutaneous injection. After 3 min, the animals were placed three at a time into an IVIS Lumina III In Vivo Imaging System, then imaged at 3 min intervals for 1 min exposure times.

2.10.3 Treatment of tumour-bearing mice with TMZ and/or FK866

Once the presence of tumours was confirmed, the mice were randomised to one of four different treatment groups. After a total of 2 weeks post-injection, the mice were treated with either:

- 1% dimethyl sulfoxide (DMSO) in saline
- TMZ (30 mg/kg) in 1% DMSO in saline once a day for 5 days
- FK866 (20 mg/kg) in 1% DMSO in saline once a day for 5 days, followed by 2 days without, then once again for 5 days

- Combined TMZ and FK866 in 1% DMSO in saline given as above

After a total of 4 weeks post-injection, all of the mice were euthanised using 20 mg pentobarbitone sodium and perfused through the heart with PBS followed by 4% paraformaldehyde (PFA) in PBS. The brains were removed and fixed in 4% PFA for up to 1 week, at which point they were either placed into 30% sucrose solution in PBS, or into PBS only to be used for Free-of-Acrylamide SDS-based Tissue Clearing (FASTClear). After the brains had been submerged in 30% sucrose for 2 days, they were snap frozen in 2-methylbutane (-80°C) to be preserved.

2.10.4 FASTClear

Tissue clearing and staining was carried out by Tsz Wing Chau on mouse brain sections FASTClear as described previously (Perbellini et al., 2017), followed by imaging using confocal microscopy. Images were processed and analysed using ImageJ (ver. 1.48) and ZEN (blue edition, ver. 2.3 lite).

2.11 *In silico* analysis of TCGA data

Normalised, gene-level data from The Cancer Genome Atlas (TCGA) were obtained from the University of California, Santa Cruz (UCSC) Cancer Browser. Data types used include:

- Clinical
- Microarray expression
- RNAseq expression
- Mutation call
- Methylation

Data was analysed in RStudio (ver. 1.0.153), running R (ver. 3.4.3) using scripts generated in house.

2.12 Statistics and data analysis

Biological replicates are defined as individual, isolated wells in tissue culture plates. All experiments carried out as a minimum of three biological replicates across three independent experiments. Unless otherwise specified, data analysis, statistical tests and the plotting of graphs were carried out using Microsoft Excel 2013 and GraphPad Prism 7 (ver. 7.02). The thesis was written and built using LaTeX in TeX Maker (ver. 5.0.2).

Chapter 3

Characterisation of GBM tumours and cell lines and the effects of NAMPT inhibition

The last major breakthrough in chemotherapy for GBM was that of TMZ. The addition of TMZ to radiotherapy following surgical debulking yielded a significant increase in overall survival in patients with GBM (Stupp et al., 2005). However, the increase in survival was still only very small at 2.5 months. Even this breakthrough was muted by the discovery of a highly specific defence mechanism in the form of MGMT, which renders TMZ largely useless. Clearly, more therapeutic options are required for patients with GBM. Targeting NAD biosynthesis may be one such option. Cancer cells require a large pool of NAD to be able to drive cellular metabolism, proliferation through the regulation of the cell cycle, and DNA repair through the action of the PARP family. The main pathway by which cancer cells generate NAD is through the recycling of Nam by the enzyme NAMPT. Therefore, inhibiting NAMPT may block NAD production and target multiple cellular pathways that GBM cells rely on for survival. In order to determine whether NAMPT inhibition in GBM could be a useful treatment, it was first important to identify the molecular phenotype of GBM cells, and their response to NAMPT inhibition. *In silico* analyses were carried out using the publicly available TCGA data to determine whether GBM tumours exhibit aberrant expression of genes involved in NAD biosynthesis. Furthermore,

the NAMPT inhibitor FK866 was tested on both established and primary GBM cells *in vitro*.

3.1 Variability in the expression of genes involved in NAD biosynthesis in GBM samples from TCGA

I first wanted to determine whether there were any significant changes in the expression of genes involved in NAD biosynthesis between healthy tissue and tumour tissue. TCGA database contains RNAseq data for patients with GBM (n = 172), which includes data on healthy tissue, primary tumour tissue and recurrent tumour tissue. Box and whisker plots were generated for each of four key genes involved in the regulation of NAD biosynthesis: NAMPT, NAPRT, NT5E and QPRT. There was a significant increase in the expression of NAMPT and NT5E in primary tumour tissue compared to healthy control tissue ($P < 0.05$, Fig. 3.1). There also appeared to be further increases in the expression of these genes in recurrent tumour tissue when compared to primary tissue, although these differences were not significant. However, there were no clear differences in the expression of NAPRT or QPRT in these samples. These results indicate that increased expression of the key enzymes involved in NAD biosynthesis, NAMPT and NT5E, occurs during oncongenic transformation.

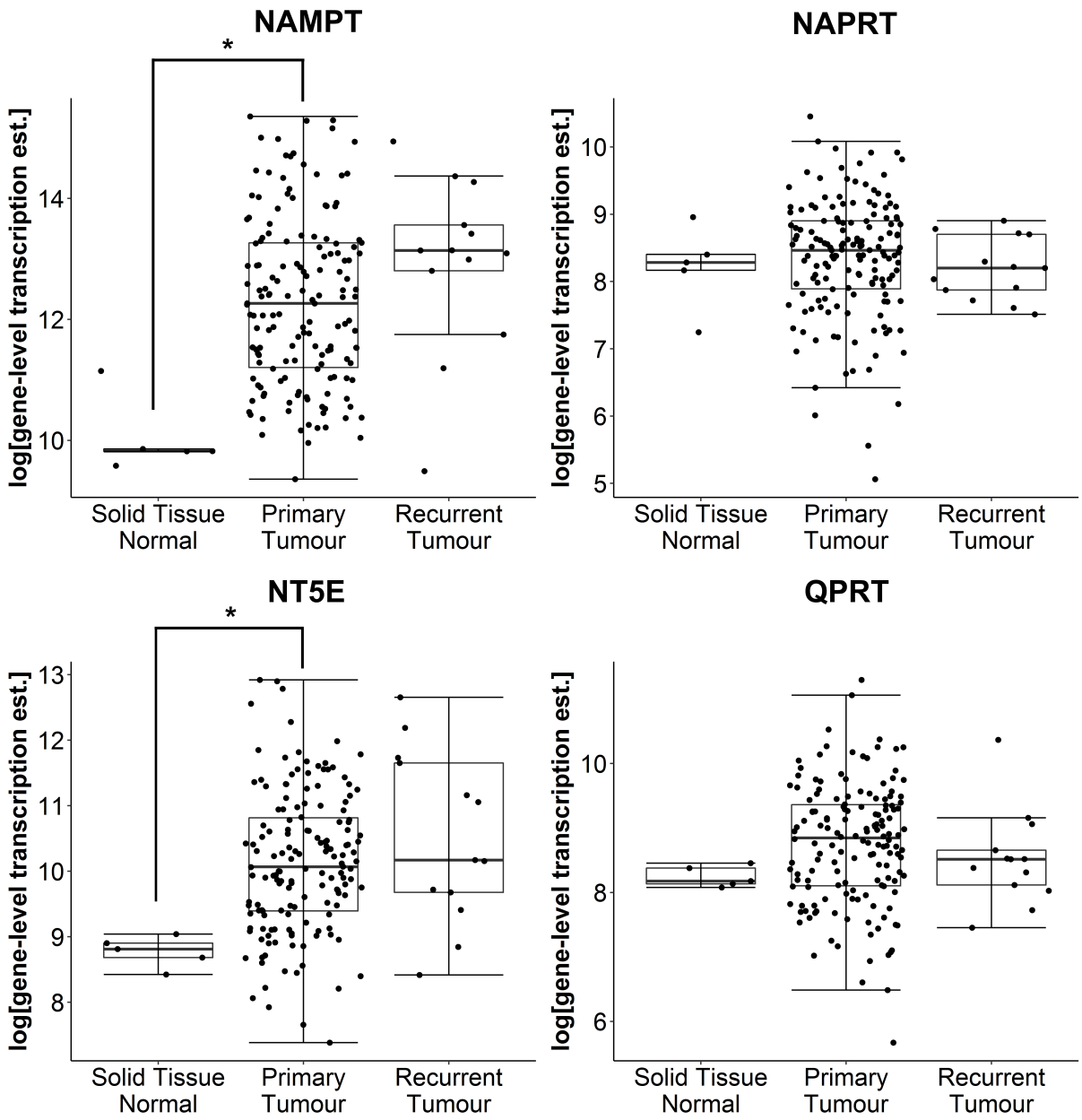


Figure 3.1: **Key genes involved in NAD biosynthesis are upregulated in GBM tumours compared to healthy tissue.** Box and whisker plots showing the distribution of expression of NAMPT, NAPRT, NT5E and QPRT between healthy, primary tumour and recurrent tumour tissue. * $P < 0.05$, two-way ANOVA with Tukey's HSD post-hoc test. TCGA RNAseq data (n = 172). Lines represent the median, interquartile range (IQR) and upper and lower extremes calculated using 1.5[IQR].

I next wanted to identify whether any of these key genes were related to overall survival in patients with GBM tumours. Microarray expression data (n = 539) or RNAseq data (n = 172) from TCGA were used to separate patients into high, intermediate or low expression groups based on tertiles, and Kaplan-Meir plots (KM plots) were generated for each gene individually.

Elevated expression of either NAMPT or NT5E was associated with significantly poorer overall survival ($P < 0.05$, Fig. 3.2). Notably, patients with very low expression of NAMPT have a far better prognosis, with four times as many patients surviving beyond two years. Furthermore, patients whose tumours had elevated expression of NAPRT seemed to have much poorer survival in the very short term (< 500 days), although this is not statistically significant ($P = 0.0548$, Fig. 3.2). These results further reinforce the importance of NAMPT, NT5E and perhaps NAPRT in the progression/recurrence of GBM tumours.

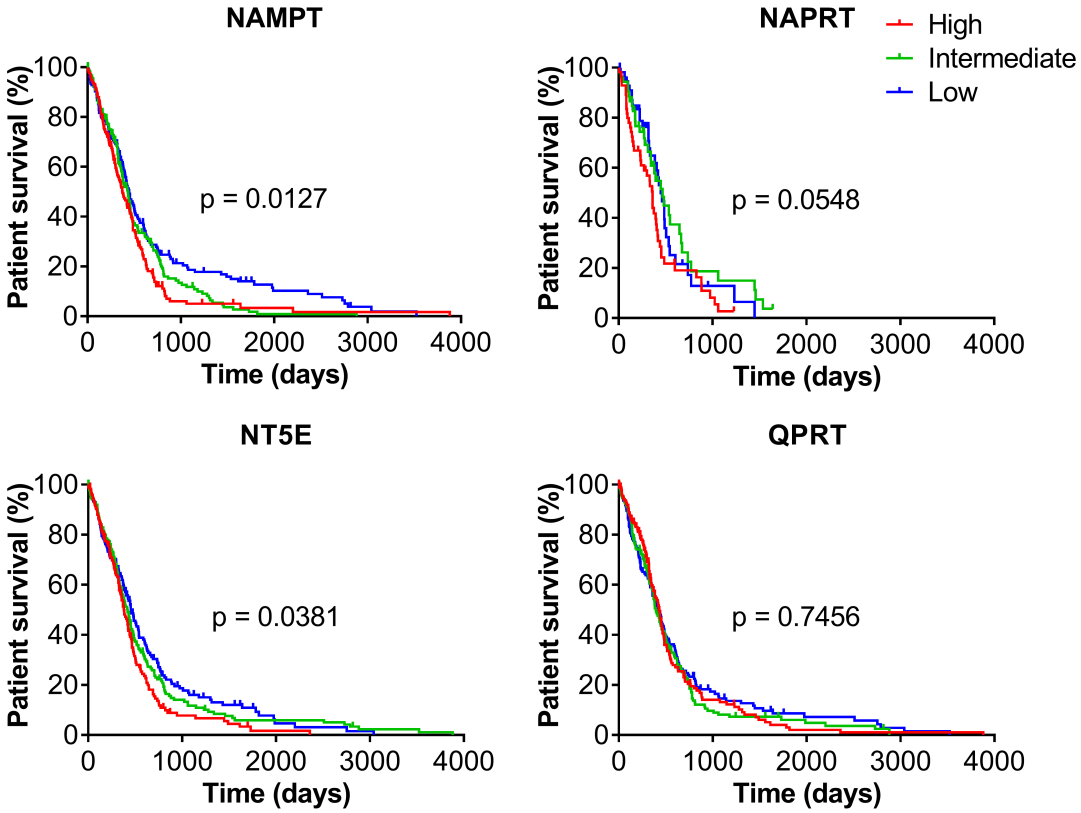


Figure 3.2: **Elevated expression of key genes involved in NAD biosynthesis leads to poorer overall survival in patients with GBM.** Kaplan-Meir plots showing the survival of patients with GBM tumours, separated according to tertile expression of NAMPT, NAPRT, NT5E and QPRT. P values calculated using the log-rank test (Mantel-Cox). TCGA microarray data (n = 539) for NAMPT, NT5E and QPRT. TCGA RNAseq data (n = 172) for NAPRT.

Given that genes involved in NAD biosynthesis appeared to have a strong link with the development and progression/recurence of GBM, I then wanted to identify whether there were any patterns in the NAD biosynthetic profiles of patient tumours that matched well known clinical characteristics or specific mutations. There were a total of 149 samples with match-

ing clinical, gene expression (RNAseq) and mutation data available in TCGA database, the majority of which were primary tumour samples. A heatmap was generated for the expression of all of the genes involved in NAD biosynthesis, with both genes and patients clustered based on a standard distance matrix. Key clinical information, including well-established GBM subtypes (Verhaak et al., 2010), as well as the sample type (primary or recurrent GBM) were included. The mutation status for common mutated genes in GBM were also included, as well as a classifier column showing which pathway each gene belongs to within NAD biosynthesis. Whilst TP53, PTEN, EGFR and RB1 mutations were evenly distributed between all of the patients, ATRX and IDH1 were often found in patients with the proneural subtype, and they appear to cluster together based on their expression of genes involved in NAD biosynthesis. In addition, most of the genes involved in the kynurenine pathway formed a single cluster, suggesting that these genes tend to be co-expressed/repressed. The two key genes that regulate the nicotinic acid pathway, NAPRT and NADSYN1, were also tightly clustered, whilst those regulating the NAD salvage pathway (NT5E, NMRK1 and NMRK2) showed no distinct grouping. The heatmap clearly indicates that the expression of genes involved in NAD biosynthesis is highly variable across patient tumour tissues, and may be associated with mutation status for commonly mutated genes in GBM, particularly those found in the proneural subtype.

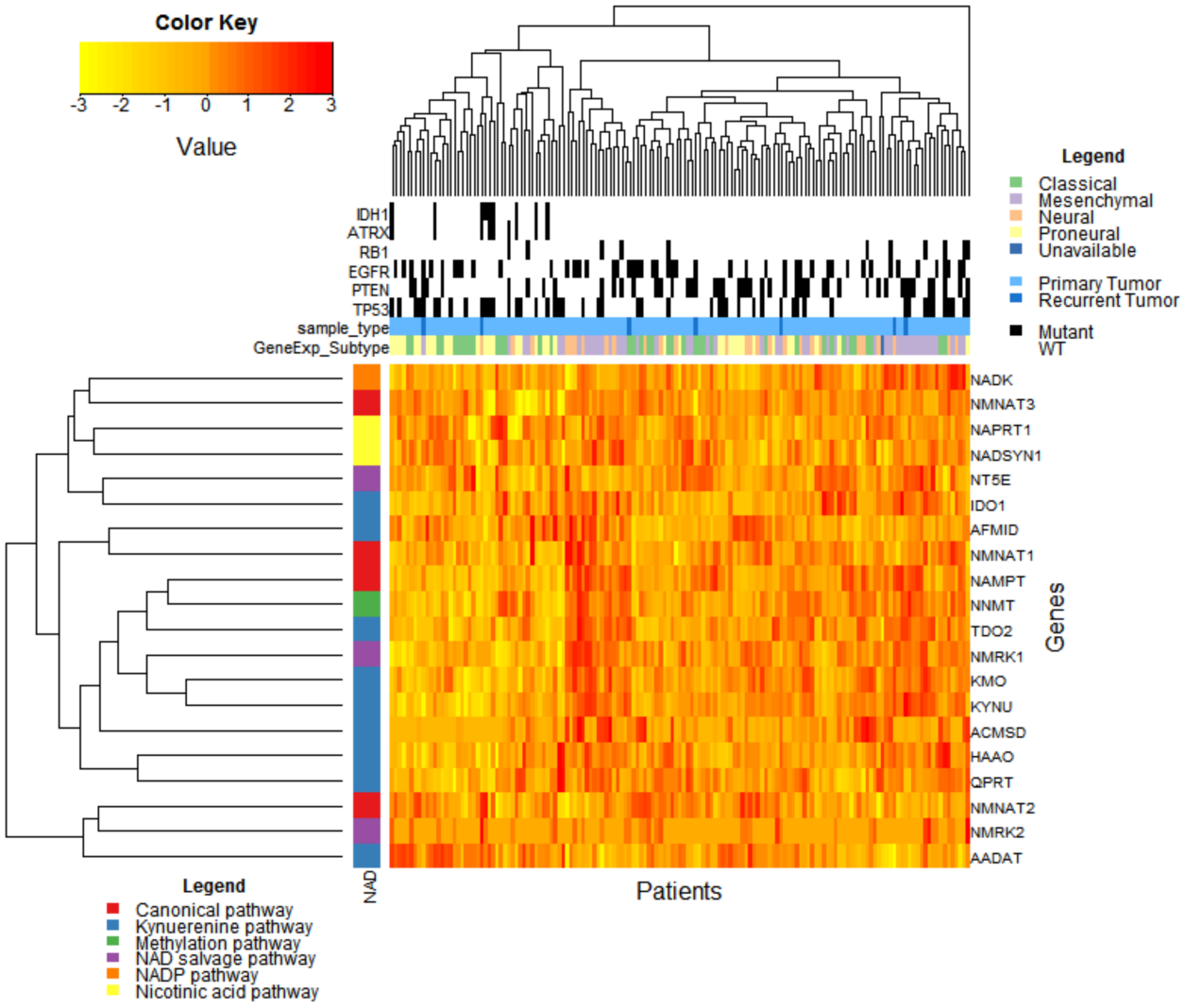


Figure 3.3: **GBM tumours cluster on mutation status for their expression of genes involved in NAD biosynthesis.** Heatmap showing scaled gene expression data (TCGA RNAseq) for genes involved in NAD biosynthesis, with indicators showing mutation status for specific genes, sample type and GBM subtype, as well as the NAD biosynthetic pathways that each gene belongs to (n = 149).

3.2 The expression of key genes involved in NAD biosynthesis varies between GBM cell lines

I next wanted to determine whether the variability in the expression of genes involved in NAD biosynthesis was also seen in GBM cell lines. Established and primary GBM cell lines were profiled for their expression of the same key genes that regulate NAD biosynthesis by both qPCR and western blot analysis. qPCR results show that both established (Fig. 3.4A) and

primary (Fig. 3.4B) GBM cell lines had a high degree of variability in their expression of genes involved in NAD biosynthesis. These results were also confirmed by western blot in established (Fig. 3.5A) and primary (Fig. 3.5B) GBM cell lines. All of the GBM cell lines expressed NAMPT to varying degrees, but staining for NAPRT indicated that cell lines either have very high levels of protein, or none at all. The expression of NT5E and QPRT was highly variable across cell lines, with some showing very high levels of protein, others only moderate levels, and some lacking any detectable protein. This further reinforces the inherent variability in the expression of genes involved in NAD biosynthesis between different GBM tumours.

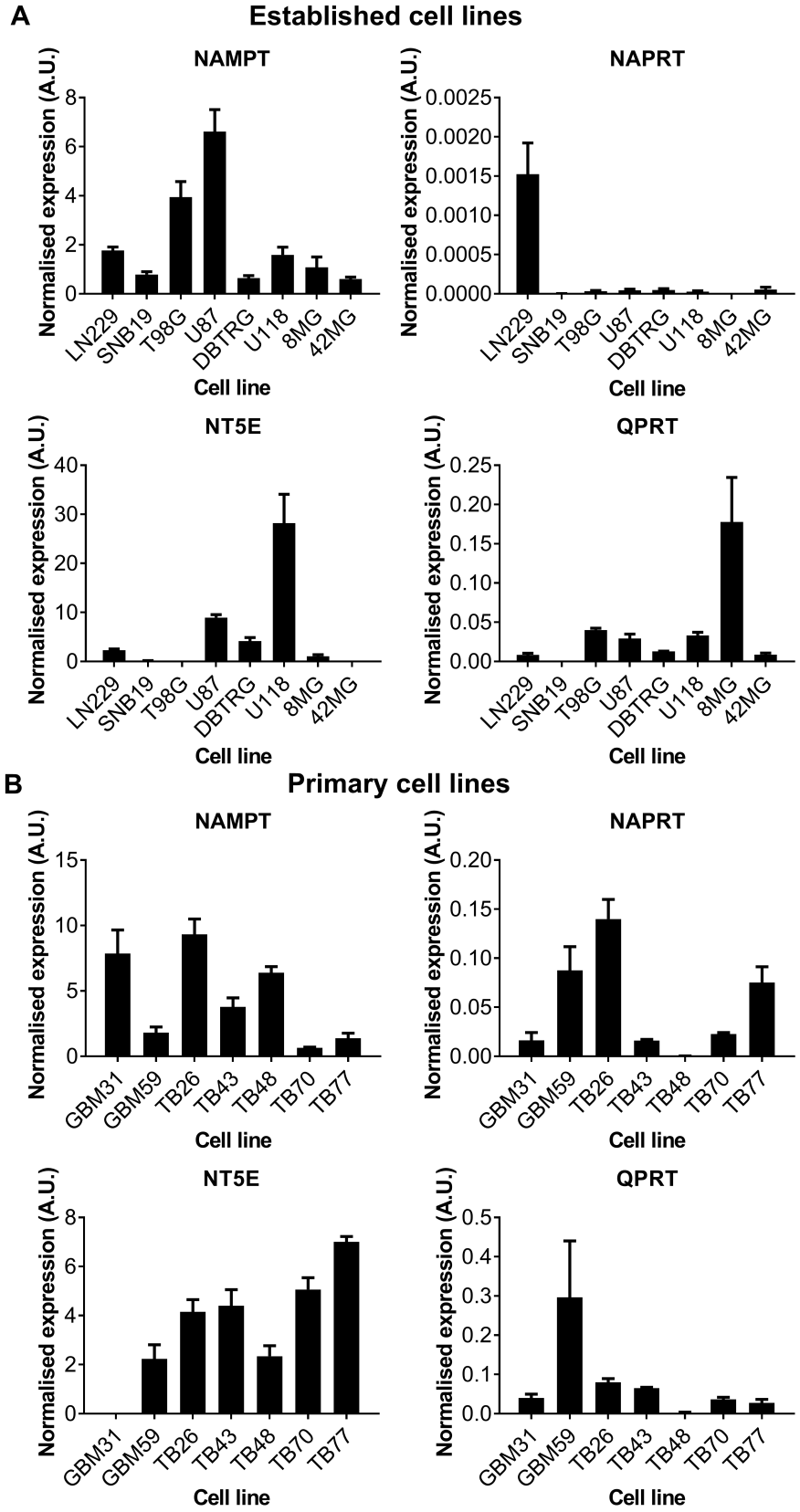


Figure 3.4: **Expression of genes involved in NAD biosynthesis is highly variable across GBM cell lines.** Bar charts showing qPCR data for key genes involved in NAD biosynthesis in (A) established and (B) primary GBM cell lines. Gene expression normalised to HPRT control. Data representative of three biological replicates. Error bars represent standard error of the mean (SEM).

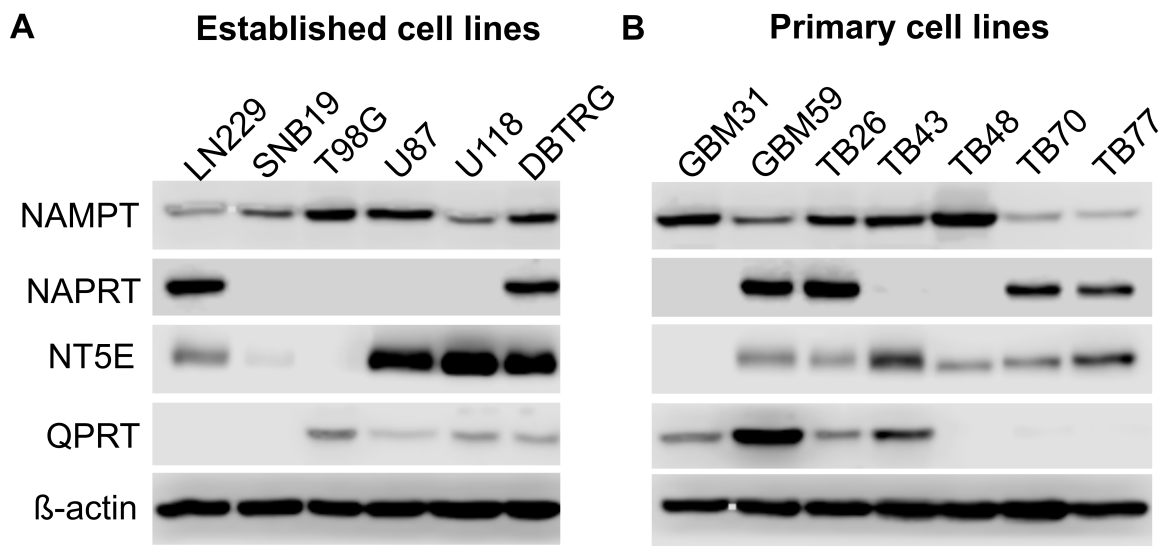


Figure 3.5: **Protein levels of genes involved in NAD biosynthesis are highly variable between GBM cell lines.** Western blot images showing protein bands for key enzymes involved in NAD biosynthesis in (A) established and (B) primary GBM cell lines.

3.3 Proliferation assays show variability in the sensitivity of GBM cell lines to NAMPT inhibition

To determine whether NAMPT inhibition could be an effective therapy in patients with GBM, established and primary GBM cell lines were treated with increasing concentrations of FK866 between 1 and 256 nM. Samples were analysed by SRB assay at 3, 6 and 9 days post-treatment. FK866 showed a time and dose dependent effect on all cell lines (Fig. 3.6, 3.7). FK866 appeared to have a relatively small therapeutic window in GBM cell lines (Fig. 3.8). Most of the GBM cell lines were highly sensitive to FK866, with IC_{50} values ranging from 5 to 35 nM (Table 3.1). However, 42MG cells showed hypersensitivity to FK866, with the IC_{50} below 1 nM. The established cell line DBTRG showed marked resistance to FK866, as did the primary cell line TB48. Another of the primary cell lines, GBM59, showed moderate sensitivity to FK866. These results suggest that whilst there is some variability in the sensitivity of GBM cell lines to FK866, most cell lines respond at very low concentrations.

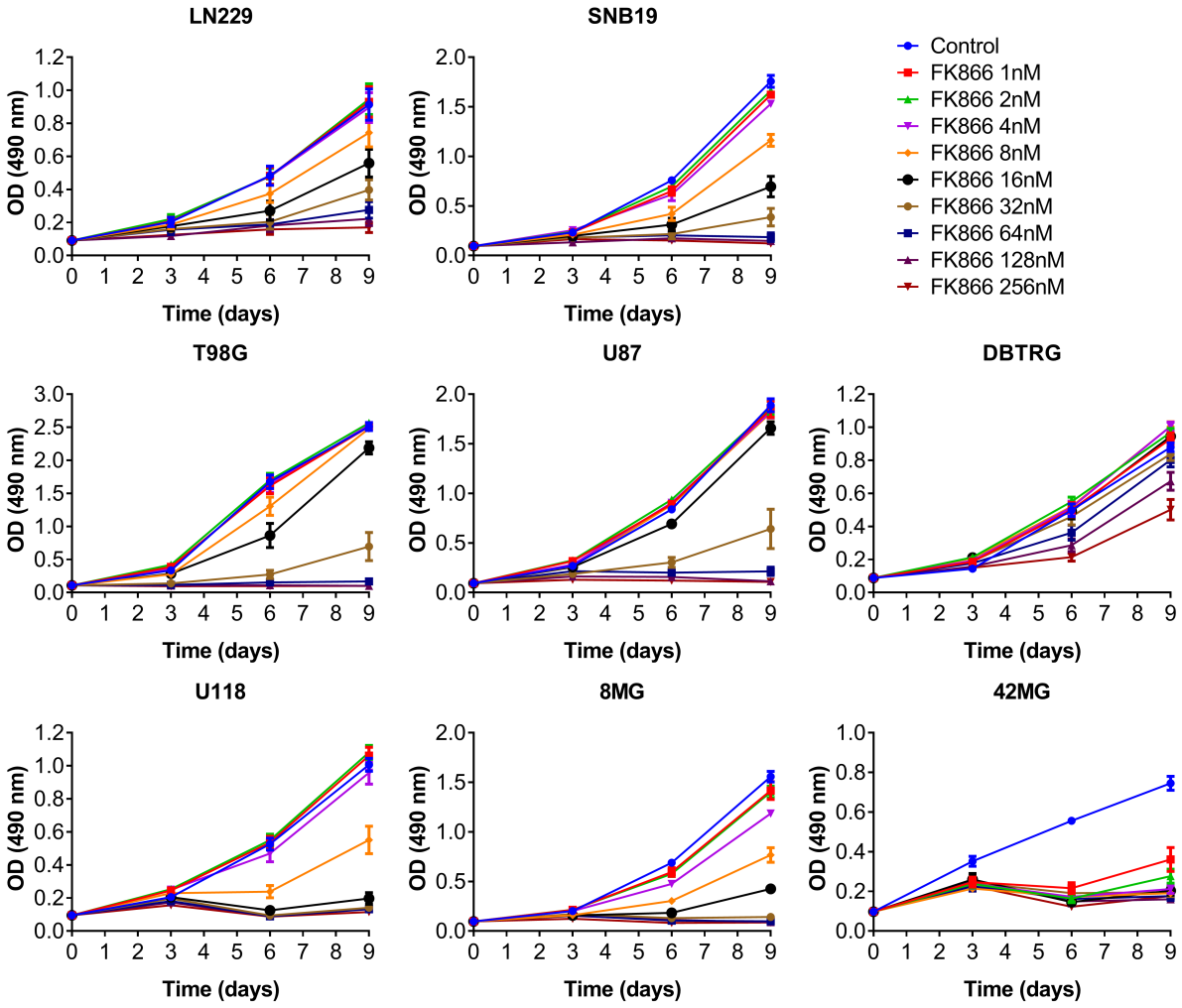


Figure 3.6: **FK866 has time and dose dependent effects on established GBM cell lines.** Dot and line plots showing proliferation measured by SRB assay (optical density (OD) 490 nm) over time in established GBM cell lines treated with increasing concentrations of FK866. Data representative of three independent experiments (n = 9 biological replicates). Error bars represent SEM.

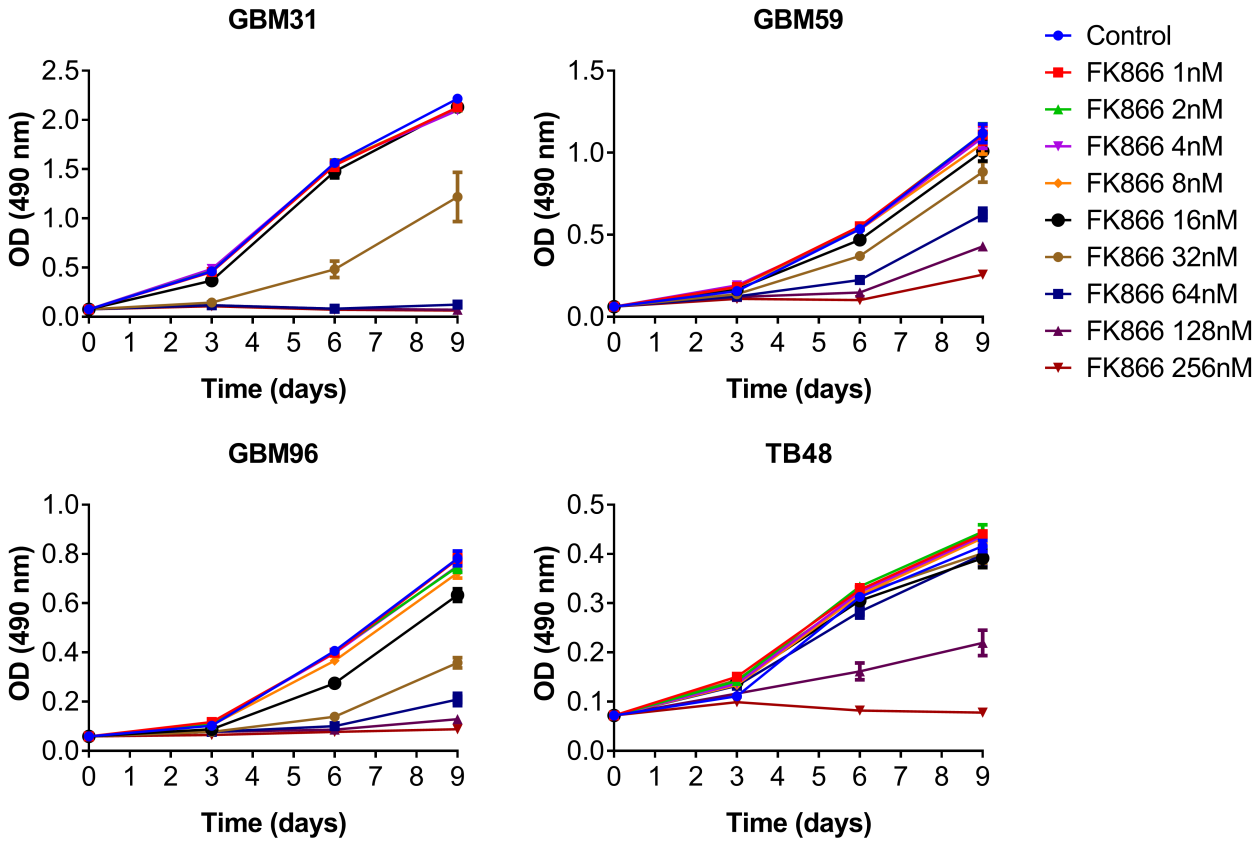


Figure 3.7: **FK866 has time and dose dependent effects on primary GBM cell lines.** Dot and line plots showing proliferation measured by SRB assay (OD 490 nm) over time in primary GBM cell lines treated with increasing concentrations of FK866. Data representative of three independent experiments (n = 9 biological replicates). Error bars represent SEM.

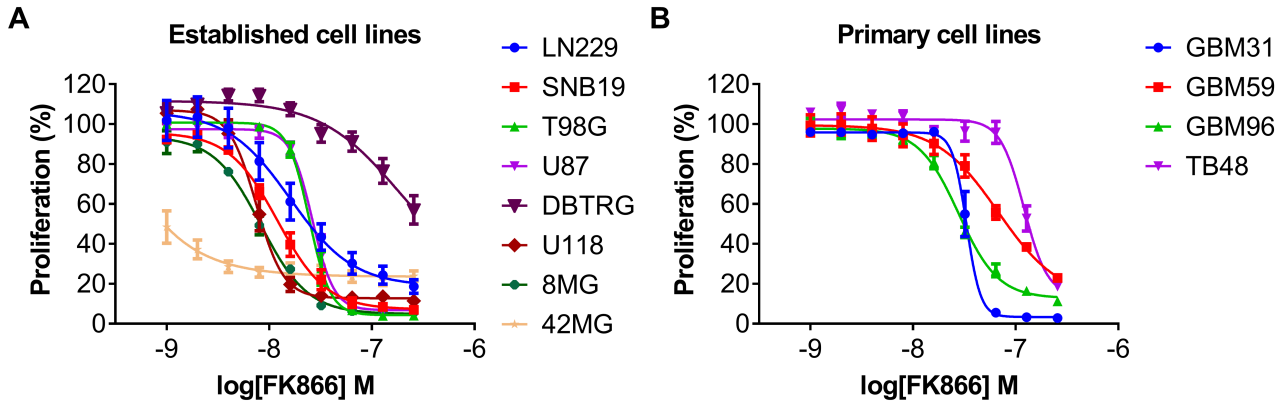


Figure 3.8: **NAMPT inhibition reduces proliferation in GBM cell lines.** Dot and line plots generated from SRB assay data showing changes in proliferation with increasing doses of FK866 in GBM cell lines in both (A) established and (B) primary GBM cell lines. Data from day 9 only. Lines of best fit represent a sigmoidal dose response curve. Proliferation normalised to vehicle control. Data representative of three independent experiments (n = 9 biological replicates). Error bars represent SEM.

Cell line	**FK866 IC50** (nM)
LN229	16.06
SNB19	12.06
T98G	24.47
U87	26.26
DBTRG	180.30
U118	7.46
8MG	8.28
42MG	<1.00
GBM31	33.22
GBM59	67.59
GBM96	27.79
TB48	120.40

Table 3.1: **Table showing the IC_{50} values for FK866 in different GBM cell lines.** IC_{50} values calculated using a sigmoidal dose response curve. Data representative of three independent experiments (n = 9 biological replicates).

3.4 NAMPT inhibition does not affect apoptosis or cell death in GBM cell lines

Given that FK866 was able to inhibit proliferation in a number of GBM cell lines, I next wanted to determine the exact method by which FK866 elicited this response. The GBM cell lines LN229 and U87 were treated with FK866 (20 nM) or vehicle control, and analysed at 3, 6 and 9 days post-treatment. At each timepoint, samples were stained with either Annexin V or trypan blue to assess apoptosis and cell viability/cell death, respectively. There was a very small but significant decrease in the population of live cells in LN229 cells treated with FK866 at day 6, but this was not seen at any other timepoint ($P < 0.05$, Fig. 3.9A, C). Neither cell line showed any significant change in the early/late apoptotic or dead cell populations at any timepoint (Fig. 3.9B).

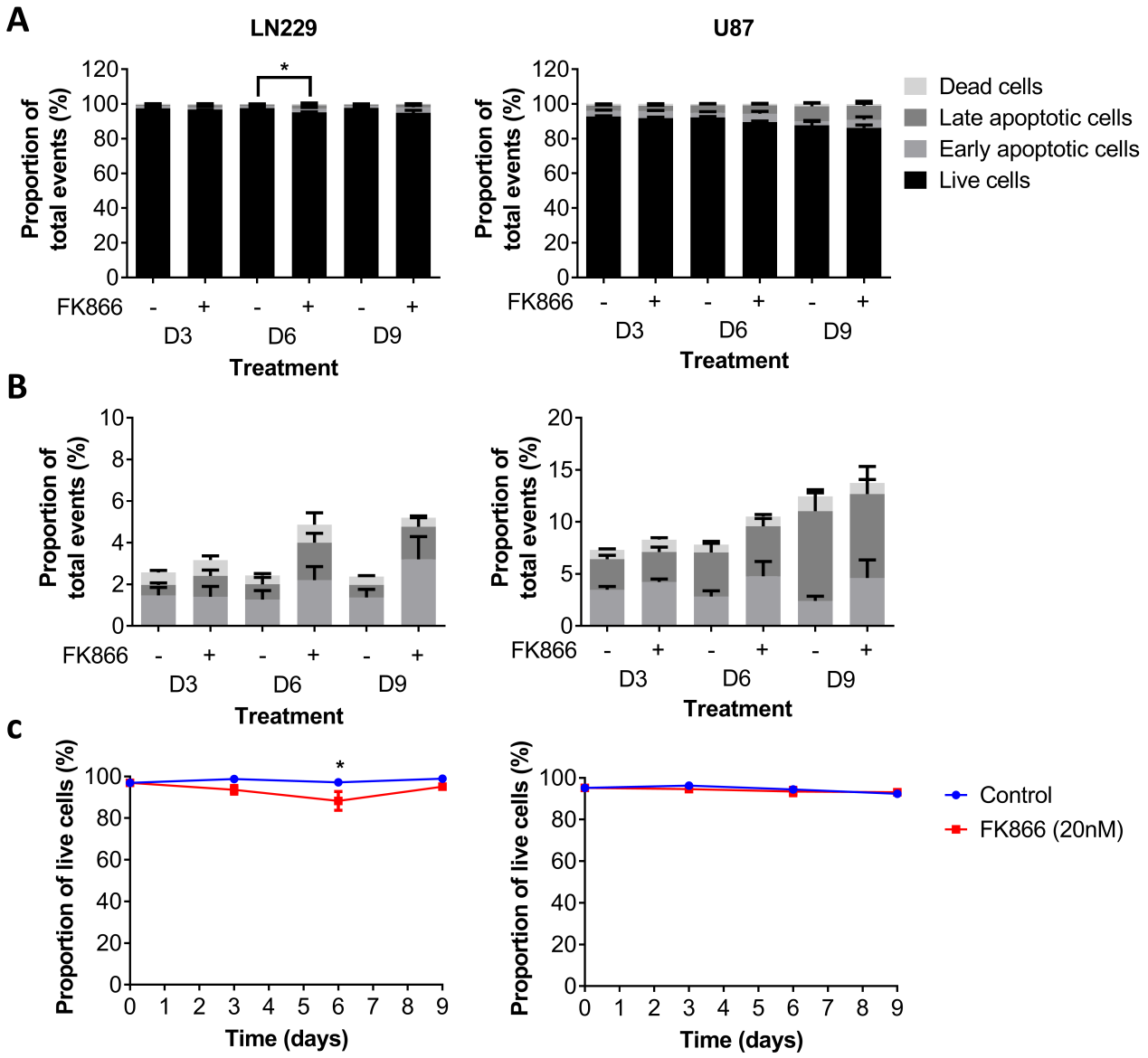


Figure 3.9: **FK866 does not activate apoptosis or initiate cell death in GBM cell lines.** (A) Stacked bar graphs showing the proportion of cells in different phases of apoptosis when treated with FK866 (20 nM) at different timepoints. (B) Line graphs showing the change in viability in GBM cells treated with FK866 (20 nM) over time. * $P < 0.05$, two-way ANOVA with Tukey's HSD post-hoc test. Data representative of three independent experiments (n = 3 biological replicates). Error bars represent SEM.

3.5 NAMPT inhibition causes a G_2/M cell cycle block in GBM cell lines

Given that FK866 did not appear to initiate apoptosis or cell death, I next looked to another major aspect of cell growth; the cell cycle. LN229 and U87 cell lines were treated with FK866 (20 nM) or vehicle control. At 3, 6 and 9 days post-treatment, the cells were fixed in methanol and stained with PI, then analysed on a flow cytometer. In LN229 cells, treatment with FK866 led to a shift in the cell cycle, with a significant decrease in the G_1/G_0 population, and a significant increase in the G_2/M population ($P < 0.05$, Fig. 3.10). This suggests that FK866 causes a G_2/M phase block, preventing the cells from completing mitosis and therefore inhibiting proliferation. Somewhat surprisingly, the same pattern was not established in the U87 cell line.

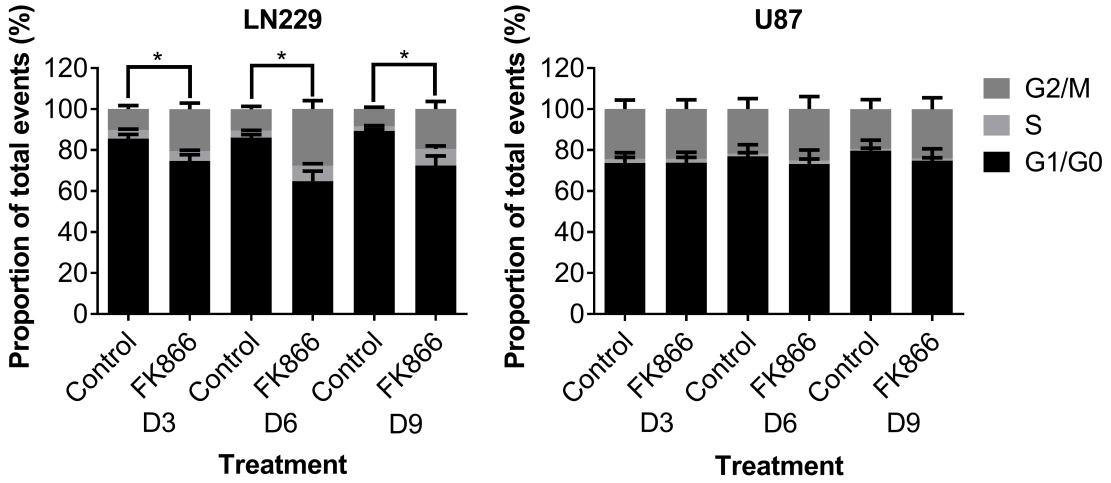


Figure 3.10: **FK866 causes a G_2/M cell cycle arrest in GBM cells.** Stacked bar graphs showing the proportion of cells in each stage of the cell cycle when treated with FK866 (20 nM) at different timepoints. * $P < 0.05$, two-way ANOVA with Tukey's HSD post-hoc test. Data representative of three independent experiments (n = 3 biological replicates). Error bars represent SEM.

3.6 Discussion

The data presented here highlight the variability both in the expression of enzymes involved in NAD biosynthesis within GBM tumours, and their relationship with survival in patients with

GBM. Consistent with previous results, both NAMPT and NT5E are upregulated in GBM tissue compared to normal healthy control tissue, and high expression of either of them is linked to lower overall survival times (Reddy et al., 2008; Xu et al., 2013). Furthermore, the expression of NAMPT is slightly higher in recurrent GBM tissue, suggesting that it may contribute to chemo- or radio-resistance during treatment of the primary tumour. The relationship between IDH1 and ATRX mutations is consistent with patterns seen in low grade gliomas. These two mutations are often seen together, along with TP53 mutations (The Cancer Genome Atlas Research Network, 2015). Therefore, these samples are highly likely to be secondary GBMs that have developed over a much longer period of time from low grade gliomas. The clustering of IDH1 mutations by their expression of genes involved in NAD biosynthesis is consistent with its recently reported effects on NAPRT activity Tateishi et al., 2015. Inhibition of NAPRT activity by IDH1-derived 2HG prevents the cells from utilising NA to produce NAD, and cancer cells may upregulate other NAD biosyntheitc pathways to compensate. Whilst NAPRT expression is not specifically increased in either primary or recurrent GBM tumours compared to healthy control tissue, its levels do appear to correlate with survival. Whilst NAPRT has previously been demonstrated to be mutated or amplified in numerous cancers, it has not previously been associated with survival (Piacente et al., 2017). The data here also show that QPRT is neither upregulated in GBM tissue, nor associated with survival in patients with GBM. This is somewhat at odds with another study, which demonstrated that QPRT was upregulated in GBM compared to low grade gliomas, and its expression is associated with survival in the Rembrandt dataset (Sahm et al., 2013). This suggests that changes in QPRT expression may be unique to secondary GBMs, which progress from a low grade glioma, but do not occur in primary GBMs.

There are clearly differences in the expression of key NAD biosynthetic genes within both established and primary GBM cell lines. In addition, the protein levels of each of these enzymes correlate well with their expression levels, indicating that there is little post-translational regulation of these genes. This further highlights the variability in the activities of different NAD biosynthetic pathways between GBM tumours. In particular, NAPRT is only expressed in $\sim$46% of the cell lines screened. This is consistent with previous results, which have demon-

strated that 50-70% of GBM cell lines lack detectable NAPRT protein, and would likely benefit from treatment with NAMPT inhibitors (Shames et al., 2013; Cole et al., 2017). It is particularly interesting that the expression levels of NAPRT are much higher in primary GBM cell lines compared to established cell lines. This suggests that NAPRT expression is lost in most GBM cell lines when grown in lab culture conditions. Normal culture media contains 32.8 µM Nam, but no NA (Thermo Fisher Scientific, 2018). These conditions create an environment where NAPRT expression is not advantageous, but high levels of NAMPT may promote proliferation in some of the cells. This could lead to selection of these cells in culture, resulting in the eventual elimination of the NAPRT expressing cells.

Treatment of both established and primary GBM cell lines with FK866 showed that it has both time- and dose- dependent effects. FK866 is known to be a highly specific inhibitor of NAMPT, and therefore the effects on proliferation are directly attributable to this interaction (Hasmann and Schemainda, 2003). In some of the cell lines, there appeared to be a slight recovery in proliferation between 6 and 9 days, which could indicate either detoxification/elimination of FK866, or the development of a resistant sub-population. The minimal effect of FK866 on apoptosis and cell death is consistent with published data (Zhang et al., 2012b). Much higher concentrations are required to initiate apoptosis than to inhibit proliferation (Yang et al., 2015c). The G_2/M cell cycle block seen in LN229 cells is also consistent with previous results in C6 glioma cells (Zhang et al., 2012b). The lack of any response in U87 cells likely represents a failure to achieve sufficient NAD depletion to cause a significant shift in the cell cycle. Whilst time- and dose-dependent studies should that FK866 concentrations as low as 16 µM could limit proliferation, the IC_{50} for U87 cells is actually 26.26 µM (Table 3.1). Higher concentrations would likely yield similar results to those seen with LN229.

Chapter 4

The role of alternative NAD biosynthetic pathways in resistance to NAMPT inhibition

In silico and *in vitro* data indicated that whilst there was variability in the expression of genes involved in NAD biosynthesis in GBM tumours, GBM cells were highly sensitive to NAMPT inhibitors. I next aimed to determine what mechanisms could affect sensitivity to NAMPT inhibitors in GBM cells by investigating different resistance pathways. Identifying which pathways contribute to resistance to NAMPT inhibitors could allow us to select a subset of GBM patients most likely to benefit from treatment with this class of compounds. To determine the roles of different NAD biosynthetic pathways in resistance to NAMPT inhibition, it was necessary to interrogate each pathway individually. This allowed me to identify the contribution of each pathway to NAD biosynthesis independent of other factors. To do this, I selected four different GBM cell lines that expressed some of the key genes involved in NAD biosynthesis, but lacked at least one. These are summarised in Table 4.1.

4.1 GBM cells expressing NAPRT utilise NA as an alternative source of NAD during treatment with a NAMPT inhibitor

NAPRT is part of the Preiss-Handler pathway, which allows the generation of NAD from dietary NA through the action of NAPRT, the NMNAT family, and NADSYN1. To determine whether this pathway could affect the efficacy of NAMPT inhibitors in GBM, four different GBM cell lines were treated with FK866 (20 nM), both alone and in combination with the NAD precursor NA (10 µM). Proliferation was measured by SRB assay at 3, 6 and 9 days. FK866 treatment led to a significant decrease in proliferation in all cell lines ($P < 0.05$, Fig. 4.1). The addition of NA to FK866-treated cells completely restored proliferation to that of the untreated controls in LN229 and U87 cell lines ($P < 0.05$, Fig. 4.1). However, there was no rescue in proliferation in either SNB19 or T98G cells. These results were consistent with the expression of NAPRT in these four cell lines (Figs. 3.4, 3.5).

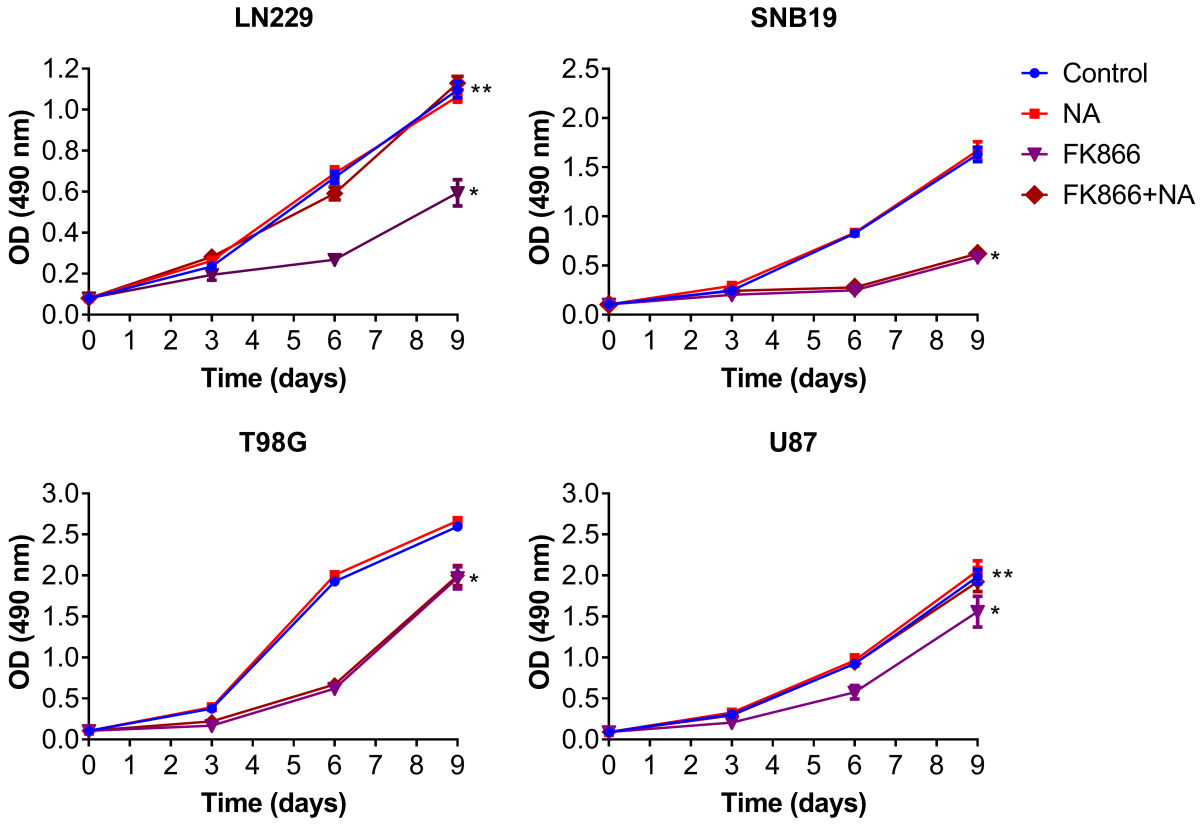


Figure 4.1: **NA rescues proliferation in GBM cells treated with FK866.** Dot and line plots showing proliferation measured by SRB assay [OD 490 nm] for different combinations of FK866 (20 nM) and the NAD precursor NA (10 µM). * $P < 0.05$ Control vs FK866, ** $P < 0.05$ FK866 vs FK866+NA, two-way ANOVA with Tukey's HSD post-hoc test. Data representative of three independent experiments (n = 9 biological replicates). Error bars represent SEM.

Given that NA was able to completely restore proliferation in some GBM cell lines, I wanted to determine whether this was directly linked to the recovery or maintenance of NAD and/or NADH levels. LN229 was chosen for these experiments, as it is sensitive to FK866, and expresses all of the key genes involved in the different metabolic pathways, namely NAMPT, NAPRT, NT5E and QPRT. LN229 cells were treated with FK866 (20 nM) with or without NA (10 µM). The Promega NAD/NADH-Glo Assay was then used to quantify NAD and NADH levels at 0, 12, 24, 48 and 72 hours. These early timepoints were chosen because whilst FK866 treatment tends to have a delayed effect on proliferation, studies have shown that it rapidly depletes NAD levels (Hasmann and Schemainda, 2003; Goellner et al., 2011; Grozio et al., 2013; Sociali et al., 2015). FK866 caused a rapid decline in both NAD and NADH levels between 0 and 24 hours, after which NAD levels were maintained at significantly lower levels compared to

vehicle control for the duration of the experiment ($P < 0.05$, Fig. 4.2). However, there was still a small pool of NADH present in the cells even at 72 h. Alone, NA boosted NAD levels in LN229 cells compared to vehicle control, resulting in a significant increase in the NAD/NADH ratio at 12 and 24 h ($P < 0.05$, Fig. 4.2). In the presence of FK866, NA was able to maintain both NAD and NADH levels at much higher levels compared to FK866 alone, very close to those seen in the vehicle control ($P < 0.05$, Fig. 4.2). Furthermore, the NAD/NADH ratio was maintained at almost exactly the same level as the vehicle control when FK866-treated cells were supplemented with NA. These results show that the changes seen in proliferation with NAMPT inhibition are directly linked to NAD levels, and NAD levels can be maintained with an exogenous supply of NA.

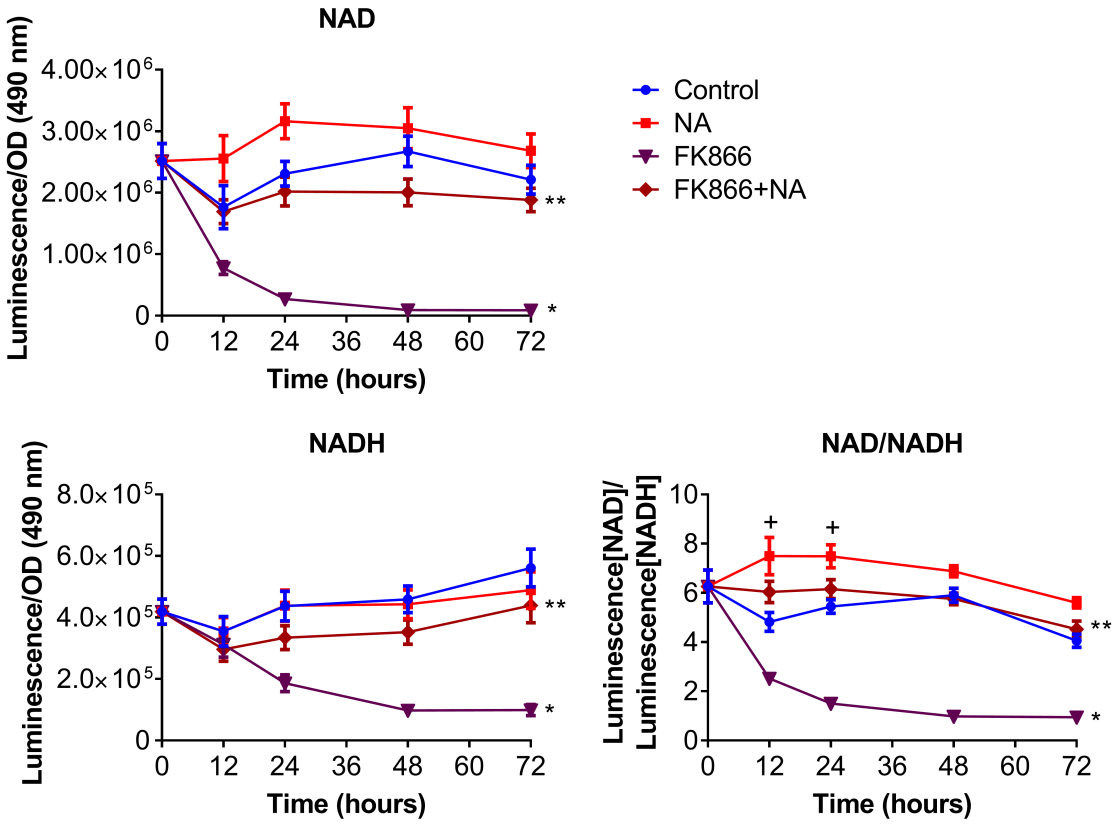


Figure 4.2: **NA maintains NAD and NADH levels in LN229 cells treated with FK866.** NAD and NADH levels were measured using the Promega NAD/NADH-Glo Assay in LN229 cells treated with FK866 (20 nM) with or without NA (10 µM). * $P < 0.05$ Control vs FK866, ** $P < 0.05$ FK866 vs FK866+NA, $^{+}$ $P < 0.05$ Control vs NA, two-way ANOVA with Tukey's HSD post-hoc test. Data representative of three independent experiments (n = 9 biological replicates). Error bars represent SEM.

Despite seeing little to no change in apoptosis or cell viability with FK866 treatment, I wanted to investigate whether or not NAD precursors, or inhibitors of other NAD biosynthetic pathways, could have an effect, either independently, or in an FK866-treated setting. LN229 cells were treated with FK866 (20 nM) with or without NA (10 µM), then apoptosis and cell viability were measured using Annexin V and trypan blue staining respectively at 3, 6 and 9 days. Consistent with previous results, the addition of FK866 did not significantly alter the apoptotic profile of LN229 cells at any timepoint (Fig. 4.3A). There was a very small drop in cell viability in LN229 cells treated with FK866 which could be reversed by the addition of NA, but this was not statistically significant (Fig. 4.3B). This indicates that the primary rescue mechanism using NA does not relate to the activation of apoptosis or cell death.

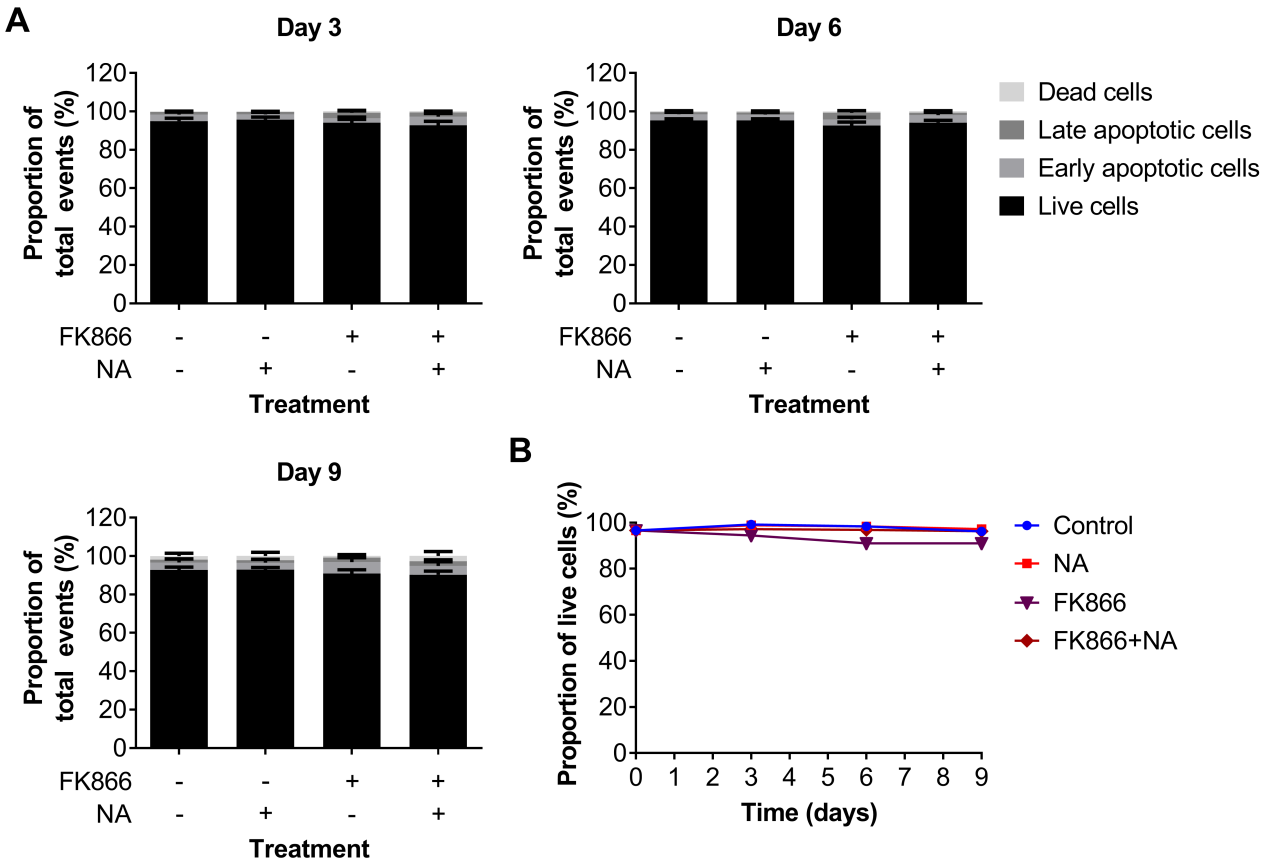


Figure 4.3: **NA does not affect apoptosis or cell viability when added to FK866 in LN229 cells.** LN229 cells were treated with FK866 (20 nM) with or without NA (10 µM). (A) bar charts showing Annexin V staining at 3, 6 and 9 days (B) dot and line graph showing the proportion of viable cells over time. Data representative of three independent experiments (n = 3 biological replicates). Error bars represent SEM.

I previously demonstrated that FK866 caused a block in the cell cycle at G_2/M phase (Fig. 3.10). To determine whether the addition of NA could reverse this phenotype, LN229 cells were treated with FK866 (20 nM) with or without NA (10 µM), stained with PI and analysed by flow cytometry. Alone, FK866 caused a significant drop in the number of cells in G_1/G_0 and a significant increase in the number of cells in G_2/M at days 6 and 9 ($P < 0.05$, Fig. 4.4). The addition of NA to FK866-treated LN229 cells resulted in maintenance of a normal cell cycle compared to cells treated with FK866 alone, also at days 6 and 9 ($P < 0.05$, Fig. 4.4). This shows that NA is able to completely restore a normal cell cycle in GBM cells treated with FK866.

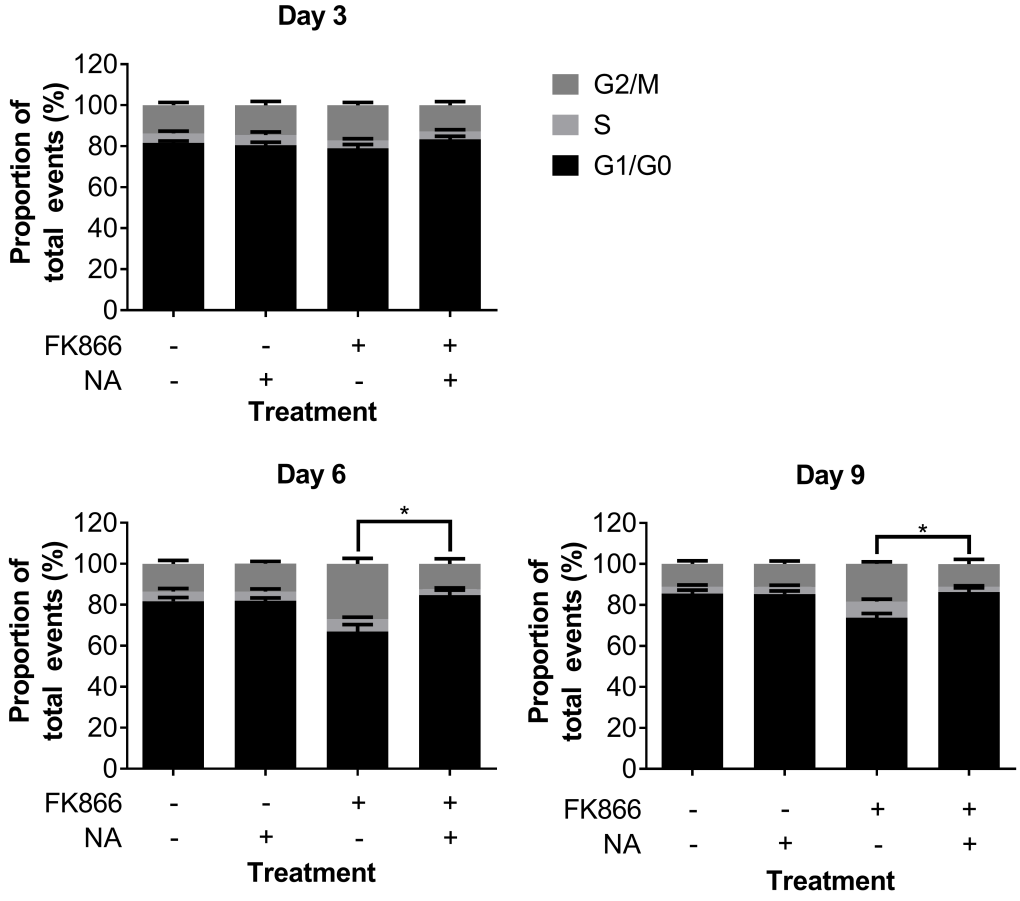


Figure 4.4: **NA restores a normal cell cycle in LN229 cells treated with FK866.** LN229 cells were treated with FK866 (20 nM) with or without NA (10 µM), and cells were fixed at 3, 6 and 9 days. Cell cycle status was determined by PI staining and flow cytometry. * $P < 0.05$, two-way ANOVA with Tukey's HSD post-hoc test. Data representative of three independent experiments (n = 3 biological replicates). Error bars represent SEM.

4.2 NT5E activity is required in GBM to fuel NAD biosynthesis from NMN in the presence of NAMPT inhibitors

NT5E has only recently been identified as a major source of NAD production (Grozio et al., 2013). NT5E is able to metabolise the conversion of NAD or NMN to NR, which can then pass through nucleotide transporters in the cell membrane and fuel NAD biosynthesis through the action of NMRK1/2. To determine whether this pathway could affect the efficacy of NAMPT inhibitors in GBM, four different GBM cell lines were treated with FK866 (20 nM), NMN (10 µM) and the NT5E inhibitor APCP (100 µM) alone and various combinations. Proliferation was measured by SRB assay at 3, 6 and 9 days. The data showed also that the addition of NMN to FK866 significantly increased proliferation in all cell lines ($P < 0.05$, Fig. 4.5A, B). Furthermore, in the LN229 and SNB19 cell lines, the addition of the NT5E inhibitor APCP significantly limited the rescue induced by NMN ($P < 0.05$, Fig. 4.5A, B). These results suggest that NT5E activity is required to allow exogenous NMN to support proliferation in some GBM cell lines.

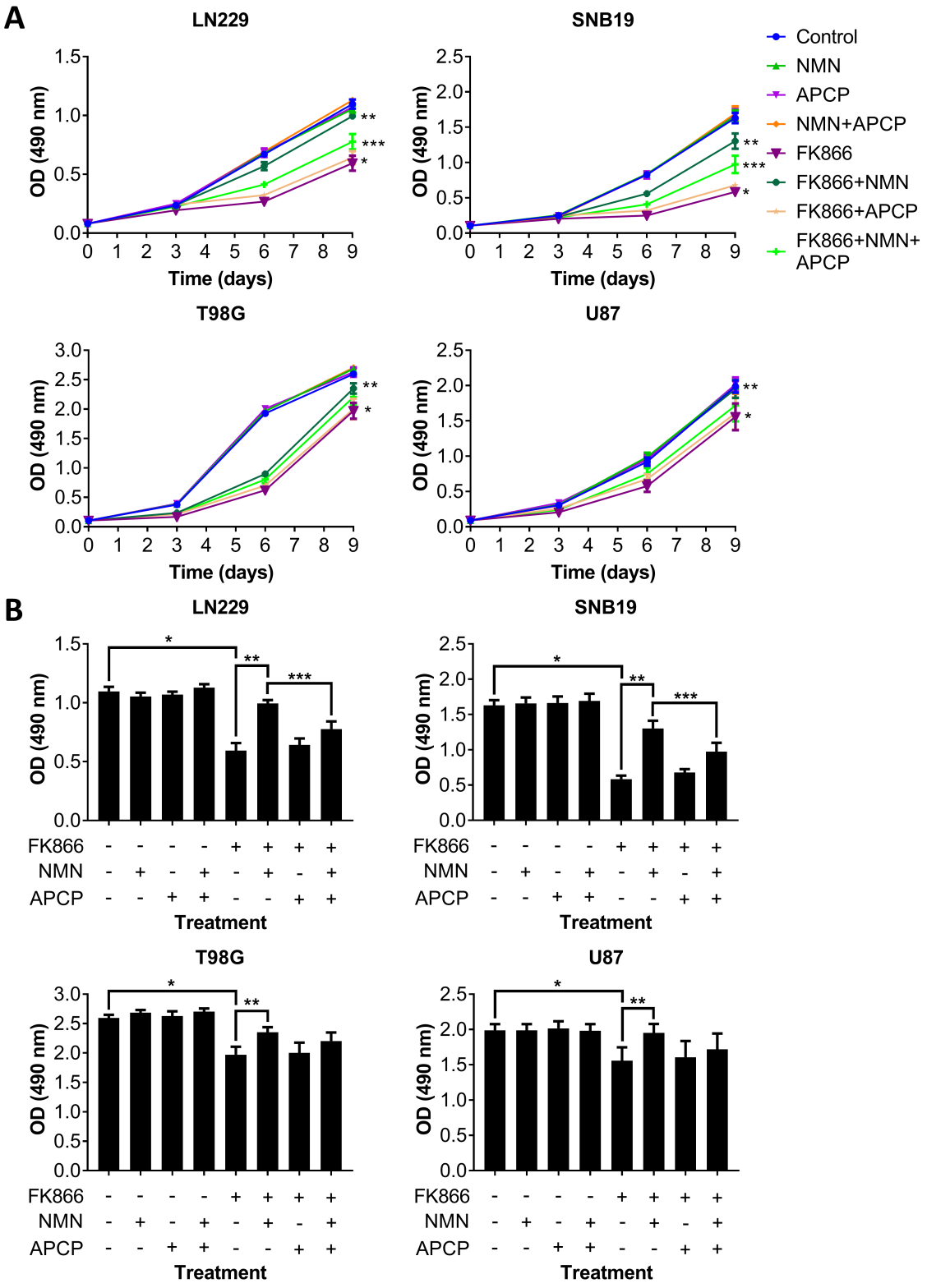


Figure 4.5: **NMN rescues proliferation in GBM cells treated with FK866.** Dot and line plots showing proliferation measured by SRB assay (OD 490 nm) for different combinations of FK866 (20 nM), the NAD precursor NMN (10 µM) and the NT5E inhibitor APCP (100 µM). * $P < 0.05$ Control vs FK866, ** $P < 0.05$ FK866 vs FK866+NMN, *** $P < 0.05$ FK866+NMN vs FK866+NMN+APCP, two-way ANOVA with Tukey's HSD post-hoc test. Data representative of three independent experiments (n = 9 biological replicates). Error bars represent SEM.

Considering that NMN was able to partially restore proliferation in all GBM cell lines, I wanted to determine whether this was directly linked to the recovery or maintenance of NAD and/or NADH levels. LN229 cells were treated with FK866 (20 nM), NMN (10 µM) and APCP (100 µM) alone and in various combinations. The Promega NAD/NADH-Glo Assay was then used to quantify NAD and NADH levels at 0, 12, 24, 48 and 72 hours. Alone, NMN had no effect on NAD or NADH levels, or the NAD/NADH ratio. Furthermore, in the presence of FK866, NMN was only able to maintain NAD and NADH levels slightly higher than FK866 alone, but this was not statistically significant. These results show that whilst NMN may be able to support proliferation in the presence of FK866, it only has a very small affect on NAD and NADH levels.

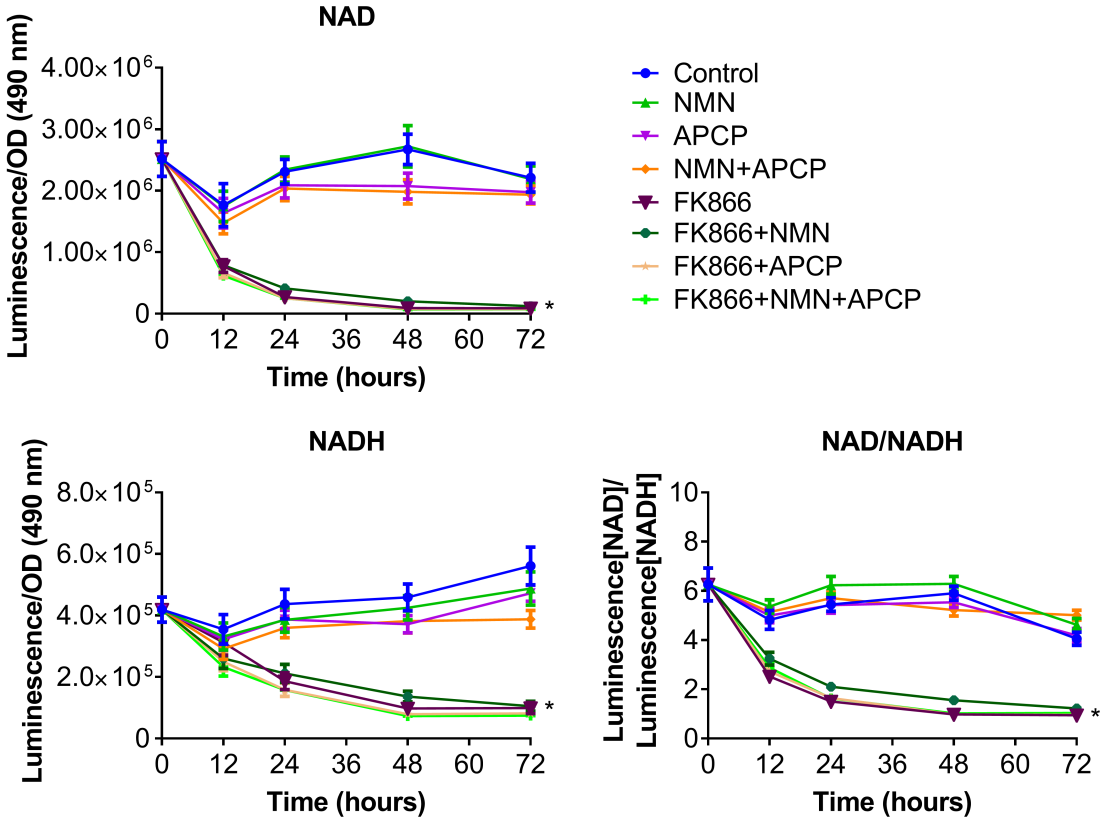


Figure 4.6: **NMN partially maintains NAD and NADH levels in LN229 cells treated with FK866.** NAD and NADH levels were measured using the Promega NAD/NADH-Glo Assay in LN229 cells treated with FK866 (20 nM), NMN (10 µM) and APCP (100 µM) alone and in various combinations. * $P < 0.05$ Control vs FK866, two-way ANOVA with Tukey's HSD post-hoc test. Data representative of three independent experiments (n = 9 biological replicates). Error bars represent SEM.

I next wanted to determine whether the restoration of proliferation by NMN or inhibition of NT5E using APCP could affect apoptosis or cell viability in GBM cells treated with FK866. LN229 cells were treated with FK866 (20 nM), NMN (10 µM) and APCP (100 µM) alone and in various combinations, then apoptosis and cell viability were measured using Annexin V and trypan blue staining respectively at 3, 6 and 9 days. There was no effect on apoptosis (Fig. 4.7A), and whilst there was a very small drop in cell viability in LN229 cells treated with FK866 which could be reversed by the addition of NMN, this was not statistically significant (Fig. 4.7B). Furthermore, the addition of APCP did not alter this effect. This indicates that the primary rescue mechanism using NMN does not relate to the activation of apoptosis and cell death, and combined inhibition of NAMPT and NT5E has no effect on apoptosis or cell viability in GBM cells.

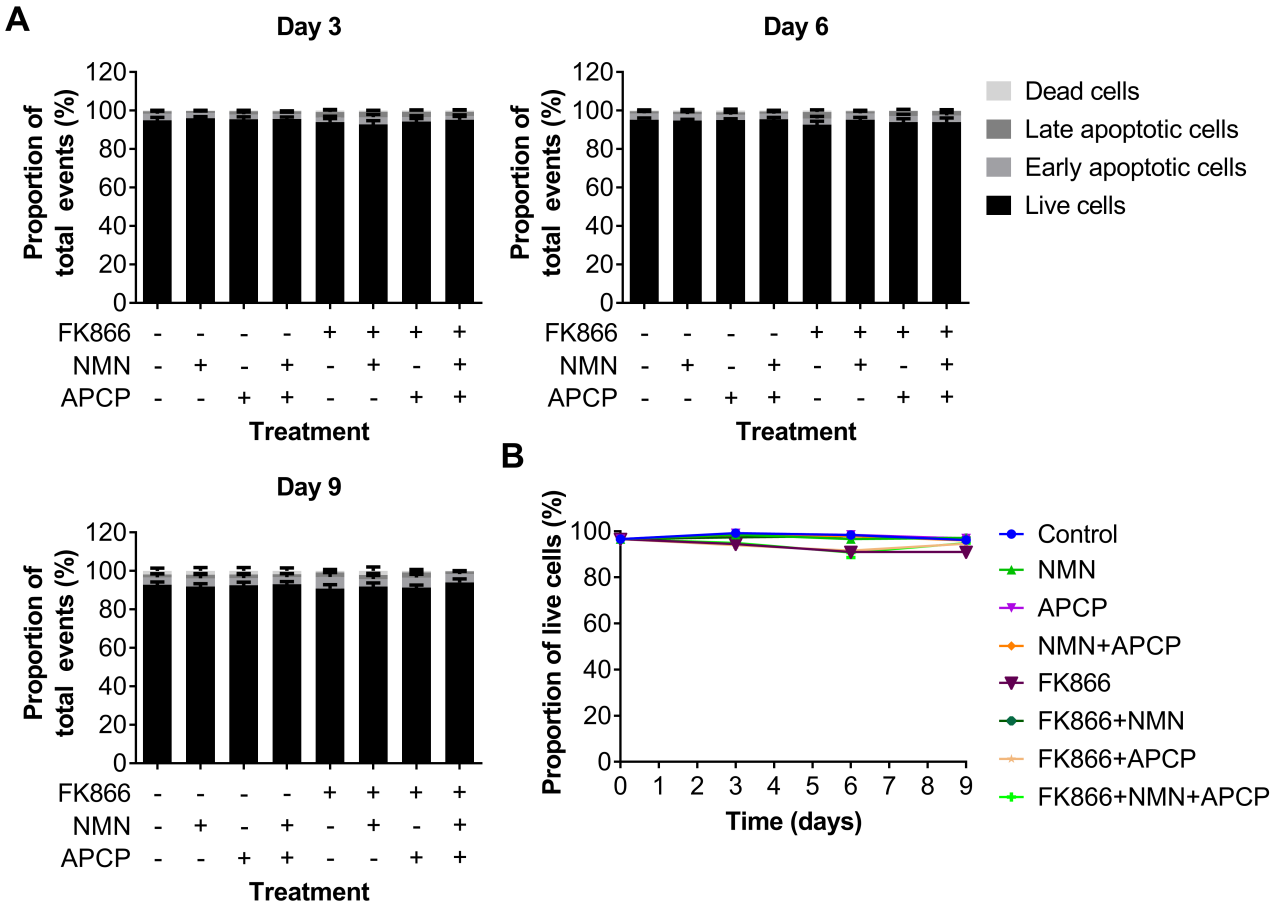


Figure 4.7: **NMN does not affect apoptosis or cell viability when added to FK866 in LN229 cells.** LN229 cells were treated with FK866 (20 nM), NMN (10 µM) and APCP (100 µM) alone and in various combinations. (A) bar charts showing Annexin V staining at 3, 6 and 9 days (B) dot and line graph showing the proportion of viable cells over time. Data representative of three independent experiments (n = 3 biological replicates). Error bars represent SEM.

To determine whether the addition of NMN could reverse the changes seen in the cell cycle with FK866 treatment, LN229 cells were treated with FK866 (20 nM), NMN (10 µM) and APCP (100 µM) alone and in various combinations, stained with PI and analysed by flow cytometry. The addition of NMN to FK866-treated cells resulted in the maintenance of a normal cell cycle compared to cells treated with FK866 alone at days 6 and 9 ($P < 0.05$, Fig. 4.8). In addition, the NT5E inhibitor APCP was able to completely block this recovery, also at 6 and 9 days ($P < 0.05$, Fig. 4.8). This further proves the link between NT5E activity and the ability of GBM cells to utilise extracellular NMN as a source of NAD.

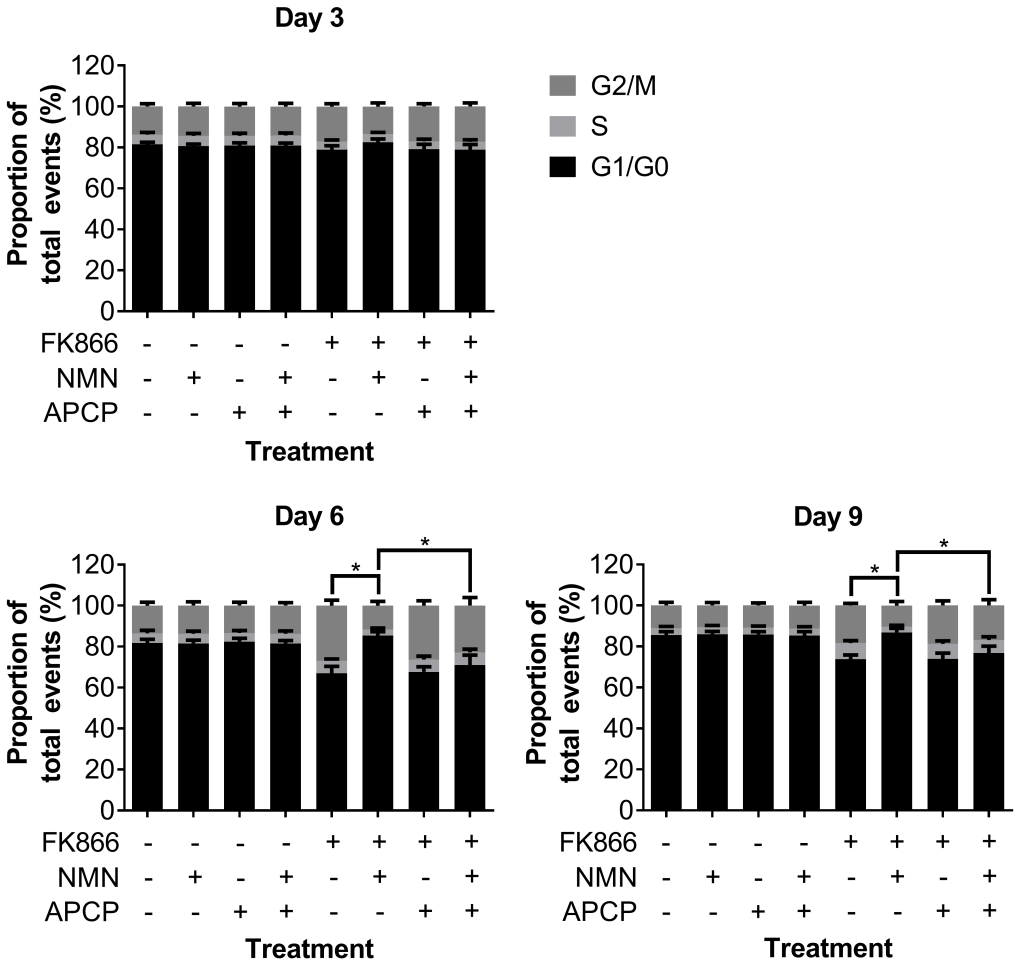


Figure 4.8: **NMN restores a normal cell cycle in LN229 cells treated with FK866.** LN229 cells were treated with FK866 (20 nM), NMN (10 µM) and APCP (100 µM) alone and in various combinations, and cells were fixed at 3, 6 and 9 days. Cell cycle status was determined by PI staining and flow cytometry. * $P < 0.05$, two-way ANOVA with Tukey's HSD post-hoc test. Data representative of three independent experiments (n = 3 biological replicates). Error bars represent SEM.

4.3 QA promotes proliferation in GBM cells treated with a NAMPT inhibitor

QPRT metabolises the final step in the kynurenine pathway, catalysing the conversion of QA to the NAD precursor NaMN. This joins into the NAPRT pathway, with NAD being generated through the action of the NMNAT family and NADSYN1. To determine whether this pathway could affect the efficacy of NAMPT inhibitors in GBM, four different GBM cell lines were

treated with FK866 (20 nM), QA (100 µM) and the QPRT inhibitor phthalic acid (PA) (10 µM) alone and in various combinations. Proliferation was measured by SRB assay at 3, 6 and 9 days. The data showed that the addition of QA to FK866 significantly increased proliferation in LN229, T98G and U87 cells ($P < 0.05$, Fig. 4.9A, B). However, the addition of the QPRT inhibitor PA only suppressed this recovery in U87 cells. It had no effect on LN229 or T98G cells. Further validation of these experiments showed that increasing the concentration of PA from 10 µM to 100 µM led to no significant difference in any of the responsive cell lines, indicating that PA is not able to block this effect (Fig. 4.10).

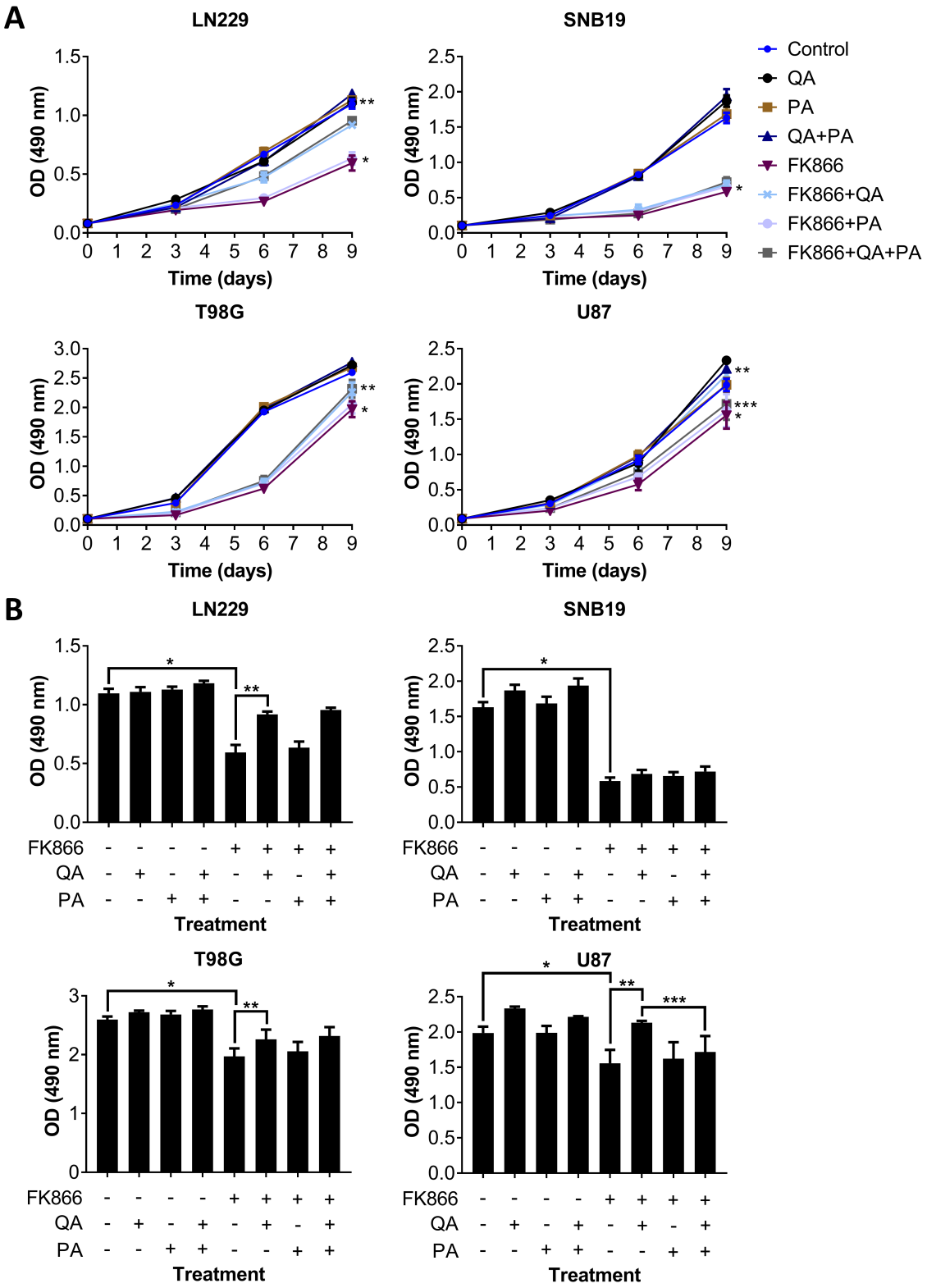


Figure 4.9: **QA rescues proliferation in GBM cells treated with FK866.** Dot and line plots showing proliferation measured by SRB assay (OD 490 nm) for different combinations of FK866 (20 nM), the NAD precursor QA (100 µM) and the QPRT inhibitor PA (10 µM). * $P < 0.05$ Control vs FK866, ** $P < 0.05$ FK866 vs FK866+QA, *** $P < 0.05$ FK866+QA vs FK866+QA+PA, two-way ANOVA with Tukey's HSD post-hoc test. Data representative of three independent experiments (n = 9 biological replicates). Error bars represent SEM.

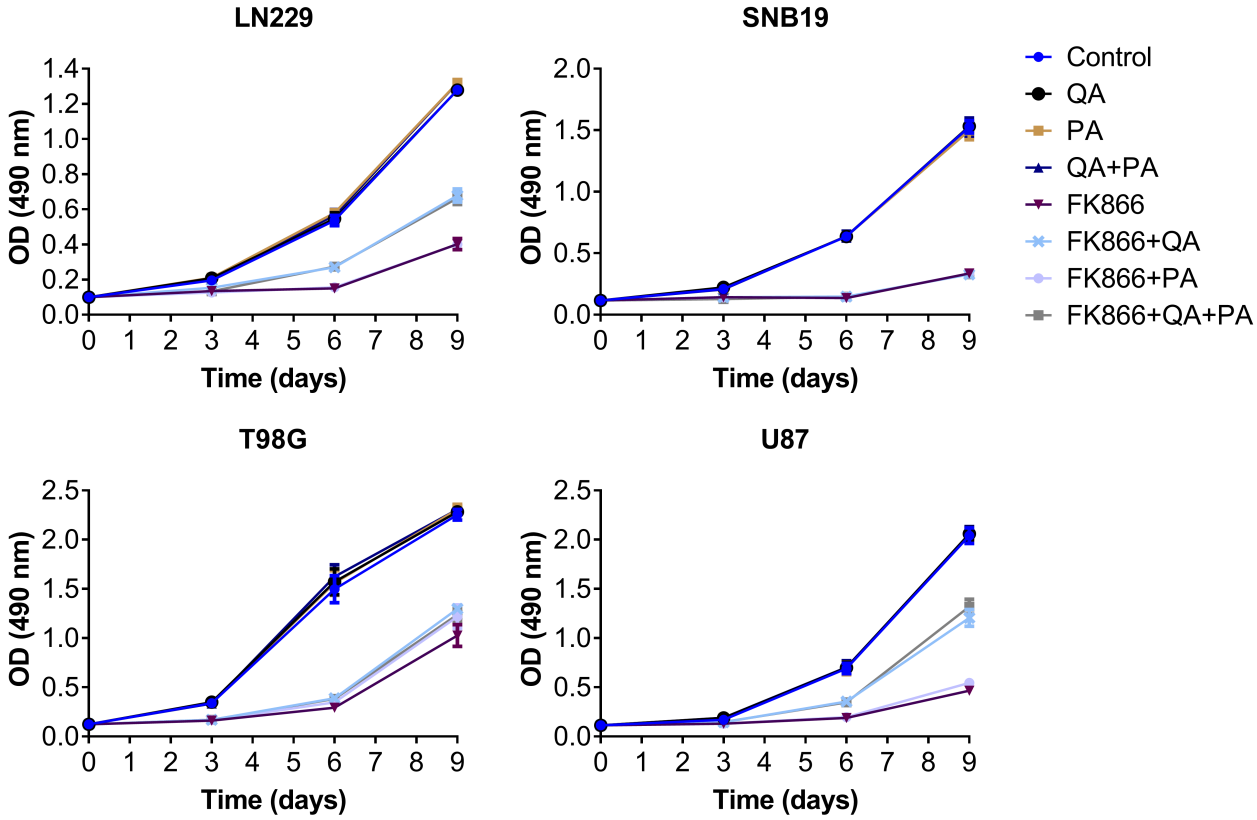


Figure 4.10: **Increased concentrations of PA does not lead to inhibition of QA mediated recovery in FK866 treated cells.** Dot and line plots showing proliferation measured by SRB assay (OD 490 nm) in cells treated with combinations of FK866 (20 nM), QA (100 µM) and PA (100 µM). Data representative of three independent experiments (n = 9 biological replicates). Error bars represent SEM.

Whilst QA was able to partially restore proliferation in some GBM cell lines, PA appeared to have no real effect. I next wanted to determine whether QA was directly affecting NAD or NADH levels. LN229 cells were treated with FK866 (20 nM), QA (100 µM) and PA (10 µM) alone and in various combinations. The Promega NAD/NADH-Glo Assay was then used to quantify NAD and NADH levels at 0, 12, 24, 48 and 72 hours. Neither QA nor PA had any effect on NAD or NADH levels either alone or in combination with FK866. This suggests that QA rescues proliferation in GBM cells through different mechanisms to the other two pathways.

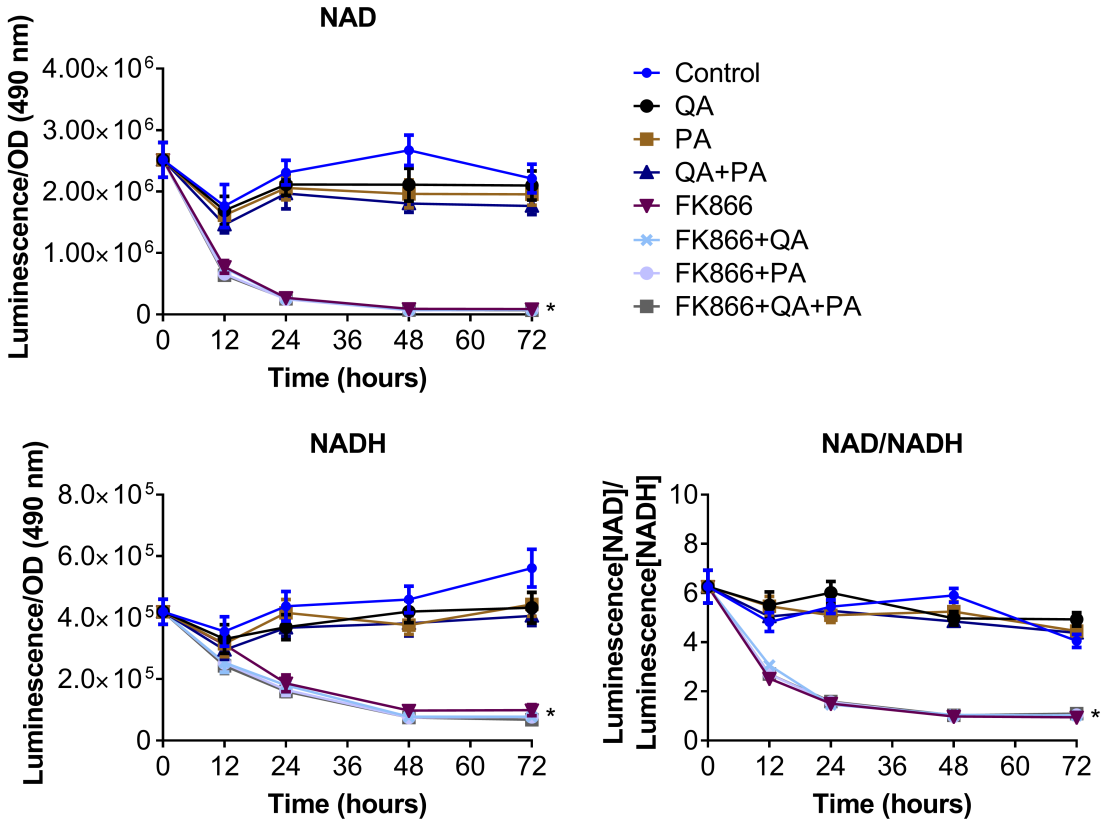


Figure 4.11: **QA does not maintain NAD and NADH levels in LN229 cells treated with FK866.** NAD and NADH levels were measured using the Promega NAD/NADH-Glo Assay in LN229 cells treated with FK866 (20 nM), QA (10 µM) and PA (10 µM) alone and in various combinations. * $P < 0.05$ Control vs FK866, two-way ANOVA with Tukey's HSD post-hoc test. Data representative of three independent experiments (n = 9 biological replicates). Error bars represent SEM.

I next wanted to determine whether QA or PA could have any effect on apoptosis or cell viability in cells treated with FK866. LN229 cells were treated with FK866 (20 nM), QA (100 µM) and PA (10 µM) alone and in various combinations, then apoptosis and cell viability were measured using Annexin V and trypan blue staining respectively at 3, 6 and 9 days. Consistent with previous results, the addition of FK866 did not significantly alter the apoptotic profile (Fig. 4.12A) or cell viability (Fig. 4.12B) in LN229 cells at any timepoint, and neither QA nor PA had any effect. This further reinforces the trend that FK866 does not initiate cell death, but rather blocks proliferation, and interference with other NAD biosynthetic pathways cannot alter this phenotype.

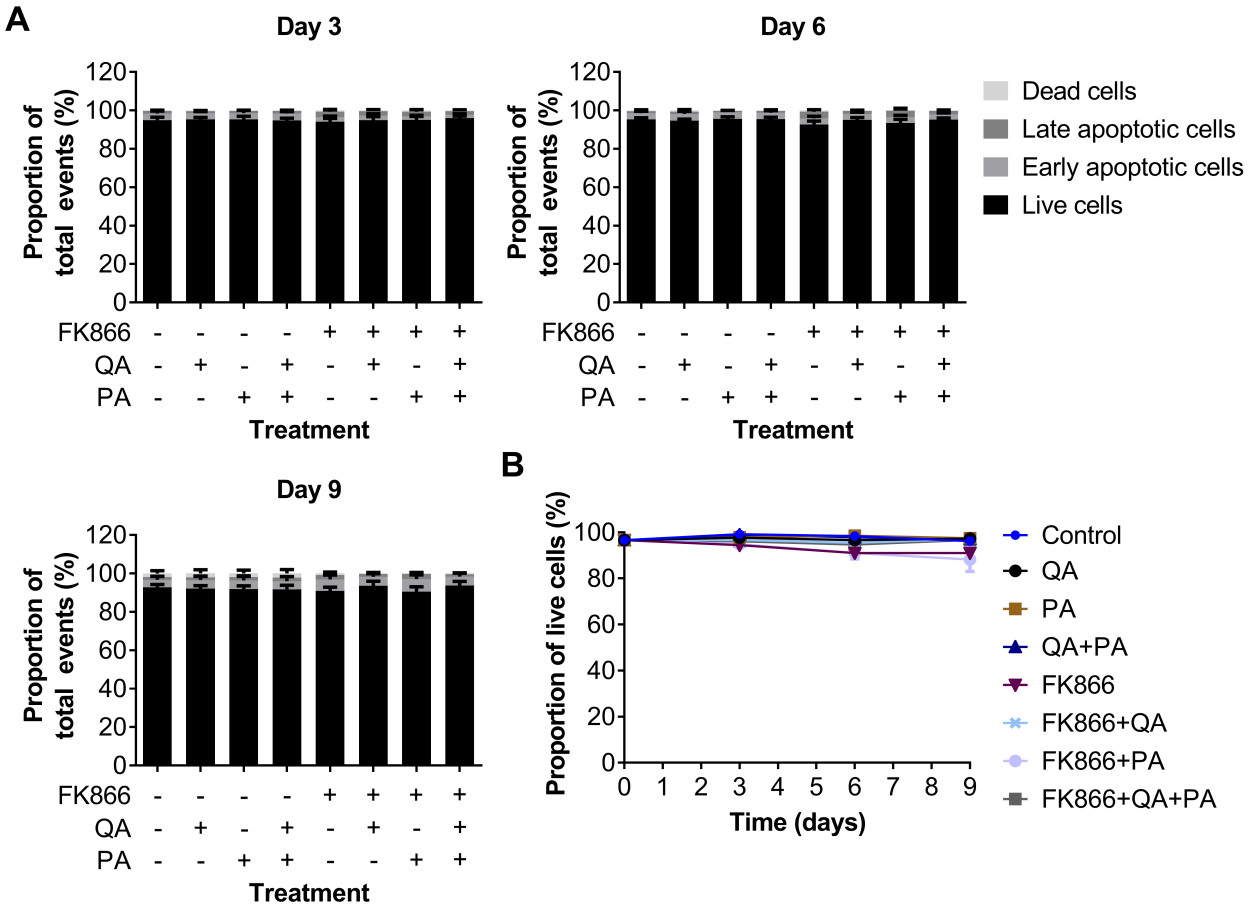


Figure 4.12: **QA does not affect apoptosis or cell viability when added to FK866 in LN229 cells.** LN229 cells were treated with FK866 (20 nM), QA (10 µM) and PA (10 µM) alone and in various combinations. (A) bar charts showing Annexin V staining at 3, 6 and 9 days (B) dot and line graph showing the proportion of viable cells over time. Data representative of three independent experiments (n = 3 biological replicates). Error bars represent SEM.

To determine whether the addition of QA could reverse the G_2/M cell cycle block caused by FK866, LN229 cells were treated with FK866 (20 nM), QA (100 µM) and PA (10 µM) alone and in various combinations, stained with PI and analysed by flow cytometry. The addition of QA to FK866-treated LN229 cells partially restored a normal cell cycle compared to FK866 treatment alone, but this was only significant at day 9 ($P < 0.05$, Fig. 4.13). The QPRT inhibitor PA did not have any effect on the cell cycle in any combination. This supports the idea that QA is able to rescue GBM cells from the effects of FK866, but suggests that this is through other mechanisms.

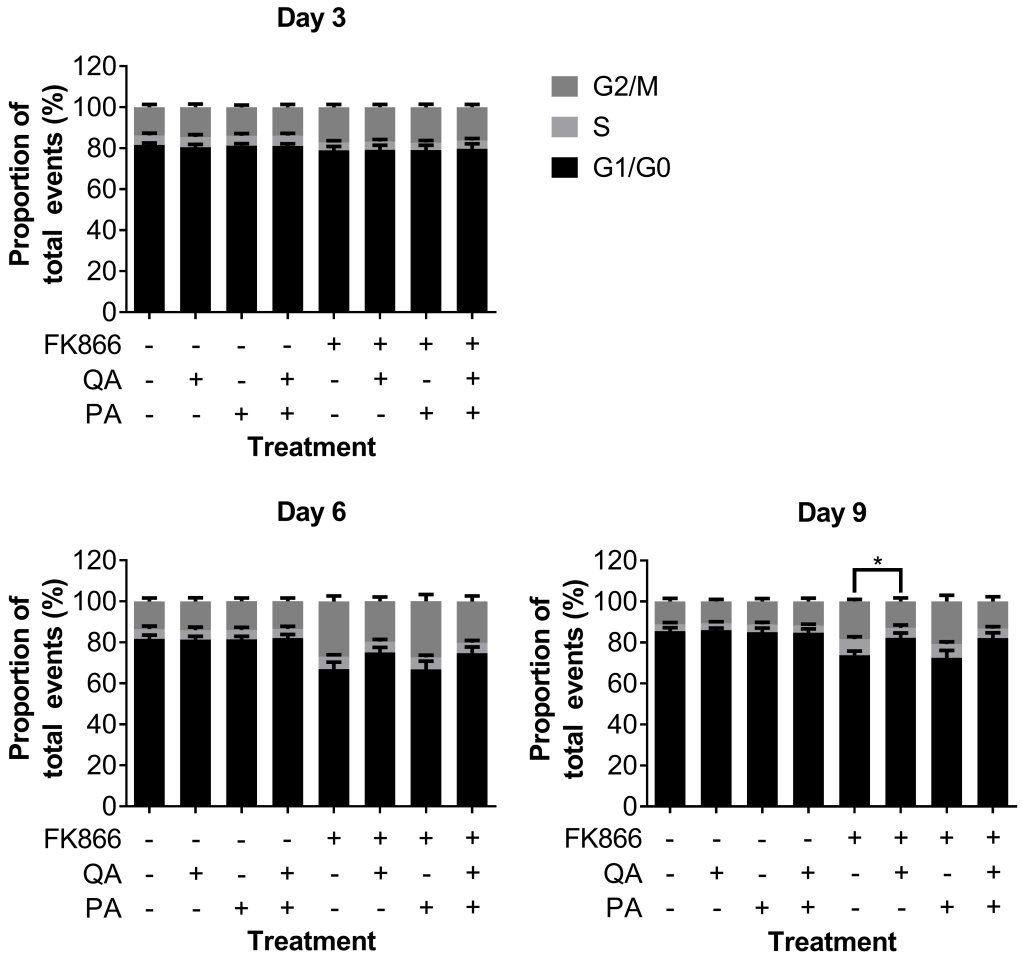


Figure 4.13: **QA restores a normal cell cycle in LN229 cells treated with FK866.** LN229 cells were treated with FK866 (20 nM), QA (10 µM) and PA (10 µM) alone and in various combinations, and cells were fixed at 3, 6 and 9 days. Cell cycle status was determined by PI staining and flow cytometry. * $P < 0.05$, two-way ANOVA with Tukey's HSD post-hoc test. Data representative of three independent experiments (n = 3 biological replicates). Error bars represent SEM.

4.4 shRNA mediated knockdown of genes involved in NAD biosynthesis in LN229 cells is insufficient to replicate results seen with molecular inhibitors

To validate the results seen with the molecular inhibitors for each pathway, I next wanted to block the expression of specific genes involved in NAD biosynthesis and test the rescue with specific NAD precursors. NAMPT, NAPRT, NT5E and QPRT genes were knocked down

individually in LN229 cells with shRNA-based plasmids using Metafectene. Cell lines with stable integration of the shRNA plasmid were selected for using puromycin. Cell lines with stable knockdown of each gene were confirmed using qPCR (Fig. 4.14A) and western blot (Fig. 4.14B). The cell lines with the greatest knockdown of each gene were selected for further experiments (NAMPT KD ALL, NAPRT KD 2, NT5E KD 1, QPRT KD 2).

Each knockdown line was used in proliferation assays corresponding to their specific pathway. Cell lines were treated with FK866 (20 nM) and either NA (10 µM), NMN (10 µM) with APCP (100 µM), or QA (100 µM) with PA (10 µM). Proliferation was measured by SRB assay at 3, 6 and 9 days. Knockdown of each gene resulted in changes to the proliferation of each cell line compared to the original parent line (Fig. 4.15A). FK866 significantly inhibited proliferation in all cell lines ($P < 0.05$, Fig. 4.15B). Consistent with previous experiments, supplementation with NA restored normal levels of proliferation in all cell lines ($P < 0.05$, Fig. 4.15B). In addition, supplementation with NMN could also restore proliferation to levels matching the controls, and this rescue could be significantly reduced by the addition of the NT5E inhibitors APCP ($P < 0.05$, Fig. 4.15B). However, none of the knockdown lines were able to properly replicate the effects seen with the molecular inhibitors. Knockdown of NT5E led to a slight decrease in the rescue seen when NMN is added to FK866-treated cells, but this was not significant.

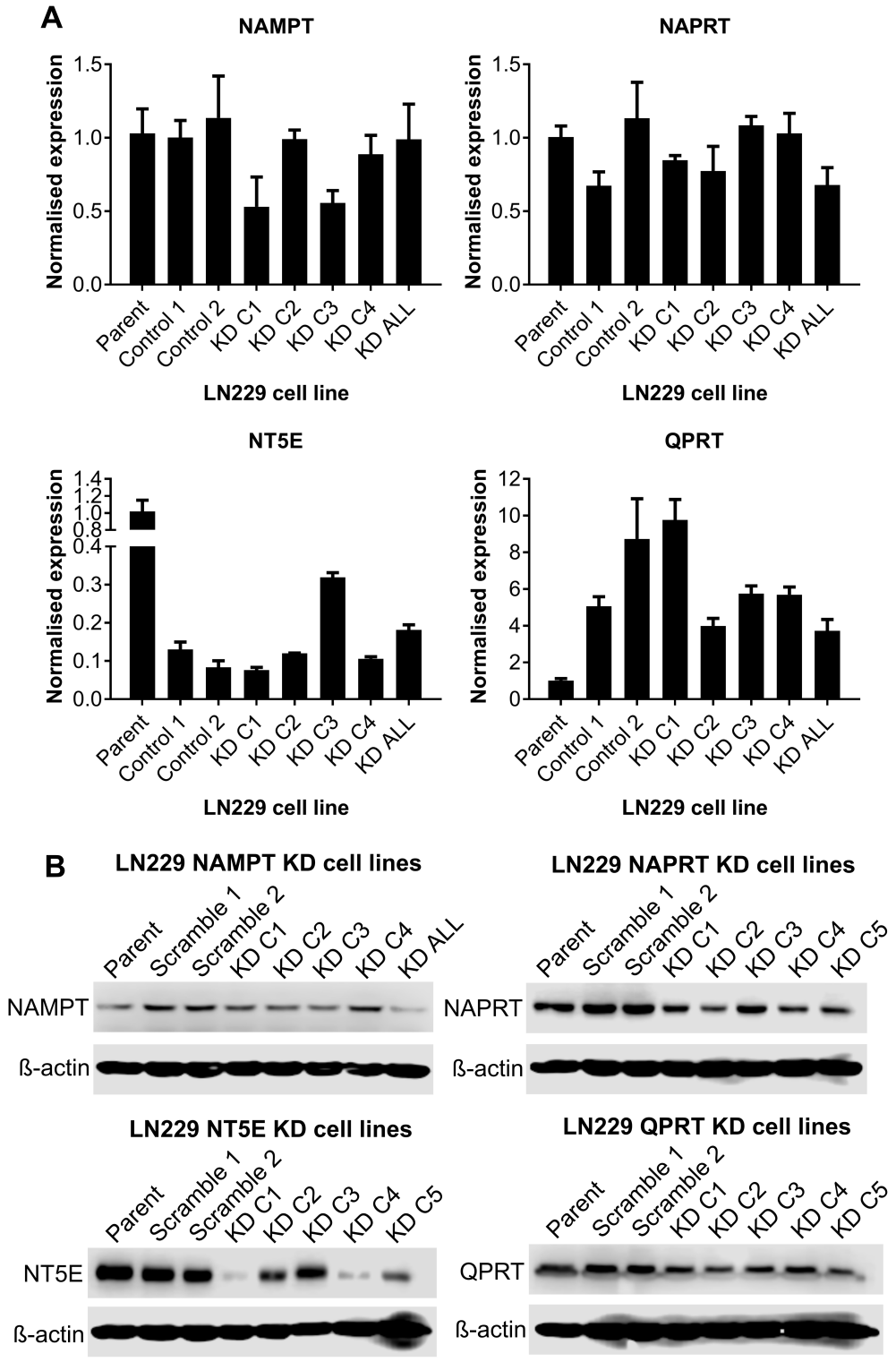


Figure 4.14: **shRNA-mediated knockdown of genes involved in NAD biosythesis in LN229 cells**. LN229 cells were transfected with shRNA-based plasmids carrying transcripts targeting genes involved in NAD biosynthesis, including NAMPT, NAPRT, NT5E and QPRT. Four different shRNA plasmids targeted against a specific gene were transfected in to LN229 cells both individually (KD1-4), and all at the same time (KD ALL). In addition, LN229 cells were transfected with two individual control plasmids (Scramble 1, Scramble 2). Expression of the genes was measured by (A) qPCR and (B) western blot. Data representative of three biological replicates. Error bars represent SEM.

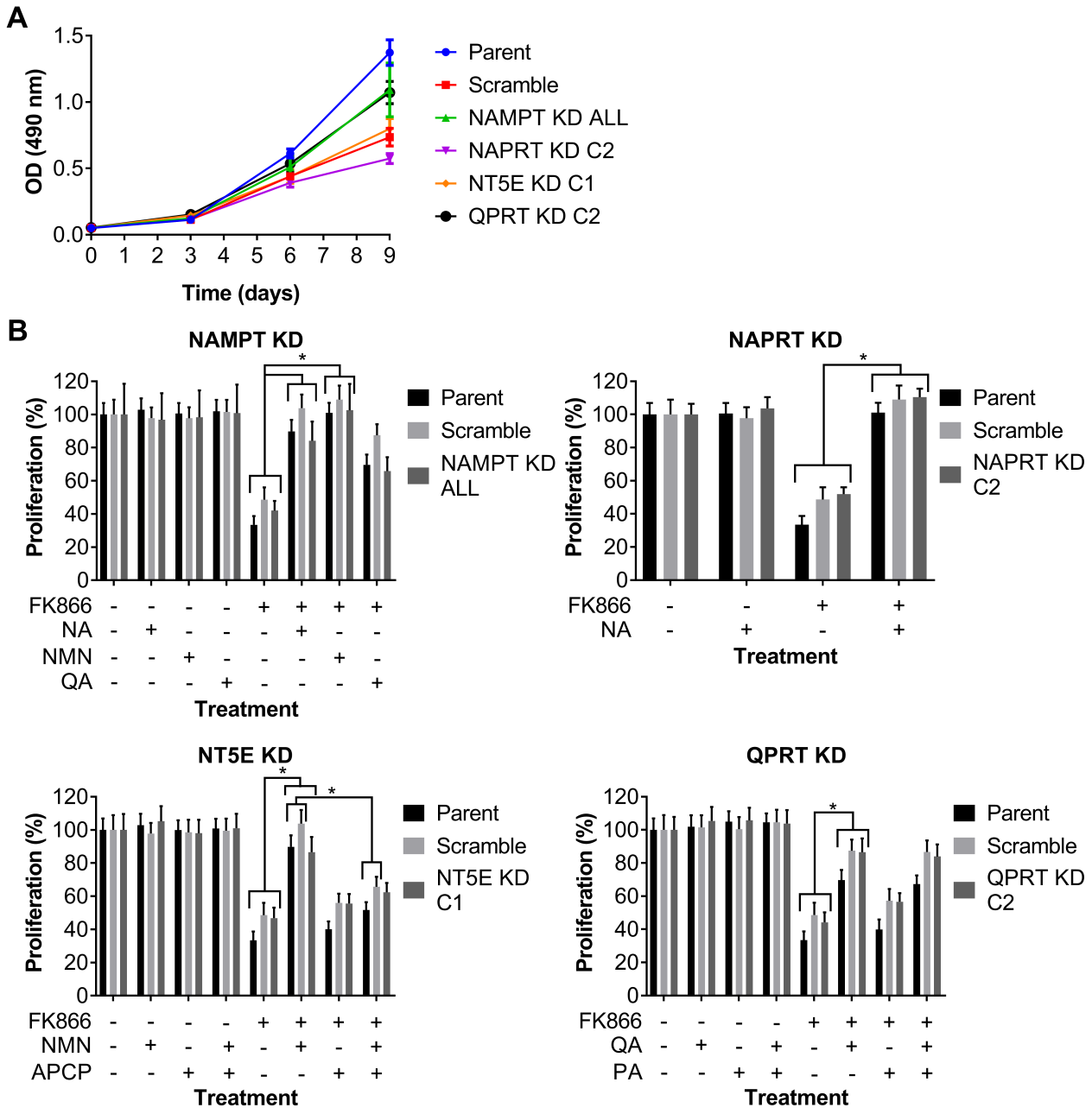


Figure 4.15: **shRNA mediated knockdowns of genes involved in NAD biosynthesis in LN229 cells do not replicate results seen with molecular inhibitors**. (A) Dot and line plot showing proliferation measured by SRB assay [OD 490 nm] for the LN229 knockdown lines. (B) Bar charts showing the changes in proliferation measured by SRB assay in the LN229 knockdown lines with different combinations of FK866 (20 nM) and the various NAD precursors/inhibitors, including NA (10 µM), NMN (10 µM), QA (10 µM), APCP (100 µM) and PA (10 µM). * $P < 0.05$, two-way ANOVA with Tukey's HSD post-hoc test. Data representative of three independent experiments (n = 9 biological replicates). Error bars represent SEM.

4.5 Discussion

These results show that multiple pathways can contribute to the resistance of GBM cells to NAMPT inhibitors, but only in the presence of specific NAD precursors, and where key enzymes are expressed. A summary of the different GBM cell lines, their expression and protein levels of some of these key enzymes, and their responses to FK866, can be seen in Table 4.1. Administration of FK866 to LN229 cells reduces both NAD and NADH levels, and whilst it has no effect on apoptosis or cell death, it does inhibit proliferation by inducing a G_2/M cell cycle block. Supplementation with NA completely restores a normal cell cycle, proliferation and NAD/NADH levels in FK866-treated LN229 cells, which express NAPRT. On the other hand, NA is unable to rescue proliferation in FK866-treated SNB19 and T98G cells, both of which lack NAPRT. This is consistent with previous data, which also showed that this phenotype can be completely reversed by supplementation with NA as demonstrated here (Cerna et al., 2012; Zhang et al., 2012b). Surprisingly, U87 cells are also rescued from FK866 treatment by the addition of NA, even though they lack expression of NAPRT. It is possible that NAPRT expression is epigenetically regulated in this cell line, and is induced upon NAD depletion. Studies have shown that NAPRT is regulated in tumours by promoter-methylation (Shames et al., 2013). The stress induced by rapid NAD depletion could lead to changes in epigenetic regulation and increase expression of NAPRT. Alternatively, FK866 treatment and supplementation with NA could select for a small sub-population that express NAPRT. Further studies are required to confirm this.

In addition to the role of NAPRT in the response of cancer cells to NAMPT inhibitors, this study also provides evidence for the role of NT5E in this system. It was previously accepted the primary role of NT5E in cancer was related to its effects on the immune system, degrading extracellular AMP to immunosuppressive adenosine to inhibit tumour killing by the immune system (Allard et al., 2016a). In addition, increases in extracellular adenosine alter purinergic signalling to promote cancer cell survival (Antonioli et al., 2013). However, it was recently been demonstrated that NT5E is a major regulator of cancer cell metabolism, and is linked to resistance of ovarian cancer cells to platinum therapy (Nevedomskaya et al., 2016). The role of NT5E in NAD metabolism was also only recently established, based on its structural similarities

to NAD nucleotidase from *H. influenzae* (Garavaglia et al., 2012). Further work indicated that this activity could promote resistance to NAMPT inhibitors, and simultaneous inhibition of NAMPT and NT5E could be a promising therapeutic strategy (Grozio et al., 2013; Sociali et al., 2015). The data presented here shows that NT5E activity is required for NMN-mediated rescue of GBM cells treated with FK866. LN229 and SNB19 both appear to express NT5E, and both can be rescued from FK866 treatment with the addition of NMN. Furthermore, the addition of the NT5E inhibitor APCP partially reverses this effect, consistent with its role as a competitive inhibitor (Synnestvedt, 2002). However, there are also some inconsistent results with the NMN and APCP data. Despite lacking expression of NT5E, T98G cells are still partially rescued from FK866 treatment with the addition of NMN, although the effect size is very small, and APCP has no effect. Furthermore, whilst U87 cells do express NT5E, and NMN is able to rescue them from FK866 treatment, APCP also has no effect. It is possible that some of the NMN in the media is broken down in to other NAD precursors through different mechanisms, which could allow T98G cells to produce NAD. As described previously, APCP functions as a competitive inhibitor, and due to the small effect size of FK866 on U87 cells, it could be that the inhibition of NT5E at this concentration of APCP is not sufficient to significantly limit the rescue with NMN. Surprisingly, despite clear increases in proliferation in FK866-treated cells supplemented with NMN, there were no significant changes in NAD or NADH levels. This gives more evidence to the possibility that FK866 treatment selects for a resistant subpopulation that is either less dependent on NAD-mediated activities, or is able to maintain NAD levels above the threshold required to inhibit cell growth.

Finally, the data presented here shows that whilst the NAD precursor QA is able to rescue GBM cells from the effects of FK866, this pathway may be less efficient at promoting NAD biosynthesis. Like NT5E, the kynurenine pathway also plays a role in modulating the immune system in response to cancer cells (Adams et al., 2014). However, this is generally attributed to IDO and TDO activity. Studies have shown that astrocytoma cells exhibit deficiencies in other enzymes of the kynurenine pathway, including KYNU, kynurenine 3-monooxygenase (KMO) and 3-hydroxyanthranilate 3,4-dioxygenase (HAAO) (Heyes et al., 1997). More recently, it was demonstrated that primary astrocytes and neurons depend on NAD generated through the

kynurenine pathway (Braidy et al., 2011). This suggests that whilst brain cancers cannot utilise the *de novo* pathway to generate NAD, normal healthy brain tissue can, which would allow NAMPT inhibitors to selectively kill cancer cells only. Whilst the expression of QPRT showed some inconsistencies with protein levels, it correlates very well with the ability of QA to restore proliferation in FK866-treated cells. QPRT is expressed in LN229, T98G and U87, all of which demonstrate partial restoration of proliferation when supplemented with FK866. SNB19, the only cell line lacking any detectable form of QPRT, could not be rescued from FK866-induced growth inhibition by the addition of QA. However, the restoration of a normal cell cycle was minimal in LN229 cells treated with FK866, indicating that this molecule is a poor source of NAD. Furthermore, the QPRT inhibitor, PA, was only able to block this rescue in U87 cells. It had no effect on LN229 or SNB19 cells. This suggests that PA is questionable as an inhibitor of QPRT. In addition to this, neither QA, nor PA had any effect on NAD or NADH levels in FK866 treated GBM cells. Similar to NMN, this could be because FK866 selects for a small subpopulation of resistant cells that can tolerate low levels of NAD for extended periods of time.

Parameter	**LN229**	**SNB19**	**T98G**	**U87**
NAMPT expression	+	+	++	++
NAMPT protein	+	+	++	++
NAPRT expression	++	-	-	-
NAPRT protein	++	-	-	-
NT5E expression	+	-	-	+
NT5E protein	+	+/-	-	++
QPRT expression	+	-	+	+
QPRT protein	-	-	+	+/-
FK866 IC_{50} (nM)	16.06	12.06	24.47	26.26
NA rescue	+	-	-	+
NMN rescue	+	+	+	+
APCP inhibition of NMN rescue	+	+	-	-
QA rescue	+	-	+	+
PA inhibition of QA rescue	-	-	-	+

Table 4.1: **Table summarising GBM cell lines, their responses to FK866, and their rescue with different NAD precursors**. Includes data from SRB assays (both FK866 titrations and rescue proliferation experiments) and both qPCR and western blot.

To try to confirm the dependencies of these rescue mechanisms on specific enzymes, shRNA-mediated knockdowns were generated against NAMPT, NAPRT, NT5E and QPRT. The best knockdown lines available were chosen for further experiments. Consistent with previous results, FK866 significantly limited proliferation, and both NA and NMN rescued the cells. However, none of the knockdowns for genes involved in NAD biosynthesis were able to replicate the results seen with specific inhibitors. This is most likely because the shRNA-mediated knockdowns for each of the genes involved in NAD biosynthesis did not achieve sufficient suppression of gene expression. As NAMPT is clearly essential for NAD biosynthesis, it could be that knockdown of this gene is only possible in cells where appropriate NAD precursors are already available. Only cells with partial knockdown of NAMPT can survive in this environment. As for the other knockdown lines, there were no sufficient knockdowns in for NAPRT and QPRT, as well as clear discrepancies between the expression and protein levels in in QPRT. All of the transfected cell

lines, including the scramble, had lower proliferation rates than the parental control, indicting that the transfection process selects for a population with slightly lower growth rates. None of the cell lines showed significant alterations in proliferation, compared to the scramble control line, that is consistent with the role of that specific gene in cancer. It may be possible to achieve efficient knockdowns through more targeted means, such as the CRISPR-Cas9 system (Qi et al., 2013).

Chapter 5

RNA sequencing of FK866-resistant and FK866-sensitive GBM cell lines

It is clear that specific GBM cell lines are able to resist treatment with NAMPT inhibitors, but this relies on the appropriate NAD precursors and cellular machinery being in place to function. Given that some GBM cell lines show inherent resistance and hypersensitivity to FK866 (Fig. 3.8), it would be useful to identify how these different cell lines respond to FK866 treatment *in vitro*. This could also provide insight into how NAMPT inhibitors cause a cell cycle block, leading to an arrest of proliferation. The FK866-sensitive line 42MG and the FK866-resistant line DBTRG were treated with FK866 (20 nM) for 24 h. RNA was extracted and the samples subject to RNAseq, with analysis and data processing to generate datasets with lists of differentially expressed genes.

5.1 NAMPT inhibition significantly alters gene expression profiles in both FK866-sensitive and FK866-resistant GBM cell lines

After data quality control, lists of differentially expressed genes were generated for control versus FK866-treated samples in each cell line. Figure 5.1 shows the log[fold change (FC)] versus the mean of normalised counts for each gene, with significantly altered transcripts highlighted in

red ($P < 0.1$). There were a total of 115 significantly altered transcripts matched to ENSEMBL IDs in 42MG cells, 113 of which were mapped to a specific gene. In the DBTRG cells, there were 195 significantly altered transcripts matched to ENSEMBL IDs, of which 194 were mapped to a specific gene.

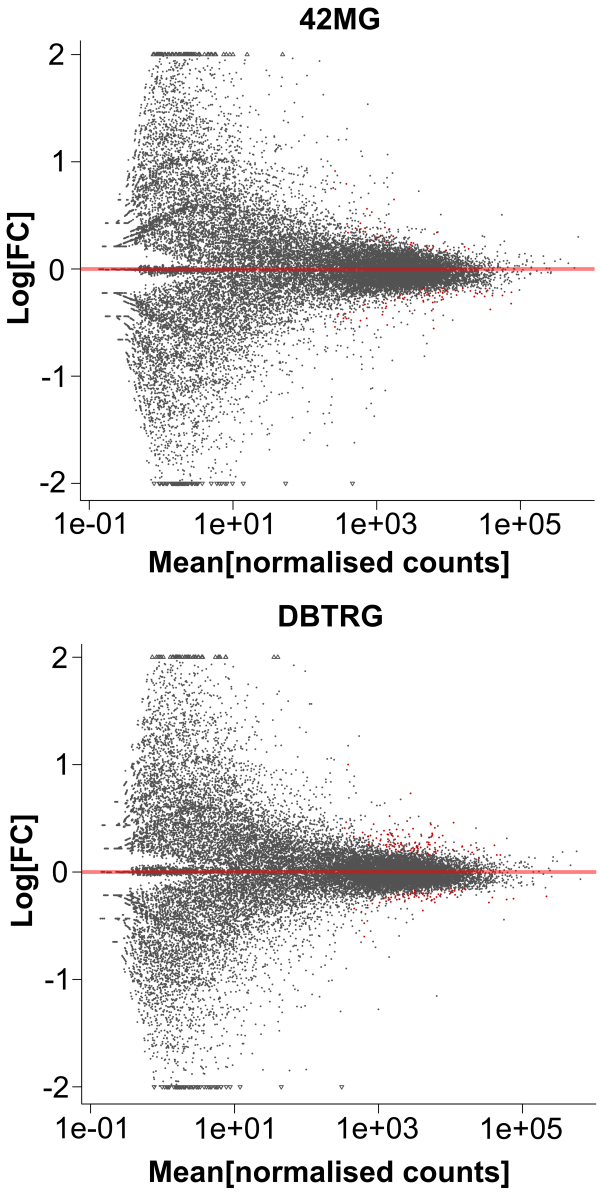


Figure 5.1: **FK866 treatment in 42MG and DBTRG cells causes significant changes in gene expression**. Scattergraphs showing the fold change in gene expression against the mean of normalised counts across replicates. Data representative of three biological replicates. Points in red are significantly differentially expressed ($P < 0.1$).

5.2 NAMPT inhibition disrupts the cell cycle and the unfolded protein response in FK866-sensitive 42MG cells

Given that we had lists of significantly differentially expressed genes with FK866 treatment, the next step was to determine what pathways these mapped to in the cells. The list of differentially expressed genes in 42MG cells (n = 113, Fig. B.1) was subjected to GSEA in Enrichr. GO analysis revealed that the most commonly altered biological processes related to mitosis, apoptosis and pathways involved in the unfolded protein response (Fig. 5.2). The molecular functions and cellular compartments reflected these processes, with microtubule activity, RNA binding and CDK activity, as well as the mitotic spindle and endoplasmic reticulum all being enriched (Fig. 5.2). Exhaustive functional pathway analysis from five different databases indicated that there were clear changes in the cell cycle and apoptosis, as well as other, more specific pathways such as FOXM1, E2F and RB signalling (Fig. 5.2). The most common transcription factors appearing in the top 10 hits across five different databases for TF regulation were FOXM1, the E2F family members E2F1 and E2F4, TP53, MYC and nuclear transcription factor Y subunit alpha (NFYA) (Fig. 5.3). The most common PPI were those involving TP53, CDK1, CDK2 and polo-like kinase 1 (PLK1) (Fig. 5.3). There were also changes in the expression of enzymes known to regulate specific metabolite levels, particularly those involved in ACoA production and NADPH. The top 10 differentially expressed genes for 42MG cells treated with FK866 can be seen in Table 5.1. Out of the top ten hits, two were also predictive of survival in patients with GBM, both of which belong to the heat shock protein (HSP) family. Furthermore, an additional six genes were both differentially expressed with FK866 treatment and demonstrated a link to survival in patients with GBM (Fig. B.1).

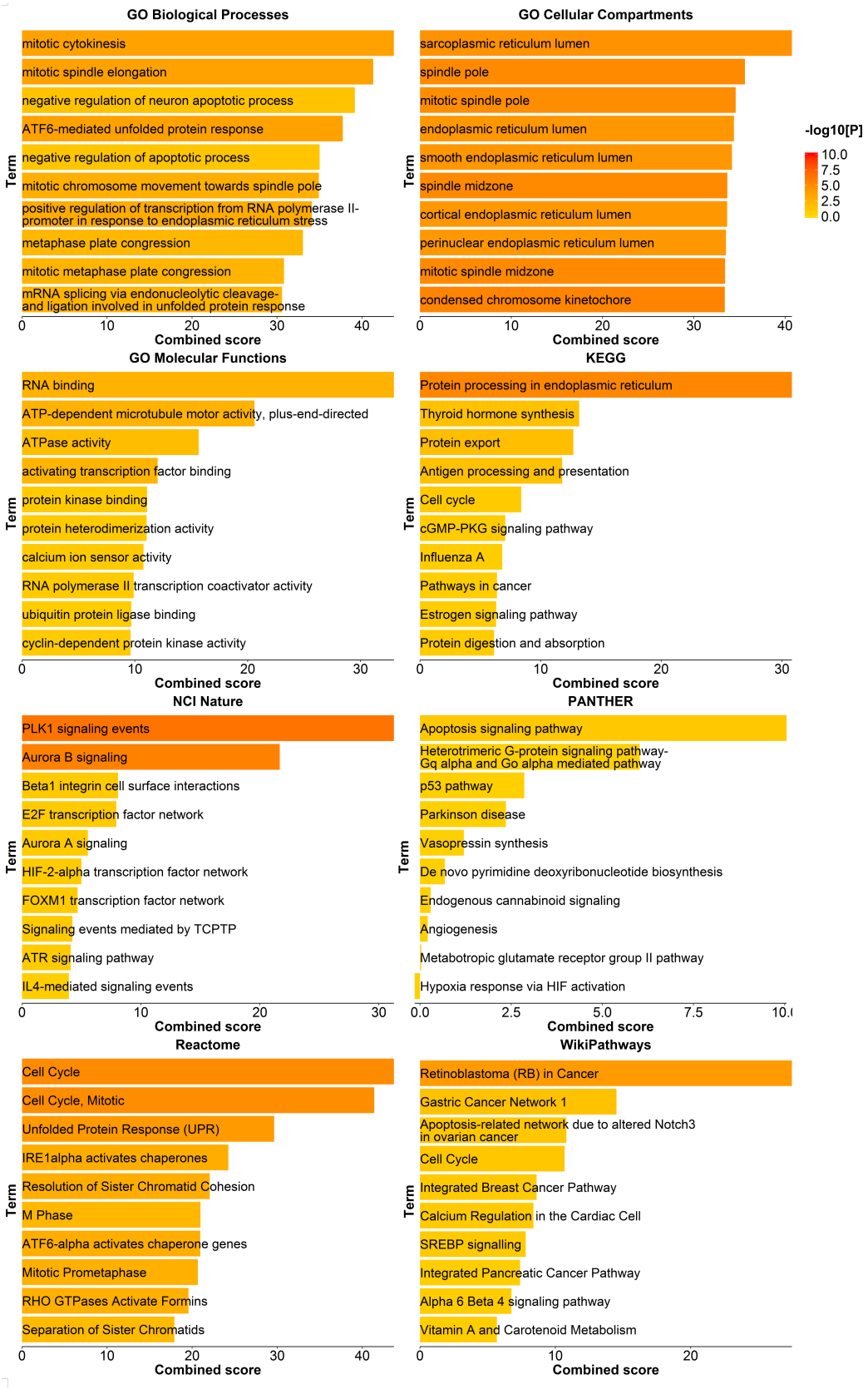


Figure 5.2: **Bar charts showing the top hits from gene set enrichment analysis for GO and cellular pathways in 42MG cells treated with FK866.** The list of differentially expressed genes for 42MG cells treated with FK866 (n = 113) was subject to GSEA in Enrichr. The combined score represents a combination of the Z-score and the P-value. Bars are coloured according to their significance (-log10[P]).

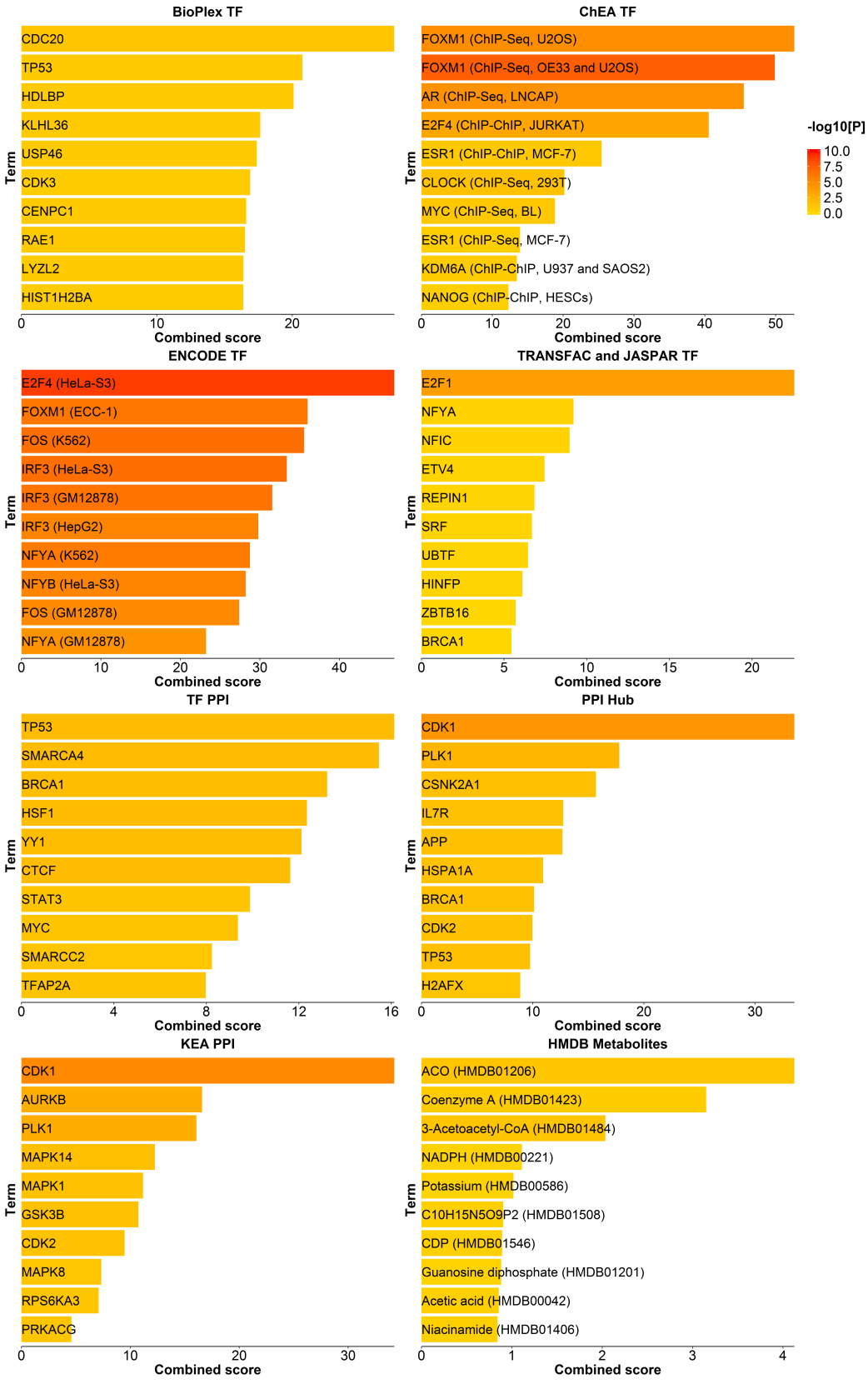


Figure 5.3: **Bar charts showing the top hits from gene set enrichment analysis for TF, PPI and metabolites in 42MG cells treated with FK866.** The list of differentially expressed genes for 42MG cells treated with FK866 (n = 113) was subject to TF network and PPI analysis in Enrichr. The combined score represents a combination of the Z-score and the *P*-value. Bars are coloured according to their significance (-log10[*P*]).

ENSEMBL ID	**Gene**	**Gene name**	**Fold change**	**Adjusted P value**	**Poor survival group**
ENSG00000044574	HSPA5	Heat shock protein family A (Hsp70) member 5	-1.297	1.94E-06	High expression ($P = 0.008$)
ENSG00000123485	HJURP	Holliday junction recognition protein	-1.235	0.001	None
ENSG00000166598	HSP90B1	Heat shock protein 90 beta family member 1	-1.249	0.001	High expression ($P = 0.020$)
ENSG00000168010	ATG16L2	Autophagy related 16 like 2	1.346	0.004	None
ENSG00000163659	TIPARP	TCDD inducible poly(ADP-ribose) polymerase	-1.311	0.004	None
ENSG00000128965	CHAC1	ChaC glutathione specific gamma-glutamylcyclotransferase 1	1.478	0.006	None
ENSG00000145050	MANF	Mesencephalic astrocyte derived neurotrophic factor	-1.234	0.006	None
ENSG00000178913	TAF7	TATA-box binding protein associated factor 7	-1.239	0.006	None
ENSG00000100321	SYNGR1	Synaptogyrin 1	1.237	0.007	None
ENSG00000136541	ERMN	Ermin	-1.375	0.011	None

Table 5.1: **Table showing the top 10 differentially expressed genes in 42MG cells treated with FK866.** Effects on survival were determined by analysis of either microarray (n = 539) or RNAseq (n = 172) data from TCGA, separated into tertiles of gene expression, by two-way ANOVA with Tukey's HSD post-hoc test.

5.3 NAMPT inhibition specifically alters the G_1/S phase of the cell cycle and HIF signalling in FK866-resistant DBTRG cells

The same data analysis was applied to the list of differentially expressed genes in the DBTRG cell line (n = 193). GO analysis revealed that the most common biological processes related to differentially expressed genes were associated with gene transcription, specifically by RNA polymerase II, as well as regulation of transcription related to the G_1/S phase transition in the cell cycle (Fig. 5.4). Consistent with altered transcription, the most common GO cellular compartment was the endoplasmic reticulum, although the methylosome was also highly ranked. The top hits for GO molecular functions were also related to biological functions, with RNA polymerase II transcription appearing multiple times, but ATPase activity was also highly ranked. Functional pathway analysis indicated that that were clear alterations in HIF signalling, the cell cycle including G_1/S phase transition and cell cycle checkpoints, as well as TP53 and integrin signalling (Fig. 5.2). The most common transcription factors appearing in the top 10 hits across five different databases of TF regulation were HIF1, HDAC1, HDAC2, E2F4, E2F7, CDKN1A and CDKN1B (Fig. 5.5). The most common PPI were those involving CDK1 and CDK2 (Fig. 5.3). There were also changes in the expression of enzymes known to regulate specific metabolite levels, particularly those involved in proline and hydroxyproline metabolism. The top 10 differentially expressed genes for DBTRG cells treated with FK866 can be seen in table 5.2. Out of the top 10 hits, two were also predictive of survival in patients with GBM, including VEGF, a well known GBM associated gene, and ADAM metallopeptidase with thrombospondin type 1 motif (ADAMTS)14. Finally, there were 32 other genes that were not only differentially expressed with FK866 treatment, but also linked to altered survival in patients with GBM (Table B.1).

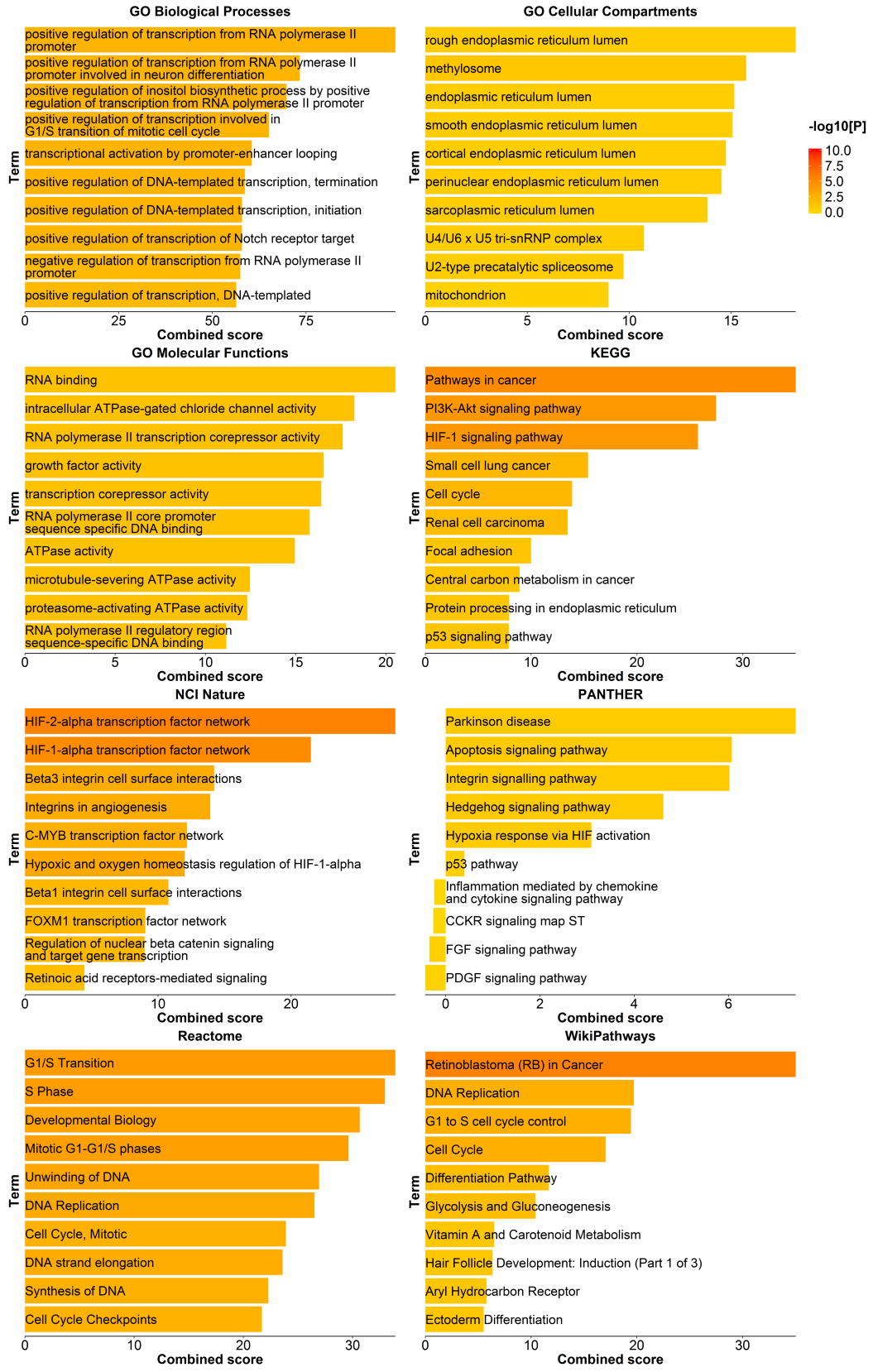


Figure 5.4: **Bar charts showing the top hits from gene set enrichment analysis for GO and cellular pathways in DBTRG cells treated with FK866.** The list of differentially expressed genes for DBTRG cells treated with FK866 (n = 193) was subject to GSEA in Enrichr. The combined score represents a combination of the Z-score and the P value. Bars are coloured according to their significance (-log10[P]).

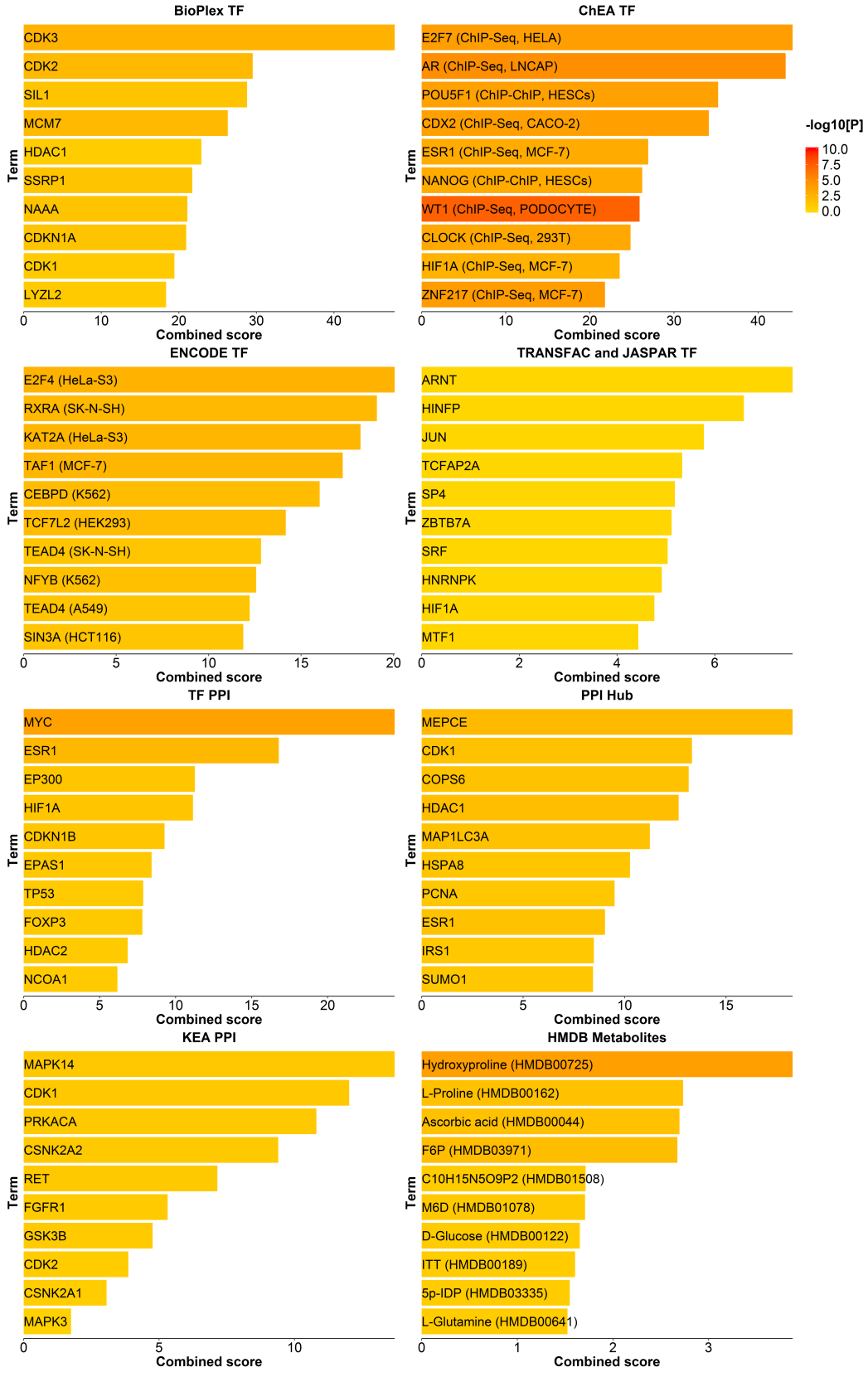


Figure 5.5: **Bar charts showing the top hits from gene set enrichment analysis for TF, PPI and metabolites in DBTRG cells treated with FK866.** The list of differentially expressed genes for DBTRG cells treated with FK866 (n = 113) was subject to TF network and PPI analysis in Enrichr. The combined score represents a combination of the Z-score and the P value. Bars are coloured according to their significance (-log10[P]).

ENSEMBL ID	**Gene**	**Gene name**	**Fold change**	**Adjusted P value**	**Poor survival group**
ENSG00000162496	DHRS3	Dehydrogenase/reductase 3	2.005	4.32E-14	None
ENSG00000107731	UNC5B	Unc-5 netrin receptor B	1.378	2.29E-09	None
ENSG00000159399	HK2	Hexokinase 2	1.392	2.43E-08	None
ENSG00000104081	BMF	Bcl2 modifying factor	1.361	8.08E-08	None
ENSG00000175727	MLXIP	MLX interacting protein	1.263	1.42E-07	None
ENSG00000095752	IL11	Interleukin 11	-1.514	1.69E-06	None
ENSG00000138316	ADAMTS14	ADAM metallopeptidase with thrombospondin type 1 motif 14	1.665	1.78E-06	High expression ($P = 0.031$)
ENSG00000179981	TSHZ1	Teashirt zinc finger homeobox 1	1.274	1.78E-06	None
ENSG00000120093	HOXB3	Homeobox B3	1.332	1.67E-05	None
ENSG00000112715	VEGFA	Vascular endothelial growth factor A	1.215	2.00E-05	High expression ($P = 0.00027$)

Table 5.2: **Table showing the top 10 differentially expressed genes in DBTRG cells treated with FK866.** Effects on survival were determined by analysis of either microarray (n = 539) or RNAseq (n = 172) data from TCGA, separated into tertiles of gene expression, by two-way ANOVA with Tukey's HSD post-hoc test.

5.4 Changes to E2F/RB, CDK and HSP cell signalling events occur in both FK866-sensitive and FK866-resistant GBM cells

GSEA indicated that FK866 treatment in both cell lines lead to alterations in numerous pathways involved in control of the cell cycle, including E2F/RB and CDK signalling. In addition, across the two cell lines, there were 13 differentially expressed genes found in both, which indicate common responses to FK866 (Table 5.3). This included two members of the HSP family, namely HSPA5 and HSPA8, which are involved in the unfolded protein response, as well as VEGFA, a well established GBM-associated gene that was also predictive of survival in TCGA data.

ENSEMBL ID	**Gene**	**Gene name**	**42MG FC**	**42MG Adj[P]**	**DBTRG FC**	**DBTRG Adj[P]**	**Poor survival group**
ENSG00000044574	HSPA5	Heat shock protein family A (Hsp70) member 5	-1.297	1.94E-06	-1.177	0.015	High expression ($P = 0.0081$)
ENSG00000112715	VEGFA	Vascular endothelial growth factor A	1.161	0.011	1.215	2.00E-05	High expression ($P = 0.00027$)
ENSG00000120075	HOXB5	Homeobox B5	1.447	0.057	1.365	1.85E-04	None
ENSG00000094804	CDC6	Cell division cycle 6	-1.208	0.014	-1.209	0.004	None
ENSG00000120437	ACAT2	Acetyl-CoA acetyltransferase 2	-1.151	0.071	-1.195	0.003	None
ENSG00000137868	STRA6	Stimulated by retinoic acid 6	1.184	0.025	1.213	0.016	None
ENSG00000171848	RRM2	Ribonucleotide reductase regulatory subunit M2	-1.148	0.070	-1.174	0.006	None
ENSG00000213676	ATF6B	Activating transcription factor 6 beta	1.145	0.065	1.162	0.008	None
ENSG00000109971	HSPA8	Heat shock protein family A (Hsp70) member 8	-1.161	0.068	-1.186	0.009	None
ENSG00000181938	GINS3	GINS complex subunit 3	-1.284	0.014	-1.182	0.090	None

ENSG00000170860	LSM3	LSM3 homolog, U6 small nuclear RNA and mRNA degradation associated	-1.172	0.057	-1.162	0.029	None
ENSG00000198830	HMGN2	High mobility group nucleosomal binding domain 2	-1.146	0.041	-1.132	0.044	None
ENSG00000164032	H2AFZ	H2A histone family member Z	-1.131	0.071	-1.113	0.099	None

Table 5.3: **Table showing differentially expressed genes with FK866 treatment in 42MG and DBTRG cell lines.** Genes are sorted based on adjusted P values for both cell lines. Effects on survival were determined by analysis of either microarray (n = 539) or RNAseq (n = 172) data from TCGA, separated into tertiles of gene expression, by two-way ANOVA with Tukey's HSD post-hoc test.

5.5 Discussion

5.5.1 FK866-sensitive 42MG cells

42MG, the FK866-sensitive cell line, showed marked changes in genes involved in mitosis and apoptosis. This is consistent with a G_2/M cell cycle arrest, and the alterations to apoptotic signalling may represent known changes induced by treatment with NAMPT inhibitors, including caspase activation and phosphatidylserine (PS) presentation (Feng et al., 2016a; Tateishi et al., 2016).

Analysis of gene expression networks altered by FK866 treatment revealed FOXM1 as a major transcriptional regulator of the response. FOXM1 is involved in GBM pathogenesis and the stemness of cancer cells. It is an important factor in the Wnt/β-catenin signalling pathway in glioma, and acts by binding to β-catenin directly and upregulating its transcriptional activity (Zhang et al., 2011b). FOXM1 is also essential for the translocation of GLI family zinc finger 1 (GLI1) to the nucleus, which promotes a cancerous phenotype, and the two have been shown to be co-expressed in GBM samples (Xue et al., 2015). In addition, FOXM1 has been shown to contribute to radioresistance in GBM cells, and inhibitors of FOXM1 are able to sensitise cells to radiation *in vivo* (Lee et al., 2015b). These results indicate that FK866 treatment leads to a growth suppressive phenotype in GBM cells regulated by FOXM1 expression.

Another set of transcription factors that were highlighted by gene expression network analysis was the E2F family. The E2F proteins are linked to control of the cell cycle in cancer (Sala et al., 1994). E2F1 and E2F4 are key regulators of genes that promote GBM proliferation and survival (Donaires et al., 2017). Both are predicted to play a role in the regulation of genes involved in the response to FK866 treatment. They have previously been implicated in the regulation of the RB signalling pathway (Dirks et al., 1998; Jiang et al., 2010). RB is mutated in a small proportion of GBM (TCGA, 2008). GSEA indicated that RB signalling was also altered upon FK866 treatment in 42MG cells. Like the E2F family, RB also plays a role in control of the cell cycle (Nozaki et al., 1999); indeed, E2F and RB directly interact to promote and inhibit progression through the cell cycle, acting as oncogenes and tumours suppressors respectively (Takahashi et al., 2000). They may be key regulators of the G_2/M cell cycle block

seen with FK866 treatment. It has also been reported that RB directly inhibits E2F1 to induce autophagy (Jiang et al., 2010). This is consistent with the induction of autophagy by FK866 in GBM cells (Yang et al., 2015c). However, others have demonstrated that E2F1 is also involved in the suppression of growth and activation of apoptosis in glioma through upregulation of BCL2, apoptosis regulator (BCL2) (Fueyo et al., 1998; Shu et al., 2000; Gomez-Manzano et al., 2001). Whilst E2F1 acts primarily as an oncogene, it also has tmour suppressor properties under certain circumstances.

In addition to the changes in gene transcription networks, FK866 also yielded alterations to protein-protein interactions in 42MG cells. In particular, CDK1 was ranked the highest in two different databases. CDK1 is a major regulator of the G_2/M checkpoint, and helps coordinate organisation of the mitotic machinery (Asghar et al., 2015). In GBM, CDK1 is upregulated compared to normal neural cell lines, and was recently implicated in the response of GBM cells to TMZ (Bo et al., 2017; Song et al., 2017). However, whilst CDK inhibitors have been trialled for GBM, most target other CDKs (Lubanska and Porter, 2017). The full role of CDK1 in GBM is still not fully understood, and more work is required to determine its role in the response of GBM cells to FK866.

Both GSEA and PPI databases indicated that PLK1 signalling was altered in 42MG cells treated with FK866. PLK1 stabilises the NAD-consuming tankyrase (TNKS) enzyme, which is involved in regulation of telomere lengthening and spindle-pole assembly during mitosis (Ha et al., 2012). PLK1 was identified as a potential therapeutic target in GBM by a small molecule screen (Danovi et al., 2013). Inhibition of PLK1 has been shown to cause cell cycle arrest and apoptosis in GBM cells (Pezuk et al., 2013a), as well as sensitising cells to radiation (Tandle et al., 2013; Pezuk et al., 2013b). Others have shown that the effects of PLK1 inhibition are the result of a corresponding decrease in the expression of SRY-box 2 (SOX2), and that inhibition of PLK1 can even reduce tumour growth *in vivo* (Lee et al., 2012). In addition, inhibition of PLK1 sensitises EGFR-mutated GBM cells to TMZ (Shen et al., 2015c). Furthermore, it has been demonstrated that inhibition of VEGF leads to a loss of PLK1, and the combination of VEGF and EGFR inhibitors acts synergistically (Momeny et al., 2017). Alterations to PLK1 signalling upon FK866 treatment are potentially mediated by reductions in TNKS activity due

to a reduction in the NAD pool.

RNAseq also revealed that aurora kinase (AURK) signalling was altered upon FK866 treatment in 42MG cells. AURK signalling is closely related to PLK1 signalling, and the two have been implicated in the spindle assembly during mitosis (Asteriti et al., 2015). Expression of AURKA or AURKB is associated with poor prognosis in GBM (Zeng et al., 2007; Barton et al., 2010; Lehman et al., 2012). AURKA activates Wnt/β-catenin signalling and self renewal in GSCs (Xia et al., 2013). Furthermore, inhibitors of AURKA or AURKB have demonstrated significant anti-neoplastic effects both *in vitro* and *in vivo*, including sensitisation to both TMZ and radiation (Li et al., 2009a; Borges et al., 2012; Diaz et al., 2012; Lee et al., 2013; Hong et al., 2014c; Van Brocklyn et al., 2014). The combination of NAMPT and AURK inhibitors is yet to be tested in any cancer, and could offer a novel therapeutic strategy by disrupting the cell cycle and initiating apoptosis.

In addition to general changes to signalling pathways in 42MG cells treated with FK866, there were significant changes in the expression of specific genes. Out of the top 10 differentially expressed genes, two are HSPs which are also predicted to have an effect on survival in GBM, namely HSPA5 and HSP90B1. Both genes are downregulated upon FK866 treatment. HSPA5, also known as GRP78, is a key regulator of the unfolded protein response, which is one of the pathways highlighted by GSEA. Expression of HSPA5 is upregulated in glioma cell lines, where it inhibits apoptosis and promotes resistance to radiation, TMZ, other DNA-damaging drugs and endoplasmic reticulum stress (Pyrko et al., 2007; Lee et al., 2008; Suyama et al., 2011; Huynh et al., 2015). HSPA5 also promotes Akt and MAPK signalling in glioma (Zhang et al., 2011a). Studies have demonstrated that inhibition of cell surface-bound HSPA5 suppresses proliferation in glioma cells (Kang et al., 2016). In addition, HSP90B1, also known as GRP94, has been implicated in the unfolded protein response, and was reported to promote glioma growth through activation of the Wnt/β-catenin pathway (Epple et al., 2013; Hu et al., 2015). This suggests that downregulation of HSPs plays a role in the effects of FK866 on GBM cells, possibly through regulation of the unfolded protein response.

FK866 also significantly downregulated the expression of one of the members of the PARP family, TCDD inducible PARP (TIPARP). TIPARP has been linked to metabolic activi-

ties in the liver, including drug detoxification through cytochrome P450 family 1 subfamily A (CYP1A)1 and regulation of LXR receptors (MacPherson et al., 2013; Bindesboll et al., 2016). TIPARP also suppresses gluconeogenesis by inhibiting phosphoenolpyruvate carboxykinase (PEPCK) upon stimulation by aryl hydrocarbon receptor (AHR) signalling (Diani-Moore et al., 2013). More recently, it was demonstrated that AHR signalling pathway is upregulated in meningioma (Talari et al., 2018). However, whilst it is clear that NAD depletion though inhibition of NAMPT could limit TIPARP activity, the exact role of this protein in GBM pathology is yet to be understood.

Another gene with significantly altered gene expression in FK866-treated 42MG cells is holliday junction recognition protein (HJURP). HJURP interacts with CENPA to facilitate its deposition at centromeres during mitosis (Foltz et al., 2009; Dunleavy et al., 2009). HJURP is thought to maintain chromosomal stability in cancer cells to allow them to survive and proliferate (Kato et al., 2007). Whilst HJURP expression was not predictive of survival in the GBM database of TCGA, previous studies have demonstrated that it is linked to prognosis in GBM, breast and liver cancer (Hu et al., 2010; De Tayrac et al., 2011; Valente et al., 2013; Montes de Oca et al., 2015; Hu et al., 2017). Furthermore, a non-synonymous single nucleotide polymorphism (SNP) in Chinese populations predisposes them to hepatocellular carcinoma (Huang et al., 2016). More recently, it was demonstrated that knockdown of HJURP in bladder cancer cells decreased SIRT1 phosphorylation and therefore activity (Cao et al., 2017a). This illustrates a direct link between HJURP activity and NAD metabolism through its consumption by SIRT1. There may be a close association between these systems, which is interrupted when cells are treated with NAMPT inhibitors such as FK866.

Finally, GSEA on 42MG cells treated with FK866 suggested that changes in the expression of enzymes involved in metabolism were likely to alter the levels of metabolites recorded in the Human Metabolome Database (HMDB). These included ACoA and its derivatives, suggesting that there are likely to be alterations to glycolysis and the entry of pyruvate into the TCA cycle. This is consistent with the reported effects of NAMPT inhibitors on cellular metabolism (Tan et al., 2013; Tan et al., 2015). These results could be confirmed using labelled glucose studies to prove changes in the rates of glycolysis and therefore labelling of TCA cycle intermediates.

5.5.2 FK866-resistant DBTRG cells

DBTRG, the FK866-resistant cell line, was also treated with FK866 and subject to analysis using the same methods. GSEA indicated that there were also changes in genes involved in the cell cycle in this cell line, but these were specifically related to G_1/S phase, RNA polymerase II activity and DNA synthesis, as opposed to G_2/M phase as it was in 42MG. Interestingly, HIF signalling was also implicated in the response of these cells to FK866, as was PI3K/Akt signalling.

Transcription factor network analysis indicated that FK866 triggered changes in genes regulated by HIF1, which is consistent with the changes to HIF signalling seen with GSEA. Whilst HIF signalling is known to promote glycolysis through upregulation of GLUT1, LDHA and PDK1, its roles in NAD metabolism are poorly understood (Semenza et al., 1996; Kim et al., 2006a; Pore et al., 2006). Studies have demonstrated that NAMPT is a target of HIF2 in chondrocytes, and is required for the activation of SIRT2/4 and multiple matrix metallopeptidase (MMP) enzymes (Yang et al., 2015d; Oh et al., 2015). Inhibition of HIF1 leads to a reduction in NAD/NADP levels, but has not specifically been linked to NAMPT activity (Ban et al., 2017). However, multiple studies have shown direct links between hypoxia and the NAD-consuming SIRT family, which clearly demonstrates that NAD metabolism plays an important role in the adaptation of cells to a hypoxic environment (Lim et al., 2010; Finley et al., 2011; Laemmle et al., 2012; Seo et al., 2015).

Like 42MG, treatment of DBTRG cells with FK866 yielded changes in the expression of genes regulated by the E2F family, specifically E2F4 and E2F7. As described previously, the E2F family is linked to control of the cell cycle and proliferation in cancer. Whilst E2F4 was also highlighted in 42MG cells, changes in the expression of genes regulated by E2F7 are unique to DBTRG. In contrast to E2F4, which acts primarily as an oncogene, E2F7 is thought to act as a tumour suppressor by suppressing E2F1 activity and therefore inhibiting proliferation (De Bruin et al., 2003; Endo-Munoz et al., 2009). It promotes cellular senescence through its interactions with the RB and TP53 pathways (Aksoy et al., 2012; Di Iasio and Zauli, 2013). E2F7 has also been implicated in the DNA damage response (Panagiotis Zalmas et al., 2008; Zalmas et al., 2013). E2F7 also promotes miRNA-129-mediated autophagy and limits glioma

growth *in vivo* (Chen et al., 2016). In addition, E2F7 inhibits the expression of numerous other miRNAs known to promote proliferation (Mitxelena et al., 2016). Despite this there is evidence to suggest that E2F7 it may have oncogenic properties in some cancers. Knockdown of E2F7 in endometrial cancer cells suppresses proliferation (Li et al., 2015a). E2F7 promotes resistance to tamoxifen, and is associated with relapse and poor prognosis in breast cancer (Chu et al., 2015). Furthermore, elevated expression of E2F7 is correlated with CDK1 in glioma, and is indicative of poor prognosis (Yin et al., 2016). Clearly, E2F7 has a diverse range of activities in different cancers. Changes in the expression of genes regulated by E2F7 induced by FK866 treatment in DBTRG cells may represent a protective phenotype that limits proliferation but maintains cell viability.

Again, as with 42MG cells, FK866 induces changes in gene expression networks and PPIs linked to the CDK family. This includes CDK1, CDK2, CDKN1A and CDKN1B. Both CDK1 and CDK2 are significantly enriched in GSCs (Bo et al., 2017). As described previously, CDK1 plays a major role in regulation of the G_2/M cell cycle checkpoint through regulation of the mitotic machinery. In GBM, CDK1 is upregulated and is implicated in their response to TMZ (Song et al., 2017). On the other hand, CDK2 regulates DNA replication during S phase of the cell cycle through its interactions with cyclin A and cyclin E, and is directly inhibited by CDKN1A and CDKN1B, (Asghar et al., 2015). Clearly, FK866 treatment in DBTRG cells leads to changes in the expression of numerous genes in this signalling pathway. In GBM, mutant EGFR downregulates CDKN1B, leading to increased cyclin A and CDK2 activity (Narita et al., 2002). Low expression of CDKN1B, but not CDKN1A, has also been associated with poor prognosis in glioma (Kirla et al., 2003). CDK2 has recently been implicated in the resistance of GBM cells to radiation (Wang et al., 2016c). Changes in CDK signalling affecting regulation of the cell cycle could represent the FK866-resistant phenotype seen in DBTRG cells.

In addition to the clear changes in cell cycle signalling induced by FK866, there were also specifically altered genes involved in other pathways. DBTRG cells exhibited a two-fold upregulation of dehydrogenase/reductase 3 (DHRS3), a gene involved in retinal metabolism (Lundová et al., 2015); however, its role in cancer is largely unknown. One study demonstrated that DHRS3 is frequently deleted in neuroblastoma (Cerignoli et al., 2002), and it is a known target

of TP53 (Kirschner et al., 2010; Deisenroth et al., 2011). It is unclear what role DHRS3 could play in the response of GBM cells to NAMPT inhibition.

FK866 also caused an upregulation of HK2, a gene with well-established roles in GBM (Sanzey et al., 2015). The Warburg effect is promoted by high levels of HK2 in GBM (Wolf et al., 2011). Knockdown or inhibition of HK2 sensitises GBM cells to radiation-induced DNA damage (Vartanian et al., 2016). Furthermore, mTOR promotes OXPHOS and suppresses HK2 activity under irradiation (Lu et al., 2015). Upregulation of HK2 in FK866-treated cells could represent a compensatory mechanism in response to loss of NAD-dependent GAPDH activity, promoting glycolysis and therefore ATP production.

BCL2-modifying factor (BMF) was also upregulated by FK866 treatment in DBTRG cells. BMF binds pro-survival BCL2 proteins to trigger apoptosis in response to events such as TGFβ activation, MAPK inhibition or increased AMPK activity (Ramjaun et al., 2007; VanBrocklin et al., 2009; Kilbride et al., 2010). BMF is also involved in tumour development in MYC-mutated mice (Frenzel et al., 2009). In glioma, the proteasome inhibitor Bortezomib induces BMF activation in a JNK-dependent manner, triggering apoptosis (Tianhu et al., 2010). Studies have demonstrated that BMF mediates cytotoxicity of HDAC inhibitors, as well as the glycolytic inhibitor 2DG (Zhang et al., 2006; Zagorodna et al., 2012). NAMPT inhibitors have not previously been associated with BCL2-mediated apoptosis, but given the upregulation of BMF seen in FK866-resistant cells here, it could be an interesting avenue to pursue.

FK866 treatment also led to a decrease in the expression of ADAMTS14 in DBTRG cells. Very little is known about ADAMTS14 in normal cellular biology, let alone cancer. Analysis of TCGA data indicated that it is predictive of survival in patients with GBM. The ADAMTS family is involved in modification of extracellular-matrix proteins (Bolz et al., 2001). Early work indicated that genetic polymorphisms in ADAMTS14 may play a role in multiple sclerosis and osteoarthritis (Goertsches et al., 2005; Rodriguez-Lopez et al., 2009). More recently, it was demonstrated that genetic polymorphisms in ADAMTS14 predispose smokers to oral cancer (Su et al., 2016). Furthermore, the same polymorphisms predispose to liver cancer, and interestingly, hypermethylation of both ADAMTS14 and MGMT is seen in patients with colorectal cancer (Sheu et al., 2017; Alonso et al., 2015). This is especially important in GBM,

as MGMT methylation is a well-established marker of TMZ sensitivity. It remains to be seen exactly what role ADAMTS14 plays in GBM, and how it might affect the response of cells to NAMPT inhibition or TMZ.

Finally, GSEA on DBTRG cells treated with FK866 suggested that changes in the expression of enzymes involved in metabolism were likely to alter the levels of certain metabolites. These included proline and hydroxyproline, which could indicate altered proline metabolism induced by FK866. However, these effects can only be confirmed by measuring them directly.

5.5.3 Consistent effects on both cell lines

Given that RB, E2F and CDK signalling are altered in both cell lines, this indicates a consistent response to NAMPT inhibition across samples related to regulation of the cell cycle. In both cell lines, there were also changes in the expression of specific genes involved in the cell cycle, including CDC6, GINS complex subunit 3 (GINS3) and ribonucleotide reductase regulatory subunit M2 (RRM2). There were also changes in the expression of genes involved in DNA synthesis, which is consistent with alterations in the cell cycle, specifically S phase. These include H2A histone family member Z (H2AFZ), high mobility group nucleosomal-binding domain 2 (HMGN2), homeobox B5 (HOXB5) and LSM3 homolog, U6 small nuclear RNA and mRNA degradation-associated (LSM3). This data suggested that FK866 significantly disrupts the cell cycle in GBM cells, which is consistent with pathway and transcription factor analysis in both cell lines.

In particular, HOXB5 was upregulated ∼1.4 fold in both cell lines. HOXB5 is a DNA-binding protein; however, its exact role in cellular biology is poorly understood (Galang and Hauser, 1993). HOXB5 is hypermethylated in some ovarian cancer samples, but highly expressed in others, as well as in oral cancers (Wu et al., 2007; Morgan et al., 2010; Tucci et al., 2011). In breast cancer, HOXB5 increases both proliferation and invasion by significantly increasing EGFR levels and inducing an EMT phenotype (Lee et al., 2015a). HOXB5 promotes an aggressive, invasive phenotype in gastric cancer by upregulating β-catenin signalling (Hong et al., 2015a). Recent work showed that knockdown of HOXB5 in NSCLC cells could block proliferation, migration and invasion through a loss of Wnt/βcatenin signalling, further rein-

forcing this phenotype (Zhang et al., 2018). The EGFR and Wnt/β-catenin signalling pathways are known to share numerous targets that promote cell survival and proliferation (Paul et al., 2013). The upregulation of HOXB5 in GBM cells in response to FK866 may represent an attempt to overcome the block in cell growth, by increasing the activity of these pathways to promote proliferation.

Changes in the expression of multiple HSPs and the gene activating transcription factor 6 (ATF6)B indicated alterations in the unfolded protein response of the endoplasmic reticulum. HSPA5 and HSPA8 were significantly downregulated in both cell lines, albeit only by a small magnitude. In contrast, ATF6B expression was significantly increased in both cell lines. GBM cells are known to exhibit aberrant expression of the unfolded protein response machinery (Graner, 2015). This is thought to allow them to produce proteins quickly, resulting in rapid proliferation and alterations to the extracellular matrix that promote invasion. ATF6 responds to endoplasmic reticulum stress by promoting the expression of genes that aid the refolding of proteins and therefore cell survival (Hetz and Papa, 2018). In GBM, ATF6 promotes resistance to chemotherapy and radiation (Dadey et al., 2015). ATF6B negatively regulates ATF6 activity by blocking its induction of HSPA5 (Thuerauf et al., 2004). In addition, knockdown of ATF6B leads to increased cell viabilty (Thuerauf et al., 2007). These data suggested that FK866 treatment in GBM cells inhibits the unfolded protein response, which may contribute to its anti-proliferative activities.

Finally, FK866 treatment induced a small increase in the expression of VEGFA in both cell lines. Previous studies have demonstrated that FK866 may trigger decreases in VEGF expression in gastric cancer cells (Bi et al., 2011). The combination of NAMPT, VEGF and Erb-B2 receptor tyrosine kinase 2 (HER2) expression has been suggested to be used as a diagnostic criterion in breast cancer (Zhu et al., 2016). Aberrant VEGF activity is a well-established phenotype in GBM. Increases in VEGF signalling are strongly associated with GBM progression, promoting angiogenesis to facilitate the delivery of blood, and therefore oxygen and nutrients, to the tumour (Robles Irizarry et al., 2012). VEGF signalling is mediated by the PI3K/Akt and MAPK pathways, and anti-VEGF therapies have resulted in increases in progression-free survival (PFS) in patients with GBM. Increased production of VEGFA induced

by FK866 treatment could potentially be a double-edged sword. Whilst it would promote angiogenesis and potentially tumour growth, it could also improve the delivery of cytotoxic drugs. More work is required to fully elucidate the role of VEGF signalling in the response of GBM cells to NAMPT inhibition.

Chapter 6

The effects of combined TMZ and FK866 treatment on GBM cell lines

It is clear that NAMPT inhibition has significant inhibitory effects on the cell cycle and proliferation in GBM cells, and is therefore a promising therapeutic option. However, patients with GBM will almost always be given the gold standard of care, consisting of surgical debulking followed by radiotherapy and chemotherapy in the form of TMZ. I hypothesised that inhibition of NAMPT, thus leading to a drop in NAD levels, could sensitise cells to TMZ by preventing PARP-mediated DNA repair. Therefore, I next aimed to determine whether FK866 could act synergistically with TMZ *in vitro*.

6.1 Proliferation assays show variability in the sensitivity of GBM cell lines to TMZ, correlated with MGMT expression

To assess the effects of combined treatment with TMZ and FK866, I first had to determine the sensitivity of GBM cells to TMZ independently. A panel of established and primary GBM cell lines were treated with increasing concentrations of TMZ, between 2 and 512 nM. Samples were analysed by SRB assay at 3, 6 and 9 days post treatment. TMZ demonstrated a time- and dose-dependent effect on all cell lines (Fig. 6.1, 6.2). The therapeutic window was relatively

wide across the different GBM cells lines (Fig. 6.3). IC_{50} data shows that there were subsets of sensitive and resistant cell lines (Fig. 6.3), which were consistent with their expression of MGMT (Fig. 6.4, Table 6.1). These results highlight the variability in the sensitivity of GBM cells to TMZ, and the importance of MGMT in TMZ resistance.

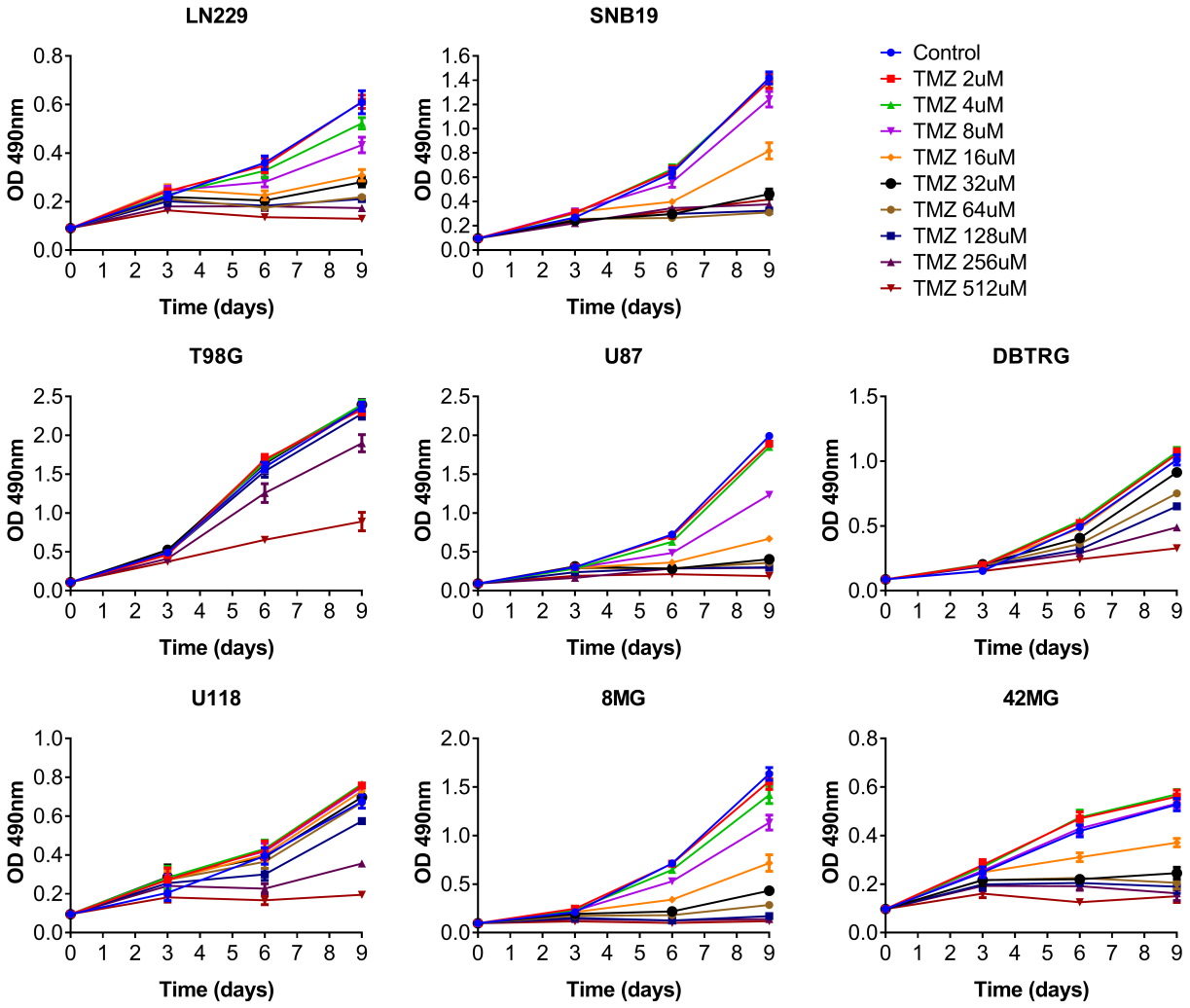


Figure 6.1: **TMZ has time and doses dependent effects on established GBM cell lines.** Dot and line plots showing proliferation measured by SRB assay (OD 490 nm) over time in established GBM cell lines treated with increasing concentrations of TMZ. Data representative of three independent experiments (n = 9 biological replicates). Error bars represent SEM.

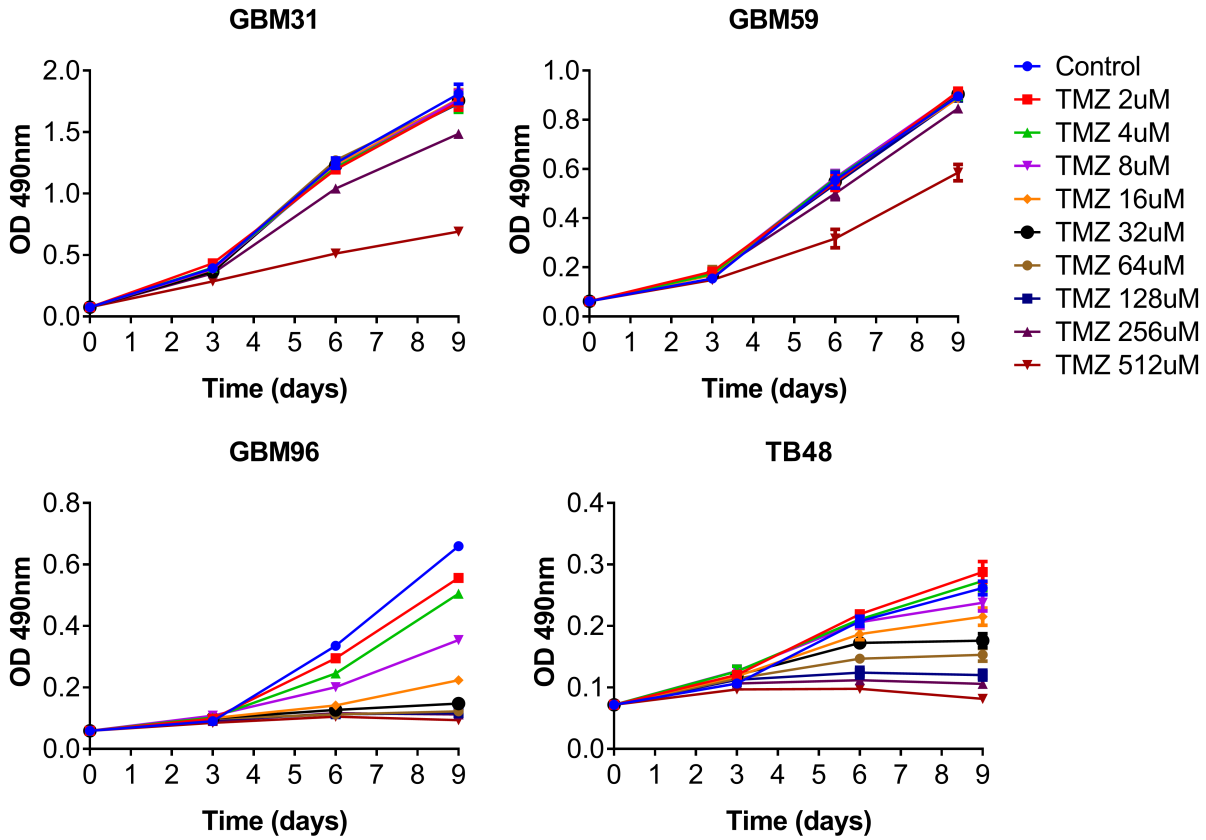


Figure 6.2: **TMZ has time and doses dependent effects on primary GBM cell lines.** Dot and line plots showing proliferation measured by SRB assay (OD 490 nm) over time in primary GBM cell lines treated with increasing concentrations of TMZ. Data representative of three independent experiments (n = 9 biological replicates). Error bars represent SEM.

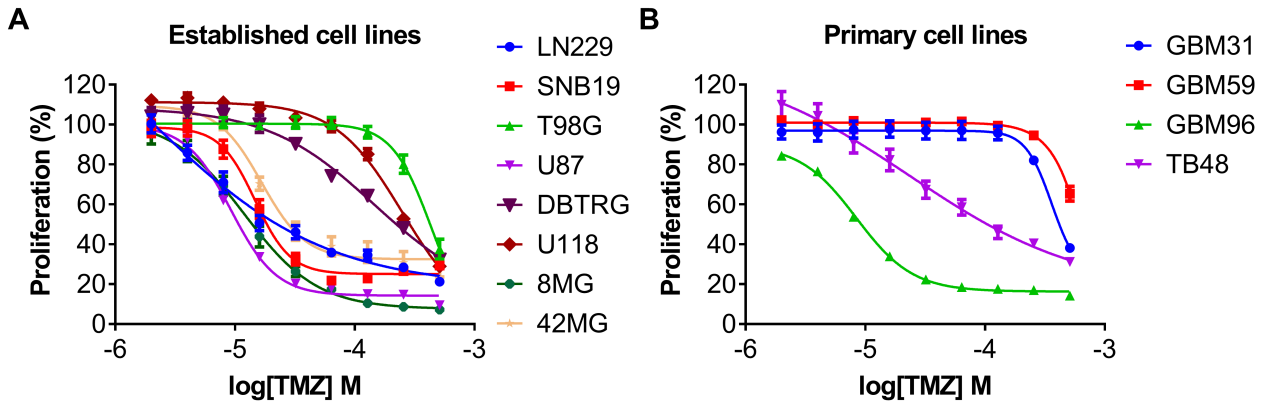


Figure 6.3: **Sensitivity to TMZ is highly variable across GBM cell lines.** Dot and line plots generated from SRB assay data showing changes in proliferation with increasing doses of TMZ in both (A) established and (B) primary GBM cell lines. Data from day 9 only. Lines of best fit represent a sigmoidal dose response curve. Proliferation normalised to vehicle control. Data representative of three independent experiments (n = 9 biological replicates). Error bars represent SEM.

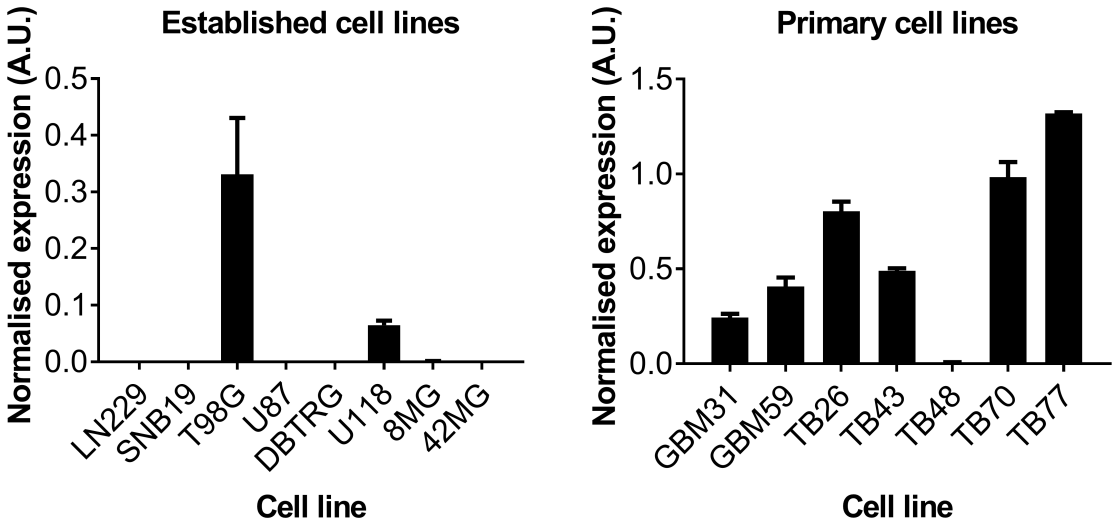


Figure 6.4: **The expression of MGMT is highly variable across established and primary GBM cell lines.** qPCR data for baseline expression of MGMT in GBM cell lines. Data representative of three independent experiments (n = 3 biological replicates). Error bars represent SEM.

Cell line	**TMZ IC50** (µM)	**MGMT status**
LN229	2.07	-
SNB19	14.75	-
T98G	433.40	+
U87	9.27	-
DBTRG	144.20	-
U118	249.80	+
8MG	11.93	-/+
42MG	16.67	-
GBM31	361.70	+
GBM59	> 512.00	+
GBM96	8.43	-
TB48	64.00	-/+

Table 6.1: **Table showing the IC_{50} values for TMZ and MGMT status in different GBM cell lines.** IC_{50} values calculated using a sigmoidal dose response curve. Data representative of three independent experiments (n = 9 biological replicates).

6.2 The combination of TMZ and FK866 significantly limits the proliferation of GBM cells compared to either alone

The next step was to look at the combined effect of TMZ and FK866 on proliferation. The LN229 and U87 cell lines were selected, because of their sensitivity to both TMZ and FK866, and their lack of MGMT expression. Short range TMZ titrations were tested with or without FK866 on LN229 and U87 cell lines. Independent FK866 and TMZ proliferation assay data were used to select a range of concentrations of each. Samples were analysed by SRB assay at 3, 6 and 9 days post-treatment. Independently, TMZ and FK866 exhibited time and dose dependent effects consistent with previous experiments (Fig. 6.5). Increasing concentrations of both FK866 and TMZ demonstrated additive effects in both GBM cell lines (Fig. 6.6A). The combination of TMZ and FK866 was significantly more effective at inhibiting proliferation than either drug used alone in both cell lines ($P < 0.05$, Fig. 6.6B).

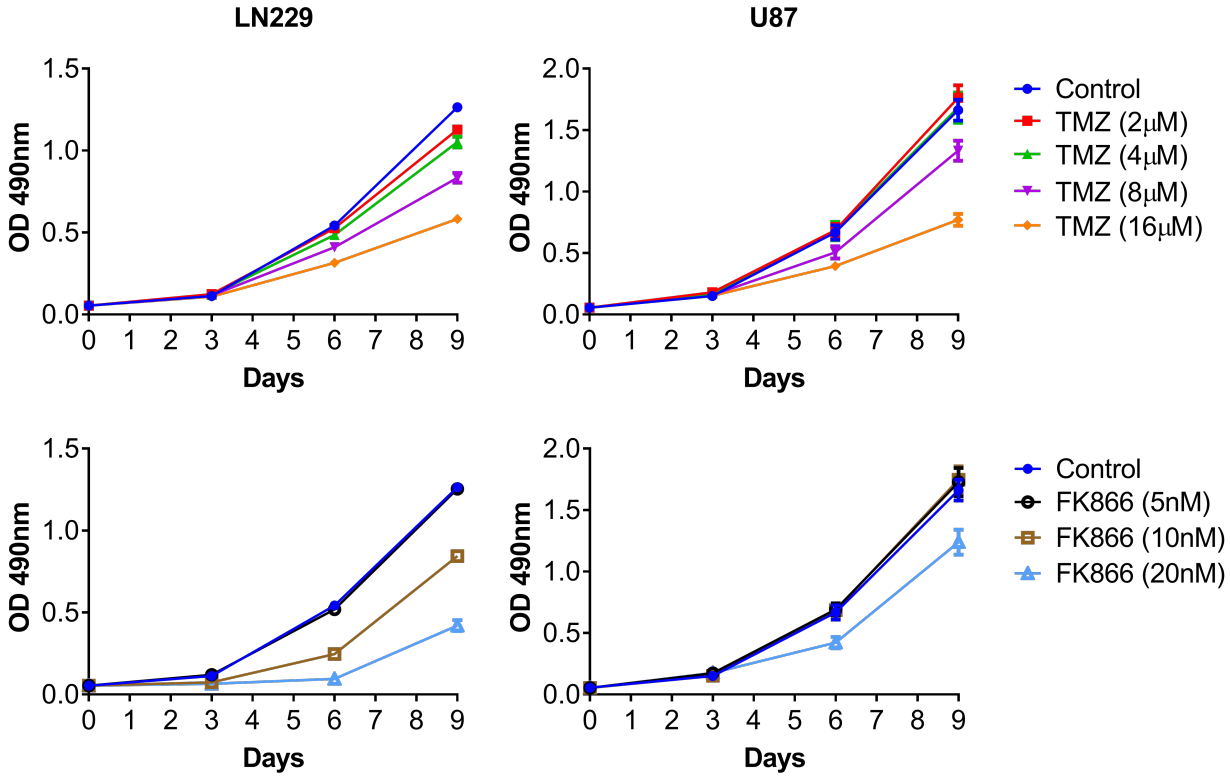


Figure 6.5: **TMZ and FK866 have time and dose dependent effects on LN229 and U87 cell lines.** Dot and line plots showing proliferation measured by SRB assay (OD 490 nm) over time in LN229 and U87 cell lines treated with increasing concentrations of TMZ or FK866. Data representative of three independent experiments (n = 9 biological replicates). Error bars represent SEM.

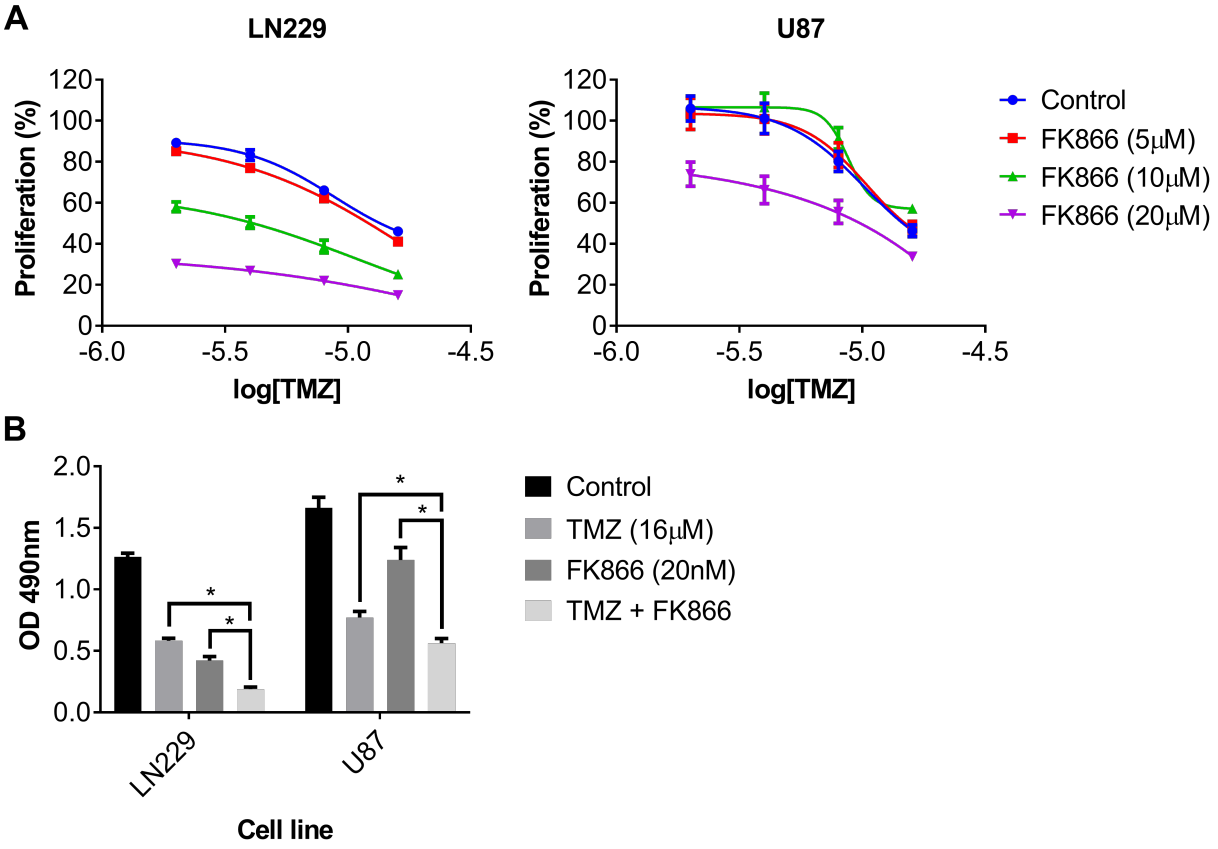


Figure 6.6: **FK866 yields additive effects when combined with TMZ in GBM cells.** (A) Data from SRB assays at day 9 for increasing concentrations of TMZ, with or without different concentrations of FK866. (B) Data from day 9 for the highest concentrations of each drug only. * $P < 0.05$, two-way ANOVA with Tukey's HSD post-hoc test. Data representative of three independent experiments (n = 9 biological replicates). Error bars represent SEM.

6.3 FK866 increases the G_2/M cell cycle block caused by TMZ treatment in GBM cells

Given that I saw additive effects when combining TMZ and FK866, the next step was to determine the mechanism by which these agents inhibit proliferation. LN229 and U87 cells were treated with TMZ (20 µM) and FK866 (20 nM) either alone or in combination. Samples were stained with annexin V or PI to measure apoptosis and cell death respectively at 3, 6 and 9 days post-treatment. In both LN229 and U87 cells, TMZ caused a significant decrease in the proportion of live cells ($P < 0.05$, Fig. 6.7). TMZ treatment also increased the proportion of early apoptotic cells in U87, and both early and late apoptotic cells in LN229 ($P < 0.05$, 6.8).

However, FK866 had no effect on apoptosis, neither independently, nor in combination with TMZ. PI staining for the cell cycle showed that TMZ causes a large shift in the cell cycle in LN229 and U87 cells. The proportion of cells in G_1/G_0 decreased and the proportion in G_2/M increased after 3 days and was maintained at 6 and 9 days ($P < 0.05$, Fig. 6.9). FK866 showed no effect on the cell cycle in U87 cells, but it decreased the proportion of cells in G_1/G_0 and increased the proportion in G_2/M phase in LN229 cells. Furthermore, the addition of FK866 to TMZ yielded a further shift in the cell cycle in LN229 cells, although this was not significant ($P = 0.088$, Fig. 6.9).

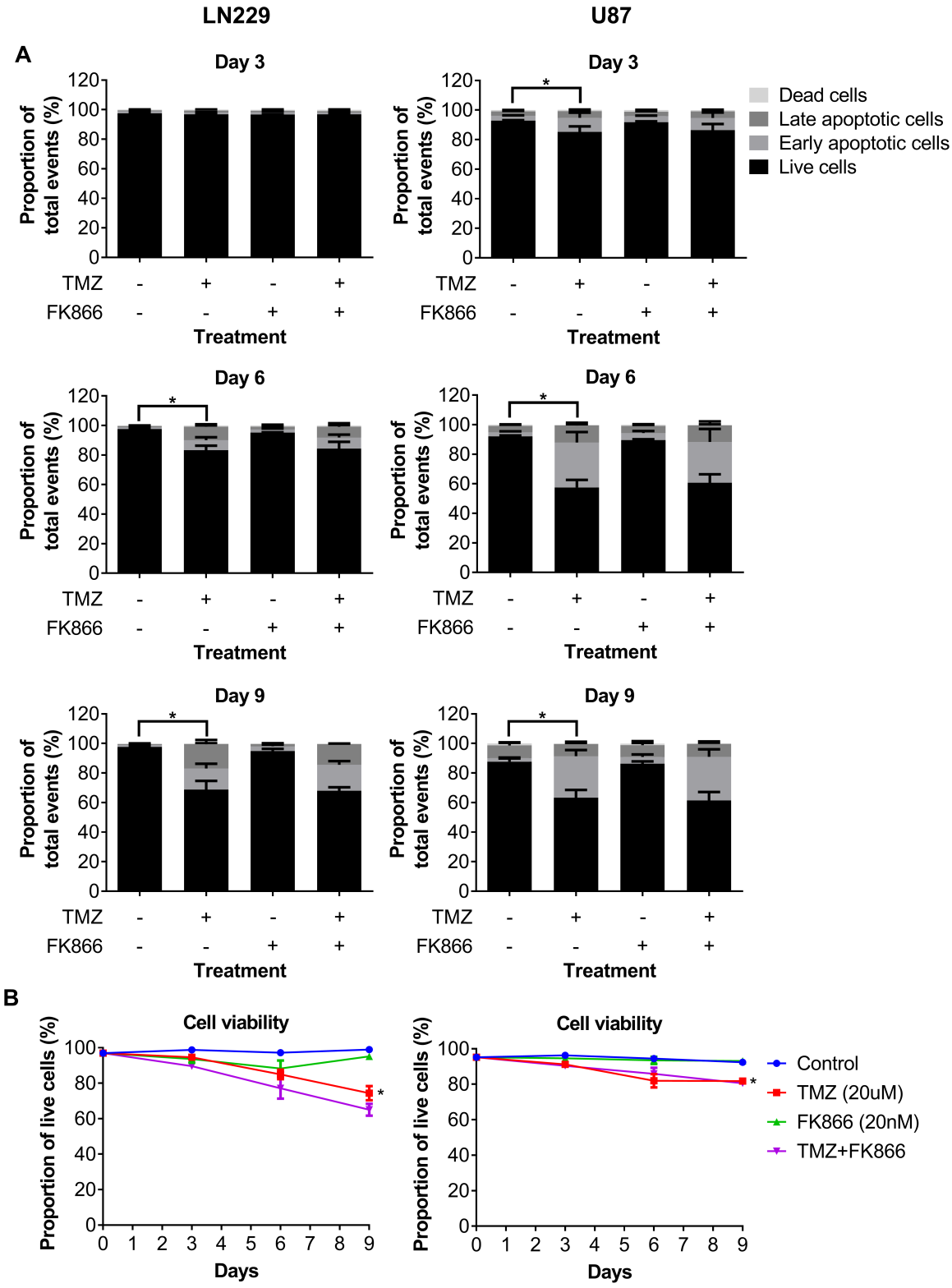


Figure 6.7: **TMZ decreases the proportions of live GBM cells.** (A) Annexin V and (B) trypan blue staining showing changes in apoptosis and cell death in GBM cells treated with TMZ (20 µM) and FK866 (20 nM). * $P < 0.05$, Control vs TMZ, two-way ANOVA with Tukey's HSD post-hoc test. Data representative of three independent experiments (n = 3 biological replicates). Error bars represent SEM.

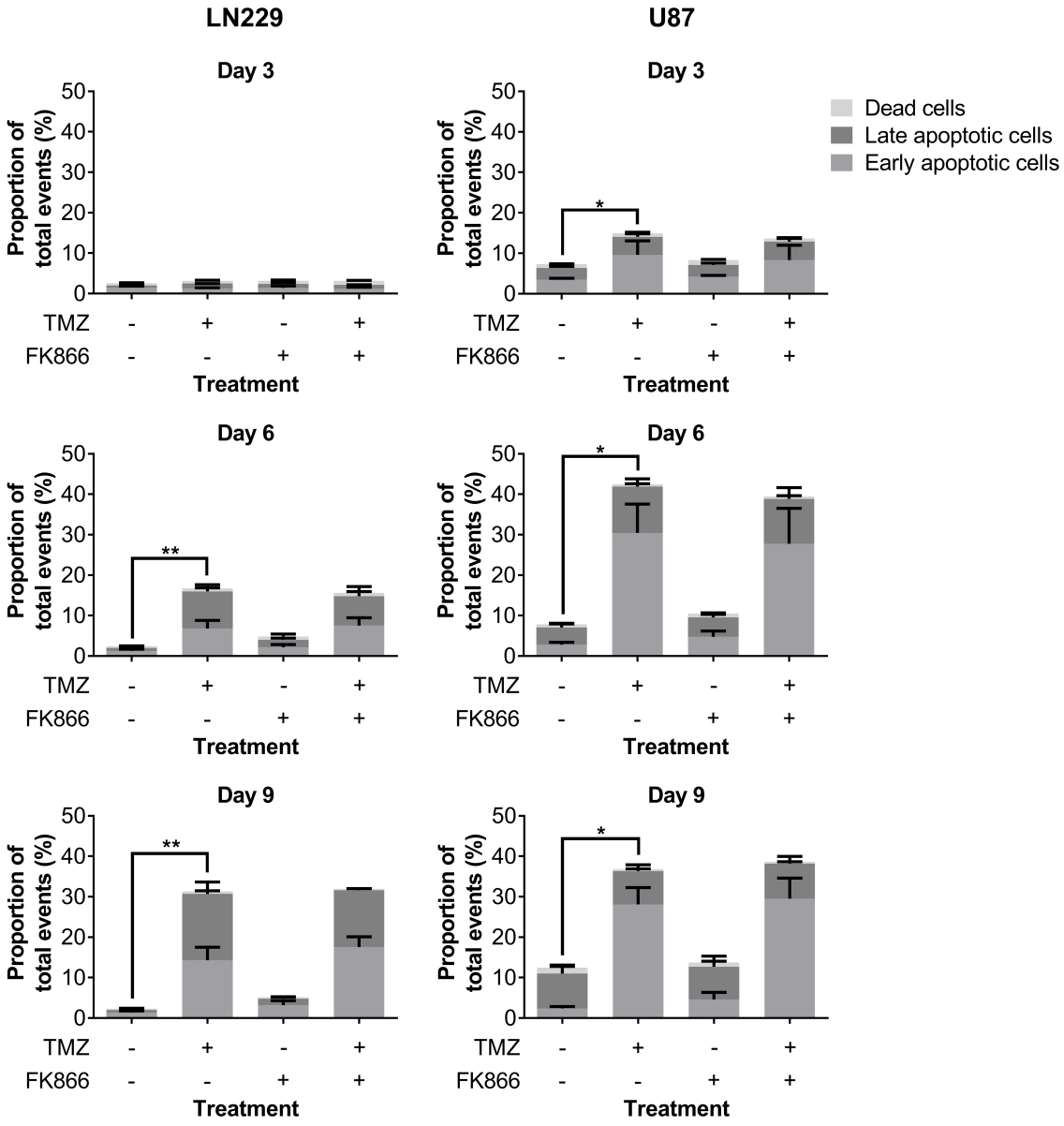


Figure 6.8: **TMZ activates apoptosis in GBM cells.** Annexin V staining showing changes in apoptosis in GBM cells treated with TMZ (20 µM) and FK866 (20 nM). * $P < 0.05$, early apoptotic cells, ** $P < 0.05$, early and late apoptotic cells, two-way ANOVA with Tukey's HSD post-hoc test. Data representative of three independent experiments (n = 3 biological replicates). Error bars represent SEM.

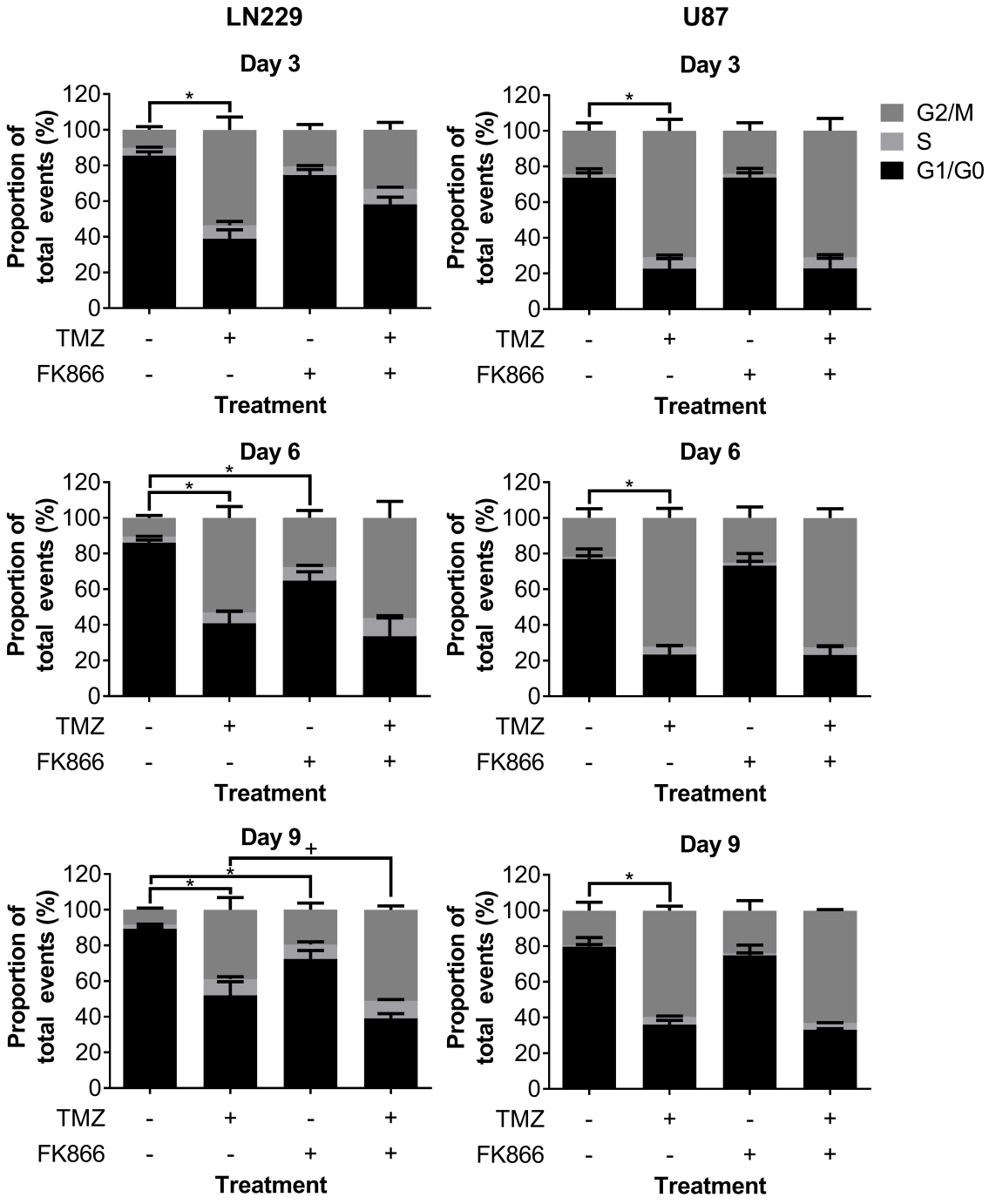


Figure 6.9: **TMZ and FK866 lead to a G_2/M cell cycle block.** PI staining showing the changes in the cell cycle in GBM cells treated with TMZ (20 µM) and FK866 (20 nM). * $P < 0.05$, + $P = 0.088$, two-way ANOVA with Tukey's HSD post-hoc test. Data representative of three independent experiments (n = 3 biological replicates). Error bars represent SEM.

6.4 The combination of TMZ and FK866 significantly alters the expression of genes involved in NAD biosynthesis, energy production and regulation of the cell cycle

I next wanted to determine whether treatment with TMZ with and without FK866 could significantly alter the expression of genes involved in NAD biosynthesis, proliferation, DNA repair and bioenergetics. LN229 cells were treated with TMZ (20 µM) and FK866 (20 nM) alone and in combination, and RNA was extracted at 24, 48 and 72 h. cDNA was synthesised and qPCR's were carried out for numerous genes involved in NAD biosynthesis, as well as PARP 1 and 2, SIRTs 1-7 and PPARGC1 A and B. Treatment of LN229 cells with FK866 in the presence or absence of TMZ resulted in a significant increase in the expression of NAMPT at 48 and 72 h ($P < 0.05$, Fig. 6.10). There were no clear changes in the expression of NAPRT, but there was a steady decrease in the expression of NT5E in all groups. Somewhat surprisingly, QPRT, IDO1 and NMNAT1 expression was significantly increased only in the groups that were not treated with FK866, whereas KYNU expression significantly increased in cells treated with both TMZ and FK866 only ($P < 0.05$, Fig. 6.10). In addition, in cells treated with FK866 either alone or in combination with TMZ, the expression of SIRT1 and PPARGC1A significantly increased rapidly between 24 h and 48 h ($P < 0.05$, Fig. 6.11), but then quickly dropped again. On the other hand, high levels of PPARGC1B were maintained in cells treated with both TMZ and FK866 ($P < 0.05$, Fig. 6.11). Finally, the expression of SIRT7 increased slightly in FK866 treated groups, although this was only significant in the FK866 only group ($P < 0.05$, Fig. 6.11). There were no clear changes in the expression of other genes involved in NAD metabolism or NAD consuming proteins such as the PARPs or other SIRTs (Fig. 6.12). Surprisingly, these results could not be recapitulated in U87 cells, suggesting that there may be very different mechanisms involved in the response of these two cells lines to combined TMZ and FK866 treatment (Fig. 6.13).

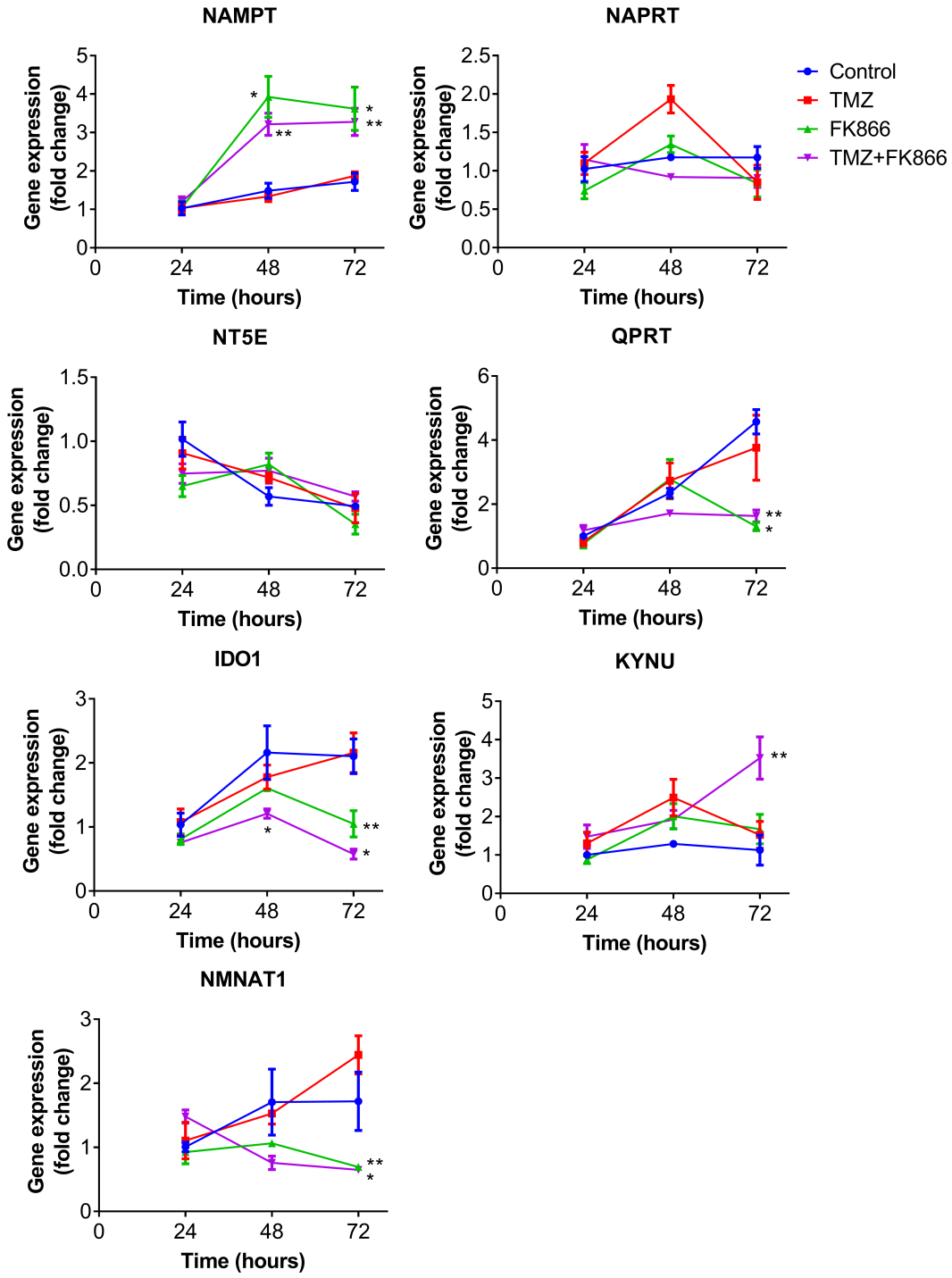


Figure 6.10: **The expression of genes involved in NAD biosynthesis are altered upon treatment of LN229 cells with TMZ and FK866.** qPCR data from LN229 cells treated with TMZ (20 µM) and FK866 (20 nM) at 24, 48 and 72 h. * $P < 0.05$ Control vs FK866, ** $P < 0.05$ Control vs TMZ+FK866, two-way ANOVA with Tukey's HSD post-hoc test. Data representative of three independent experiments (n = 3 biological replicates). Error bars represent SEM.

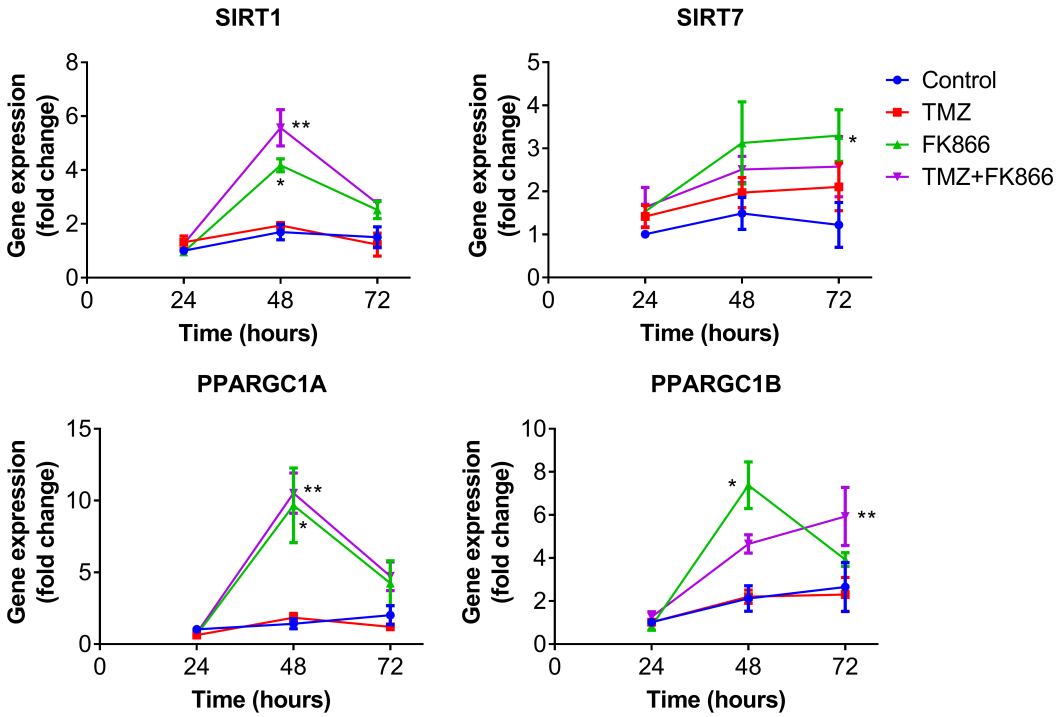


Figure 6.11: **The expression of genes related to cell cycle control and bioenergetics are altered upon treatment of LN229 cells with TMZ and FK866.** qPCR data from LN229 cells treated with TMZ (20 µM) and FK866 (20 nM) at 24, 48 and 72 h. * $P < 0.05$ Control vs FK866, ** $P < 0.05$ Control vs TMZ+FK866, two-way ANOVA with Tukey's HSD post-hoc test. Data representative of three independent experiments (n = 3 biological replicates). Error bars represent SEM.

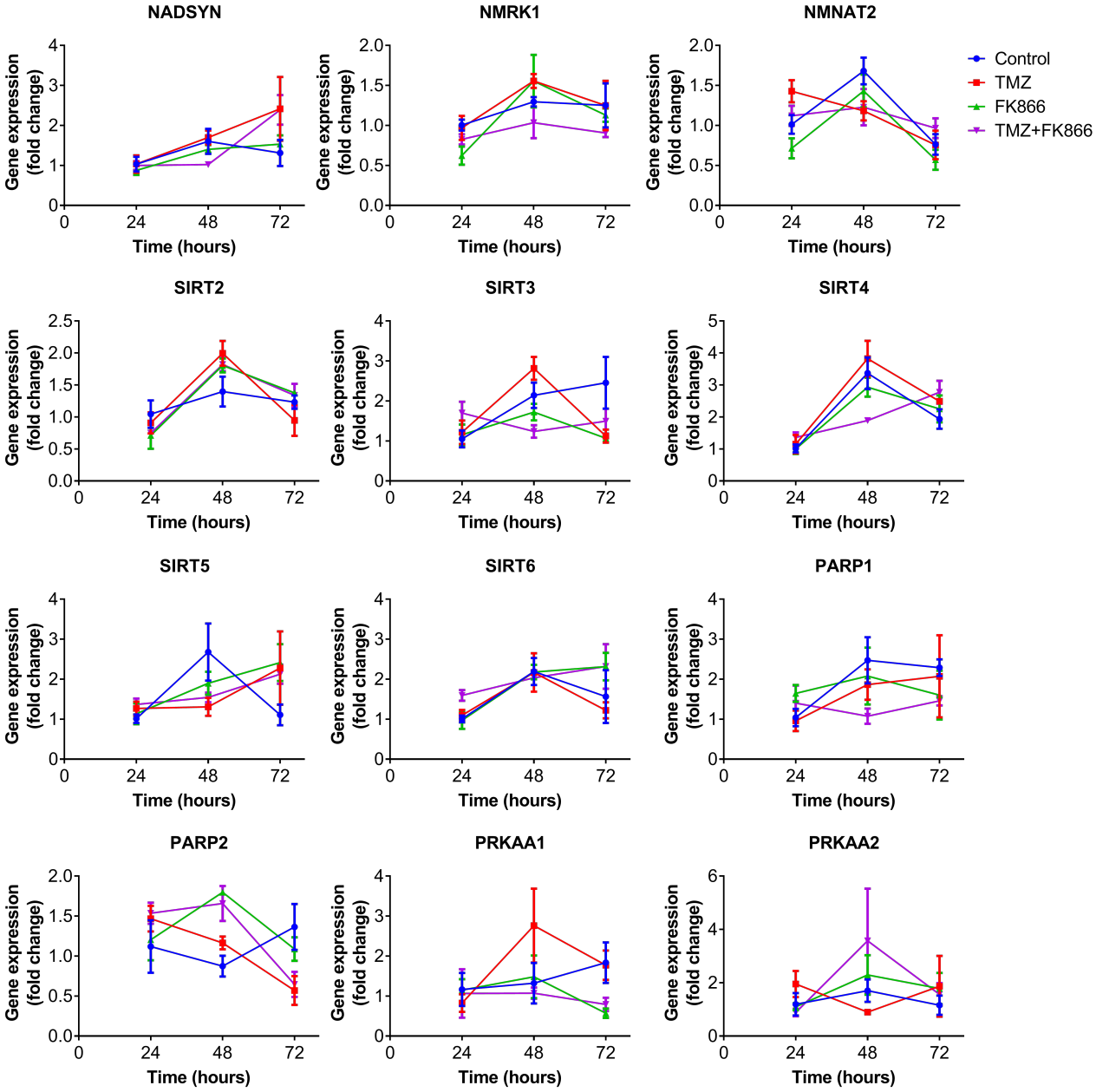


Figure 6.12: **Changes in the expression of other genes involved in NAD biosynthesis/consumption and bioenergetics in LN229 cells treated with TMZ and FK866.** Dot and line plots showing the changes in gene expression over time (qPCR data) in LN229 cells treated with TMZ (20 µM) and FK866 (20 nM), either alone or in combination. Data representative of three independent experiments (n = 3 biological replicates). Error bars represent SEM.

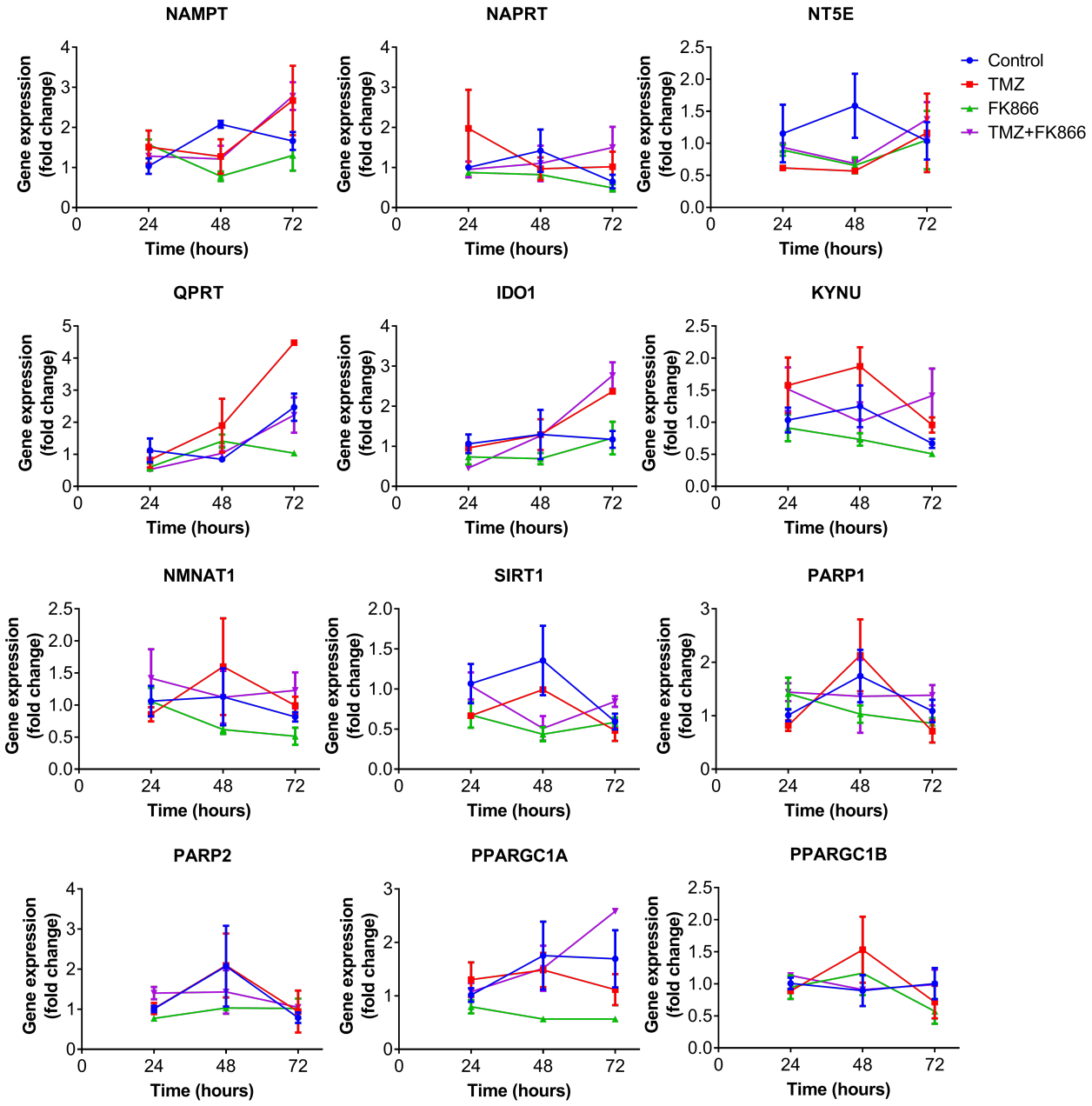


Figure 6.13: **Changes in the expression of genes involved in NAD biosynthesis/consumption and bioenergetics in U87 cells treated with TMZ and FK866.** Dot and line plots showing the changes in gene expression over time (qPCR data) in U87 cells treated with TMZ (20 µM) and FK866 (20 nM), either alone or in combination. Data representative of three independent experiments (n = 3 biological replicates). Error bars represent SEM.

6.5 Discussion

The results presented here demonstrated that both established and primary GBM cell lines are ∼1,000 times more sensitive to FK866 than they are to TMZ, which is consistent with other studies (Goellner et al., 2011). Proliferation assay data suggest that the combination of FK866 (20 nM) and TMZ (16 µM) is additive as opposed to synergistic. It is necessary to use both at growth inhibitory concentrations to achieve any sort of combined effect. This could be confirmed using the method proposed by Chou-Talalay combination index (Chou, 2007). The combination of TMZ and FK866 limits proliferation by initiating a G_2/M cell cycle block better than either drug alone in LN229 cells. The shift in the cell cycle to a G_2/M block is often observed in GBM cells treated with TMZ (Hirose et al., 2001; Kanzawa et al., 2004), and has also been linked to the action of FK866 in GBM cells (Zhang et al., 2012b). Surprisingly, U87 does not show a clear change in the cell cycle with FK866 treatment, despite a small decrease in proliferation. Given the previous discrepancies seen with the FK866 rescue experiments in U87, it is possible that this cell line is highly unique, and its responses to FK866 could be mechanistically different from the other cell lines. A recent study showed that the combination of TMZ and NAMPT inhibition could also induce apoptosis and necrosis in GBM cells, through the activation of caspase-1, 3 and 9 and increased production of ROS, dependent on c-Jun/JNK signaling (Feng et al., 2016a). More work is required to determine if this occurs in the cell lines used here, and how the different NAD biosynthetic pathways might affect the responses of these cells to NAMPT inhibitors.

Treatment of LN229 cells with TMZ and FK866 led to significant changes in the expression of genes involved in NAD biosynthesis, as well as some SIRTs and the PPARGC1 genes. Increases in the expression of NAMPT in response to FK866 treatment suggest an attempt to compensate for the loss of its activity. It is clear that a reduction in NAD levels in LN229 cells alters epigenetic regulation of NAMPT to promote its expression. Whilst the induction of KYNU expression in LN229 cells treated with FK866 would promote NAD biosynthesis through the kynurenine pathway, the suppression of QPRT, IDO1 and NMNAT1 expression is somewhat surprising. QA is able to restore proliferation in FK866 treated LN229 cells, so one would assume that these genes would also be upregulated in response to NAMPT inhibition, but

the exact opposite is observed. Studies have shown that in GBM, both QPRT and IDO2 are expressed at higher levels compared to normal cells (Adams et al., 2014). Changes in the expression of these genes may be more directly related to the effects of TMZ as opposed to FK866 treatment. The rapid but transient induction of SIRT1 could represent the shift in the cell cycle seen with FK866 treatment. SIRT1 is known to regulate the expression of transcription factors that control the cell cycle, including RB and members of the E2F family, such as E2F1 (Wang et al., 2006a; Wong and Weber, 2007). Changes in the expression of SIRT1 are also consistent with alterations to FOXM1 signalling seen in the FK866-sensitive 42MG cells, as SIRT1 expression is directly regulated by FOXM1 (Zhu et al., 2014). The parallel increases in PPARGC1A/B and SIRT1 also indicated a link between the two proteins. PGC1α is well established as a key regulator of cell metabolism. It promotes mitochondrial biogenesis and OXPHOS to increase ATP production, as well as having roles in lipid and carbohydrate metabolism (Liang and Ward, 2006). All of these activities rely on NAD to properly function. Studies have demonstrated that SIRT1 directly deacetylates and therefore activates PGC1α to promote an oxidative phenotype (Nemoto et al., 2005). Treatment of GBM cells with FK866 reduced NAD levels and would therefore decrease the activity of SIRT1, leading to a loss of PGC1α activity. The transient increase in the expression of these two genes may represent another compensatory mechanism to maintain a normal cell cycle and energy production under the stress of NAD depletion. Their corresponding decline at 72 h could represent the point at which the cells enter senescence. The decrease seen in the expression of NT5E across all groups suggest that this is not related to TMZ or FK866 treatment, but rather reflects some changes that occur to cells grown in culture conditions. NT5E has previously been associated with extracellular matrix interactions in glioma cells (Cappellari and Vasques, 2012). Changes to the extracellular matrix are likely to occur as cells adhere to a culture plate, proliferate and migrate in to open space, which could lead to decreases in NT5E expression. Furthermore, NT5E expression is epigenetically regulated through CpG island methylation (Wang et al., 2012; Lo Nigro et al., 2012). Epigenetic regulation could explain the lack of these responses in U87 cells. There may be other factors, including gene silencing by promoter methylation, miRNA interference or protein degradation that lead to inconsistencies between gene expression

and protein levels. In addition, divergent responses to FK866 treatment have previously been reported in lung cancer (Xiao et al., 2016). This reinforces the importance of identifying subpopulations of patients whose tumours are most likely to respond to NAMPT inhibitors.

Chapter 7

The effects of combined TMZ and FK866 therapy *in vivo*

7.1 NAMPT inhibition synergises with TMZ to reduce tumour burden in mice

In order to determine whether NAMPT inhibition would be a viable option for the treatment of GBM clinically, we used a well established *in vivo* model of GBM tumours using U87-GFP/Luc cells. A total of 2×10^5 U87-GFP/Luc cells were injected into the right cerebral hemisphere of nude (CD1-*Foxn1*$^{nu/nu}$) mice, and tumours were allowed to establish for 10 days, at which point they were imaged using the IVIS. After 2 weeks, mice were randomised to four different treatment groups:

- 1% DMSO in saline once a day for 5 days a week for 2 weeks
- TMZ (30 mg/kg) in 1% DMSO in saline once a day for 5 days a week for 1 week
- FK866 (20 mg/kg) in 1% DMSO in saline once a day for 5 days a week for 2 weeks
- Combined TMZ and FK866 in 1% DMSO in saline administered as described above

The mice were imaged using the IVIS every 3-4 days. When the animals in the control group started to become symptomatic (∼4 weeks), all of the animals were culled, perfused with 4% PFA and the brains were removed and fixed in 4% PFA. Images showing the radiance from

the tumours seen in each animal from the final round of imaging can be seen in Fig. 7.1. None of the drug combinations had any significant effect on mouse weight over the course of the experiment (Fig. 7.2).

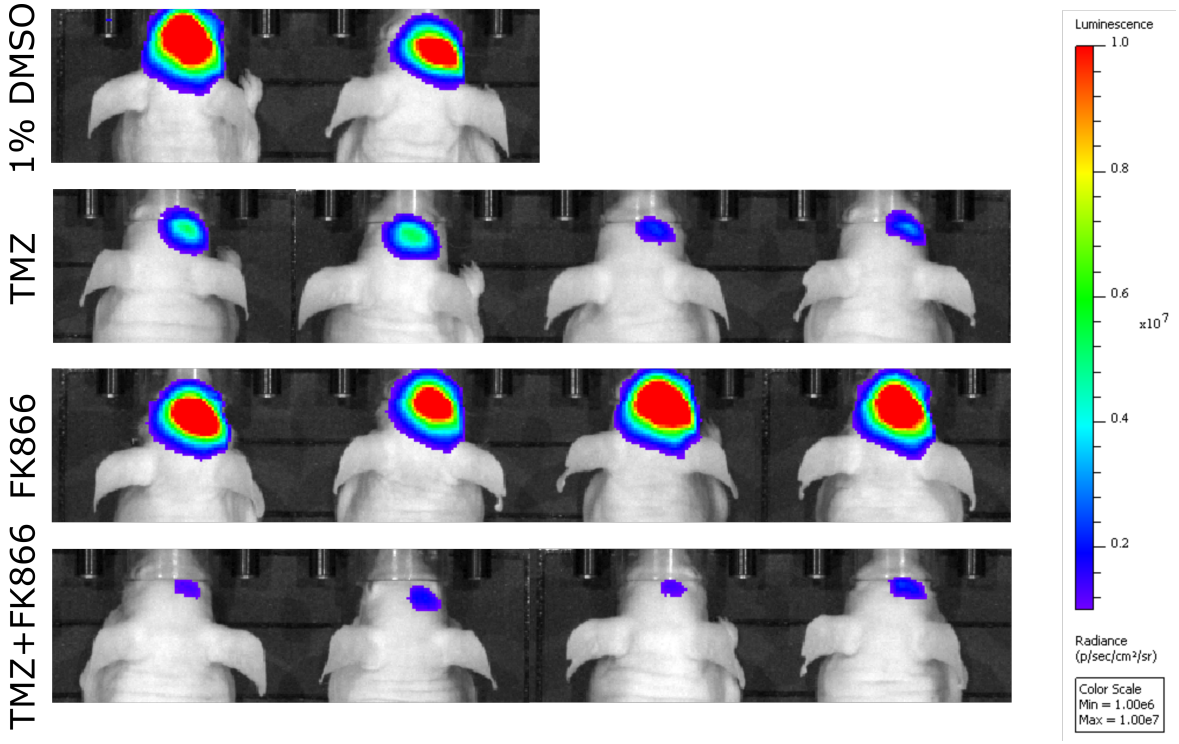


Figure 7.1: **Images of the tumours in all mice taken from the final round of imaging on the IVIS.** All images normalised to a standard scale of radiance (p/sec/cm^2/sr). Data unavailable for two of the mice in the control group.

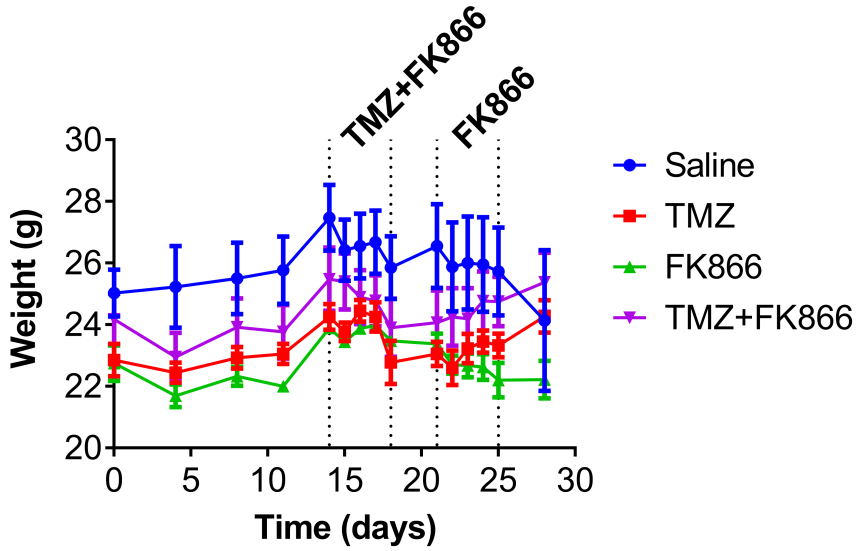


Figure 7.2: **Dot and line plot showing the average weight of animals in each treatment group over the course of the study.** Day 0 marks the day at which U87-GFP/Luc cells were implanted into the right cerebral hemisphere of the mice. Drug treatment periods are labelled with dotted lines (once a day for 5 days in a week). Data representative of four mice.

As expected, the saline-treated group had very large tumours, and two of the mice became symptomatic and had to be sacrificed before the final round of imaging could take place. Whilst FK866 alone did not appear to have much of an effect on tumour growth, the mice in this group were completely asymptomatic, and showed little to no weight loss (Fig. 7.3A). TMZ clearly reduced tumour burden in the mice, but the addition of FK866 reduced tumour size even further, to approximately half that of the TMZ only treated group (Fig. 7.3A, B). Whilst this difference was not significant in the raw radiance values, when the data was normalised to the initial tumour size from the first IVIS scan at day 10, the addition of FK866 to TMZ significantly reduced tumour burden at the last two timepoints ($P < 0.05$, Fig. 7.3C, D).

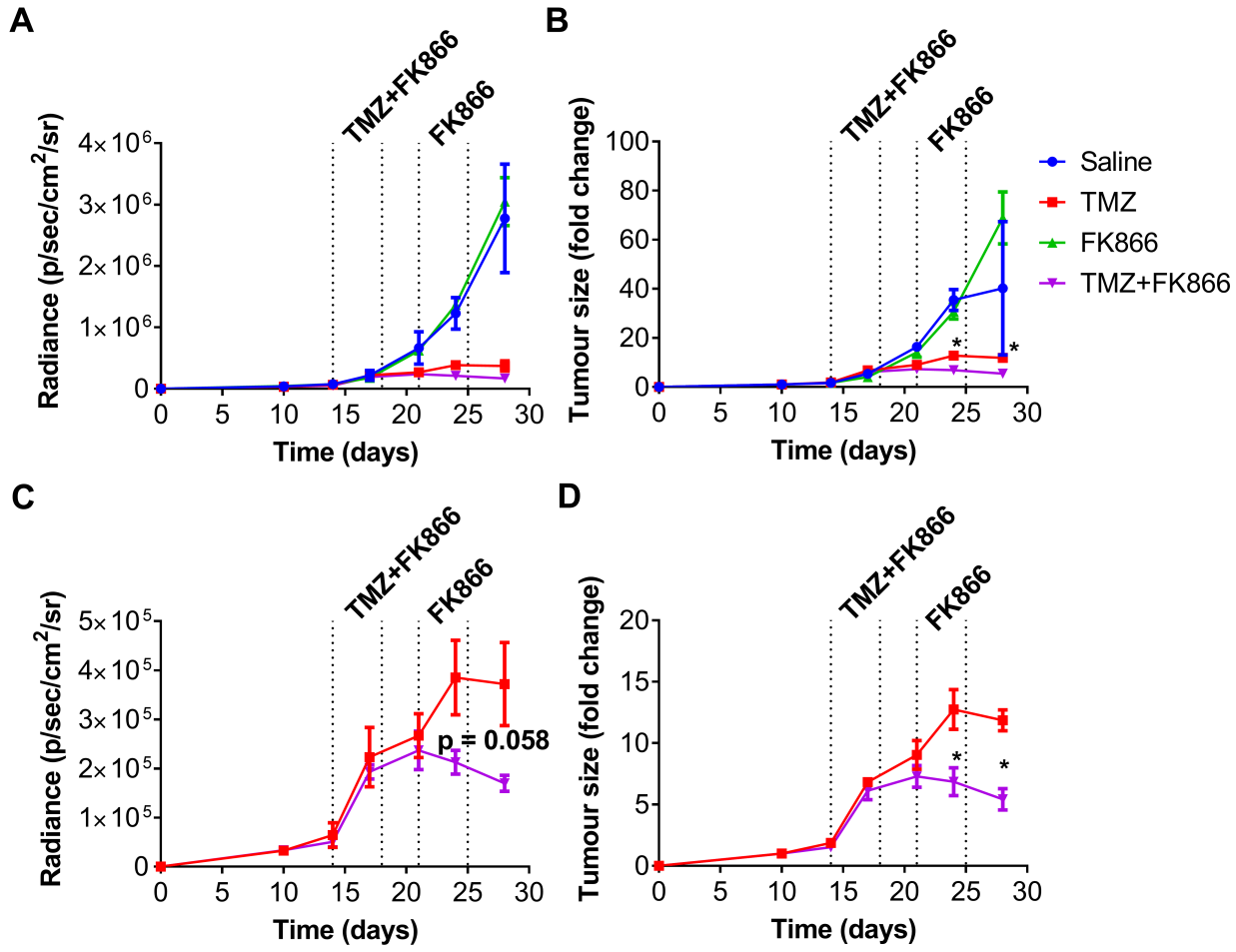


Figure 7.3: **Dot and line graphs showing the change in tumour size over time in the four treatment groups.** (A) Tumour radiance plotted over time for all four treatment groups. (B) Fold change in tumour size plotted against time for all four treatment groups. (C) Tumour radiance plotted over time for TMZ treated groups only. (D) Fold change in tumour size plotted over time for TMZ treated groups only. * $P < 0.05$, TMZ vs TMZ+ FK866, two-way ANOVA with Tukey's HSD post-hoc test. Data representative of four mice. Error bars represent SEM.

7.2 FK866 inhibits proliferation and stabilises GBM tumours *in vivo*

In order to get a more detailed view of the microstructure of the tumours, we carried out imaging using a modified version of the tissue clearing CLARITY procedure (Chung et al., 2013) known as FASTClear (Perbellini et al., 2017) on mouse brain sections. Images of the mouse brains used for FASTClear can be seen in the appendix (Fig. B.1). Samples were

subject to the FASTClear protocol and stained with an antibody targeting Ki-67, as well as tomato lectin to stain blood vessels. Representative images from each treatment group can be seen in Fig. 7.4. The tumour in the control mouse filled almost the entirety of the right hemisphere, significantly disrupting the normal brain structure, and also had large numbers of proliferative (Ki-67$^+$) cells, and showed vast central necrotic areas with no staining. TMZ treatment clearly reduced tumour size, as well as reducing the number of proliferative cells, and reducing the tumours impact on overall brain structure. Whilst the tumour was still quite large in the FK866 treated mouse, there appeared to be fewer proliferative cells, no core necrosis, well defined tumour boundaries, and only partial disruption of normal brain structure. Finally, in the TMZ+FK866 treated mouse, the tumour was too small to detect by this method, and there was no Ki-67 staining and no disruption to normal brain structure.

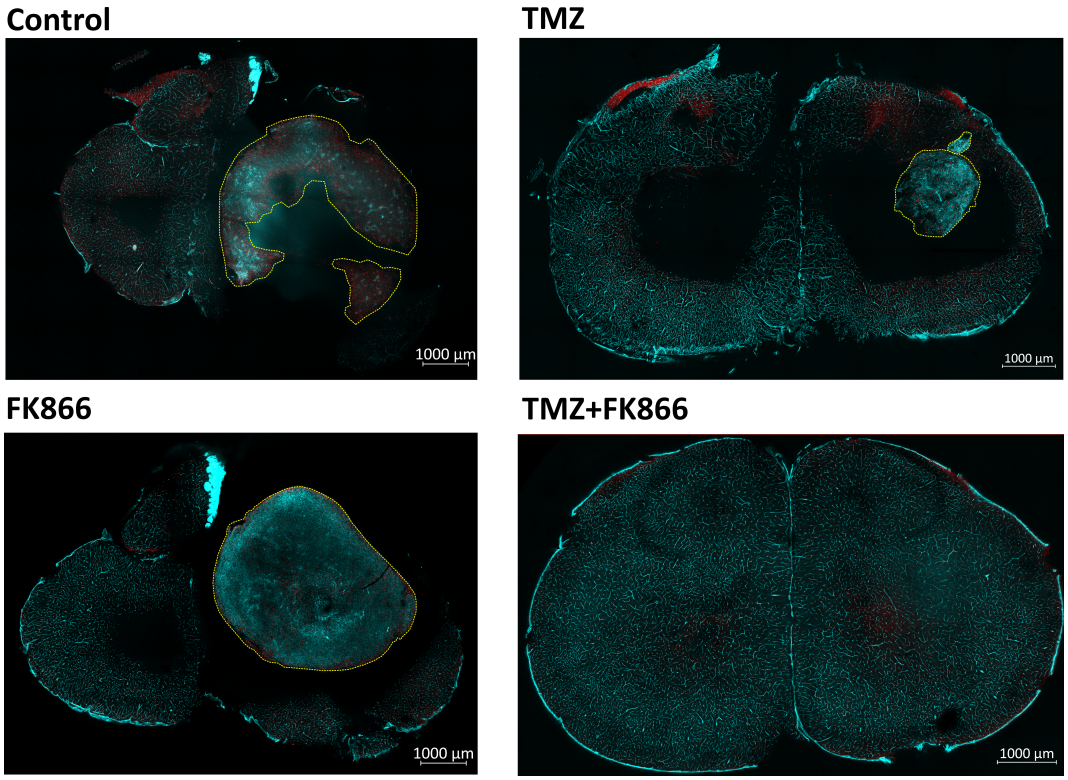


Figure 7.4: **Confocal microscope images of mouse brain sections stained with Ki-67 and tomato lectin**. Representative images for the mice in each treatment group. Green staining is tomato lectin, which indicates blood vessels. Red staining is Ki-67, which shows proliferative cells. Yellow dashed lines enclose tumour tissue. Scale bars show 1000 µm. FASTClear carried out and images obtained by Tsz Wing Chau.

7.3 Discussion

The results presented here indicate that, when combined with TMZ, FK866 significantly inhibits the growth of intracranial GBM tumours, and initiates tumour regression at an earlier stage. This leads to a reduction in tumour burden by ∼50%. Whilst FK866 is unable to inhibit tumour growth when used independently, it may prevent the development of large, necrotic regions often seen in GBM tumours, and decrease the proportion of proliferative (Ki-67$^+$) cells at the tumour periphery. It is possible that the concentration of FK866 in the brain *in vivo* is lower than the doses used *in vitro*, which would explain the relatively poor response. This could be due to any number of factors, including metabolism of the drug by the liver, or failure of the drug to localise to the brain and penetrate the BBB. It is important to note that whilst there was a significant difference in the growth of tumours in the TMZ versus the TMZ+FK866 group, some of the tumours between the groups were still remarkably similar in size. Further repeat experiments are required to ensure that this effect is robust and reproducible. However, the results presented here are generally consistent with published data. Previous studies have shown that treatment of mice bearing intracranial primary GBM tumours with GMX1778 leads to a reduction in the number of Ki-67$^+$ cells in the tumour, as well as an increase in their survival time (Tateishi et al., 2015). However, when the same group used U87 cells, they did not observe the same increase in survival (Tateishi et al., 2016). Furthermore, when they attempted to combine this with TMZ they used a subcutaneous model of U87 cells. Whilst they used very similar doses of both TMZ and FK866, and the pattern of change appeared to be very similar to the data presented here, they did not observe a significant decrease in tumour growth with the addition of FK866 to TMZ (Tateishi et al., 2017). This suggests that the effects of combined FK866 and TMZ are dependent on the unique biology of the brain and its interactions with GBM cells.

Chapter 8

General discussion

GBM is a devastating form of cancer, with a median survival time of only 14.2 months (Johnson and O'Neill, 2012). The last major breakthrough in the treatment of GBM was over 10 years ago, with the addition of TMZ to surgery and radiation (Stupp et al., 2005). Since then, attempts have been made to target specific signalling pathways in GBM, such as the EGFR, PI3K/Akt, AMPK and mTOR pathways, but these are yet to show significant clinical benefits (Pitz et al., 2015; Chinnaiyan et al., 2017; Ma et al., 2015; Artene et al., 2018; Schiff et al., 2018; ClinicalTrials.gov, 2018). Furthermore, targeted therapies are often only effective in cancers that display specific genetic alterations, such as PARP inhibitors in BRCA-mutated cancers, which do not occur in GBM (Wesseling et al., 2015; Ohmoto and Yachida, 2017). In addition, metabolic therapies including classic antimetabolites like methotrexate, glycolytic inhibitors such as 2DG and depletion of amino acids such as arginine, have all either failed or are yet to be tested in GBM (Singh et al., 2005; Herrlinger et al., 2005; Ott et al., 2013; Thongkum et al., 2017; Szlosarek et al., 2017). Inhibitors of NAMPT have demonstrated significant anti-neoplastic activity in numerous cancers, including GBM (Hasmann and Schemainda, 2003; Muruganandham et al., 2005; Pogrebniak et al., 2006; Billington et al., 2008; Nahimana et al., 2009; Patel et al., 2010; Okumura et al., 2012; Zhang et al., 2012b). Some studies have indicated that NAMPT inhibitors can enhance the effects of TMZ in GBM through multiple mechanisms (Goellner et al., 2011; Yang et al., 2015c; Feng et al., 2016a). Whilst initial clinical trials for NAMPT inhibitors have been unsuccessful, this is likely because they have been tested on highly refractory cancers, with no stratification of patients based on known

resistance mechanisms (Holen et al., 2008; Von Heideman et al., 2010; Goldinger et al., 2016; ClinicalTrials.gov, 2018).

In this study, I have demonstrated that there is a subset of patients with GBM whose tumours lack key enzymes involved in NAD biosynthetic pathways, which prevents them from using alternative sources of NAD during NAMPT inhibition. These enzymes are NAPRT, NT5E and QPRT. Whilst previous studies have analysed the effects of individual NAD biosynthetic pathways, very little work has been done showing how these pathways behave in the same cells, and how they might interact. I have shown that the expression of these genes is highly variable between GBM tumours, and both established and primary GBM cell lines. The expression of NAMPT and NT5E are both elevated in GBM tissue, and both these genes, as well as NAPRT, are associated with survival in patients with GBM. Whilst this has previously been reported for NAMPT and NT5E in GBM (Reddy et al., 2008; Xu et al., 2013), this observation has not previously been shown for NAPRT. *In vitro* data demonstrates that the NAMPT inhibitor FK866 potently limits proliferation in both established and primary GBM cell lines. Consistent with previous results, the data suggests that this is not through the activation of apoptosis or cell death, but rather the inhibition of proliferation, possibly through a G_2/M cell cycle block (Zhang, 2012). The presence of specific genes involved in NAD biosynthesis, including NAPRT, NT5E and QPRT, dictate the ability of specific NAD precursors to rescue proliferation in GBM cells treated with FK866. Furthermore, the combination of TMZ and FK866 was more effective at inhibiting the growth of GBM cells both *in vitro*, and in a murine orthotopic xenograft model of GBM using U87 cells. Whilst this is mostly consistent with preivous studies, this is the first time, to my knowledge, that a NAMPT inhibitor has been shown to be effective when combined with TMZ in an intracranial model (Zhang et al., 2012b; Yang et al., 2015c; Tateishi et al., 2015).

It has been proposed that the toxicity of NAMPT inhibitors could be mitigated by coadministration of NA, allowing increased doses to be used to achieve maximal on-target effects (Tarrant et al., 2015). Studies have demonstrated that this approach allows specific depletion of NAD levels in NAPRT-deficient tumours (Olesen et al., 2010b). This theory could be expanded to tumours that express mutant and therefore catalytically inactive forms of NAPRT

(Duarte-Pereira et al., 2014). This may be the case for glioma, where it has been demonstrated that a small percentage of tumours have deletions in the NAPRT gene (Piacente et al., 2017). Somewhat surprisingly, one study demonstrated that NAPRT-deficient tumours could be rescued by either NA or Nam *in vivo* (O'Brien et al., 2013). The authors suggested that this could be due to differences between the timing or dose of either the NAMPT inhibitor or NA, which prevents the drop in NAD levels from reaching the threshold required to inhibit tumour growth. They also suggest that these results could be due to the production of NAD precursors such as Nam by the liver to promote its competitive use as a substrate for NAMPT over the inhibitors themselves. There may be some effect from oral administration of NA or Nam and its metabolism in the gastrointestinal tract by bacteria of the human microbiome, leading to interconversion of NAD metabolites and rescue via completely different pathways. Furthermore, it has previously been demonstrated that secondary GBM tumours harbouring IDH1 mutations are highly sensitive to NAMPT inhibitors (Tateishi et al., 2015). The mutant IDH1 produces 2HG, which inhibits the activity of NAPRT and prevents synthesis of NAD from NA upon NAMPT inhibition. This suggests that NAMPT inhibitors may be effective in both primary and secondary GBM.

Whilst there have been concerns about the translation of patient stratification for NAMPT inhibitors using markers such as NAPRT, there may be other ways to go about this. Recently, it was demonstrated that the compound 2-hydroxinicotinic acid (2-HNA) can specifically inhibit the activity of NAPRT, sensitising ovarian cancer cells to FK866 (Piacente et al., 2017). This shows that it might be possible to block NAD rescue in $NAPRT^{+}$ tumours, allowing us to target a larger proportion of patients. Previous studies have shown that NAPRT activity is inhibited by a number of different metabolic compounds, including certain glycolytic intermediates, and derivatives of CoA (Galassi et al., 2012). In addition, it has been demonstrated that inhibition of NAMPT causes a glycolytic block at GAPDH, because of the dependence of this enzyme on NAD as a cofactor (Tan et al., 2013; Tan et al., 2015). This suggests that the rates of glycolysis may affect rescue from NAMPT inhibition through NAPRT, with highly glycolytic tumours being more sensitive. A better understanding of the metabolic effects of NAMPT inhibitors may allow us to select targeted therapies to interrupt other signalling pathways that

will trigger cell death in cancer cells. MAPK activation is involved in the response of GBM cells to NAMPT inhibitors, and the combination of FK866 and the MAPK1/3 inhibitor U0126 limits proliferation more effectively than either drug alone (Zhang et al., 2012b). Furthermore, NAMPT inhibitors have been demonstrated to affect EGFR/PI3K/Akt/mTOR signalling, and inhibitors of different aspects of these pathways could act synergistically (Okumura et al., 2012; Schuster et al., 2015; Zucal et al., 2015; Espindola-Netto et al., 2017).

It is also important to consider other therapies that patients with GBM may receive during a normal course of treatment. One study showed that treatment of C6 glioma cells with dexamethasone decreases proliferation but increases their expression of NT5E (Bavaresco et al., 2007). As dexamethasone is often given to patients with GBM to control oedema, this could present a problem when considering the use of NAMPT inhibitors; the upregulation of NT5E may provide an alternative path of NAD biosynthesis. Recent work has also indicated that the product of the reaction catalysed by NT5E, NR, is present in the diet (Trammell et al., 2016). Furthermore, NR increases hepatocellular NAD levels more efficiently compared to Nam and NA. This could further confound the role of NT5E in resistance to NAMPT inhibitors *in vivo*. It will be very important to stratify patients based on NT5E expression in the tumour to maximise the therapeutic benefit from NAMPT inhibitors. It is also important to note that there is another enzyme that may affect NT5E-mediated rescue from NAMPT inhibitors, CD38. CD38 has been linked to ageing and related disorders, as well as haematological cancers (Chini et al., 2018). CD38 can degrade NAD or NMN to release Nam, which is unable to fuel NAD biosynthesis if NAMPT activity is impaired (Grozio et al., 2013). High levels of CD38 have been linked to increased sensitivity to NAMPT inhibitors (Chini et al., 2014). It could be that determining the NT5E/CD38 ratio will offer a better measure of the ability of cells to be rescued from NAMPT inhibition by exogenous NAD/NMN. The rescue seen by introduction of NMN to T98G cells treated with FK866 could be due to a combination of very low levels of NT5E coupled with endogenous CD38 silencing.

Like NT5E, studies have demonstrated that dexamethasone can also increase the expression of IDO1 induced by γ-interferon, thereby increasing the activity of the kynurenine pathway, which could promote resistance to NAMPT inhibitors (Badawy, 2017). In glioma cells, TMZ

induces the expression of QPRT and promotes resistance to NAMPT inhibitors (Sahm et al., 2013). Interestingly, the authors showed that whilst glioma cells themselves lack HAAO, expression of this enzyme in local microglia may allow GBM cells to exploit their production of QA from tryptophan to support NAD biosynthesis. Given the importance of the kynurenine pathway not only in NAD biosynthesis, but in immune regulation as well, NAMPT inhibitors may be effective when combined with immune therapies. In particular, immune checkpoint inhibitors in the form of anti-PD1 and anti-CTLA4 antibodies have shown some promise in other forms of cancer, but are yet to show significant clinical benefit in GBM (Lim et al., 2018).

The results presented here demonstrate that FK866-sensitive and -resistant GBM cell lines have both shared and divergent responses to NAMPT inhibition. The FK866-sensitive 42MG cell line shows changes in FOXM1 signalling and pathways involved in the regulation of the cell cycle. On the other hand, the FK866-resistant DBTRG cell line shows changes in HIF signalling and specific changes in the regulation of the G_2/S phase of the cell cycle. Both cell lines demonstrate alterations to E2F/RB and CDK signalling in control of the cell cycle, suggesting that this is a general effect of NAMPT inhibition in GBM cells. However, many of the differences in gene expression were only very small. These targets need to be verified by qPCR to confirm the effects of FK866 on resistant and sensitive cell lines, and to identify other potential mechanisms by which GBM cells might tolerate NAD depletion.

These results also show that GBM cell lines are highly sensitive to the NAMPT inhibitor FK866, with effective doses more than 1000 times lower than TMZ. Whilst it is well established that multiple DNA repair mechanisms are involved in resistance to TMZ, their roles in the response to NAMPT inhibitors are poorly understood. Early work demonstrated that the combination of TMZ, NAMPT inhibition and an inhibitor of BER was more effective than TMZ and NAMPT inhibition alone (Goellner et al., 2011). This approach was even effective in TMZ-resistant cells with very high levels of MGMT. This suggests that FK866 could be combined with TMZ either during initial treatment to improve its efficacy in patients, or applied to patients with TMZ-resistant primary/recurrent tumours to sensitise them to TMZ. Others have reported that mutations in genes such as mutS homolog 6 (MSH6) inhibit DNA repair by MMR, and promote resistance to TMZ (Yip et al., 2009). Loss of ERCC excision repair,

endonuclease non-catalytic subunit (ERCC)1, a major component of nucleotide excision repair (NER), has previously been linked to the sensitivity of cancer cells to PARP inhibitors (Cheng et al., 2013). More recently, it was shown that lung cancer cells lacking ERCC1 are hypersensitive to NAMPT inhibitors (Touat et al., 2018). Genetic variation in genes involved in DNA repair, including the ERCC and XRCC families, have been linked to glioma risk in numerous studies (Qian et al., 2017; Liu and Jiang, 2017). In addition, the expression of ERCC proteins have been associated with sensitivity to DNA damaging agents (Chen et al., 2007; Chen et al., 2010). Knockdown of ERCC1 sensitises cells to TMZ both *in vitro* and *in vivo* (Boccard et al., 2015). Furthermore, hypermethylation of the ERCC1 promoter is associated with sensitivity to radiation in glioma cell lines (Liu et al., 2009b). This suggests the combination of TMZ and a NAMPT inhibitor could be uniquely toxic to ERCC-deficient GBM tumours. More work is required to fully explore how deficiencies or alterations in DNA repair mechanisms contribute to sensitivity to NAMPT inhibitors.

The results presented here highlight the complexity within NAD biosynthesis, which reflects cancer metabolism as a whole. Unlike classic oncogenic pathways known to drive GBM growth, such as EGFR and PI3K/Akt mutations, there are numerous different metabolic pathways that can compensate for the loss of another. These changes can be rapid and either transient or permanent, depending on the specific needs of the cell. In the context of NAD biosynthesis, these pathways only have to maintain a very small NAD pool to support cell viability. We require a more comprehensive understanding of NAD metabolism to be able to maximise the benefit of drugs that target these pathways.

8.1 Conclusion and future work

In conclusion, the data presented here indicate that NAMPT inhibitors could be an effective therapy in GBM by selecting patients whose tumours lack key enzymes required for alternative NAD biosynthetic pathways. Both *in vitro* and RNAseq data indicate that NAMPT inhibition significantly alters regulation of the cell cycle. The combination of a NAMPT inhibitor and TMZ are effective both *in vitro* and *in vivo*, and could offer significant clinical benefit to patients with GBM.

Whilst these results are promising, more work is required to fully validate them. First of all, whilst I have looked at the combination of FK866 with TMZ, most patients with a GBM tumour will also receive radiation. Testing the combination of TMZ, FK866 and radiation will give a more accurate representation of what a tumour would be exposed to *in vivo*. This could be achieved both *in vitro* and *in vivo* using the same intracranial mouse model for which I have presented data here. In addition, poor knockdown of genes involved in NAD biosynthesis meant that replication of results using targeted inhibitors could not be achieved. Efficient knockdowns could be obtained by employing the CRISPR-Cas9 system. It has been shown that this system can achieve efficient knockdown by highly specific targeting of endogenous genes (Qi et al., 2013). Building on this system, it was demonstrated that fusion of enzymatically inactive dCas9 to either VP16 tetramer activation domain (VP64) or Kruppel-associated box repressor domain (KRAB) could more efficiently upregulate or inhibit gene expression respectively (Kearns et al., 2014). This system is currently available in GBM cell lines in my lab, and could be used to validate the results presented here. In addition, it would be useful to look at autophagy, PARylation, caspase activation and γH2AX formation to gain a better understanding of how these are affected by FK866 treatment and the different rescue pathways in GBM cell lines. The NAPRT inhibitor 2-HNA could be used to further validate the role of this pathway in resistance to NAMPT inhibitors. Furthermore, it would be useful to look at the role that CD38 may play in NAD metabolism in GBM and the efficacy of NAMPT inhibitors in cells that lack this enzyme. Finally, a recent article identified Vacor as a NAMPT/NMNAT2 substrate, which produces the novel compound Vacor adenine dinucleotide (VAD) (Buonvicino et al., 2018). VAD inhibits both NAMPT and NMNAT2, triggering necrotic cell death through a total loss of energy production, and inhibits the growth of tumours *in vivo*. However, this is completely dependent on NMNAT2 expression, which further complicates the role of different enzymes in the effects of NAD depletion on cancer cells.

Whilst my work has mainly utilised established GBM cell lines, some of my results suggest that they do not fully represent the phenotype of GBM tumours. Therefore, it would be beneficial to expand some of my experiments to include primary cell lines, and to expand this to more physiological conditions, including 3D spheroid culture and hypoxic conditions. There

has also been significant interest generated in the heterogeneity of GBMs, particularly with regards to GSCs and tumour recurrence. GSCs tend to be resistant to therapy, show a highly glycolytic phenotype, and have a preference for hypoxic environments. Studies have shown that NAMPT inhibition in GSCs limits their growth *in vivo* (Gujar et al., 2016). In addition, the combination of FK866 and TMZ has been shown to be effective in GSCs (Lucena-Cacace et al., 2017). It would be interesting to see how GSCs specifically respond to FK866, and whether or not the have a variable NAD biosynthetic profile compared to normal GBM cells. It may be possible to select for GSCs from our primary tumours by culturing them in hypoxia, and then test these cells using clonogenic assays to assess their ability to establish tumours.

There is also the potential to apply the knowledge I have generated here to other cancers, particularly other brain tumours. Whilst GBM may be the most common, aggressive form of brain cancer, other brain tumours such as meningiomas, oligodendrogliomas and ependymomas may show similarities to GBM with regards to their dependence on high levels of NAD, particularly if they are also high-grade, aggressive forms. However, it would have to be confirmed that NAMPT inhibitors such as FK866 can in fact cross the BBB and have their appropriate effects. Furthermore, it may have to be combined with standard therapy for other brain tumour types to maximise its effects, which will likely differ from standard therapy used in GBM.

In order to better understand the metabolic changes resulting from NAD depletion, and the effects of different rescue pathways, one could carry out extensive metabolomic characterisation of GBM cells treated with FK866 and different NAD sources. This could include extraction of metabolites and measuring their levels directly using nuclear magnetic resonance spectroscopy or gas/liquid chromatography mass spectrometry. It would even be possible to measure cell glycolysis and oxygen consumption directly using an extracellular-flux analyser. It would also be useful to identify how different oncogenic pathways affect the response of GBM cells to NAD depletion, including TP53 and AMPK/mTOR signalling, but most importantly alterations in the EGFR/PTEN/PI3K/Akt axis. All of this work could allow us to precisely identify which GBM patients are most likely to benefit from treatment with NAMPT inhibitors, truly achieving the goal of precision medicine.

Bibliography

Abbadi, S., Rodarte, J. J., Abutaleb, A., Lavell, E., Smith, C. L., Ruff, W., ... Quinones-Hinojosa, A. (2014). Glucose-6-phosphatase Is a Key Metabolic Regulator of Glioblastoma Invasion. *Molecular Cancer Research*, *12*(11), 1547–1559.

Abolmaali, S. S., Tamaddon, A. M., & Dinarvand, R. (2013). A review of therapeutic challenges and achievements of methotrexate delivery systems for treatment of cancer and rheumatoid arthritis. *Cancer Chemotherapy and Pharmacology*, *71*(5), 1115–1130.

Aboukameel, A., Muqbil, I., Senapedis, W., Baloglu, E., Landesman, Y., Shacham, S., ... Azmi, A. S. (2017). Novel p21-Activated Kinase 4 (PAK4) Allosteric Modulators Overcome Drug Resistance and Stemness in Pancreatic Ductal Adenocarcinoma. *Molecular Cancer Therapeutics*, *16*(1), 76–87.

Abu Aboud, O., Chen, C.-H., Senapedis, W., Baloglu, E., Argueta, C., & Weiss, R. H. (2016). Dual and Specific Inhibition of NAMPT and PAK4 By KPT-9274 Decreases Kidney Cancer Growth. *Molecular Cancer Therapeutics*, *15*(9), 2119–29.

Adams, S., Teo, C., McDonald, K. L., Zinger, A., Bustamante, S., Lim, C. K., ... Guillemin, G. J. (2014). Involvement of the kynurenine pathway in human glioma pathophysiology. *PLOS One*, *9*(11), 1–28.

Agarwala, S. S. & Kirkwood, J. M. (2000). Temozolomide, a Novel Alkylating Agent with Activity in the Central Nervous System, May Improve the Treatment of Advanced Metastatic Melanoma. *The Oncologist*, *5*(2), 144–151.

Ahadova, A., Gebert, J., Von Knebel Doeberitz, M., Kopitz, J., & Kloor, M. (2015). Dose-dependent effect of 2-deoxy-D-glucose on glycoprotein mannosylation in cancer cells. *IUBMB Life*, *67*(3), 218–226.

Ahmad, F., Dixit, D., Sharma, V., Kumar, A., Joshi, S. D., Sarkar, C., & Sen, E. (2016). Nrf2-driven TERT regulates pentose phosphate pathway in glioblastoma. *Cell Death and Disease*, *7*(2213).

Ahmed, S. U., Carruthers, R., Gilmour, L., Yildirim, S., Watts, C., & Chalmers, A. J. (2015). Selective inhibition of parallel DNA damage response pathways optimizes radiosensitization of glioblastoma stem-like cells. *Cancer Research*, *75*(20), 4416–4428.

Akhavan, D., Cloughesy, T. F., & Mischel, P. S. (2010). mTOR signaling in glioblastoma: Lessons learned from bench to bedside. *Neuro-Oncology*, *12*(8), 882–889.

Aksoy, O., Chicas, A., Zeng, T., Zhao, Z., McCurrach, M., Wang, X., & Lowe, S. W. (2012). The atypical E2F family member E2F7 couples the p53 and RB pathways during cellular senescence. *Genes & Development*, *26*(14), 1546–1557.

Alaee, M., Khaghani, S., Behroozfar, K., Hesari, Z., & Ghorbanhosseini, S. S. (2017). Nicotinamide Phosphoribosyltransferase Inhibition and Apoptosis in MCF-7 Cells. *Journal of Breast Cancer*, *20*(1), 20–26.

Allard, B., Beavis, P. A., Darcy, P. K., & Stagg, J. (2016a). Immunosuppressive activities of adenosine in cancer. *Current Opinion in Pharmacology*, *29*, 7–16.

Allard, D., Allard, B., Gaudreau, P.-O., Chrobak, P., & Stagg, J. (2016b). CD73-adenosine: a next-generation target in immuno-oncology. *Immunotherapy*, *8*(2), 145–163.

Alonso, S., Dai, Y., Yamashita, K., Horiuchi, S., Dai, T., Matsunaga, A., ... Perucho, M. (2015). Methylation of MGMT and ADAMTS14 in normal colon MUCOSA: biomarkers of a field defect for cancerization preferentially targeting elder African-Americans. *Oncotarget*, *6*(5), 3420–3431.

Anastasiou, D., Poulogiannis, G., Asara, J. M., Boxer, M. B., Jiang, J.-k., Shen, M., ... Cantley, L. C. (2011). Inhibition of pyvate kinase M2 by Reactive Oxygen Species Contributes to Cellular Antioxydant Responses. *Science*, *334*(6060), 1278–1283.

Anders, S., Pyl, P. T., & Huber, W. (2015). HTSeq-A Python framework to work with high-throughput sequencing data. *Bioinformatics*, *31*(2), 166–169.

Andor, N., Harness, J. V., Muller, S., Mewes, H. W., & Petritsch, C. (2014). Expands: Expanding ploidy and allele frequency on nested subpopulations. *Bioinformatics*, *30*(1), 50–60.

Antonioli, L., Blandizzi, C., Pacher, P., & Haskó, G. (2013). Immunity, inflammation and cancer: a leading role for adenosine. *Nature Reviews Cancer*, *13*(12), 842–57.

Argiris, A., Cohen, E., Karrison, T., Esparaz, B., Mauer, A., Ansari, R., ... Vokes, E. (2006). A phase II trial of perifosine, an oral alkylphospholipid, in recurrent or metastatic head and neck cancer. *Cancer Biology & Therapy*, *5*(7), 766–770.

Artene, S. A., Tuţă, C., Dragoi, A., Alexandru, O., Stefana Oana, P., Tache, D. E., ... Dricu, A. (2018). Current and emerging EGFR therapies for glioblastoma. *Journal of Immunoassay and Immunochemistry*, *39*(1), 1–11.

Ascierto, P. A., Scala, S., Castello, G., Daponte, A., Simeone, E., Ottaiano, A., ... Logan, T. F. (2005). Pegylated arginine deiminase treatment of patients with metastatic melanoma: Results from phase I and II studies. *Journal of Clinical Oncology*, *23*(30), 7660–7668.

Asghar, U., Witkiewicz, A. K., Turner, N. C., & Knudsen, E. S. (2015). The history and future of targeting cyclin-dependent kinases in cancer therapy. *Nature Reviews Drug Discovery*, *14*(2), 130–146.

Asteriti, I. A., De Mattia, F., & Guarguaglini, G. (2015). Cross-Talk between AURKA and Plk1 in Mitotic Entry and Spindle Assembly. *Frontiers in Oncology*, *5*(283), 1–9.

Audrito, V., Serra, S., Brusa, D., Mazzola, F., Arruga, F., Vaisitti, T., ... Deaglio, S. (2015). Extracellular nicotinamide phosphoribosyltransferase (NAMPT) promotes M2 macrophage polarization in chronic lymphocytic leukemia. *Blood*, *125*(1), 111–123.

Augustin, A. (2003). PARP-3 localizes preferentially to the daughter centriole and interferes with the G1/S cell cycle progression. *Journal of Cell Science*, *116*(8), 1551–1562.

Badawy, A. A. (2017). Kynurenine pathway of tryptophan metabolism: Regulatory and functional aspects. *International Journal of Tryptophan Research*, *10*, 1–20.

Bae, S. K., Kim, S. R., Kim, J. G., Kim, J. Y., Koo, T. H., Jang, H. O., ... Bae, M. K. (2006). Hypoxic induction of human visfatin gene is directly mediated by hypoxia-inducible factor-1. *FEBS Letters*, *580*(17), 4105–4113.

Bai, P., Canto, C., Brunyánszki, A., Huber, A., Szántó, M., Cen, Y., ... Auwerx, J. (2011). PARP-2 regulates SIRT1 expression and whole-body energy expenditure. *Cell Metabolism*, *13*(4), 450–460.

Bajrami, I., Kigozi, A., Van Weverwijk, A., Brough, R., Frankum, J., Lord, C. J., & Ashworth, A. (2012). Synthetic lethality of PARP and NAMPT inhibition in triple-negative breast cancer cells. *EMBO Molecular Medicine*, *4*(10), 1087–1096.

Ban, H. S., Kim, B.-K., Lee, H., Kim, H. M., Harmalkar, D., Nam, M., ... Won, M. (2017). The novel hypoxia-inducible factor-1α inhibitor IDF-11774 regulates cancer metabolism, thereby suppressing tumor growth. *Cell Death and Disease*, *8*(e2843).

Bar, E. E. (2011). Glioblastoma, cancer stem cells and hypoxia. *Brain Pathology*, *21*(2), 119–129.

Barazzuol, L., Jena, R., Burnet, N. G., Meira, L. B., Jeynes, J. C. G., Kirkby, K. J., & Kirkby, N. F. (2013). Evaluation of poly (ADP-ribose) polymerase inhibitor ABT-888 combined with radiotherapy and temozolomide in glioblastoma. *Radiation Oncology*, *8*(65), 1–11.

Barton, V. N., Foreman, N. K., Donson, A. M., Birks, D. K., Handler, M. H., & Vibhakar, R. (2010). Aurora kinase A as a rational target for therapy in glioblastoma. *Journal of Neurosurgery: Pediatrics*, *6*(1), 98–105.

Battaglia, L., Muntoni, E., Chirio, D., Peira, E., Annovazzi, L., Schiffer, D., ... Valazza, A. (2017). Solid lipid nanoparticles by coacervation loaded with a methotrexate prodrug : preliminary study for glioma treatment. *Nanomedicine*, *12*(6), 639–656.

Bauer, D. E., Hatzivassiliou, G., Zhao, F., Andreadis, C., & Thompson, C. B. (2005). ATP citrate lyase is an important component of cell growth and transformation. *Oncogene*, *24*(41), 6314–6322.

Bavaresco, L., Bernardi, A., Braganhol, E., Cappellari, A. R., Rockenbach, L., Farias, P. F., ... Battastini, A. M. O. (2008). The role of ecto-5'-nucleotidase/CD73 in glioma cell line proliferation. *Molecular and Cellular Biochemistry*, *319*(1-2), 61–8.

Bavaresco, L., Bernardi, A., Braganhol, E., Wink, M. R., & Battastini, A. M. O. (2007). Dexamethasone inhibits proliferation and stimulates ecto-5-nucleotidase/CD73 activity in C6 rat glioma cell line. *Journal of Neuro-Oncology*, *84*(1), 1–8.

Beauparlant, P., Bédard, D., Bernier, C., Chan, H., Gilbert, K., Goulet, D., ... Watson, M. (2009). Preclinical development of the nicotinamide phosphoribosyl transferase inhibitor prodrug GMX1777. *Anti-Cancer Drugs*, *20*(5), 346–54.

Becher, O. J., Millard, N. E., Modak, S., Kushner, B. H., Haque, S., Spasojevic, I., ... Dunkel, I. J. (2017). A phase i study of single-agent perifosine for recurrent or refractory pediatric CNS and solid tumors. *PLOS One*, *12*(6), 1–15.

Beck, C., Boehler, C., Guirouilh Barbat, J., Bonnet, M. E., Illuzzi, G., Ronde, P., ... Dantzer, F. (2014a). PARP3 affects the relative contribution of homologous recombination and nonhomologous end-joining pathways. *Nucleic Acids Research*, *42*(9), 5616–5632.

Beck, C., Robert, I., Reina-San-Martin, B., Schreiber, V., & Dantzer, F. (2014b). Poly(ADP-ribose) polymerases in double-strand break repair: Focus on PARP1, PARP2 and PARP3. *Experimental Cell Research*, *329*(1), 18–25.

Beckner, M. E., Fellows-Mayle, W., Zhang, Z., Agostino, N. R., Kant, J. A., Day, B. W., & Pollack, I. F. (2010). Identification of ATP citrate lyase as a positive regulator of glycolytic function in glioblastomas. *International Journal of Cancer*, *126*(10), 2282–2295.

Behrouzfar, K., Alaee, M., Nourbakhsh, M., Gholinejad, Z., & Golestani, A. (2017). Extracellular NAMPT/visfatin causes p53 deacetylation via NAD production and SIRT1 activation in breast cancer cells. *Cell Biochemistry and Function*, *35*(6), 327–333.

Beloribi-Djefaflia, S., Vasseur, S., & Guillaumond, F. (2016). Lipid metabolic reprogramming in cancer cells. *Oncogenesis*, *5*, 1–10.

Ben-Sahra, I. & Manning, B. D. (2017). mTORC1 signaling and the metabolic control of cell growth. *Current Opinion in Cell Biology*, *45*, 72–82.

Bensaad, K., Favaro, E., Lewis, C. A., Peck, B., Lord, S., Collins, J. M., ... Harris, A. L. (2014). Fatty acid uptake and lipid storage induced by HIF-1a contribute to cell growth and survival after hypoxia-reoxygenation. *Cell Reports*, *9*(1), 349–365.

Bensaad, K., Tsuruta, A., Selak, M. A., Vidal, M. N. C., Nakano, K., Bartrons, R., ... Vousden, K. H. (2006). TIGAR, a p53-Inducible Regulator of Glycolysis and Apoptosis. *Cell*, *126*(1), 107–120.

Bhardwaj, R., Sharma, P. K., Jadon, S. P., & Varshney, R. (2012). A combination of 2-deoxy-d-glucose and 6-aminonicotinamide induces cell cycle arrest and apoptosis selectively in irradiated human malignant cells. *Tumor Biology*, *33*(4), 1021–1030.

Bi, T. Q., Che, X. M., Liao, X. H., Zhang, D. J., Long, H. L., Li, H. J., & Zhao, W. (2011). Overexpression of Nampt in gastric cancer and chemopotentiating effects of the Nampt inhibitor FK866 in combination with fluorouracil. *Oncology Reports*, *26*(5), 1251–1257.

Bieging, K. T., Mello, S. S., & Attardi, L. D. (2014). Unravelling mechanisms of p53-mediated tumour suppression. *Nature Reviews Cancer*, *14*(5), 359–370.

Billington, R. A., Genazzani, A. A., Travelli, C., & Condorelli, F. (2008). NAD depletion by FK866 induces autophagy. *Autophagy*, *4*(3), 385–387.

Binderup, E., Björkling, F., Hjarnaa, P. V., Latini, S., Baltzer, B., Carlsen, M., & Binderup, L. (2005). EB1627: A soluble prodrug of the potent anticancer cyanoguanidine CHS828. *Bioorganic and Medicinal Chemistry Letters*, *15*(10), 2491–2494.

Bindesboll, C., Tan, S., Bott, D., Cho, T., Tamblyn, L., MacPherson, L., ... Matthews, J. (2016). TCDD-inducible poly-ADP-ribose polymerase (TIPARP/PARP7) mono-ADP-ribosylates and co-activates liver X receptors. *Biochemical Journal*, *473*(7), 899–910.

Blank, M. F. & Grummt, I. (2017). The seven faces of SIRT7. *Transcription*, *8*(2), 67–74.

Bleeker, F. E., Atai, N. A., Lamba, S., Jonker, A., Rijkeboer, D., Bosch, K. S., ... Van Noorden, C. J. (2010). The prognostic IDH1R132 mutation is associated with reduced NADP+-dependent IDH activity in glioblastoma. *Acta Neuropathologica*, *119*(4), 487–494.

Bo, L., Wei, B., Li, C., Wang, Z., Gao, Z., & Miao, Z. (2017). Identification of potential key genes associated with glioblastoma based on the gene expression profile. *Oncology Letters*, *14*(2), 2045–2052.

Boccard, S. G., Marand, S. V., Geraci, S., Pycroft, L., Berger, F. R., & Pelletier, L. A. (2015). Inhibition of DNA-repair genes Ercc1 and Mgmt enhances temozolomide efficacy in gliomas treatment: a pre-clinical study. *Oncotarget*, *6*(30), 29456–68.

Bogan, K. L. & Brenner, C. (2008). Nicotinic Acid, Nicotinamide, and Nicotinamide Riboside: A Molecular Evaluation of NAD+ Precursor Vitamins in Human Nutrition. *Annual Review of Nutrition*, *28*(1), 115–130.

Bolz, H., Ramírez, A., Von Brederlow, B., & Kubisch, C. (2001). Characterization of ADAMTS14, a novel member of the ADAMTS metalloproteinase family. *Biochimica et Biophysica Acta - Gene Structure and Expression*, *1522*(3), 221–225.

Borges, K. S., Castro-Gamero, A. M., Moreno, D. A., Da Silva Silveira, V., Brassesco, M. S., De Paula Queiroz, R. G., ... Tone, L. G. (2012). Inhibition of Aurora kinases enhances chemosensitivity to temozolomide and causes radiosensitization in glioblastoma cells. *Journal of Cancer Research and Clinical Oncology*, *138*(3), 405–414.

Bott, A. J., Peng, I. C., Fan, Y., Faubert, B., Zhao, L., Li, J., ... Zong, W. X. (2015). Oncogenic Myc Induces Expression of Glutamine Synthetase through Promoter Demethylation. *Cell Metabolism*, *22*(6), 1068–1077.

Bowlby, S. C., Thomas, M. J., D'Agostino, R. B., & Kridel, S. J. (2012). Nicotinamide phosphoribosyl transferase (Nampt) is required for de novo lipogenesis in tumor cells. *PLOS One*, *7*(6), 1–12.

Bracht, K., Nicholls, A. M., Liu, Y., & Bodmer, W. F. (2010). 5-Fluorouracil response in a large panel of colorectal cancer cell lines is associated with mismatch repair deficiency. *British Journal of Cancer*, *103*(3), 340–346.

Braidy, N., Guillemin, G. J., & Grant, R. (2011). Effects of kynurenine pathway inhibition on NAD + metabolism and cell viability in human primary astrocytes and neurons. *International Journal of Tryptophan Research*, *4*(1), 29–37.

Brázdová, M., Quante, T., Tögel, L., Walter, K., Loscher, C., Tichý, V., ... Tolstonog, G. V. (2009). Modulation of gene expression in U251 glioblastoma cells by binding of mutant p53 R273H to intronic and intergenic sequences. *Nucleic Acids Research*, *37*(5), 1486–1500.

Brazill, J. M., Li, C., Zhu, Y., & Zhai, R. G. (2017). NMNAT: It's an NAD+synthase... It's a chaperone... It's a neuroprotector. *Current Opinion in Genetics and Development*, *44*, 156–162.

Bruick, R. K. & McKnight, S. L. (2001). A conserved family of prolyl-4-hydroxylases that modify HIF. *Science*, *294*(5545), 1337–1340.

Buonvicino, D., Mazzola, F., Zamporlini, F., Resta, F., Ranieri, G., Camaioni, E., ... Chiarugi, A. (2018). Identification of the Nicotinamide Salvage Pathway as a New Toxification Route for Antimetabolites. *Cell Chemical Biology*, *25*(4), 471–482.

Burnstock, G. & Di Virgilio, F. (2013). Purinergic signalling and cancer. *Purinergic Signalling*, *9*(4), 491–540.

Buti, S., Leonetti, A., Dallatomasina, A., & Bersanelli, M. (2016). Everolimus in the management of metastatic renal cell carcinoma: an evidence-based review of its place in therapy. *Core Evidence*, *11*, 23–36.

Cagnetta, A., Caffa, I., Acharya, C., Soncini, D., Acharya, P., Adamia, S., ... Cea, M. (2015). APO866 increases antitumor activity of cyclosporin - A by inducing mitochondrial and endoplasmic reticulum stress in leukemia cells. *Clinical Cancer Research*, *21*(17), 3934–3945.

Caldecott, K. W. (2008). Single-strand break repair and genetic disease. *Nature Reviews Genetics*, *9*(8), 619–631.

Campbell, N., Reece, J., Urry, L., Cain, M., Wasserman, S., Minorsky, P., & Jackson, R. (2008). *Biology 8th Edition*.

Campos, B., Olsen, L. R., Urup, T., & Poulsen, H. S. (2016). A comprehensive profile of recurrent glioblastoma. *Oncogene*, *35*(45), 5819–5825.

Cantó, C., Gerhart-hines, Z., Feige, J. N., Lagouge, M., Milne, J. C., Elliott, P. J., ... Auwerx, J. (2013). AMPK regulates energy expenditure by modulating NAD+ metabolism and SIRT1 activity. *Nature*, *458*(7241), 1056–1060.

Cao, R., Wang, G., Qian, K., Chen, L., Qian, G., Xie, C., ... Wang, X. (2017a). Silencing of HJURP induces dysregulation of cell cycle and ROS metabolism in bladder cancer cells via PPARγ-SIRT1 feedback loop. *Journal of Cancer*, *8*(12), 2282–2295.

Cao, Z., Liang, N., Yang, H., & Li, S. (2017b). Visfatin mediates doxorubicin resistance in human non–small-cell lung cancer via Akt-mediated up-regulation of ABCC1. *Cell Proliferation*, *50*(5), 1–8.

Cappellari, A. & Vasques, G. (2012). Involvement of ecto-5-nucleotidase/CD73 in U138MG glioma cell adhesion. *Molecular and Cellular Biochemistry*, *359*(1-2), 315–322.

Capper, D., Simon, M., Langhans, C. D., Okun, J. G., Tonn, J. C., Weller, M., ... Hartmann, C. (2012). 2-Hydroxyglutarate concentration in serum from patients with gliomas does not correlate with IDH1/2 mutation status or tumor size. *International Journal of Cancer*, *131*(3), 766–768.

Carbonneau, M., Gagne, L. M., Lalonde, M. E., Germain, M. A., Motorina, A., Guiot, M. C., ... Mallette, F. A. (2016). The oncometabolite 2-hydroxyglutarate activates the mTOR signalling pathway. *Nature Communications*, *7*(12700), 1–12.

Carracedo, A., Cantley, L. C., & Pandolfi, P. P. (2013). Cancer metabolism: fatty acid oxidation in the limelight. *Nature Reviews Cancer*, *13*(4), 227–32.

Carracedo, A., Weiss, D., Leliaert, A. K., Bhasin, M., De Boer, V. C., Laurent, G., ... Pandolfi, P. P. (2012). A metabolic prosurvival role for PML in breast cancer. *Journal of Clinical Investigation*, *122*(9), 3088–3100.

Cea, M., Cagnetta, A., Fulciniti, M., Tai, Y. T., Hideshima, T., Chauhan, D., ... Anderson, K. C. (2012). Targeting NAD+ salvage pathway induces autophagy in multiple myeloma cells via mTORC1 and extracellular signal-regulated kinase (ERK1/2) inhibition. *Blood*, *120*(17), 3519–3529.

Cea, M., Soncini, D., Fruscione, F., Raffaghello, L., Garuti, A., Emionite, L., ... Nencioni, A. (2011). Synergistic interactions between HDAC and sirtuin inhibitors in human leukemia cells. *PLOS One*, *6*(7), 1–12.

Cejka, P., Stojic, L., Mojas, N., Russell, A. M., Heinimann, K., Cannavó, E., ... Jiricny, J. (2003). Methylation-induced G2/M arrest requires a full complement of the mismatch repair protein hMLH1. *The EMBO Journal*, *22*(9), 2245–2254.

Cerignoli, F., Guo, X., Cardinali, B., Rinaldi, C., Casaletto, J., Frati, L., ... Giannini, G. (2002). retSDR1 , a Short-Chain Retinol Dehydrogenase / Reductase , Is Retinoic Acid- inducible and Frequently Deleted in Human Neuroblastoma Cell Lines 1. *Molecular Biology*, *27*(36), 1196–1204.

Cerna, D., Li, H., Flaherty, S., Takebe, N., Coleman, C. N., & Yoo, S. S. (2012). Inhibition of nicotinamide phosphoribosyltransferase (NAMPT) activity by small molecule GMX1778 regulates Reactive Oxygen Species (ROS)-mediated cytotoxicity in a p53- and nicotinic acid phosphoribosyltransferase1 (NAPRT1)-dependent manner. *Journal of Biological Chemistry*, *287*(26), 22408–22417.

Chae, Y. K., Arya, A., Malecek, M.-K., Shin, D. S., Carneiro, B., Chandra, S., ... Giles, F. (2016). Repurposing metformin for cancer treatment: current clinical studies. *Oncotarget*, *7*(26), 40767–40780.

Chalhoub, N. & Baker, S. J. (2009). PTEN and the PI3-kinase pathway in cancer. *Annual Review of Pathology*, *4*(1), 127–50.

Chalkiadaki, A. & Guarente, L. (2015). The multifaceted functions of sirtuins in cancer. *Nature Reviews Cancer*, *15*(10), 608–624.

Chan, M., Gravel, M., Bramoull??, A., Bridon, G., Avizonis, D., Shore, G. C., & Roulston, A. (2014). Synergy between the NAMPT inhibitor GMX1777(8) and pemetrexed in non-small cell lung cancer cells is mediated by PARP activation and enhanced NAD consumption. *Cancer Research*, *74*(21), 5948–5954.

Chang, S. M., Wen, P., Cloughesy, T., Greenberg, H., Schiff, D., Conrad, C., ... Prados, M. D. (2005). Phase II study of CCI-779 in patients with recurrent glioblastoma multiforme. *Investigational New Drugs*, *23*(4), 357–361.

Chee, K. G., Longmate, J., Quinn, D. I., Chatta, G., Pinski, J., Twardowski, P., ... Lara, P. N. (2007). The AKT inhibitor perifosine in biochemically recurrent prostate cancer: A phase II California/Pittsburgh cancer consortium trial. *Clinical Genitourinary Cancer*, *5*(7), 433–437.

Chen, C., Shi, Y., Li, Y., He, Z. C., Zhou, K., Zhang, X. N., ... Bian, X. W. (2017). A glycolysis-based ten-gene signature correlates with the clinical outcome, molecular subtype and IDH1 mutation in glioblastoma. *Journal of Genetics and Genomics*, *44*(11), 519–530.

Chen, E. Y., Tan, C. M., Kou, Y., Duan, Q., Wang, Z., Meirelles, G. V., ... Ma'ayan, A. (2013). Enrichr: interactive and collaborative HTML5 gene list enrichment analysis tool. *BMC bioinformatics*, *14*(1), 128.

Chen, H.-Y., Shao, C.-J., Chen, F.-R., Kwan, A.-L., & Chen, Z.-P. (2010). Role of ERCC1 promoter hypermethylation in drug resistance to cisplatin in human gliomas. *International Journal of Cancer*, *126*(8), 1944–1954.

Chen, H., Shao, C., Shi, H., Mu, Y., Sai, K., & Chen, Z. (2007). Single nucleotide polymorphisms and expression of ERCC1 and ERCC2 vis-à-vis chemotherapy drug cytotoxicity in human glioma. *Journal of Neuro-Oncology*, *82*(3), 257–262.

Chen, X., Zhang, Y., Shi, Y., Lian, H., Tu, H., Han, S., ... Liu, W. (2016). MiR-129 triggers autophagic flux by regulating a novel Notch-1/ E2F7/Beclin-1 axis to impair the viability of human malignant glioma cells. *Oncotarget*, *7*(8), 9222–35.

Chendong, Y., Sudderth, J., Tuyen, D., Bachoo, R. G., McDonald, J. G., & DeBerardinis, R. J. (2009). Glioblastoma cells require glutamate dehydrogenase to survive impairments of glucose metabolism or Akt signaling. *Cancer Research*, *69*(20), 7986–7993.

Cheng, C. L. (2005). Poly(ADP-ribose) polymerase-1 inhibition reverses temozolomide resistance in a DNA mismatch repair-deficient malignant glioma xenograft. *Molecular Cancer Therapeutics*, *4*(9), 1364–1368.

Cheng, H., Zhang, Z., Borczuk, A., Powell, C. A., Balajee, A. S., Lieberman, H. B., & Halmos, B. (2013). PARP inhibition selectively increases sensitivity to cisplatin in ERCC1-low non-small cell lung cancer cells. *Carcinogenesis*, *34*(4), 739–749.

Cheng, Y., Zhang, Y., Zhang, L., Ren, X., Huber-Keener, K. J., Liu, X., ... Yang, J.-M. (2012). MK-2206, a Novel Allosteric Inhibitor of Akt, Synergizes with Gefitinib against Malignant Glioma via Modulating Both Autophagy and Apoptosis. *Molecular Cancer Therapeutics*, *11*(1), 154–164.

Chesnelong, C., Chaumeil, M. M., Blough, M. D., Al-Najjar, M., Stechishin, O. D., Chan, J. A., ... Cairncross, J. G. (2014). Lactate dehydrogenase A silencing in IDH mutant gliomas. *Neuro-Oncology*, *16*(5), 686–695.

Chini, C. C., Guerrico, a. M., Nin, V., Camacho-Pereira, J., Escande, C., Barbosa, M. T., & Chini, E. N. (2014). Targeting of NAD metabolism in pancreatic cancer cells: potential novel therapy for pancreatic tumors. *Clinical Cancer Research*, *20*(1), 120–130.

Chini, E. N., Chini, C. C., Espindola Netto, J. M., de Oliveira, G. C., & van Schooten, W. (2018). The Pharmacology of CD38/NADase: An Emerging Target in Cancer and Diseases of Aging. *Trends in Pharmacological Sciences*, *39*(4), 424–436.

Chinnaiyan, P., Won, M., Wen, P. Y., Rojiani, A. M., Werner-Wasik, M., Shih, H. A., ... Mehta, M. P. (2017). A randomized phase II study of everolimus in combination with chemoradiation in newly diagnosed glioblastoma: Results of NRG Oncology RTOG 0913. *Neuro-Oncology*, *20*(5), 666–673.

Chou, T.-c. (2007). Theoretical Basis , Experimental Design , and Computerized Simulation of Synergism and Antagonism in Drug Combination Studies. *Pharmacological Reviews*, *58*(3), 621–681.

Chu, J., Zhu, Y., Liu, Y., Sun, L., Lv, X., Wu, Y., ... Liu, Q. (2015). E2F7 overexpression leads to tamoxifen resistance in breast cancer cells by competing with E2F1 at miR-15a/16 promoter. *Oncotarget*, *6*(31), 31944–57.

Chung, K., Wallace, J., Kim, S. Y., Kalyanasundaram, S., Andalman, A. S., Davidson, T. J., ... Deisseroth, K. (2013). Structural and molecular interrogation of intact biological systems. *Nature*, *497*(7449), 332–337.

Cianfanelli, V., Fuoco, C., Lorente, M., Salazar, M., Quondamatteo, F., Gherardini, P. F., ... Cecconi, F. (2015). AMBRA1 links autophagy to cell proliferation and tumorigenesis by promoting c-Myc dephosphorylation and degradation. *Nature Cell Biology*, *17*(1), 20–30.

Ciccia, A. & Elledge, S. J. (2010). The DNA Damage Response: Making It Safe to Play with Knives. *Molecular Cell*, *40*(2), 179–204.

ClinicalTrials.gov. (2018). Clinical Trials.

Cole, J., Guiot, M.-C., Gravel, M., Bernier, C., Shore, G. C., & Roulston, A. (2017). Novel NAPRT specific antibody identifies small cell lung cancer and neuronal cancers as promising clinical indications for a NAMPT inhibitor/niacin co-administration strategy. *Oncotarget*, *8*(44), 77846–77859.

Cooper, I., Last, D., Guez, D., Sharabi, S., Elhaik Goldman, S., Lubitz, I., ... Mardor, Y. (2015). Combined local blood–brain barrier opening and systemic methotrexate for the treatment of brain tumors. *Journal of Cerebral Blood Flow & Metabolism*, *35*(6), 967–976.

CRUK. (2016). CancerStats: Cancer Statistics for the UK.

Csibi, A., Lee, G., Yoon, S. O., Tong, H., Ilter, D., Elia, I., ... Blenis, J. (2014). The mTORC1/S6K1 pathway regulates glutamine metabolism through the eif4b-dependent control of c-Myc translation. *Current Biology*, *24*(19), 2274–2280.

D'Atri, S., Tentori, L., Lacal, P. M., Graziani, G., Pagani, E., Benincasa, E., ... Medicine, E. (1998). Involvement of the Mismatch Repair System in Temozolomide-Induced Apoptosis. *Molecular Pharmacology*, *54*(2), 334–341.

Dadey, D. Y. A., Kapoor, V., Khudanyan, A., Urano, F., Kim, A. H., Thotala, D., & Hallahan, D. E. (2015). The ATF6 pathway of the ER stress response contributes to enhanced viability in glioblastoma. *Oncotarget*, *7*(2), 2080–92.

Dan, L., Klimenkova, O., Klimiankou, M., Klusman, J. H., van den Heuvel-Eibrink, M. M., Reinhardt, D., ... Skokowa, J. (2012). The role of sirtuin 2 activation by nicotinamide phosphoribosyltransferase in the aberrant proliferation and survival of myeloid leukemia cells. *Haematologica*, *97*(4), 551–559.

Dang, C. V. (2012). Links between metabolism and cancer. *Genes & Development*, *26*, 877–890.

Dang, L., White, D. W., Gross, S., Bennett, B. D., Bittinger, M. a., Driggers, E. M., ... Su, S. M. (2009). Cancer-associated IDH1 mutations produce 2-hydroxyglutarate. *Nature*, *462*(7274), 739–744.

Dang, W. (2014). The controversial world of sirtuins. *Drug Discovery Today: Technologies*, *12*, 9–17.

Daniele, S., Costa, B., Zappelli, E., Da Pozzo, E., Sestito, S., Nesi, G., ... Martini, C. (2015). Combined inhibition of AKT/mTOR and MDM2 enhances Glioblastoma Multiforme cell apoptosis and differentiation of cancer stem cells. *Scientific Reports*, *5*(9956), 1–14.

Danovi, D., Folarin, A., Gogolok, S., Ender, C., Elbatsh, A. M. O., Engström, P. G., ... Pollard, S. M. (2013). A High-Content Small Molecule Screen Identifies Sensitivity of Glioblastoma Stem Cells to Inhibition of Polo-Like Kinase 1. *PLOS One*, *8*(10), 1–13.

Dantzer, F., Giraud-Panis, M.-J., Jaco, I., Ame, J.-C., Schultz, I., Blasco, M., ... Schreiber, V. (2004). Functional Interaction between Poly(ADP-Ribose) Polymerase 2 (PARP-2) and TRF2: PARP Activity Negatively Regulates TRF2. *Molecular and Cellular Biology*, *24*(4), 1595–1607.

Davis, C., Naci, H., Gurpinar, E., Poplavska, E., Pinto, A., & Aggarwal, A. (2017). Availability of evidence of benefits on overall survival and quality of life of cancer drugs approved by European Medicines Agency: retrospective cohort study of drug approvals 2009-13. *The British Medical Journal*, *359*, 1–13.

De Bonis, P., Anile, C., Pompucci, A., Fiorentino, A., Balducci, M., Chiesa, S., ... Mangiola, A. (2013). The influence of surgery on recurrence pattern of glioblastoma. *Clinical Neurology and Neurosurgery*, *115*(1), 37–43.

De Bruin, A., Maiti, B., Jakoi, L., Timmers, C., Buerki, R., & Leone, G. (2003). Identification and Characterization of E2F7, a Novel Mammalian E2F Family Member Capable of Blocking Cellular Proliferation. *Journal of Biological Chemistry*, *278*(43), 42041–42049.

De Figueiredo, L. F., Gossmann, T. I., Ziegler, M., & Schuster, S. (2011). Pathway analysis of NAD + metabolism. *Biochemical Journal*, *439*(2), 341–348.

De Salvo, M., Maresca, G., D'Agnano, I., Marchese, R., Stigliano, A., Gagliassi, R., ... Bucci, B. (2011). Temozolomide induced c-Myc-mediated apoptosis via Akt signalling in MGMT expressing glioblastoma cells. *International Journal of Radiation Biology*, *87*(5), 518–533.

De Tayrac, M., Aubry, M., Saïkali, S., Etcheverry, A., Surbled, C., Guénot, F., ... Mosser, J. (2011). A 4-gene signature associated with clinical outcome in high-grade gliomas. *Clinical Cancer Research*, *17*(2), 317–327.

Deberardinis, R. J. & Cheng, T. (2010). Q's next: The diverse functions of glutamine in metabolism, cell biology and cancer. *Oncogene*, *29*(3), 313–324.

Decker, D., Kinzie, J., Evans, R., Abu-Zahra, H., & Al-Sarraf, M. (1987). Pilot Study of Combination 5-Fluorouracil, Cisdiamminedichloroplatinum II, and Radiation Therapy for Grade III and IV Astrocytomas. *American Journal of Cancer Research*, *10*(5), 444–447.

Deisenroth, C., Itahana, Y., Tollini, L., Jin, A., & Zhang, Y. (2011). p53-inducible DHRS3 is an endoplasmic reticulum protein associated with lipid droplet accumulation. *Journal of Biological Chemistry*, *286*(32), 28343–28356.

Demir, M. K., Hakan, T., Akinci, O., & Berkman, Z. (1987). Primary cerebellar glioblastoma multiforme. *Diagnostic and Interventional Radiology*, *5*, 231–236.

Denny, B. J., Wheelhouse, R. T., Stevens, M. F. G., Tsang, L. L. H., & Slack, J. A. (1994). NMR and Molecular Modeling Investigation of the Mechanism of Activation of the Antitumor Drug Temozolomide and Its Interaction with DNA. *Biochemistry*, *33*(31), 9045–9051.

Di Iasio, M. G. & Zauli, G. (2013). The non-genotoxic activator of the p53 pathway Nutlin-3 shifts the balance between E2F7 and E2F1 transcription factors in leukemic cells. *Investigational New Drugs*, *31*(2), 458–460.

Diani-Moore, S., Zhang, S., Ram, P., & Rifkind, A. B. (2013). Aryl hydrocarbon receptor activation by dioxin targets phosphoenolpyruvate carboxykinase (PEPCK) for ADP-ribosylation via 2,3,7,8-Tetrachlorodibenzo-p- dioxin (TCDD)-inducible poly(ADP-ribose) polymerase (TiPARP). *Journal of Biological Chemistry*, *288*(30), 21514–21525.

Diaz, R. J., Golbourn, B., Shekarforoush, M., Smith, C. A., & Rutka, J. T. (2012). Aurora kinase B/C inhibition impairs malignant glioma growth in vivo. *Journal of Neuro-Oncology*, *108*(3), 349–360.

Dickerson, T., Jauregui, C. E., & Teng, Y. (2017). Friend or foe? Mitochondria as a pharmacological target in cancer treatment. *Future Medicinal Chemistry*, *9*(18), 2197–2210.

Dietrich, J., Rao, K., Pastorino, S., & Kesari, S. (2011). Corticosteroids in brain cancer patients : benefits and pitfalls. *Expert Review Cinical Pharmacology*, *4*(2), 233–242.

Dirks, P. B., Rutka, J. T., Hubbard, S. L., Mondal, S., & Hamel, P. A. (1998). The E2F-family proteins induce distinct cell cycle regulatory factors in p16-arrested, U343 astrocytoma cells. *Oncogene*, *17*(7), 867–876.

Djerassi, I., Farber, S., Abir, E., & Neikirk, W. (1967). Continuous infusion of methotrexate in children with acute leukaemia. *Cancer*, *20*, 233–242.

Donaires, F. S., Godoy, P. R., Leandro, G. S., Puthier, D., & Sakamoto-Hojo, E. T. (2017). E2F transcription factors associated with up-regulated genes in glioblastoma. *Cancer Biomarkers*, *18*(2), 199–208.

Donawho, C. K., Luo, Y., Luo, Y., Penning, T. D., Bauch, J. L., Bouska, J. J., ... Frost, D. J. (2007). ABT-888, an orally active poly(ADP-ribose) polymerase inhibitor that potenti-

ates DNA-damaging agents in preclinical tumor models. *Clinical Cancer Research*, *13*(9), 2728–2737.

Dong, G., Chen, W., Wang, X., Yang, X., Xu, T., Wang, P., ... Sheng, C. (2017). Small Molecule Inhibitors Simultaneously Targeting Cancer Metabolism and Epigenetics: Discovery of Novel Nicotinamide Phosphoribosyltransferase (NAMPT) and Histone Deacetylase (HDAC) Dual Inhibitors. *Journal of Medicinal Chemistry*, *60*(19), 7965–7983.

Dryden, S. C., Nahhas, F. A., Nowak, J. E., Goustin, A.-s., & Tainsky, M. A. (2003). Role for Human SIRT2 NAD-Dependent Deacetylase Activity in Control of Mitotic Exit in the Cell Cycle Role for Human SIRT2 NAD-Dependent Deacetylase Activity in Control of Mitotic Exit in the Cell Cycle. *Molecular and Cellular Biology*, *23*(9), 3173–3185.

Du, F., Okuno, E., Whetsell, W. O., Köhler, C., & Schwarcz, R. (1991). Immunohistochemical localization of quinolinic acid phosphoribosyltransferase in the human neostriatum. *Neuroscience*, *42*(2), 397–406.

Duarte-Pereira, S., Pereira-Castro, I., Silva, S. S., Gonçalves, M., Neto, C., Teixeira da Costa, L., ... Silva, R. M. (2016). Extensive regulation of nicotinate phosphoribosyltransferase (NAPRT) expression in human tissues and tumors. *Oncotarget*, *7*(2), 1973–83.

Duarte-Pereira, S., Silva, S. S., Azevedo, L., Castro, L., Amorim, A., & Silva, R. M. (2014). NAMPT and NAPRT1: novel polymorphisms and distribution of variants between normal tissues and tumor samples. *Scientific Reports*, *4*(6311), 1–7.

Dunleavy, E. M., Roche, D., Tagami, H., Lacoste, N., Ray-Gallet, D., Nakamura, Y., ... Almouzni-Pettinotti, G. (2009). HJURP Is a Cell-Cycle-Dependent Maintenance and Deposition Factor of CENP-A at Centromeres. *Cell*, *137*(3), 485–497.

Egler, R., Ahuja, S., & Matloub, Y. (2016). L-asparaginase in the treatment of patients with acute lymphoblastic leukemia. *Journal of Pharmacology and Pharmacotherapeutics*, *7*(2), 62.

Egler, V., Korur, S., Failly, M., Boulay, J. L., Imber, R., Lino, M. M., & Merlo, A. (2008). Histone deacetylase inhibition and blockade of the glycolytic pathway synergistically induce glioblastoma cell death. *Clinical Cancer Research*, *14*(10), 3132–3140.

Elkhaled, A., Jalbert, L. E., Phillips, J. J., Yoshihara, H. A. I., Parvataneni, R., Srinivasan, R., ... Nelson, S. J. (2012). Magnetic Resonance of 2-Hydroxyglutarate in IDH1-Mutated Low-Grade Gliomas. *Science Translational Medicine*, *4*(116), 1–10.

Ely, J. (1954). 2-deoxy-d-glucose as an inhibitor of cancerous growth in animals. *Journal of The Franklin Institute*, *258*(2), 157–160.

Endo-Munoz, L., Dahler, A., Teakle, N., Rickwood, D., Hazar-Rethinam, M., Abdul-Jabbar, I., ... Saunders, N. (2009). E2F7 can regulate proliferation, differentiation, and apoptotic responses in human keratinocytes: Implications for cutaneous squamous cell carcinoma formation. *Cancer Research*, *69*(5), 1800–1808.

Engelhard, H., Butler, A., & Bauer, K. (1989). Quantification of the c-myc oncoprotein in human glioblastoma cells and tumor tissue. *Journal of Neurosurgery*, *71*(2), 224–232.

Ensor, C. M., Holtsberg, F. W., Bomalaski, J. S., & Clark, M. a. (2002). Pegylated Arginine Deiminase (ADI-SS PEG20 , 000 mw) Inhibits Human Melanomas and Hepatocellular Carcinomas in Vitro and in Vivo and Hepatocellular Carcinomas in Vitro and in Vivo. *Cancer Research*, *62*(19), 5443–5450.

Epple, L. M., Dodd, R. D., Merz, A. L., Dechkovskaia, A. M., Herring, M., Winston, B. A., ... Graner, M. W. (2013). Induction of the Unfolded Protein Response Drives Enhanced Metabolism and Chemoresistance in Glioma Cells. *PLOS One*, *8*(8), 1–28.

Espindola-Netto, J. M., Chini, C. C., Tarragó, M., Wang, E., Dutta, S., Pal, K., ... Chini, E. N. (2017). Preclinical efficacy of the novel competitive NAMPT inhibitor STF-118804 in pancreatic cancer. *Oncotarget*, *8*(49), 85054–85067.

Esteller, M. & Herman, J. G. (2004). Generating mutations but providing chemosensitivity: The role of O 6-methylguanine DNA methyltransferase in human cancer. *Oncogene*, *23*(1), 1–8.

Farber, S., Diamond, L., Mercer, R., Sylvester, R., & Wolff, J. (1948). Temporary remissions in acute leukemia in children produced by folic acid antagonist, 4-aminopteroyl-glutamic acid (aminopterin). *New England Journal of Medicine*, *238*(23), 787–793.

Fathi, A. T., Nahed, B. V., Wander, S. A., Iafrate, A. J., Borger, D. R., Hu, R., ... Chi, A. S. (2016). Elevation of Urinary 2-Hydroxyglutarate in IDH-Mutant Glioma. *The Oncologist*, *21*(2), 214–219.

Fazeli, M. S., Keramati, M. R., Rahimi, A., Kazemeini, A., Banoei, M. M., Dashti, H., & Fazeli, R. (2016). Visfatin level in patients with colorectal adenoma. *Medical Journal of the Islamic Republic of Iran*, *30*(320), 1–4.

Fazio, N., Buzzoni, R., Baudin, E., Antonuzzo, L., Hubner, R. A., Lahner, H., ... Verslype, C. (2016). A Phase II Study of BEZ235 in Patients with Everolimus-resistant, Advanced Pancreatic Neuroendocrine Tumours. *Anticancer Research*, *36*(2), 713–719.

Feng, J., Yan, P.-F., Zhao, H.-Y., Zhang, F.-C., Zhao, W.-H., & Feng, M. (2016a). Inhibitor of Nicotinamide Phosphoribosyltransferase Sensitizes Glioblastoma Cells to Temozolomide via Activating ROS/JNK Signaling Pathway. *BioMed Research International*, *2016*(1450843), 1–11.

Feng, J., Yan, P.-F., Zhao, H.-Y., Zhang, F.-C., Zhao, W.-H., & Feng, M. (2016b). SIRT6 suppresses glioma cell growth via induction of apoptosis, inhibition of oxidative stress and suppression of JAK2/STAT3 signaling pathway activation. *Oncology Reports*, *35*(3), 1395–1402.

Feng, Z., Hu, W., De Stanchina, E., Teresky, A. K., Jin, S., Lowe, S., & Levine, A. J. (2007). The regulation of AMPK β1, TSC2, and PTEN expression by p53: Stress, cell and tissue specificity, and the role of these gene products in modulating the IGF-1-AKT-mTOR pathways. *Cancer Research*, *67*(7), 3043–3053.

Fenton, A. L., Shirodkar, P., MacRae, C. J., Meng, L., & Anne Koch, C. (2013). The PARP3-and ATM-dependent phosphorylation of APLF facilitates DNA double-strand break repair. *Nucleic Acids Research*, *41*(7), 4080–4092.

Fiedler, T., Strauss, M., Hering, S., Redanz, U., William, D., Rosche, Y., ... Maletzki, C. (2015). Arginine deprivation by arginine deiminase of Streptococcus pyogenes controls primary glioblastoma growth in vitro and in vivo. *Cancer Biology & Therapy*, *16*(7), 1047–1055.

Figueiro, F., de Oliveira, C. P., Bergamin, L. S., Rockenbach, L., Mendes, F. B., Jandrey, E. H. F., ... Battastini, A. M. O. (2016). Methotrexate up-regulates ecto-5-nucleotidase/CD73 and reduces the frequency of T lymphocytes in the glioblastoma microenvironment. *Purinergic Signalling*, *12*(2), 303–312.

Figueiró, F., Mendes, F. B., Corbelini, P. F., Janarelli, F., Helena, E., Jandrey, F., ... Battastini, A. M. O. (2014). A Monastrol-derived Compound , LaSOM 63 , Inhibits Ecto-5 ' Nucleotidase / CD73 Activity and Induces Apoptotic Cell Death of Glioma Cell Lines. *Anticancer Research*, *34*(4), 1837–42.

Finley, L. W., Carracedo, A., Lee, J., Souza, A., Egia, A., Zhang, J., ... Haigis, M. C. (2011). SIRT3 Opposes Reprogramming of Cancer Cell Metabolism through HIF1α Destabilization. *Cancer Cell*, *19*(3), 416–428.

Flavin, R., Peluso, S., Nguyen, P., & Loda, M. (2010). Fatty acid synthase as a potential therapeutic target in cancer. *Future Oncology*, *6*(4), 551–562.

Foltz, D. R., Jansen, L. E., Bailey, A. O., Yates, J. R., Bassett, E. A., Wood, S., ... Cleveland, D. W. (2009). Centromere-Specific Assembly of CENP-A Nucleosomes Is Mediated by HJURP. *Cell*, *137*(3), 472–484.

Ford, E., Voit, R., Liszt, G., Magin, C., Grummt, I., & Guarente, L. (2006). Mammalian Sir2 homolog SIRT7 is an activator of RNA polymerase I transcription service Mammalian Sir2 homolog SIRT7 is an activator of RNA polymerase I transcription. *Genes & Development*, *20*(9), 1075–1080.

Frenzel, A., Labi, V., Chmelewskij, W., Ploner, C., Geley, S., & Fiegl, H. (2009). Suppression of B cell lymphomagenesis by the BH3-only proteins Bmf and Bad Suppression of B cell lymphomagenesis by the BH3-only proteins Bmf and Bad. *Blood*, *115*(5), 995–1005.

Fueyo, J., Gomez-Manzano, C., Yung, W., Liu, T., Alemany, R., McDonnell, T., ... Kyritsis, A. (1998). Overexpression of E2F-1 in glioma triggers apoptosis and suppresses tumor growth in vitro and in vivo. *Nature Medicine*, *4*(6), 685–690.

Fulciniti, M., Martinez-Lopez, J., Senapedis, W., Oliva, S., Bandi, R., Amodio, N., ... Munshi, N. (2017). Functional role and therapeutic targeting of p21-activated kinase 4 in multiple myeloma. *Blood*, *129*(16), 2233–2246.

Galang, C. K. & Hauser, C. a. (1993). Cooperative DNA binding of the human HoxB5 (Hox-2.1) protein is under redox regulation in vitro. *Molecular and Cellular Biology*, *13*(8), 4609–17.

Galassi, L., Di Stefano, M., Brunetti, L., Orsomando, G., Amici, A., Ruggieri, S., & Magni, G. (2012). Characterization of human nicotinate phosphoribosyltransferase: Kinetic studies, structure prediction and functional analysis by site-directed mutagenesis. *Biochimie*, *94*(2), 300–309.

Galia, A., Calogero, A., Condorelli, R., Fraggetta, F., La Corte, A., Ridolfo, F., ... Salemi, M. (2012). PARP-1 protein expression in glioblastoma multiforme. *European Journal of Histochemistry*, *56*(1), 45–48.

Gao, P., Tchernyshyov, I., Chang, T. C., Lee, Y. S., Kita, K., Ochi, T., ... Dang, C. V. (2009). C-Myc suppression of miR-23a/b enhances mitochondrial glutaminase expression and glutamine metabolism. *Nature*, *458*(7239), 762–765.

Gao, Z.-W., Dong, K., & Zhang, H.-Z. (2014). The roles of CD73 in cancer. *BioMed Research International*, *2014*, 1–9.

Garavaglia, S., Bruzzone, S., Cassani, C., Canella, L., Allegrone, G., Sturla, L., ... Rizzi, M. (2012). The high-resolution crystal structure of periplasmic Haemophilus influenzae NAD nucleotidase reveals a novel enzymatic function of human CD73 related to NAD metabolism. *Biochemical Journal*, *441*(1), 131–41.

Garten, A., Schuster, S., Penke, M., Gorski, T., de Giorgis, T., & Kiess, W. (2015). Physiological and pathophysiological roles of NAMPT and NAD metabolism. *Nature Reviews Endocrinology*, *11*(9), 1–12.

Gehrke, I., Bouchard, E. D. J., Beiggi, S., Poeppl, A. G., Johnston, J. B., Gibson, S. B., & Banerji, V. (2014). On-target effect of FK866, a nicotinamide phosphoribosyl transferase inhibitor, by apoptosis-mediated death in chronic lymphocytic leukemia cells. *Clinical Cancer Research*, *20*(18), 4861–4872.

Gholinejad, Z., Kheiripour, N., Nourbakhsh, M., Ilbeigi, D., Behroozfar, K., Hesari, Z., ... Einollahi, N. (2017). Extracellular NAMPT/Visfatin induces proliferation through ERK1/2 and AKT and inhibits apoptosis in breast cancer cells. *Peptides*, *92*, 9–15.

Ghosh, S., Tewari, R., Dixit, D., & Sen, E. (2010). TNF-alpha induced oxidative stress dependent Akt signaling affects actin cytoskeletal organization in glioma cells. *Neurochemistry International*, *56*(1), 194–201.

Gil Del Alcazar, C. R., Hardebeck, M. C., Mukherjee, B., Tomimatsu, N., Gao, X., Yan, J., ... Burma, S. (2014). Inhibition of DNA double-strand break repair by the dual PI3K/mTOR inhibitor NVP-BEZ235 as a strategy for radiosensitization of glioblastoma. *Clinical Cancer Research*, *20*(5), 1235–1248.

Glazer, E. S., Piccirillo, M., Albino, V., Di Giacomo, R., Palaia, R., Mastro, A. A., ... Izzo, F. (2010). Phase II Study of Pegylated Arginine Deiminase for Nonresectable and Metastatic Hepatocellular Carcinoma. *Journal of Clinical Oncology*, *28*(13), 2220–2226.

Godlewski, J., Nowicki, M. O., Bronisz, A., Nuovo, G., Palatini, J., De Lay, M., ... Lawler, S. E. (2010). MicroRNA-451 Regulates LKB1/AMPK Signaling and Allows Adaptation to Metabolic Stress in Glioma Cells. *Molecular Cell*, *37*(5), 620–632.

Goellner, E. M., Grimme, B., Brown, A. R., Lin, Y.-C., Wang, X.-H., Sugrue, K. F., ... Sobol, R. W. (2011). Overcoming temozolomide resistance in glioblastoma via dual inhibition of NAD+ biosynthesis and base excision repair. *Cancer Research*, *71*(6), 2308–17.

Goertsches, R., Comabella, M., Navarro, A., Perkal, H., & Montalban, X. (2005). Genetic association between polymorphisms in the ADAMTS14 gene and multiple sclerosis. *Journal of Neuroimmunology*, *164*(1-2), 140–147.

Goldinger, S., Bischof, S., Fink-Puches, R., Klemke, C., Dreno, B., Bagot, M., & DUmmer, R. (2016). Efficacy and Safety of APO866 in Patients With Refractory or Relapsed Cutaneous T-Cell Lymphoma: A Phase 2 Clinical Trial. *JAMA Dermatology*, *152*(7), 837–839.

Gomez-Manzano, C., Mitlianga, P., Fueyo, J., Lee, H.-y., Hu, M., Spurgers, K. B., ... Yung, W. K. A. (2001). Transfer of E2F-1 to Human Glioma Cells Results in Transcriptional Up-Regulation of Bcl-2. *Cancer Research*, *61*(18), 6693–6697.

Graner, M. W. (2015). The unfolded protein response in glioblastomas: targetable or trouble? *Future Science OA*, *1*(2), 1–11.

Grozio, A., Sociali, G., Sturla, L., Caffa, I., Soncini, D., Salis, A., ... Bruzzone, S. (2013). CD73 protein as a source of extracellular precursors for sustained NAD+ biosynthesis in FK866-treated tumor cells. *The Journal of Biological Chemistry*, *288*(36), 25938–49.

Grube, S., Dünisch, P., Freitag, D., Klausnitzer, M., Sakr, Y., Walter, J., ... Ewald, C. (2014). Overexpression of fatty acid synthase in human gliomas correlates with the WHO tumor grade and inhibition with Orlistat reduces cell viability and triggers apoptosis. *Journal of Neuro-Oncology*, *118*(2), 277–287.

Guastella, A. R., Michelhaugh, S. K., Klinger, N. V., Kupsky, W. J., Polin, L. A., Muzik, O., ... Mittal, S. (2016). Tryptophan PET Imaging of the Kynurenine Pathway in Patient-Derived Xenograft Models of Glioblastoma. *Molecular Imaging*, *15*, 1–11.

Gujar, A. D., Le, S., Mao, D. D., Dadey, D. Y. A., Turski, A., Sasaki, Y., ... Kim, A. H. (2016). An NAD +-dependent transcriptional program governs self-renewal and radiation resistance in glioblastoma. *Proceedings of the National Academy of Sciences of the United States of America*, *113*(51), 8247–8256.

Guo, D., Bell, E., & Chakravarti, a. (2013a). Lipid metabolism emerges as a promising target for malignant glioma therapy. *CNS oncology*, *2*(3), 289–299.

Guo, D., Hildebrandt, I. J., Prins, R. M., Soto, H., Mazzotta, M. M., Dang, J., ... Mischel, P. S. (2009a). The AMPK agonist AICAR inhibits the growth of EGFRvIII-expressing glioblastomas by inhibiting lipogenesis. *Proceedings of the National Academy of Sciences of the United States of America*, *106*(31), 12932–12937.

Guo, D., Prins, R. M., Dang, J., Kuga, D., Iwanami, A., Soto, H., ... Mischel, P. S. (2009b). EGFR signaling through an Akt-SREBP-1-dependent, rapamycin-resistant pathway sensitizes glioblastomas to antilipogenic therapy. *Science Signaling*, *2*(101), 1–13.

Guo, D., Reinitz, F., Youssef, M., Hong, C., Nathanson, D., Akhavan, D., ... Mischel, P. S. (2011). An LXR agonist promotes glioblastoma cell death through inhibition of an EGFR/AKT/SREBP-1/LDLR-dependent pathway. *Cancer Discovery*, *1*(5), 442–456.

Guo, J., Lam, L. T., Longenecker, K. L., Bui, M. H., Idler, K. B., Glaser, K. B., ... Huang, T. H. (2017). Identification of novel resistance mechanisms to NAMPT inhibition via the de novo NAD+biosynthesis pathway and NAMPT mutation. *Biochemical and Biophysical Research Communications*, *491*(3), 681–686.

Guo, P., Nie, Q., Lan, J., Ge, J., Qiu, Y., & Mao, Q. (2013b). C-Myc negatively controls the tumor suppressor PTEN by upregulating miR-26a in glioblastoma multiforme cells. *Biochemical and Biophysical Research Communications*, *441*(1), 186–190.

Gupta, S. K., Mladek, A. C., Carlson, B. L., Boakye-Agyeman, F., Bakken, K. K., Kizilbash, S. H., ... Sarkaria, J. N. (2014). Discordant in vitro and in vivo chemopotentiating effects of the PARP inhibitor veliparib in temozolomide-sensitive versus -resistant glioblastoma multiforme xenografts. *Clinical Cancer Research*, *20*(14), 3730–3741.

Ha, G. H., Kim, H. S., Go, H., Lee, H., Seimiya, H., Chung, D. H., & Lee, C. W. (2012). Tankyrase-1 function at telomeres and during mitosis is regulated by Polo-like kinase-1-mediated phosphorylation. *Cell Death and Differentiation*, *19*(2), 321–332.

Haenni, S. S., Hassa, P. O., Altmeyer, M., Fey, M., Imhof, R., & Hottiger, M. O. (2008). Identification of lysines 36 and 37 of PARP-2 as targets for acetylation and auto-ADP-ribosylation. *International Journal of Biochemistry and Cell Biology*, *40*(10), 2274–2283.

Haigis, M. C., Mostoslavsky, R., Haigis, K. M., Fahie, K., Christodoulou, D. C., Murphy, A. J. J., ... Guarente, L. (2006). SIRT4 Inhibits Glutamate Dehydrogenase and Opposes the Effects of Calorie Restriction in Pancreatic β Cells. *Cell*, *126*(5), 941–954.

Hallows, W. C., Yu, W., Smith, B. C., Devires, M. K., Ellinger, J. J., Someya, S., ... Denu, J. M. (2011). Sirt3 Promotes the Urea Cycle and Fatty Acid Oxidation during Dietary Restriction. *Molecular Cell*, *41*(2), 139–149.

Hanai, J. I., Doro, N., Sasaki, A. T., Kobayashi, S., Cantley, L. C., Seth, P., & Sukhatme, V. P. (2012). Inhibition of lung cancer growth: ATP citrate lyase knockdown and statin treatment leads to dual blockade of mitogen-activated protein Kinase (MAPK) and Phosphatidylinositol 3-kinase (PI3K)/AKT pathways. *Journal of Cellular Physiology*, *227*(4), 1709–1720.

Hanzlikova, H., Gittens, W., Krejcikova, K., Zeng, Z., & Caldecott, K. W. (2017). Overlapping roles for PARP1 and PARP2 in the recruitment of endogenous XRCC1 and PNKP into oxidized chromatin. *Nucleic Acids Research*, *45*(5), 2546–2557.

Hara, N., Yamada, K., Shibata, T., Osago, H., Hashimoto, T., & Tsuchiya, M. (2007). Elevation of cellular NAD levels by nicotinic acid and involvement of nicotinic acid phosphoribosyltransferase in human cells. *Journal of Biological Chemistry*, *282*(34), 24574–24582.

Hasmann, M. & Schemainda, I. (2003). FK866, a Highly Specific Noncompetitive Inhibitor of Nicotinamide Phosphoribosyltransferase, Represents a Novel Mechanism for Induction of Tumor Cell Apoptosis. *Cancer Research*, *63*(21), 7436–7442.

Hassan, S. B., Lövborg, H., Lindhagen, E., Karlsson, M. O., & Larsson, R. (2006). CHS 828 kill tumour cells by inhibiting the nuclear factor-κB translocation but unlikely through down-regulation of proteasome. *Anticancer Research*, *26*(6), 4431–4436.

Hatzivassiliou, G., Zhao, F., Bauer, D. E., Andreadis, C., Shaw, A. N., Dhanak, D., ... Thompson, C. B. (2005). ATP citrate lyase inhibition can suppress tumor cell growth. *Cancer Cell*, *8*(4), 311–321.

He, X., Nie, H., Hong, Y., Sheng, C., Xia, W., & Ying, W. (2012). SIRT2 activity is required for the survival of C6 glioma cells. *Biochemical and Biophysical Research Communications*, *417*(1), 468–472.

Hegi, M. E., Liu, L., Herman, J. G., Stupp, R., Wick, W., Weller, M., ... Gilbert, M. R. (2008). Correlation of O6-methylguanine methyltransferase (MGMT) promoter methylation with clinical outcomes in glioblastoma and clinical strategies to modulate MGMT activity. *Journal of Clinical Oncology*, *26*(25), 4189–4199.

Heiden, M. G. V., Cantley, L. C., & Thompson, C. B. (2009). Understanding the Warburg Effect: The Metabolic Requirements of Cell Proliferation. *Science*, *324*(5930), 1029–1033.

Henderson, D. J. P., Miranda, J. L., & Emerson, B. M. (2017). The beta-NAD+ salvage pathway and PKC-mediated signaling influence localized PARP-1 activity and CTCF Poly(ADP)ribosylation. *Oncotarget*, *8*(39), 64698–64713.

Hensley, C. T., Wasti, A. T., & Deberardinis, R. J. (2013). Glutamine and cancer: cell biology, physiology, and clinical opportunities. *The Journal of Clinical Investigation*, *123*(9), 3678–3684.

Herrlinger, U., Rieger, J., Steinbach, J. P., Nägele, T., Dichgans, J., & Weller, M. (2005). UKT-04 trial of continuous metronomic low-dose chemotherapy with methotrexate and cyclophosphamide for recurrent glioblastoma. *Journal of Neuro-Oncology*, *71*(3), 295–299.

Heske, C. M., Davis, M. I., Baumgart, J. T., Wilson, K., Gormally, M. V., Chen, L., ... Thomas, C. J. (2017). Matrix screen identifies synergistic combination of PARP inhibitors and nicotinamide phosphoribosyltransferase (NAMPT) inhibitors in Ewing sarcoma. *Clinical Cancer Research*, *23*(23), 7301–7311.

Hetz, C. & Papa, F. R. (2018). The Unfolded Protein Response and Cell Fate Control. *Molecular Cell*, *69*(2), 169–181.

Heyes, M. P., Chen, C. Y., Major, E. O., & Saito, K. (1997). Different kynurenine pathway enzymes limit quinolinic acid formation by various human cell types. *Biochemical Journal*, *326*, 351–356.

Hirai, H., Sootome, H., Nakatsuru, Y., Miyama, K., Taguchi, S., Tsujioka, K., ... Kotani, H. (2010). MK-2206, an Allosteric Akt Inhibitor, Enhances Antitumor Efficacy by Standard Chemotherapeutic Agents or Molecular Targeted Drugs In vitro and In vivo. *Molecular Cancer Therapeutics*, *9*(7), 1956–1967.

Hirose, Y., Berger, M. S., & Pieper, R. O. (2001). p53 Effects Both the Duration of G 2 /M Arrest and the Fate of Temozolomide-treated Human Glioblastoma Cells 1. *Cancer Research*, *61*(5), 1957–1963.

Hjarnaa, P.-j. V., Jonsson, E., Latini, S., Dhar, S., Larsson, R., Bramm, E., & Skov, T. (1999). CHS 828 , a Novel Pyridyl Cyanoguanidine with Potent Antitumor Activity in Vitro and in Vivo CHS 828 , a Novel Pyridyl Cyanoguanidine with Potent Antitumor Activity in Vitro and in Vivo. *Cancer Research*, *59*(22), 5751–5757.

Ho Yang, S., Li, S., Lu, G., Xue, H., Kim, D. H., Zhu, J.-J., ... Liu, Y. (2016). Metformin treatment reduces temozolomide resistance of glioblastoma cells. *Oncotarget*, *7*(48), 78787–78803.

Holen, K., Saltz, L. B., Hollywood, E., Burk, K., & Hanauske, A. R. (2008). The pharmacokinetics, toxicities, and biologic effects of FK866, a nicotinamide adenine dinucleotide biosynthesis inhibitor. *Investigational New Drugs*, *26*(1), 45–51.

Hong, C.-S., Jeong, O., Piao, Z., Guo, C., Jung, M.-R., Choi, C., & Park, Y.-K. (2015a). HOXB5 induces invasion and migration through direct transcriptional up-regulation of B-catenin in human gastric carcinoma. *Biochemical Journal*, *472*(3), 393–403.

Hong, D. S., Henary, H., Falchook, G. S., Naing, A., Fu, S., Moulder, S., ... Kurzrock, R. (2014a). First-in-human study of pbi-05204, an oleander-derived inhibitor of akt, fgf-2, nf-kb and p70s6k, in patients with advanced solid tumors. *Investigational New Drugs*, *32*(6), 1204–1212.

Hong, S. M., Park, C. W., Kim, S. W., Nam, Y. J., Yu, J. H., Shin, J. H., ... Choi, K. Y. (2015b). NAMPT suppresses glucose deprivation-induced oxidative stress by increasing NADPH levels in breast cancer. *Oncogene*, *35*(27), 3544–54.

Hong, S. Y., Yu, F. X., Luo, Y., & Hagen, T. (2016). Oncogenic activation of the PI3K/Akt pathway promotes cellular glucose uptake by downregulating the expression of thioredoxin-interacting protein. *Cellular Signalling*, *28*(5), 377–383.

Hong, S., Zhao, B., Lombard, D. B., Fingar, D. C., & Inoki, K. (2014b). Cross-talk between sirtuin and mammalian target of rapamycin complex 1 (mTORC1) signaling in the regulation of S6 kinase 1 (S6K1) phosphorylation. *Journal of Biological Chemistry*, *289*(19), 13132–13141.

Hong, X., O'Donnell, J. P., Salazar, C. R., Van Brocklyn, J. R., Barnett, K. D., Pearl, D. K., ... Lehman, N. L. (2014c). The selective Aurora-A kinase inhibitor MLN8237 (alisertib) potently inhibits proliferation of glioblastoma neurosphere tumor stem-like cells and potentiates the effects of temozolomide and ionizing radiation. *Cancer Chemotherapy and Pharmacology*, *73*(5), 983–990.

Houtkooper, R. H., Cantó, C., Wanders, R. J., & Auwerx, J. (2010). The secret life of NAD+: An old metabolite controlling new metabolic signaling pathways. *Endocrine Reviews*, *31*(2), 194–223.

Hovstadius, P., Larsson, R., Jonsson, E., Skov, T., Kissmeyer, A.-M., Krasilnikoff, K., ... Ahlgren, J. (2002). A phase I study of CHS 828 in patients with solid tumors. *Clinical Cancer Research*, *8*(9), 2843–2850.

Hu, B., Wang, Q., Wang, Y., & Chen, J. (2017). Holliday junction – recognizing protein promotes cell proliferation and correlates with unfavorable clinical outcome of hepatocellular carcinoma. *OncoTargets and Therapy*, *10*, 2601–2607.

Hu, T., Xie, N., Qin, C., Wang, J., & You, Y. (2015). Glucose-regulated protein 94 is a novel glioma biomarker and promotes the aggressiveness of glioma via Wnt/β-catenin signaling pathway. *Tumor Biology*, *36*(12), 9357–9364.

Hu, Z., Huang, G., Sadanandam, A., Gu, S., Lenburg, M. E., Pai, M., ... Mao, J. H. (2010). The expression level of HJURP has an independent prognostic impact and predicts the sensitivity to radiotherapy in breast cancer. *Breast Cancer Research*, *12*(2), 1–15.

Huang, W., Zhang, H., Hao, Y., Xu, X., Zhai, Y., Wang, S., ... Zhou, G. (2016). A non-synonymous single nucleotide polymorphism in the HJURP gene associated with susceptibility to hepatocellular carcinoma among Chinese. *PLOS One*, *11*(2), 1–15.

Hung, A. C., Lo, S., Hou, M. F., Lee, Y. C., Tsai, C. H., Chen, Y. Y., ... Yuan, S. S. F. (2016). Extracellular visfatin-promoted malignant behavior in breast cancer is mediated through c-Abl and STAT3 activation. *Clinical Cancer Research*, *22*(17), 4478–4490.

Huynh, T. T., Lin, C. M., Lee, W. H., Wu, A. T., Lin, Y. K., Lin, Y. F., ... Wang, L. S. (2015). Pterostilbene suppressed irradiation-resistant glioma stem cells by modulating GRP78/miR-205 axis. *Journal of Nutritional Biochemistry*, *26*(5), 466–475.

Ichimura, K., Pearson, D. M., Kocialkowski, S., Bäcklund, L. M., Chan, R., Jones, D. T. W., & Collins, V. P. (2009). IDH1 mutations are present in the majority of common adult gliomas but rare in primary glioblastomas. *Neuro-Oncology*, *11*(4), 341–347.

Imaoka, N., Hiratsuka, M., Osaki, M., Kamitani, H., Kambe, A., Fukuoka, J., ... Oshimura, M. (2012). Prognostic significance of sirtuin 2 protein nuclear localization in glioma: An immunohistochemical study. *Oncology Reports*, *28*(3), 923–930.

Iwadate, Y., Fujimoto, S., Tagawa, M., Namba, H., Sueyoshi, K., Hirose, M., & Sakiyama, S. (1996). Association of p53 gene mutation with decreased chemosensitivity in human malignant gliomas. *International Journal of Cancer*, *69*(3), 236–240.

Izzo, F., Marra, P., Beneduce, G., Castello, G., Vallone, P., De Rosa, V., ... Curley, S. A. (2004). Pegylated arginine deiminase treatment of patients with unresectable hepatocellular carcinoma: Results from phase I/II studies. *Journal of Clinical Oncology*, *22*(10), 1815–1822.

Jackson, M., Hassiotou, F., & Nowak, A. (2014). Glioblastoma stem-like cells: At the root of tumor recurrence and a therapeutic target. *Carcinogenesis*, *36*(2), 177–185.

Jagtap, P. & Szabo, C. (2005). Poly(ADP-ribose) polymerase and the therapeutic effects of its inhibitors. *Nature Reviews Drug Discovery*, *4*(5), 421–440.

Janiszewska, M., Suva, M. L., Riggi, N., Houtkooper, R. H., Auwerx, J., Clement-Schatlo, V., ... Stamenkovic, I. (2012). Imp2 controls oxidative phosphorylation and is crucial for preserving glioblastoma cancer stem cells. *Genes & Development*, *26*(17), 1926–1944.

Jiang, H., Martin, V., Gomez-Manzano, C., Johnson, D. G., Alonso, M., White, E., ... Fueyo, J. (2010). The RB-E2F1 Pathway Regulates Autophagy. *Cancer Research*, *70*(20), 7882–7893.

Johnson, D. R. & O'Neill, B. P. (2012). Glioblastoma survival in the United States before and during the temozolomide era. *Journal of Neuro-Oncology*, *107*(2), 359–364.

Jones, J. E., Esler, W. P., Patel, R., Lanba, A., Vera, N. B., Pfefferkorn, J. A., & Vernochet, C. (2017). Inhibition of Acetyl-CoA carboxylase 1 (ACC1) and 2 (ACC2) reduces proliferation and de novo lipogenesis of EGFRvIII human glioblastoma cells. *PLOS One*, *12*(1), 1–20.

Jones, R. G., Plas, D. R., Kubek, S., Buzzai, M., Mu, J., Xu, Y., ... Thompson, C. B. (2005). AMP-activated protein kinase induces a p53-dependent metabolic checkpoint. *Molecular Cell*, *18*(3), 283–293.

Joshi, S., Singh, A. R., & Durden, D. L. (2014). MDM2 regulates hypoxic hypoxia-inducible factor 1α stability in an E3 ligase, proteasome, and PTEN-phosphatidylinositol 3-kinase-AKT-dependent manner. *Journal of Biological Chemistry*, *289*(33), 22785–22797.

Ju, H. Q., Zhuang, Z. N., Li, H., Tian, T., Lu, Y. X., Fan, X. Q., ... Xu, R. H. (2016). Regulation of the Nampt-mediated NAD salvage pathway and its therapeutic implications in pancreatic cancer. *Cancer Letters*, *379*(1), 1–11.

Kalinina, J., Carroll, A., Wang, L., Yu, Q., Mancheno, D. E., Wu, S., ... Van Meir, E. G. (2012). Detection of "oncometabolite" 2-hydroxyglutarate by magnetic resonance analysis as a biomarker of IDH1/2 mutations in glioma. *Journal of Molecular Medicine*, *90*(10), 1161–1171.

Kane, D. A. (2014). Lactate oxidation at the mitochondria: A lactate-malate-aspartate shuttle at work. *Frontiers in Neuroscience*, *8*(366), 1–6.

Kang, B. R., Yang, S. H., Chung, B. R., Kim, W., & Kim, Y. S. (2016). Cell surface GRP78 as a biomarker and target for suppressing glioma cells. *Scientific Reports*, *6*(34922), 1–7.

Kanzawa, T., Germano, I. M., Komata, T., Ito, H., Kondo, Y., & Kondo, S. (2004). Role of autophagy in temozolomide-induced cytotoxicity for malignant glioma cells. *Cell Death and Differentiation*, *11*(4), 448–457.

Kao, G. D., Jiang, Z., Fernandes, A. M., Gupta, A. K., & Maity, A. (2007). Inhibition of phosphatidylinositol-3-OH kinase/Akt signaling impairs DNA repair in glioblastoma cells following ionizing radiation. *Journal of Biological Chemistry*, *282*(29), 21206–21212.

Karran, P. (2001). Mechanisms of tolerance to DNA damaging therapeutic drugs. *Carcinogenesis*, *22*(12), 1931–1937.

Kasznicki, J., Sliwinska, A., & Drzewoski, J. (2014). Metformin in cancer prevention and therapy. *Annals of Translational Medicine*, *2*(6), 57.

Kathagen-Buhmann, A., Schulte, A., Weller, J., Holz, M., Herold-Mende, C., Glass, R., & Lamszus, K. (2016). Glycolysis and the pentose phosphate pathway are differentially associated with the dichotomous regulation of glioblastoma cell migration versus proliferation. *Neuro-Oncology*, *18*(9), 1219–1229.

Kato, H., Ito, E., Shi, W., Alajez, N. M., Yue, S., Lee, C., ... Liu, F. F. (2010). Efficacy of combining GMX1777 with radiation therapy for human head and neck carcinoma. *Clinical Cancer Research*, *16*(3), 898–911.

Kato, T., Sato, N., Hayama, S., Yamabuki, T., Ito, T., Miyamoto, M., ... Daigo, Y. (2007). Activation of Holliday junction-recognizing protein involved in the chromosomal stability and immortality of cancer cells. *Cancer Research*, *67*(18), 8544–8553.

Kearns, N. A., Genga, R. M. J., Enuameh, M. S., Garber, M., Wolfe, S. A., & Maehr, R. (2014). Cas9 effector-mediated regulation of transcription and differentiation in human pluripotent stem cells. *Development*, *141*(1), 219–223.

Kennedy, C. R., Tilkens, S. B., Guan, H., Garner, J. A., Or, P. M., & Chan, A. M. (2013). Differential sensitivities of glioblastoma cell lines towards metabolic and signaling pathway inhibitions. *Cancer Letters*, *336*(2), 299–306.

Khan, M., Saif, A., Sandler, S., & Mirrakhimov, A. E. (2014). Idelalisib for the Treatment of Chronic Lymphocytic Leukemia. *Future Oncology*, *12*(18), 2077–2094.

Khan, Z. A., Tripathi, R., & Mishra, B. (2012). Methotrexate: a detailed review on drug delivery and clinical aspects. *Expert Opinion on Drug Delivery*, *9*(2), 151–169.

Khurshed, M., Molenaar, R. J., Lenting, K., Leenders, W. P., & van Noorden, C. J. (2017). In silico gene expression analysis reveals glycolysis and acetate anaplerosis in IDH1 wild-type glioma and lactate and glutamate anaplerosis in IDH1-mutated glioma. *Oncotarget*, *8*(30), 49165–49177.

Kilbride, S. M., Farrelly, A. M., Bonner, C., Ward, M. W., Nyhan, K. C., Concannon, C. G., ... Prehn, J. H. M. (2010). AMP-activated protein kinase mediates apoptosis in response to bioenergetic stress through activation of the pro-apoptotic Bcl-2 homology domain-3-only protein BMF. *Journal of Biological Chemistry*, *285*(46), 36199–36206.

Kim, E. H., Lee, J. H., Oh, Y., Koh, I., Shim, J. K., Park, J., ... Kang, S. G. (2017). Inhibition of glioblastoma tumorspheres by combined treatment with 2-deoxyglucose and metformin. *Neuro-Oncology*, *19*(2), 197–207.

Kim, H. S., Vassilopoulos, A., Wang, R. H., Lahusen, T., Xiao, Z., Xu, X., ... Deng, C. X. (2011). SIRT2 Maintains Genome Integrity and Suppresses Tumorigenesis through Regulating APC/C Activity. *Cancer Cell*, *20*(4), 487–499.

Kim, I. & He, Y.-Y. (2013). Targeting the AMP-Activated Protein Kinase for Cancer Prevention and Therapy. *Frontiers in Oncology*, *3*(175), 1–12.

Kim, J., Lee, I. H., Cho, H. J., Park, C. K., Jung, Y. S., Kim, Y., ... Nam, D. H. (2015). Spatiotemporal Evolution of the Primary Glioblastoma Genome. *Cancer Cell*, *28*(3), 318–328.

Kim, J. W., Tchernyshyov, I., Semenza, G. L., & Dang, C. V. (2006a). HIF-1-mediated expression of pyruvate dehydrogenase kinase: A metabolic switch required for cellular adaptation to hypoxia. *Cell Metabolism*, *3*(3), 177–185.

Kim, M. K., Lee, J. H., Kim, H., Park, S. J., Kim, S. H., Kang, G. B., ... Eom, S. H. (2006b). Crystal Structure of Visfatin/Pre-B Cell Colony-enhancing Factor 1/Nicotinamide Phosphoribosyltransferase, Free and in Complex with the Anti-cancer Agent FK-866. *Journal of Molecular Biology*, *362*(1), 66–77.

Kirla, R. M., Haapasalo, H. K., Kalimo, H., & Salminen, E. K. (2003). Low expression of p27 indicates a poor prognosis in patients with high-grade astrocytomas. *Cancer*, *97*(3), 644–648.

Kirsch, W. M. & Leitner, J. W. (1967). A comparison of the anaerobic glycolysis of human brain and glioblastoma. *Journal of Neurosurgery*, *27*(1), 45–51.

Kirschner, R. D., Rother, K., Müller, G. A., & Engeland, K. (2010). The retinal dehydrogenase/reductase retSDR1/DHRS3 gene is activated by p53 and p63 but not by mutants derived from tumors or EEC/ADULT malformation syndromes. *Cell Cycle*, *9*(11), 2177–2188.

Kitange, G. J., Carlson, B. L., Schroeder, M. A., Grogan, P. T., Lamont, J. D., Decker, P. A., ... Sarkaria, J. N. (2009). Induction of MGMT expression is associated with temozolomide resistance in glioblastoma xenografts. *Neuro-Oncology*, *11*(3), 281–291.

Klingler-Hoffmann, M., Bukczynska, P., & Tiganis, T. (2003). Inhibition of phosphatidylinositol 3-kinase signaling negates the growth advantage imparted by a mutant epidermal growth factor receptor on human glioblastoma cells. *International Journal of Cancer*, *105*(3), 331–339.

Kmiecik, J., Poli, A., Brons, N. H. C., Waha, A., Eide, G. E., Enger, P. Ø., ... Chekenya, M. (2013). Elevated CD3+ and CD8+ tumor-infiltrating immune cells correlate with prolonged survival in glioblastoma patients despite integrated immunosuppressive mechanisms in the tumor microenvironment and at the systemic level. *Journal of Neuroimmunology*, *264*(1-2), 71–83.

Koh, M. Y., Darnay, B. G., & Powis, G. (2008). Hypoxia-Associated Factor, a Novel E3-Ubiquitin Ligase, Binds and Ubiquitinates Hypoxia-Inducible Factor 1, Leading to Its Oxygen-Independent Degradation. *Molecular and Cellular Biology*, *28*(23), 7081–7095.

Kohnken, R., Kodigepalli, K. M., & Wu, L. (2015). Regulation of deoxynucleotide metabolism in cancer: Novel mechanisms and therapeutic implications. *Molecular Cancer*, *14*(1), 1–11.

Korkola, J. E., Collisson, E. A., Heiser, L., Oates, C., Bayani, N., Itani, S., ... Gray, J. W. (2015). Decoupling of the PI3K Pathway via Mutation Necessitates Combinatorial Treatment in HER2+ Breast Cancer. *PLOS One*, *10*(7), 1–19.

Kostaras, X., Cusano, F., Kline, G. A., Roa, W., & Easaw, J. (2014). Use of dexamethasone in patients with high-grade glioma: a clinical practice guideline. *Current Oncology*, *21*(3), e493–503.

Kotliarova, S., Pastorino, S., Kovell, L. C., Kotliarov, Y., Song, H., Zhang, W., ... Fine, H. A. (2008). Glycogen synthase kinase-3 inhibition induces glioma cell death through c-MYC, nuclear factor-κB, and glucose regulation. *Cancer Research*, *68*(16), 6643–6651.

Kreisl, T. N., Lassman, A. B., Mischel, P. S., Rosen, N., Scher, H. I., Teruya-Feldstein, J., ... Abrey, L. E. (2009). A pilot study of everolimus and gefitinib in the treatment of recurrent glioblastoma (GBM). *Journal of Neuro-Oncology*, *92*(1), 99–105.

Kucharzewska, P., Christianson, H. C., & Belting, M. (2015). Global profiling of metabolic adaptation to hypoxic stress in human glioblastoma cells. *PLOS One*, *10*(1), 1–22.

Kuleshov, M. V., Jones, M. R., Rouillard, A. D., Fernandez, N. F., Duan, Q., Wang, Z., ... Ma'ayan, A. (2016). Enrichr: a comprehensive gene set enrichment analysis web server 2016 update. *Nucleic Acids Research*, *44*(1), 90–97.

Kushner, B. H., Cheung, N. K. V., Modak, S., Becher, O. J., Basu, E. M., Roberts, S. S., ... Dunkel, I. J. (2017). A phase I/Ib trial targeting the Pi3k/Akt pathway using perifosine: Long-term progression-free survival of patients with resistant neuroblastoma. *International Journal of Cancer*, *140*(2), 480–484.

Kutuzov, M. M., Khodyreva, S. N., Amé, J. C., Ilina, E. S., Sukhanova, M. V., Schreiber, V., & Lavrik, O. I. (2013). Interaction of PARP-2 with DNA structures mimicking DNA repair intermediates and consequences on activity of base excision repair proteins. *Biochimie*, *95*(6), 1208–1215.

Kutuzov, M. M., Khodyreva, S. N., Ilina, E. S., Sukhanova, M. V., Amé, J. C., & Lavrik, O. I. (2015). Interaction of PARP-2 with AP site containing DNA. *Biochimie*, *112*, 10–19.

Laemmle, A., Lechleiter, A., Roh, V., Schwarz, C., Portmann, S., Furer, C., ... Stroka, D. (2012). Inhibition of SIRT1 impairs the accumulation and transcriptional activity of HIF-1α protein under hypoxic conditions. *PLOS One*, *7*(3), 1–12.

Langhans, J., Schneele, L., Trenkler, N., von Bandemer, H., Nonnenmacher, L., Karpel-Massler, G., ... Westhoff, M.-A. (2017). The effects of PI3K-mediated signalling on glioblastoma cell behaviour. *Oncogenesis*, *6*(11), 1–9.

Larsen, J. T., Shanafelt, T. D., Leis, J. F., LaPlant, B., Call, T., Pettinger, A., ... Ding, W. (2017). Akt inhibitor MK-2206 in combination with bendamustine and rituximab in relapsed or refractory chronic lymphocytic leukemia: Results from the N1087 alliance study. *American Journal of Hematology*, *92*(8), 759–763.

Lassen, U., Sorensen, M., Gaziel, T. B., Hasselbalch, B., & Poulsen, H. S. (2013). Phase II study of bevacizumab and temsirolimus combination therapy for recurrent glioblastoma multiforme. *Anticancer Research*, *33*(4), 1657–1660.

Lee, C., Fotovati, A., Triscott, J., Chen, J., Venugopal, C., Singhal, A., ... Dunn, S. E. (2012). Polo-like kinase 1 inhibition kills glioblastoma multiforme brain tumor cells in part through loss of SOX2 and delays tumor progression in mice. *Stem Cells*, *30*(6), 1064–1075.

Lee, H. K., Xiang, C., Cazacu, S., Finniss, S., Kazimirsky, G., Lemke, N., ... Brodie, C. (2008). GRP78 is overexpressed in glioblastomas and regulates glioma cell growth and apoptosis. *Neuro-Oncology*, *10*(3), 236–243.

Lee, P. Y., Chen, C. L., Lin, Z. Z., Cheng, A. L., Chen, E. I., Whang-Peng, J., & Huang, C. Y. F. (2013). The aurora kinases inhibitor VE-465 is a novel treatment for glioblastoma multiforme. *Oncology*, *84*(6), 326–335.

Lee, Y.-C., Yang, Y.-H., Su, J.-H., Chang, H.-L., Hou, M.-F., & Yuan, S.-S. F. (2011). High Visfatin Expression in Breast Cancer Tissue Is Associated with Poor Survival. *Cancer Epidemiology Biomarkers & Prevention*, *20*(9), 1892–1901.

Lee, J.-Y., Hur, H., Yun, H. J., Kim, Y., Yang, S., Kim, S. I., & Kim, M. H. (2015a). HOXB5 Promotes the Proliferation and Invasion of Breast Cancer Cells. *International Journal of Biological Sciences*, *11*(6), 701–711.

Lee, Y., Kim, K. H., Kim, D. G., Cho, H. J., Kim, Y., Rheey, J., ... Nam, D. H. (2015b). FoxM1 promotes stemness and radio- resistance of glioblastoma by regulating the master stem cell regulator Sox2. *PLOS One*, *10*(10), 1–18.

Lehman, N. L., O'Donnell, J. P., Whiteley, L. J., Stapp, R. T., Lehman, T. D., Roszka, K. M., ... Poisson, L. M. (2012). Aurora A is differentially expressed in gliomas, is associated with

patient survival in glioblastoma, and is a potential chemotherapeutic target in gliomas. *Cell Cycle*, *11*(3), 489–502.

Levy, D., Kahana, J., & Kumar, R. (2009). AKT inhibitor, GSK690693, induces growth inhibition and apoptosis in acute lymphoblastic leukemia cell lines. *Blood*, *113*(8), 1723–1729.

Li, D., Bi, F. F., Chen, N. N., Cao, J. M., Sun, W. P., Zhou, Y. M., ... Yang, Q. (2014a). A novel crosstalk between BRCA1 and poly (ADP-ribose) polymerase 1 in breast cancer. *Cell Cycle*, *13*(21), 3442–3449.

Li, D., Chen, N. N., Cao, J. M., Sun, W. P., Zhou, Y. M., Li, C. Y., & Wang, X. X. (2014b). BRCA1 as a nicotinamide adenine dinucleotide (NAD)-dependent metabolic switch in ovarian cancer. *Cell Cycle*, *13*(16), 2564–2571.

Li, J., Anderson, M. G., Tucker, L. A., Shen, Y., Glaser, K. B., & Shah, O. J. (2009a). Inhibition of Aurora B kinase sensitizes a subset of human glioma cells to TRAIL concomitant with induction of TRAIL-R2. *Cell Death and Differentiation*, *16*(3), 498–511.

Li, Q., Qiu, X. M., Li, Q. H., Wang, X. Y., Li, L., Xu, M., ... Xiao, Y. B. (2015a). MicroRNA-424 may function as a tumor suppressor in endometrial carcinoma cells by targeting E2F7. *Oncology Reports*, *33*(5), 2354–2360.

Li, W., Ma, X., Li, N., Liu, H., Dong, Q., Zhang, J., ... Wang, W. (2016). Resveratrol inhibits Hexokinases II mediated glycolysis in non-small cell lung cancer via targeting Akt signaling pathway. *Experimental Cell Research*, *349*(2), 320–327.

Li, W., Saud, S. M., Young, M. R., Chen, G., & Hua, B. (2015b). Targeting AMPK for cancer prevention and treatment. *Oncotarget*, *6*(10), 7365–7378.

Li, Y., Guessous, F., Kwon, S., Kumar, M., Ibidapo, O., Fuller, L., ... Abounader, R. (2008). PTEN has tumor-promoting properties in the setting of gain-of-function p53 mutations. *Cancer Research*, *68*(6), 1723–1731.

Li, Z., Bao, S., Wu, Q., Wang, H., Eyler, C., Sathornsumetee, S., ... Rich, J. N. (2009b). Hypoxia-Inducible Factors Regulate Tumorigenic Capacity of Glioma Stem Cells. *Cancer Cell*, *15*(6), 501–513.

Liang, H. & Ward, W. F. (2006). PGC-1a : a key regulator of energy metabolism. *Advances in Physiology Education*, *30*(1), 145–151.

Liang, Y. C., Hsu, C. Y., Yao, Y. L., & Yang, W. M. (2013). PARP-2 regulates cell cycle-related genes through histone deacetylation and methylation independently of poly(ADP-ribosyl)ation. *Biochemical and Biophysical Research Communications*, *431*(1), 58–64.

Lim, J.-H., Lee, Y.-M., Chun, Y.-S., Chen, J., Kim, J.-E., & Park, J.-W. (2010). Sirtuin 1 Modulates Cellular Responses to Hypoxia by Deacetylating Hypoxia-Inducible Factor 1α. *Molecular Cell*, *38*(6), 864–878.

Lim, M., Xia, Y., Bettegowda, C., & Weller, M. (2018). Current state of immunotherapy for glioblastoma. *Nature Reviews Clinical Oncology*, *15*, 422–442.

Lin, C.-Y. & Gustafsson, J.-Å. (2015). Targeting liver X receptors in cancer therapeutics. *Nature Reviews Cancer*, *15*(4), 216–224.

Lino, M. M. & Merlo, A. (2011). PI3Kinase signaling in glioblastoma. *Journal of Neuro-Oncology*, *103*(3), 417–427.

Liu, H. Y., Li, Q. R., Cheng, X. F., Wang, G. J., & Hao, H. P. (2016). NAMPT inhibition synergizes with NQO1-targeting agents in inducing apoptotic cell death in non-small cell lung cancer cells. *Chinese Journal of Natural Medicines*, *14*(8), 582–589.

Liu, K. & Jiang, Y. (2017). Polymorphisms in DNA Repair Gene and Susceptibility to Glioma: A Systematic Review and Meta-Analysis Based on 33 Studies with 15 SNPs in 9 Genes. *Cellular and Molecular Neurobiology*, *37*(2), 263–274.

Liu, Y., Scheurer, M. E., El-Zein, R., Cao, Y., Do, K. A., Gilbert, M., ... Bondy, M. L. (2009a). Association and interactions between DNA repair gene polymorphisms and adult glioma. *Cancer Epidemiology Biomarkers and Prevention*, *18*(1), 204–214.

Liu, Y. C., Li, F., Handler, J., Huang, C. R. L., Xiang, Y., Neretti, N., ... Dang, C. V. (2008). Global regulation of nucleotide biosynthetic genes by c-myc. *PLOS One*, *3*(7), 1–13.

Liu, Z. G., Chen, H. Y., Cheng, J. J., Chen, Z. P., Li, X. N., & fei Xia, Y. (2009b). Relationship between methylation status of ERCC1 promoter and radiosensitivity in glioma cell lines. *Cell Biology International*, *33*(10), 1111–1117.

Lo Nigro, C., Monteverde, M., Lee, S., Lattanzio, L., Vivenza, D., Comino, A., ... Crook, T. (2012). NT5E CpG island methylation is a favourable breast cancer biomarker. *British Journal of Cancer*, *107*(1), 75–83.

Lombardi, G., Corona, G., Bellu, L., Puppa, A. D., Pambuku, A., Fiduccia, P., ... Zagonel, V. (2015). Diagnostic Value of Plasma and Urinary 2-Hydroxyglutarate to Identify Patients With Isocitrate Dehydrogenase-Mutated Glioma. *The Oncologist*, *20*(5), 562–567.

Longley, D. B., Harkin, D. P., & Johnston, P. G. (2003). 5-Fluorouracil: Mechanisms of action and clinical strategies. *Nature Reviews Cancer*, *3*(5), 330–338.

Loseva, O., Jemth, A. S., Bryant, H. E., Schüler, H., Lehtiö, L., Karlberg, T., & Helleday, T. (2010). PARP-3 is a mono-ADP-ribosylase that activates PARP-1 in the absence of DNA. *Journal of Biological Chemistry*, *285*(11), 8054–8060.

Louis, D. N., Perry, A., Reifenberger, G., von Deimling, A., Figarella-Branger, D., Cavenee, W. K., ... Ellison, D. W. (2016). The 2016 World Health Organization Classification of Tumors of the Central Nervous System: a summary. *Acta Neuropathologica*, *131*(6), 803–820.

Love, M. I., Huber, W., & Anders, S. (2014). Moderated estimation of fold change and dispersion for RNA-seq data with DESeq2. *Genome Biology*, *15*(12), 550.

Lu, C.-L., Qin, L., Liu, H.-C., Candas, D., Fan, M., & Li, J. J. (2015). Tumor Cells Switch to Mitochondrial Oxidative Phosphorylation under Radiation via mTOR-Mediated Hexokinase II Inhibition - A Warburg-Reversing Effect. *PLOS One*, *10*(3), 1–20.

Lu, Y., Kwintkiewicz, J., Liu, Y., Tech, K., Frady, L. N., Su, Y. T., ... Wu, J. (2017). Chemosensitivity of IDH1-mutated gliomas due to an impairment in PARP1-mediated DNA repair. *Cancer Research*, *77*(7), 1709–1718.

Lubanska, D. & Porter, L. (2017). Revisiting CDK Inhibitors for Treatment of Glioblastoma Multiforme. *Drugs in R&D*, *17*(2), 255–263.

Lucena-Cacace, A., Otero-Albiol, D., & Jiménez-García, M. P. (2017). NAMPT overexpression induces cancer stemness and defines a novel tumor signature for glioma prognosis. *Oncotarget*, *8*(59), 99514–99530.

Lukey, M. J., Katt, W. P., & Cerione, R. A. (2017). Targeting amino acid metabolism for cancer therapy. *Drug Discovery Today*, *22*(5), 796–804.

Luna, A., Aladjem, M. I., & Kohn, K. W. (2013). SIRT1/PARP1 crosstalk: Connecting DNA damage and metabolism. *Genome Integrity*, *4*(1), 1–11.

Lundová, T., Zemanová, L., Malčeková, B., Skarka, A., Štambergová, H., Havránková, J., ... Wsól, V. (2015). Molecular and biochemical characterisation of human short-chain dehydrogenase/reductase member 3 (DHRS3). *Chemico-Biological Interactions*, *234*, 178–187.

Luo, J., Nikolaev, A. Y., Imai, S.-i., Chen, D., Su, F., Shiloh, A., ... Gu, W. (2001). Negative control of p53 by Sir2alpha promotes cell survival under stress. *Cell*, *107*(2), 137–48.

Lv, X., Zhang, L., Zhu, Y., Said, H. M., Shi, J., & Xu, G. (2015). Regulative effect of Nampt on tumor progression and cell viability in human colorectal cancer. *Journal of Cancer*, *6*(9), 849–858.

Ma, D. J., Galanis, E., Anderson, S. K., Schiff, D., Kaufmann, T. J., Peller, P. J., ... Sarkaria, J. N. (2015). A phase II trial of everolimus, temozolomide, and radiotherapy in patients with newly diagnosed glioblastoma: NCCTG N057K. *Neuro-Oncology*, *17*(9), 1261–1269.

Machado, L. E., Alvarenga, A. W., da Silva, F. F., Roffé, M., Begnami, M. D., Torres, L. F. B., ... Hajj, G. N. M. (2018). Overexpression of mTOR and p(240–244)S6 in IDH1 Wild-Type Human Glioblastomas Is Predictive of Low Survival. *Journal of Histochemistry & Cytochemistry*, *66*(6), 403–414.

MacPherson, L., Tamblyn, L., Rajendra, S., Bralha, F., McPherson, J. P., & Matthews, J. (2013). 2,3,7,8-Tetrachlorodibenzo-p-dioxin poly(ADP-ribose) polymerase (TiPARP, ARTD14) is a mono-ADP-ribosyltransferase and repressor of aryl hydrocarbon receptor transactivation. *Nucleic Acids Research*, *41*(3), 1604–1621.

Mai, W. X., Gosa, L., Daniels, V. W., Ta, L., Tsang, J. E., Higgins, B., ... Nathanson, D. A. (2017). Cytoplasmic p53 couples oncogene-driven glucose metabolism to apoptosis and is a therapeutic target in glioblastoma. *Nature Medicine*, *23*(11), 1342–1351.

Maira, S.-M., Stauffer, F., Brueggen, J., Furet, P., Schnell, C., Fritsch, C., ... Garcia-Echeverria, C. (2008). Identification and characterization of NVP-BEZ235, a new orally available dual phosphatidylinositol 3-kinase/mammalian target of rapamycin inhibitor with potent in vivo antitumor activity. *Molecular Cancer Therapeutics*, *7*(7), 1851–1863.

Majewska, E. & Szeliga, M. (2017). AKT/GSK3β Signaling in Glioblastoma. *Neurochemical Research*, *42*(3), 918–924.

Majuelos-Melguizo, J., Rodríguez, M. I., López-Jiménez, L., Rodríguez-Vargas, J. M., Martí Martín-Consuegra, J. M., Serrano-Sáenz, S., ... Javier Oliver, F. (2015). PARP targeting counteracts gliomagenesis through induction of mitotic catastrophe and aggravation of deficiency in homologous recombination in PTEN-mutant glioma. *Oncotarget*, *6*(7), 4790–4803.

Malanga, M. & Althaus, F. R. (2005). The role of poly(ADP-ribose) in the DNA damage signaling network. *Biochemistry and Cell Biology*, *83*(3), 354–364.

Maldi, E., Travelli, C., Caldarelli, A., Agazzone, N., Cintura, S., Galli, U., ... Genazzani, A. A. (2013). Nicotinamide phosphoribosyltransferase (NAMPT) is over-expressed in melanoma lesions. *Pigment Cell and Melanoma Research*, *26*(1), 144–146.

Mao, Z., Hine, C., Tian, X., Van Meter, M., Au, M., Vaidya, A., ... Gorbunova, V. (2011). SIRT6 promotes DNA repair under stress by activating PARP1. *Science*, *332*(6036), 1443–1446.

Martinsson, P., De la Torre, M., Binderup, L., Nygren, P., & Larsson, R. (2001a). Cell death with atypical features induced by the novel antitumoral drug CHS 828, in human U-937 GTB cells. *European Journal of Pharmacology*, *417*(3), 181–187.

Martinsson, P., Ekelund, S., Nygren, P., & Larsson, R. (2002). The combination of the antitumoural pyridyl cyanoguanidine CHS 828 and etoposide in vitro-from cytotoxic synergy to complete inhibition of apoptosis. *British Journal of Pharmacology*, *137*(4), 568–573.

Martinsson, P., Liminga, G., Dhar, S., De la Torre, M., Lukinius, A., Jonsson, E., ... Larsson, R. (2001b). Temporal effects of the novel antitumour pyridyl cyanoguanidine (CHS 828) on human lymphoma cells. *European Journal of Cancer*, *37*(2), 260–267.

Masui, K., Tanaka, K., Akhavan, D., Babic, I., Gini, B., Matsutani, T., ... Mischel, P. S. (2013). MTOR complex 2 controls glycolytic metabolism in glioblastoma through FoxO acetylation and upregulation of c-Myc. *Cell Metabolism*, *18*(5), 726–739.

Mateo, J., Ganji, G., Lemech, C., Burris, H. A., Han, S. W., Swales, K., ... Arkenau, H. T. (2017). A first-time-in-human study of GSK2636771, a phosphoinositide 3 kinase beta-selective inhibitor, in patients with advanced solid tumors. *Clinical Cancer Research*, *23*(19), 5981–5992.

Mathias, R. A., Greco, T. M., Oberstein, A., Budayeva, H. G., Chakrabarti, R., Rowland, E. A., ... Cristea, I. M. (2014). Sirtuin 4 is a lipoamidase regulating pyruvate dehydrogenase complex activity. *Cell*, *159*(7), 1615–1625.

Matoba, S., Kang, J., Patino, W., Wragg, A., Boehm, M., Gavrilova, O., ... Hwang, P. (2006). p53 Regulates Mitochondrial Respiration. *Science*, *312*(5780), 1650–1653.

McKean-Cowdin, R., Barnholtz-Sloan, J., Inskip, P. D., Ruder, A. M., Butler, M., Rajaraman, P., ... Wrensch, M. (2009). Associations between polymorphisms in DNA repair genes and glioblastoma. *Cancer Epidemiology Biomarkers and Prevention*, *18*(4), 1118–1126.

Mei, Z., Zhang, X., Yi, J., Huang, J., He, J., & Tao, Y. (2016). Sirtuins in metabolism, DNA repair and cancer. *Journal of Experimental & Clinical Cancer Research*, *35*(1), 1–14.

Menendez, J. A. & Lupu, R. (2017). Fatty acid synthase (FASN) as a therapeutic target in breast cancer. *Expert Opinion on Therapeutic Patents*, *21*(11), 1001–1016.

Menssen, a., Hydbring, P., Kapelle, K., Vervoorts, J., Diebold, J., Luscher, B., ... Hermeking, H. (2012). The c-MYC oncoprotein, the NAMPT enzyme, the SIRT1-inhibitor DBC1, and the SIRT1 deacetylase form a positive feedback loop. *Proceedings of the National Academy of Sciences of the United States of America*, *109*(4), 187–196.

Michelakis, E. D., Sutendra, G., Dromparis, P., Webster, L., Haromy, A., Niven, E., ... Petruk, K. C. (2010). Metabolic Modulation of Glioblastoma with Dichloroacetate. *Science Translational Medicine*, *2*(31), 1–9.

Migita, T., Okabe, S., Ikeda, K., Igarashi, S., Sugawara, S., Tomida, A., ... Seimiya, H. (2013). Inhibition of ATP citrate lyase induces an anticancer effect via reactive oxygen species: AMPK as a predictive biomarker for therapeutic impact. *American Journal of Pathology*, *182*(5), 1800–1810.

Mihaylova, M. M. & Shaw, R. J. (2011). The AMPK signalling pathway coordinates cell growth, autophagy and metabolism. *Nature Cell Biology*, *13*(9), 1016–1023.

Miller, D. R. (2006). A tribute to Sidney Farber - The father of modern chemotherapy. *British Journal of Haematology*, *134*(1), 20–26.

Minor, R. K., Smith, D. L., Sossong, A. M., Kaushik, S., Poosala, S., Spangler, E. L., ... Mattison, J. A. (2010). Chronic ingestion of 2-deoxy-d-glucose induces cardiac vacuolization and increases mortality in rats. *Toxicology and Applied Pharmacology*, *243*(3), 332–339.

Mitxelena, J., Apraiz, A., Vallejo-Rodriguez, J., Malumbres, M., & Zubiaga, A. M. (2016). E2F7 regulates transcription and maturation of multiple microRNAs to restrain cell proliferation. *Nucleic Acids Research*, *44*(12), 5557–5570.

Miyazaki, T., Moritake, K., Yamada, K., Hara, N., Osago, H., Shibata, T., ... Tsuchiya, M. (2009). Indoleamine 2,3-dioxygenase as a new target for malignant glioma therapy. Laboratory investigation. *Journal of Neurosurgery*, *111*(2), 230–7.

Mohammad, R. M., Li, Y., Muqbil, I., Aboukameel, A., Senapedis, W., Baloglu, E., ... Azmi, A. S. (2017). Targeting Rho GTPase effector p21 activated kinase 4 (PAK4) suppresses p-Bad-microRNA drug resistance axis leading to inhibition of pancreatic ductal adenocarcinoma proliferation. *Small GTPases*, *0*(0), 1–11.

Mohanti, B. K., Rath, G. K., Anantha, N., Kannan, V., Das, B. S., Chandramouli, B. A., ... Jain, V. (1996). Improving cancer radiotherapy with 2-deoxy-d-glucose: phase I/II clinical trials on human cerebral gliomas. *International Journal of Radiation Oncology Biology Physics*, *35*(1), 103–111.

Mojas, N., Lopes, M., & Jiricny, J. (2007). Mismatch repair-dependent processing of methylation damage gives rise to persistent single-stranded gaps in newly replicated DNA. *Genes & Development*, *21*(24), 3342–3355.

Momcilovic, M. & Shackelford, D. B. (2015). Targeting LKB1 in cancer – exposing and exploiting vulnerabilities. *British Journal of Cancer*, *113*(4), 574–584.

Momeny, M., Moghaddaskho, F., Gortany, N. K., Yousefi, H., Sabourinejad, Z., Zarrinrad, G., ... Ghaffari, S. H. (2017). Blockade of vascular endothelial growth factor receptors by tivozanib has potential anti-tumour effects on human glioblastoma cells. *Scientific Reports*, *7*(44075), 1–12.

Montes de Oca, R., Gurard-Levin, Z. A., Berger, F., Rehman, H., Martel, E., Corpet, A., ... Almouzni, G. (2015). The histone chaperone HJURP is a new independent prognostic marker for luminal A breast carcinoma. *Molecular Oncology*, *9*(3), 657–674.

Montraveta, A., Xargay-Torrent, S., López-Guerra, M., Rosich, L., Pérez-Galán, P., Salaverria, I., ... Colomer, D. (2014). Synergistic anti-tumor activity of acadesine (AICAR) in combination with the anti-CD20 monoclonal antibody rituximab in in vivo and in vitro models of mantle cell lymphoma. *Oncotarget*, *5*(3), 726–39.

Moore, Z., Chakrabarti, G., Luo, X., Ali, A., Hu, Z., Fattah, F. J., ... Boothman, D. A. (2015). NAMPT inhibition sensitizes pancreatic adenocarcinoma cells to tumor-selective, PAR-independent metabolic catastrophe and cell death induced by β-lapachone. *Cell Death and Disease*, *6*(e1599).

Morales, J. C., Li, L., Fattah, F. J., Dong, Y., Bey, E. A., Patel, M., ... Boothman, D. A. (2014). Review of Poly (ADP-ribose) Polymerase (PARP) Mechanisms of Action and Rationale for Targeting in Cancer and Other Diseases. *Critical Reviews in Eukaryotic Gene Expression*, *24*(1), 15–28.

Morgan, R., Plowright, L., Harrington, K. J., Michael, A., & Pandha, H. S. (2010). Targeting HOX and PBX transcription factors in ovarian cancer. *BMC Cancer*, *10*(89), 1–9.

Morgillo, F., Della Corte, C. M., Diana, A., di Mauro, C., Ciaramella, V., Barra, G., ... Orditura, M. (2017). Phosphatidylinositol 3-kinase (PI3Kalpha)/AKT axis blockade with taselisib or ipatasertib enhances the efficacy of anti-microtubule drugs in human breast cancer cells. *Oncotarget*, *8*(44), 76479–76491.

Morrish, F., Isern, N., Sadilek, M., Jeffrey, M., & Hockenbery, D. M. (2009). C-Myc activates multiple metabolic networks to generate substrates for cell-cycle entry. *Oncogene*, *28*(27), 2485–2491.

Munoz, J. L., Walker, N. D., Scotto, K. W., & Rameshwar, P. (2015). Temozolomide competes for P-glycoprotein and contributes to chemoresistance in glioblastoma cells. *Cancer Letters*, *367*(1), 69–75.

Murnyák, B., Kouhsari, M. C., Hershkovitch, R., Kálmán, B., Marko-Varga, G., Klekner, Á., & Hortobágyi, T. (2017). PARP1 expression and its correlation with survival is tumour molecular subtype dependent in glioblastoma. *Oncotarget*, *8*(28), 46348–46362.

Muruganandham, M., Alfieri, A. A., Matei, C., Chen, Y., Sukenick, G., Schemainda, I., ... Koutcher, J. A. (2005). Metabolic Signatures Associated with a NAD Synthesis Inhibitor - Induced T umor Apoptosis Identified by 1 H-Decoupled- 31 P Magnetic Resonance Spectroscopy. *Cancer Therapy: Preclinical*, *11*(9), 3503–3513.

Nahimana, A., Attinger, A., Aubry, D., Greaney, P., Ireson, C., Thougaard, A. V., ... Duchosal, M. a. (2009). The NAD biosynthesis inhibitor APO866 has potent antitumor activity against hematologic malignancies The NAD biosynthesis inhibitor APO866 has potent antitumor activity against hematologic malignancies. *Blood*, *113*(14), 3276–3286.

Nakagawa, T., Lomb, D. J., Haigis, M. C., & Guarente, L. (2009). SIRT5 Deacetylates Carbamoyl Phosphate Synthetase 1 and Regulates the Urea Cycle. *Cell*, *137*(3), 560–570.

Narayan, R. S., Fedrigo, C. A., Brands, E., Dik, R., Stalpers, L. J., Baumert, B. G., ... Sminia, P. (2017). The allosteric AKT inhibitor MK2206 shows a synergistic interaction with chemotherapy and radiotherapy in glioblastoma spheroid cultures. *BMC Cancer*, *17*(204), 1–8.

Narita, Y., Nagane, M., Mishima, K., Huang, H. J., Furnari, F. B., & Cavenee, W. K. (2002). Mutant epidermal growth factor receptor signaling down-regulates p27 through activation of the phosphatidylinositol 3-kinase/Akt pathway in glioblastomas. *Cancer Research*, *62*(22), 6764–6769.

NCBI. (2018). PubMed.

Nemoto, S., Fergusson, M. M., & Finkel, T. (2005). SIRT1 functionally interacts with the metabolic regulator and transcriptional coactivator PGC-1α. *Journal of Biological Chemistry*, *280*(16), 16456–16460.

Netland, I. A., Førde, H. E., Sleire, L., Leiss, L., Rahman, M. A., Skeie, B. S., ... Goplen, D. (2016). Dactolisib (NVP-BEZ235) toxicity in murine brain tumour models. *BMC Cancer*, *16*(657), 1–12.

Neubauer, K., Bednarz Misa, I., Diakowska, D., Kapturkiewicz, B., Gamian, A., & Krzystek-Korpacka, M. (2015). Nampt/PBEF/visfatin upregulation in colorectal tumors, mirrored in normal tissue and whole blood of colorectal cancer patients, is associated with metastasis, hypoxia, IL1 β, and anemia. *BioMed Research International*, *2015*(523930), 1–12.

Nevedomskaya, E., Perryman, R., Solanki, S., Syed, N., Mayboroda, O. A., & Keun, H. C. (2016). A Systems Oncology Approach Identifies NT5E as a Key Metabolic Regulator in Tumor Cells and Modulator of Platinum Sensitivity. *Journal of Proteome Research*, *15*(1), 280–290.

Newlands, E. S., Stevens, M. F., Wedge, S. R., Wheelhouse, R. T., & Brock, C. (1997). Temozolomide: A review of its discovery, chemical properties, pre-clinical development and clinical trials. *Cancer Treatment Reviews*, *23*(1), 35–61.

Nikiforov, A., Dölle, C., Niere, M., & Ziegler, M. (2011). Pathways and subcellular compartmentation of NAD biosynthesis in human cells: from entry of extracellular precursors to mitochondrial NAD generation. *The Journal of Biological Chemistry*, *286*(24), 21767–78.

Nikiforov, A., Kulikova, V., & Ziegler, M. (2015). The human NAD metabolome: Functions, metabolism and compartmentalization. *Critical Reviews in Biochemistry and Molecular Biology*, *50*(4), 284–297.

Nishida, Y., Rardin, M. J., Carrico, C., He, W., Sahu, A. K., Gut, P., ... Verdin, E. (2015). SIRT5 Regulates both Cytosolic and Mitochondrial Protein Malonylation with Glycolysis as a Major Target. *Molecular Cell*, *59*(2), 321–332.

Nitta, M., Kozono, D., Kennedy, R., Stommel, J., Ng, K., Zinn, P. O., ... Chen, C. C. (2010). Targeting EGFR induced oxidative stress by PARP1 inhibition in glioblastoma therapy. *PLOS One*, *5*(5), 1–9.

Novellasdemunt, L., Tato, I., Navarro-Sabate, A., Ruiz-Meana, M., Méndez-Lucas, A., Perales, J. C., ... Luis Rosa, J. (2013). Akt-dependent activation of the heart 6-phosphofructo-2-kinase/fructose-2, 6-bisphosphatase (PFKFB2) isoenzyme by amino acids. *Journal of Biological Chemistry*, *288*(15), 10640–10651.

Nozaki, M., Tada, M., Kobayashi, H., Zhang, C. L., Sawamura, Y., Abe, H., ... Van Meir, E. G. (1999). Roles of the functional loss of p53 and other genes in astrocytoma tumorigenesis and progression. *Neuro-Oncology*, *1*(2), 124–137.

O'Brien, T., Oeh, J., Xiao, Y., Liang, X., Vanderbilt, A., Qin, A., ... Sampath, D. (2013). Supplementation of nicotinic acid with NAMPT inhibitors results in loss of in vivo efficacy in NAPRT1-deficient tumor models. *Neoplasia*, *15*(12), 1314–1329.

Oh, H., Kwak, J. S., Yang, S., Gong, M. K., Kim, J. H., Rhee, J., ... Chun, J. S. (2015). Reciprocal regulation by hypoxia-inducible factor-2α and the NAMPT-NAD+-SIRT axis in articular chondrocytes is involved in osteoarthritis. *Osteoarthritis and Cartilage*, *23*(12), 2288–2296.

Ohmoto, A. & Yachida, S. (2017). Current status of poly(ADP-ribose) polymerase inhibitors and future directions. *OncoTargets and Therapy*, *10*, 5195–5208.

Oizel, K., Chauvin, C., Oliver, L., Gratas, C., Geraldo, F., Jarry, U., ... Pecqueur, C. (2017). Efficient mitochondrial glutamine targeting prevails over glioblastoma metabolic plasticity. *Clinical Cancer Research*, *23*(20), 6292–6305.

Okumura, S., Sasaki, T., Minami, Y., & Ohsaki, Y. (2012). Nicotinamide phosphoribosyltransferase: A potent therapeutic target in non-small cell lung cancer with epidermal growth factor receptor-gene mutation. *Journal of Thoracic Oncology*, *7*(1), 49–56.

Okuyama, H., Endo, H., Akashika, T., Kato, K., & Inoue, M. (2010). Downregulation of c-MYC protein levels contributes to cancer cell survival under dual deficiency of oxygen and glucose. *Cancer Research*, *70*(24), 10213–10223.

Olesen, U. H., Christensen, M. K., Björkling, F., Jäättelä, M., Jensen, P. B., Sehested, M., & Nielsen, S. J. (2008). Anticancer agent CHS-828 inhibits cellular synthesis of NAD. *Biochemical and Biophysical Research Communications*, *367*(4), 799–804.

Olesen, U. H., Hastrup, N., & Sehested, M. (2011). Expression patterns of nicotinamide phosphoribosyltransferase and nicotinic acid phosphoribosyltransferase in human malignant lymphomas. *APMIS*, *119*(4-5), 296–303.

Olesen, U. H., Petersen, J. G., Garten, A., Kiess, W., Yoshino, J., Imai, S. I., ... Sehested, M. (2010a). Target enzyme mutations are the molecular basis for resistance towards pharmacological inhibition of nicotinamide phosphoribosyltransferase. *BMC Cancer*, *10*(677), 1–13.

Olesen, U. H., Thougaard, A. V., Jensen, P. B., & Sehested, M. (2010b). A Preclinical Study on the Rescue of Normal Tissue by Nicotinic Acid in High-Dose Treatment with APO866, a Specific Nicotinamide Phosphoribosyltransferase Inhibitor. *Molecular Cancer Therapeutics*, *9*(6), 1609–1617.

Olsen, L. S., Hjarnaa, P. J. V., Latini, S., Holm, P. K., Larsson, R., Bramm, E., ... Madsen, M. W. (2004). Anticancer agent CHS 828 suppresses nuclear factor-κB activity in cancer cells through downregulation of IKK activity. *International Journal of Cancer*, *111*(2), 198–205.

Olson, R. E. (1951). Carbohydrate Oxidation of C14-labeled Carbohydrate Intermediates in Tumor and Normal Tissue. *Cancer Research*, *11*(8), 571–584.

Opel, D., Westhoff, M. A., Bender, A., Braun, V., Debatin, K. M., & Fulda, S. (2008). Phosphatidylinositol 3-kinase inhibition broadly sensitizes glioblastoma cells to death receptor- and drug-induced apoptosis. *Cancer Research*, *68*(15), 6271–6280.

Osthus, R. C., Shim, H., Kim, S., Li, Q., Reddy, R., Mukherjee, M., ... Dang, C. V. (2000). Deregulation of glucose transporter 1 and glycolytic gene expression by c-Myc. *Journal of Biological Chemistry*, *275*(29), 21797–21800.

Ostrom, Q. T., Bauchet, L., Davis, F. G., Deltour, I., Fisher, J. L., Langer, C. E., ... Barnholtz-Sloan, J. S. (2014). The epidemiology of glioma in adults: A state of the science review. *Neuro-Oncology*, *16*(7), 896–913.

Osuka, S. & Meir, E. G. V. (2017). Overcoming therapeutic resistance in glioblastoma : the way forward. *The Journal of Clinical Investigation*, *127*(2), 415–426.

Ott, M., Litzenburger, U. M., Rauschenbach, K. J., Bunse, L., Ochs, K., Sahm, F., ... Platten, M. (2015). Suppression of TDO-mediated tryptophan catabolism in glioblastoma cells by a steroid-responsive FKBP52-dependent pathway. *Glia*, *63*(1), 78–90.

Ott, P. A., Carvajal, R. D., Pandit-Taskar, N., Jungbluth, A. A., Hoffman, E. W., Wu, B. W., ... Wolchok, J. D. (2013). Phase I/II study of pegylated arginine deiminase (ADI-PEG 20) in patients with advanced melanoma. *Investigational New Drugs*, *31*(2), 425–434.

Oudard, S., Arvelo, F., Miccoli, L., Apiou, F., Dutrillaux, A. M., Poisson, M., ... Poupon, M. F. (1996). High glycolysis in gliomas despite low hexokinase transcription and activity correlated to chromosome 10 loss. *British Journal of Cancer*, *74*(6), 839–845.

Pan, Y., Rhea, P., Tan, L., Cartwright, C., Lee, H. J., Ravoori, M. K., ... Yang, P. (2015). PBI-05204, a supercritical CO2 extract of Nerium oleander, inhibits growth of human pancreatic cancer via targeting the PI3K/mTOR pathway. *Investigational New Drugs*, *33*(2), 271–279.

Panagiotis Zalmas, L., Zhao, X., Graham, A. L., Fisher, R., Reilly, C., Coutts, A. S., & La Thangue, N. B. (2008). DNA-damage response control of E2F7 and E2F8. *EMBO Reports*, *9*(3), 252–259.

Panosyan, E. H., Wang, Y., Xia, P., Lee, W.-N. P., Pak, Y., Laks, D. R., ... Lasky, J. L. (2014). Asparagine Depletion Potentiates the Cytotoxic Effect of Chemotherapy against Brain Tumors. *Molecular Cancer Research*, *12*(5), 694–702.

Park, H.-J., Kim, S.-R., Kim, S. S., Wee, H.-J., Bae, M.-K., Ryu, M. H., & Bae, S.-K. (2014). Visfatin promotes cell and tumor growth by upregulating Notch1 in breast cancer. *Oncotarget*, *5*(13), 5087–5099.

Park, J., Chen, Y., Tishkoff, D. X., Peng, C., Tan, M., Dai, L., ... Zhao, Y. (2013). SIRT5-Mediated Lysine Desuccinylation Impacts Diverse Metabolic Pathways. *Molecular Cell*, *50*(6), 919–930.

Patel, M. A., Kim, J. E., Ruzevick, J., Li, G., & Lim, M. (2014). The future of glioblastoma therapy: synergism of standard of care and immunotherapy. *Cancers*, *6*(4), 1953–85.

Patel, S. T., Mistry, T., Brown, J. E., Digby, J. E., Adya, R., Desai, K. M., & Randeva, H. S. (2010). A novel role for the adipokine visfatin/pre-B cell colony-enhancing factor 1 in prostate carcinogenesis. *Peptides*, *31*(1), 51–57.

Paul, I., Bhattacharya, S., Chatterjee, A., & Ghosh, M. K. (2013). Current Understanding on EGFR and Wnt/β-Catenin Signaling in Glioma and Their Possible Crosstalk. *Genes and Cancer*, *4*(11-12), 427–446.

Pavlyk, I., Rzhepetskyy, Y., Jagielski, A. K., Drozak, J., Wasik, A., Pereverzieva, G., ... Redowicz, M. J. (2015). Arginine deprivation affects glioblastoma cell adhesion, invasiveness and actin cytoskeleton organization by impairment of β-actin arginylation. *Amino Acids*, *47*(1), 199–212.

Paz, M. F., Yaya-tur, R., Rojas-marcos, I., Reynes, G., Pollan, M., Aguirre-cruz, L., ... Garcı, M. (2004). CpG Island Hypermethylation of the DNA Repair Enzyme Methyltransferase Predicts Response to Temozolomide in Primary Gliomas CpG Island Hypermethylation of the DNA Repair Enzyme Methyltransferase Predicts Response to Temozolomide in Primary Gliomas. *Clinical Cancer Research*, *10*, 4933–4938.

Peck, B., Ferber, E. C., & Schulze, A. (2013). Antagonism between FOXO and MYC Regulates Cellular Powerhouse. *Frontiers in Oncology*, *3*(96), 1–6.

Perbellini, F., Liu, A. K., Watson, S. A., Bardi, I., Rothery, S. M., & Terracciano, C. M. (2017). Free-of-Acrylamide SDS-based Tissue Clearing (FASTClear) for three dimensional visualization of myocardial tissue. *Scientific Reports*, *7*(5188), 1–9.

Peterse, E., Van Den Akker, B., Niessen, B., Oosting, J., Suijker, J., De Jong, Y., ... Bovée, J. (2017). NAD Synthesis Pathway Interference Is a Viable Therapeutic Strategy for Chondrosarcoma. *Molecular Cancer Research*, *15*(12), 1714–1721.

Pezuk, J. A., Brassesco, M. S., Morales, A. G., De Oliveira, J. C., De Paula Queiroz, R. G., MacHado, H. R., ... Tone, L. G. (2013a). Polo-like kinase 1 inhibition causes decreased proliferation by cell cycle arrest, leading to cell death in glioblastoma. *Cancer Gene Therapy*, *20*(9), 499–506.

Pezuk, J. A., Brassesco, M. S., Morales, A. G., de Oliveira, J. C., de Oliveira, H. F., Scrideli, C. A., & Tone, L. G. (2013b). Inhibition of Polo-Like Kinase 1 Induces Cell Cycle Arrest and Sensitizes Glioblastoma Cells to Ionizing Radiation. *Cancer Biotherapy & Radiopharmaceuticals*, *28*(7), 516–522.

Piacente, F., Caffa, I., Ravera, S., Sociali, G., Passalacqua, M., Vellone, V. G., ... Nencioni, A. (2017). Nicotinic acid phosphoribosyltransferase regulates cancer cell metabolism, susceptibility to NAMPT inhibitors, and DNA repair. *Cancer Research*, *77*(14), 3857–3869.

Pittelli, M., Formentini, L., Faraco, G., Lapucci, A., Rapizzi, E., Cialdai, F., ... Chiarugi, A. (2010). Inhibition of nicotinamide phosphoribosyltransferase: Cellular bioenergetics reveals a mitochondrial insensitive NAD pool. *Journal of Biological Chemistry*, *285*(44), 34106–34114.

Pitz, M. W., Eisenhauer, E. A., MacNeil, M. V., Thiessen, B., Easaw, J. C., Macdonald, D. R., ... Mason, W. P. (2015). Phase II study of PX-866 in recurrent glioblastoma. *Neuro-Oncology*, *17*(9), 1270–1274.

Pogrebniak, A., Schemainda, I., Azzam, K., Pelka Fleischer, R., Nüssler, V., & Hasmann, M. (2006). Chemopotentiating effects of a novel NAD biosynthesis inhibitor, FK866, in combination with antineoplastic agents. *European Journal of Medical Research*, *11*(8), 313–321.

Pore, N., Jiang, Z., Shu, H. K., Bernhard, E., Kao, G. D., & Maity, A. (2006). Akt1 Activation Can Augment Hypoxia-Inducible Factor-1a Expression by Increasing Protein Translation through a Mammalian Target of Rapamycin–Independent Pathway. *Molecular Cancer Research*, *4*(7), 471–479.

Porta, C., Paglino, C., & Mosca, A. (2014). Targeting PI3K/Akt/mTOR Signaling in Cancer. *Frontiers in Oncology*, *4*(64), 1–11.

Pyko, I. V., Nakada, M., Sabit, H., Teng, L., Furuyama, N., Hayashi, Y., ... ichiro Hamada, J. (2013). Glycogen synthase kinase 3β inhibition sensitizes human glioblastoma cells to temozolomide by affecting O6-methylguanine DNA methyltransferase promoter methylation via c-Myc signaling. *Carcinogenesis*, *34*(10), 2206–2217.

Pyrko, P., Schöntha, A. H., Hofman, F. M., Chen, T. C., & Lee, A. S. (2007). The unfolded protein response regulator GRP78/BiP as a novel target for increasing chemosensitivity in malignant gliomas. *Cancer Research*, *67*(20), 9809–9816.

Qi, L. S., Larson, M. H., Gilbert, L. A., Doudna, J. A., Weissman, J. S., Arkin, A. P., & Lim, W. A. (2013). Repurposing CRISPR as an RNA-γuided platform for sequence-specific control of gene expression. *Cell*, *152*(5), 1173–1183.

Qian, T., Zhang, B., Qian, C., He, Y., & Li, Y. (2017). Association between common polymorphisms in ERCC gene and glioma risk. *Medicine*, *96*(20), 1–10.

Qu, Y., Zhang, J., Wu, S., Li, B., Liu, S., & Cheng, J. (2012). SIRT1 promotes proliferation and inhibits apoptosis of human malignant glioma cell lines. *Neuroscience Letters*, *525*(2), 168–172.

Quan, J. J., Song, J. N., & Qu, J. Q. (2015). PARP3 interacts with FoxM1 to confer glioblastoma cell radioresistance. *Tumor Biology*, *36*(11), 8617–8624.

Quezada, C., Garrido, W., Oyarzún, C., Fernández, K., Segura, R., Melo, R., ... San Martín, R. (2013). 5'-Ectonucleotidase Mediates Multiple-Drug Resistance in Glioblastoma Multiforme Cells. *Journal of Cellular Physiology*, *228*(3), 602–8.

Ramezani, S., Vousooghi, N., Ramezani Kapourchali, F., & Joghataei, M. T. (2017). Perifosine enhances bevacizumab-induced apoptosis and therapeutic efficacy by targeting PI3K/AKT pathway in a glioblastoma heterotopic model. *Apoptosis*, *22*(8), 1025–1034.

Ramjaun, A. R., Tomlinson, S., Eddaoudi, A., & Downward, J. (2007). Upregulation of two BH3-only proteins, Bmf and Bim, during TGFβ-induced apoptosis. *Oncogene*, *26*(7), 970–981.

Rane, C., Senapedis, W., Baloglu, E., Landesman, Y., Crochiere, M., Das-Gupta, S., & Minden, A. (2017). A novel orally bioavailable compound KPT-9274 inhibits PAK4, and blocks triple negative breast cancer tumor growth. *Scientific Reports*, *7*(42555), 1–12.

Ranson, M., Hersey, P., Thompson, D., Beith, J., McArthur, G. A., Haydon, A., ... Middleton, M. R. (2007). Randomized trial of the combination of lomeguatrib and temozolomide compared with temozolomide alone in chemotherapy naive patients with metastatic cutaneous melanoma. *Journal of Clinical Oncology*, *25*(18), 2540–2545.

Ranson, M., Middleton, M. R., Bridgewater, J., Lee, S. M., Dawson, M., Jowle, D., ... Margison, G. P. (2006). Lomeguatrib, a potent inhibitor of O6-alkylguanine-DNA- alkyltransferase: Phase I safety, pharmacodynamic, and pharmacokinetic trial and evaluation in combination with temozolomide in patients with advanced solid tumors. *Clinical Cancer Research*, *12*(5), 1577–1584.

Ratajczak, J., Joffraud, M., Trammell, S. A., Ras, R., Canela, N., Boutant, M., ... Cantó, C. (2016). NRK1 controls nicotinamide mononucleotide and nicotinamide riboside metabolism in mammalian cells. *Nature Communications*, *7*(13103), 1–12.

Ravaud, A., Cerny, T., Terret, C., Wanders, J., Bui, B. N., Hess, D., ... Twelves, C. (2005). Phase I study and pharmacokinetic of CHS-828, a guanidino-containing compound, administered orally as a single dose every 3 weeks in solid tumours: An ECSG/EORTC study. *European Journal of Cancer*, *41*(5), 702–707.

Reddy, P. S., Umesh, S., Thota, B., Tandon, A., Pandey, P., Hegde, A. S., ... Somasundaram, K. (2008). PBEF1/NAmPRTase/Visfatin: A potential malignant astrocytoma/glioblastoma serum marker with prognostic value. *Cancer Biology & Therapy*, *7*(5), 663–668.

Reitman, Z. J., Duncan, C. G., Poteet, E., Winters, A., Yan, L. J., Gooden, D. M., ... Yan, H. (2014). Cancer-Associated isocitrate dehydrogenase 1 (IDH1) R132H mutation and D-2-hydroxyglutarate stimulate glutamine metabolism under hypoxia. *Journal of Biological Chemistry*, *289*(34), 23318–23328.

Rich, M. A., Bolaffi, J. L., Knoll, J. E., CHeong, L., & Eidinoff, M. L. (1958). Growth Inhibition of a Human Tumor Cell Strain by 5-Fluorouracil, 5-Fluorouridine, and 5-Fluoro-2-deoxyuridine - Reversal Studies. *Cancer Research*, *18*(6), 730–735.

Ríos, M., Foretz, M., Viollet, B., Prieto, A., Fraga, M., García-Caballero, T., ... Señarís, R. (2014). Lipoprotein internalisation induced by oncogenic AMPK activation is essential to maintain glioblastoma cell growth. *European Journal of Cancer*, *50*(18), 3187–3197.

Rivlin, N., Brosh, R., Oren, M., & Rotter, V. (2011). Mutations in the p53 tumor suppressor gene: Important milestones at the various steps of tumorigenesis. *Genes and Cancer*, *2*(4), 466–474.

Robles Irizarry, L., Hambardzumyan, D., Nakano, I., Gladson, C. L., & Ahluwalia, M. S. (2012). Therapeutic targeting of VEGF in the treatment of glioblastoma. *Expert Opinion on Therapeutic Targets*, *16*(10), 973–984.

Rocha, C. R. R., Kajitani, G. S., Quinet, A., Fortunato, R. S., Menck, C. F. M., Ribeiro Reily Rocha, C., ... Frederico Martins Menck, C. (2016). NRF2 and glutathione are key resistance mediators to temozolomide in glioma and melanoma cells. *Oncotarget*, *7*(30), 48081–48092.

Rodriguez-Lopez, J., Pombo-Suarez, M., Loughlin, J., Tsezou, A., Blanco, F. J., Meulenbelt, I., ... Gonzalez, A. (2009). Association of a nsSNP in ADAMTS14 to some osteoarthritis phenotypes. *Osteoarthritis and Cartilage*, *17*(3), 321–327.

Röhrig, F. & Schulze, A. (2016). The multifaceted roles of fatty acid synthesis in cancer. *Nature Reviews Cancer*, *16*(11), 732–749.

Rouleau, M., McDonald, D., Gagné, P., Ouellet, M. E., Droit, A., Hunter, J. M., ... Poirier, G. G. (2007). PARP-3 associates with polycomb group bodies and with components of the DNA damage repair machinery. *Journal of Cellular Biochemistry*, *100*(2), 385–401.

Royal Society of Chemistry. (2018). ChemSpider.

Royce, M. E. & Osman, D. (2015). Everolimus in the treatment of metastatic breast cancer. *Breast Cancer: Basic and Clinical Research*, *9*, 73–79.

Ruano, Y., Ribalta, T., De Lope, Á. R., Campos-Martín, Y., Piaño, C., Pérez-Magán, E., ... Meléndez, B. (2009). Worse outcome in primary Glioblastoma multiforme with concurrent epidermal growth factor receptor and p53 alteration. *American Journal of Clinical Pathology*, *131*(2), 257–263.

Ruiz, I. M. (2014). PARP inhibitors and temozolomide in brain tumours.

Rulten, S. L., Fisher, A. E., Robert, I., Zuma, M. C., Rouleau, M., Ju, L., ... Caldecott, K. W. (2011). PARP-3 and APLF function together to accelerate nonhomologous end-joining. *Molecular Cell*, *41*(1), 33–45.

Rydström, J. (2006). Mitochondrial NADPH, transhydrogenase and disease. *Biochimica et Biophysica Acta - Bioenergetics*, *1757*(5-6), 721–726.

Sahm, F., Oezen, I., Opitz, C. A., Radlwimmer, B., Von Deimling, A., Ahrendt, T., ... Platten, M. (2013). The endogenous tryptophan metabolite and NAD+ precursor quinolinic acid confers resistance of gliomas to oxidative stress. *Cancer Research*, *73*(11), 3225–3234.

Sala, A., Nicolaides, N. C., Engelhard, A., Bellon, T., Lawe, D. C., Arnold, A., ... Calabretta, B. (1994). Correlation between E2F-1 Requirement in the S Phase and E2F-1 Transactivation of Cell Cycle-related Genes in Human Cells. *Cancer Research*, *54*(6), 1402–1406.

Salamanca-Cardona, L., Shah, H., Poot, A. J., Correa, F. M., Di Gialleonardo, V., Lui, H., ... Keshari, K. R. (2017). In Vivo Imaging of Glutamine Metabolism to the Oncometabolite 2-Hydroxyglutarate in IDH1/2 Mutant Tumors. *Cell Metabolism*, *26*(6), 830–841.

Salazar-Ramiro, A., Ramírez-Ortega, D., de La Cruz, V. P., Hérnandez-Pedro, N. Y., González-Esquivel, D. F., Sotelo, J., & Pineda, B. (2016). Role of redox status in development of Glioblastoma. *Frontiers in Immunology*, *7*(156), 1–15.

Salphati, L., Heffron, T. P., Alicke, B., Nishimura, M., Barck, K., Carano, R. A., ... Phillips, H. S. (2012). Targeting the PI3K pathway in the brain - Efficacy of a PI3K inhibitor optimized to cross the blood-brain barrier. *Clinical Cancer Research*, *18*(22), 6239–6248.

Sami, A. & Karsy, M. (2013). Targeting the PI3K/AKT/mTOR signaling pathway in glioblastoma: Novel therapeutic agents and advances in understanding. *Tumor Biology*, *34*(4), 1991–2002.

Sanai, N., Mirzadeh, Z., & Berger, M. S. (2008). Functional Outcome after Language Mapping for Glioma Resection. *New England Journal of Medicine*, *358*(1), 18–27.

Santidrian, A. F., LeBoeuf, S. E., Wold, E. D., Ritland, M., Forsyth, J. S., & Felding, B. H. (2014). Nicotinamide phosphoribosyltransferase can affect metastatic activity and cell adhesive functions by regulating integrins in breast cancer. *DNA Repair*, *23*, 79–87.

Sanzey, M., Abdul Rahim, S. A., Oudin, A., Dirkse, A., Kaoma, T., Vallar, L., ... Niclou, S. P. (2015). Comprehensive analysis of glycolytic enzymes as therapeutic targets in the treatment of glioblastoma. *PLOS One*, *10*(5), 1–16.

Sasiak, K. & Saunders, P. P. (1996). Purification and properties of a human nicotinamide ribonucleoside kinase. *Archives of Biochemistry and Biophysics*, *333*(2), 414–418.

Sawicka-Gutaj, N., Waligórska-Stachura, J., Andrusiewicz, M., Biczysko, M., Sowiński, J., Skrobisz, J., & Ruchała, M. (2015). Nicotinamide phosphorybosiltransferase overexpression in thyroid malignancies and its correlation with tumor stage and with survivin/survivin DEx3 expression. *Tumor Biology*, *36*(10), 7859–7863.

Saxena, A., Wong, L. H., Kalitsis, P., Earle, E., Shaffer, L. G., & Choo, K. H. A. (2002). Poly(ADP-ribose) polymerase 2 localizes to mammalian active centromeres and interacts with PARP-1, Cenpa, Cenpb and Bub3, but not Cenpc. *Human Molecular Genetics*, *11*(19), 2319–2329.

Schaich, M., Kestel, L., Pfirrmann, M., Robel, K., Illmer, T., Kramer, M., ... Krex, D. (2009). A MDR1 (ABCB1) gene single nucleotide polymorphism predicts outcome of temozolomide treatment in glioblastoma patients. *Annals of Oncology*, *20*(1), 175–181.

Schiff, D., Jaeckle, K. A., Anderson, S. K., Galanis, E., Giannini, C., Buckner, J. C., ... Sarkaria, J. N. (2018). Phase 1/2 trial of temsirolimus and sorafenib in the treatment of patients with recurrent glioblastoma: North Central Cancer Treatment Group Study/Alliance N0572. *Cancer*, *124*(7), 1455–1463.

Schuster, S., Penke, M., Gorski, T., Gebhardt, R., Weiss, T. S., Kiess, W., & Garten, A. (2015). FK866-induced NAMPT inhibition activates AMPK and downregulates mTOR signaling in hepatocarcinoma cells. *Biochemical and Biophysical Research Communications*, *458*(2), 334–340.

Schwartzenberg-Bar-Yoseph, F., Armoni, M., & Karnieli, E. (2004). The Tumor Suppressor p53 Down-Regulates Glucose Transporters GLUT1 and GLUT4 Gene Expression The Tumor Suppressor p53 Down-Regulates Glucose Transporters GLUT1 and GLUT4 Gene Expression. *Cancer Research*, *64*(7), 2627–2633.

Sebastián, C., Zwaans, B. M., Silberman, D. M., Gymrek, M., Goren, A., Zhong, L., ... Mostoslavsky, R. (2012). The histone deacetylase SIRT6 Is a tumor suppressor that controls cancer metabolism. *Cell*, *151*(6), 1185–1199.

Semenza, G. L. (2011). Regulation of metabolism by hypoxia-inducible factor 1. *Cold Spring Harbor Symposia on Quantitative Biology*, *76*, 347–353.

Semenza, G. L., Jiang, B. H., Leung, S. W., Passantino, R., Concordet, J. P., Maire, P., & Giallongo, A. (1996). Hypoxia Response Elements in the Aldolase A, Enolase 1,and Lactate Dehydrogenase A Gene Promoters Contain Essential Binding Sites for Hypoxia-inducible Factor 1. *Journal of Biological Chemistry*, *271*(51), 32529–32537.

Seo, K. S., Park, J. H., Heo, J. Y., Jing, K., Han, J., Min, K. N., ... Kweon, G. R. (2015). SIRT2 regulates tumour hypoxia response by promoting HIF-1α hydroxylation. *Oncogene*, *34*(11), 1354–1362.

Seront, E., Rottey, S., Filleul, B., Glorieux, P., Goeminne, J. C., Verschaeve, V., ... Machiels, J. P. (2016). Phase II study of dual phosphoinositol-3-kinase (PI3K) and mammalian target of rapamycin (mTOR) inhibitor BEZ235 in patients with locally advanced or metastatic transitional cell carcinoma. *BJU International*, *118*(3), 408–415.

Serra, V., Markman, B., Scaltriti, M., Eichhorn, P. J., Valero, V., Guzman, M., ... Baselga, J. (2008). NVP-BEZ235, a dual PI3K/mTOR inhibitor, prevents PI3K signaling and inhibits the growth of cancer cells with activating PI3K mutations. *Cancer Research*, *68*(19), 8022–8030.

Shackelford, R. E., Bui, M. M., Coppola, D., & Hakam, A. (2010). Over-expression of nicotinamide phosphoribosyltransferase in ovarian cancers. *International Journal of Clinical and Experimental Pathology*, *3*(5), 522–527.

Shackelford, R., Hirsh, S., Henry, K., Abdel-Mageed, A., Kandil, E., & Coppola, D. (2013). Nicotinamide phosphoribosyltransferase and SIRT3 expression are increased in well-differentiated thyroid carcinomas. *Anticancer Research*, *33*(8), 3047–3052.

Shahar, T., Rozovski, U., Hess, K. R., Hossain, A., Gumin, J., Gao, F., ... Lang, F. F. (2017). Percentage of mesenchymal stem cells in high-grade glioma tumor samples correlates with patient survival. *Neuro-Oncology*, *19*(5), 660–668.

Shames, D. S., Elkins, K., Walter, K., Holcomb, T., Du, P., Mohl, D., ... Belmont, L. D. (2013). Loss of NAPRT1 expression by tumor-specific promoter methylation provides a novel predictive biomarker for NAMPT inhibitors. *Clinical Cancer Research*, *19*(24), 6912–6923.

Shapiro, W. R., Green, S. B., Burger, P. C., Selker, R. G., VanGilder, J. C., Robertson, J. T., ... Mahaley, M. S. (1992). A randomized comparison of intra-arterial versus intravenous BCNU, with or without intravenous 5-fluorouracil, for newly diagnosed patients with malignant glioma. *Journal of Neurosurgery*, *76*(5), 772–781.

Sharif, T., Ahn, D. G., Liu, R. Z., Pringle, E., Martell, E., Dai, C., ... Lee, P. W. (2016). The NAD+salvage pathway modulates cancer cell viability via p73. *Cell Death and Differentiation*, *23*(4), 669–680.

Shaw, R. J. (2009). LKB1 and AMP-activated protein kinase control of mTOR signalling and growth. *Acta Physiologica*, *196*(1), 65–80.

Shaw, R. J., Kosmatka, M., Bardeesy, N., Hurley, R. L., Witters, L. A., DePinho, R. A., & Cantley, L. C. (2004). The tumor suppressor LKB1 kinase directly activates AMP-activated kinase and regulates apoptosis in response to energy stress. *Proceedings of the National Academy of Sciences of the United States of America*, *101*(10), 3329–3335.

Shen, H., Decollogne, S., Dilda, P. J., Hau, E., Chung, S. A., Luk, P. P., ... McDonald, K. L. (2015a). Dual-targeting of aberrant glucose metabolism in glioblastoma. *Journal of Experimental & Clinical Cancer Research*, *34*(1), 1–11.

Shen, H., Hau, E., Joshi, S., Dilda, P. J., & McDonald, K. L. (2015b). Sensitization of Glioblastoma Cells to Irradiation by Modulating the Glucose Metabolism. *Molecular Cancer Therapeutics*, *14*(8), 1794–804.

Shen, Y., Li, J., Nitta, M., Futalan, D., Steed, T., Treiber, J. M., ... Chen, C. C. (2015c). Orthogonal targeting of EGFRvIII expressing glioblastomas through simultaneous EGFR and PLK1 inhibition. *Oncotarget*, *6*(14), 11751–11767.

Sheu, M. J., Hsieh, M. J., Chou, Y. E., Wang, P. H., Yeh, C. B., Yang, S. F., ... Liu, Y. F. (2017). Effects of ADAMTS14 genetic polymorphism and cigarette smoking on the clinicopathologic development of hepatocellular carcinoma. *PLOS One*, *12*(2), 1–15.

Shi, F., Guo, H., Zhang, R., Liu, H., Wu, L., Wu, Q., ... Zhang, Q. (2017). The PI3K inhibitor GDC-0941 enhances radiosensitization and reduces chemoresistance to temozolomide in GBM cell lines. *Neuroscience*, *346*, 298–308.

Shu, H. K., Julin, C. M., Furman, F., Yount, G. L., Haas-Kogan, D., & Israel, M. a. (2000). Overexpression of E2F1 in glioma-derived cell lines induces a p53-independent apoptosis that is further enhanced by ionizing radiation. *Neuro-Oncology*, *2*(1), 16–21.

Shutt, D. C., O'Dorisio, M. S., Aykin-Burns, N., & Spitz, D. R. (2010). 2-deoxy-D-glucose induces oxidative stress and cell killing in human neuroblastoma cells. *Cancer Biology & Therapy*, *9*(11), 853–861.

Simon-Molas, H., Calvo-Vidal, M. N., Castaño, E., Rodríguez-García, A., Navarro-Sabaté, À., Bartrons, R., & Manzano, A. (2016). Akt mediates TIGAR induction in HeLa cells following PFKFB3 inhibition. *FEBS Letters*, *590*(17), 2915–2926.

Singh, D., Banerji, A. K., Dwarakanath, B. S., Tripathi, R. P., Gupta, J. P., Mathew, T. L., ... Jain, V. (2005). Optimizing cancer radiotherapy with 2-deoxy-D-glucose: Dose escalation studies in patients with glioblastoma multiforme. *Strahlentherapie und Onkologie*, *181*(8), 507–514.

Smolková, K. & Ježek, P. (2012). The role of mitochondrial NADPH-dependent isocitrate dehydrogenase in cancer cells. *International Journal of Cell Biology*, *2012*, 1–12.

Sociali, G., Raffaghello, L., Magnone, M., Zamporlini, F., Emionite, L., Sturla, L., ... Bruzzone, S. (2015). Antitumor effect of combined NAMPT and CD73 inhibition in an ovarian cancer model. *Oncotarget*, *7*(3), 2968–84.

Solaini, G., Sgarbi, G., & Baracca, A. (2011). Oxidative phosphorylation in cancer cells. *Biochimica et Biophysica Acta*, *1807*(6), 534–542.

Soncini, D., Caffa, I., Zoppoli, G., Cea, M., Cagnetta, A., Passalacqua, M., ... Nencioni, A. (2014). Nicotinamide phosphoribosyltransferase promotes epithelial-to-mesenchymal transition as a soluble factor independent of its enzymatic activity. *Journal of Biological Chemistry*, *289*(49), 34189–34204.

Song, Z., Pan, Y., Ling, G., Wang, S., Huang, M., Jiang, X., & Ke, Y. (2017). Escape of U251 glioma cells from temozolomide-induced senescence was modulated by CDK1/survivin signaling. *American Journal of Translational Research*, *9*(5), 2163–2180.

Srivenugopal, K. S., Yuan, X.-H., Friedman, H. S., & Ali-Osman, F. (1996). Ubiquitination-Dependent Proteolysis of O6-Methylguanine-DNA Methyltransferase in Human and Murine Tumor Cells following Inactivation with O-Benzylguanine or 1,3-Bis(2-chloroethyl)-1-nitrosourea. *Biochemistry*, *35*(4), 1328–1334.

Stewart, D. J., Dahrouge, S., & Soltys, K. (1995). A phase II study of 5-fluorouracil plus folinic acid in malignant gliomas in adults. *Journal of Neuro-Oncology*, *23*(3), 249–252.

Stincone, A., Prigione, A., Cramer, T., Wamelink, M. M., Campbell, K., Cheung, E., ... Ralser, M. (2015). The return of metabolism: Biochemistry and physiology of the pentose phosphate pathway. *Biological Reviews*, *90*(3), 927–963.

Stine, Z. E., Walton, Z. E., Altman, B. J., Hsieh, A. L., & Dang, C. V. (2015). MYC, metabolism, and cancer. *Cancer Discovery*, *5*(10), 1024–1039.

Stupp, R., Mason, W. P., Van Den Bent, M. J., Weller, M., Fisher, B., Taphoorn, M. J. B., ... Mirimanoff, R. O. (2005). Radiotherapy plus Concomitant and Adjuvant Temozolomide for Glioblastoma. *The New England Journal of Medicine*, *352*(10), 987–996.

Su, S.-C., Hsieh, M.-J., Liu, Y.-F., Chou, Y.-E., Lin, C.-W., & Yang, S.-F. (2016). ADAMTS14 Gene Polymorphism and Environmental Risk in the Development of Oral Cancer. *PLOS One*, *11*(7), 1–11.

Sun, Y., Connors, K. E., & Yang, D. Q. (2007). AICAR induces phosphorylation of AMPK in an ATM-dependent, LKB1-independent manner. *Molecular and Cellular Biochemistry*, *306*(1-2), 239–245.

Sun, Y., Zhu, S., Wu, Z., Huang, Y., Liu, C., Tang, S., & Wei, L. (2017). Elevated serum visfatin levels are associated with poor prognosis of hepatocellular carcinoma. *Oncotarget*, *8*(14), 23427–23435.

Suyama, K., Watanabe, M., Sakabe, K., Okada, Y., Matsuyama, D., Kuroiwa, M., & Mochida, J. (2011). Overexpression of GRP78 protects glial cells from endoplasmic reticulum stress. *Neuroscience Letters*, *504*(3), 271–276.

Svensson, Å., Bäckman, U., Jonsson, E., Larsson, R., & Christofferson, R. (2002). CHS 828 inhibits neuroblastoma growth in mice alone and in combination with antiangiogenic drugs. *Pediatric Research*, *51*(5), 607–611.

Syed, N., Langer, J., Janczar, K., Singh, P., Lo Nigro, C., Lattanzio, L., ... Crook, T. (2013). Epigenetic status of argininosuccinate synthetase and argininosuccinate lyase modulates autophagy and cell death in glioblastoma. *Cell Death and Disease*, *4*(e458).

Synnestvedt, K. (2002). Ecto-5'-nucleotidase (CD73) regulation by hypoxia-inducible factor-1 mediates permeability changes in intestinal epithelia. *The Journal of Clinical Investigation*, *110*(7), 993–1002.

Szlosarek, P. W., Steele, J. P., Nolan, L., Gilligan, D., Taylor, P., Spicer, J., ... Hackshaw, A. (2017). Arginine Deprivation With Pegylated Arginine Deiminase in Patients With Argininosuccinate Synthetase 1-Deficient Malignant Pleural Mesothelioma: A Randomized Clinical Trial. *JAMA Oncology*, *3*(1), 58–66.

Takahashi, Y., Rayman, J. B., & Dynlacht, B. D. (2000). Analysis of promoter binding by the E2F and pRB families in vivo: Distinct E2F proteins mediate activation and repression. *Genes & Development*, *14*(7), 804–816.

Takaku, H., Takase, M., Abe, S., Hayashi, H., & Miyasaki, K. (1992). In vivo anti-tumor activity of arginine deiminase purified from mycoplasma arginini. *International Journal of Cancer*, *51*(2), 244–249.

Takao, S., Chien, W., Madan, V., Lin, D.-C., Ding, L.-W., Sun, Q.-Y., ... Koeffler, H. P. (2017). Targeting the vulnerability to NAD+ depletion in B-cell acute lymphoblastic leukemia. *Leukemia*, *32*(3), 616–625.

Talari, N. K., Panigrahi, M. K., Madigubba, S., & Phanithi, P. B. (2018). Overexpression of aryl hydrocarbon receptor (AHR) signalling pathway in human meningioma. *Journal of Neuro-Oncology*, *137*(2), 241–248.

Tan, B., Dong, S., Shepard, R. L., Kays, L., Roth, K. D., Geeganage, S., ... Zhao, G. (2015). Inhibition of nicotinamide phosphoribosyltransferase (NAMPT), an enzyme essential for NAD+ biosynthesis, leads to altered carbohydrate metabolism in cancer cells. *Journal of Biological Chemistry*, *290*(25), 15812–15824.

Tan, B., Young, D. a., Lu, Z. H., Wang, T., Meier, T. I., Shepard, R. L., ... Zhao, G. (2013). Pharmacological inhibition of nicotinamide phosphoribosyltransferase (NAMPT), an enzyme essential for NAD+ biosynthesis, in human cancer cells: Metabolic basis and potential clinical implications. *Journal of Biological Chemistry*, *288*(5), 3500–3511.

Tanaka, K., Sasayama, T., Irino, Y., Takata, K., Nagashima, H., Satoh, N., ... Kohmura, E. (2015). Compensatory glutamine metabolism promotes glioblastoma resistance to mTOR inhibitor treatment. *Journal of Clinical Investigation*, *125*(4), 1591–1602.

Tandle, A. T., Kramp, T., Kil, W. J., Halthore, A., Gehlhaus, K., Shankavaram, U., ... Camphausen, K. (2013). Inhibition of polo-like kinase 1 in glioblastoma multiforme induces

mitotic catastrophe and enhances radiosensitisation. *European Journal of Cancer*, *49*(14), 3020–3028.

Tardito, S., Oudin, A., Ahmed, S. U., Fack, F., Keunen, O., Zheng, L., ... Gottlieb, E. (2015). Glutamine synthetase activity fuels nucleotide biosynthesis and supports growth of glutamine-restricted glioblastoma. *Nature Cell Biology*, *17*(12), 1556–1568.

Tarrant, J. M., Dhawan, P., Singh, J., Zabka, T. S., Clarke, E., Dossantos, G., ... Uppal, H. (2015). Preclinical models of nicotinamide phosphoribosyltransferase inhibitor-mediated hematotoxicity and mitigation by co-treatment with nicotinic acid. *Toxicology Mechanisms and Methods*, *25*(3), 201–211.

Taspinar, M., Ilgaz, S., Ozdemir, M., Ozkan, T., Oztuna, D., Canpinar, H., ... Ugur, H. C. (2013). Effect of lomeguatrib-temozolomide combination on MGMT promoter methylation and expression in primary glioblastoma tumor cells. *Tumor Biology*, *34*(3), 1935–1947.

Tateishi, K., Higuchi, F., Miller, J. J., Koerner, M. V., Lelic, N., Shankar, G. M., ... Cahill, D. P. (2017). The alkylating chemotherapeutic temozolomide induces metabolic stress in IDH1-mutant cancers and potentiates NAD+depletion-mediated cytotoxicity. *Cancer Research*, *77*(15), 4102–4115.

Tateishi, K., Iafrate, A. J., Ho, Q., Curry, W. T., Batchelor, T. T., Flaherty, K. T., ... Wakimoto, H. (2016). Myc-Driven glycolysis is a therapeutic target in glioblastoma. *Clinical Cancer Research*, *22*(17), 4452–4465.

Tateishi, K., Wakimoto, H., Iafrate, A. J., Tanaka, S., Loebel, F., Lelic, N., ... Cahill, D. P. (2015). Extreme Vulnerability of IDH1 Mutant Cancers to NAD+ Depletion. *Cancer Cell*, *28*(6), 773–784.

Tawbi, H. A., Villaruz, L., Tarhini, A., Moschos, S., Sulecki, M., Viverette, F., ... Kirkwood, J. M. (2011). Inhibition of DNA repair with MGMT pseudosubstrates: Phase i study of lomeguatrib in combination with dacarbazine in patients with advanced melanoma and other solid tumours. *British Journal of Cancer*, *105*(6), 773–777.

TCGA. (2008). Comprehensive genomic characterization defines human glioblastoma genes and core pathways. *Nature*, *455*(7216), 1061–1068.

Tentori, L., Portarena, I., Torino, F., Scerrati, M., Navarra, P., & Graziani, G. (2002). Poly(ADP-ribose) polymerase inhibitor increases growth inhibition and reduces G2/M cell accumulation induced by temozolomide in malignant glioma cells. *Glia*, *40*(1), 44–54.

Thakur, B. K., Dittrich, T., Chandra, P., Becker, A., Kuehnau, W., Klusmann, J. H., ... Welte, K. (2012a). Involvement of p53 in the cytotoxic activity of the NAMPT inhibitor FK866 in myeloid leukemic cells. *International Journal of Cancer*, *132*(4), 766–774.

Thakur, B. K., Dittrich, T., Chandra, P., Becker, A., Lippka, Y., Selvakumar, D., ... Welte, K. (2012b). Inhibition of NAMPT pathway by FK866 activates the function of p53 in HEK293T cells. *Biochemical and Biophysical Research Communications*, *424*(3), 371–377.

The Cancer Genome Atlas Research Network. (2015). Comprehensive, Integrative Genomic Analysis of Diffuse Lower-Grade Gliomas. *New England Journal of Medicine*, *372*(26), 2481–2498.

Theodoropoulou, S., Kolovou, P. E., Morizane, Y., Kayama, M., Nicolaou, F., Miller, J. W., ... Vavvas, D. G. (2012). Erratum: Retinoblastoma cells are inhibited by aminoimidazole carboxamide ribonucleotide (AICAR) partially through activation of AMP-dependent kinase (The FASEB Journal (2010) 24 (2620-2630) DOI:10.1096/fj.09-152546). *The FASEB Journal*, *26*(10), 4383–4384.

Thermo Fisher Scientific. (2018). DMEM, high glucose, pyruvate.

Thongkum, A., Wu, C., Li, Y. Y., Wangpaichitr, M., Navasumrit, P., Parnlob, V., ... Savaraj, N. (2017). The combination of arginine deprivation and 5-fluorouracil improves therapeutic efficacy in argininosuccinate synthetase negative hepatocellular carcinoma. *International Journal of Molecular Sciences*, *18*(6), 1–19.

Thuerauf, D. J., Marcinko, M., Belmont, P. J., & Glembotski, C. C. (2007). Effects of the isoform-specific characteristics of ATF6a and ATF6B on endoplasmic reticulum stress response gene expression and cell viability. *Journal of Biological Chemistry*, *282*(31), 22865–22878.

Thuerauf, D. J., Morrison, L., & Glembotski, C. C. (2004). Opposing roles for ATF6a and ATF6B in endoplasmic reticulum stress response gene induction. *Journal of Biological Chemistry*, *279*(20), 21078–21084.

Tian, W., Zhu, Y., Wang, Y., Teng, F., Zhang, H., Liu, G., ... Xue, F. (2013). Visfatin, a potential biomarker and prognostic factor for endometrial cancer. *Gynecologic Oncology*, *129*(3), 505–512.

Tianhu, Z., Shiguang, Z., & Xinghan, L. (2010). Bmf is upregulated by PS-341-mediated cell death of glioma cells through JNK phosphorylation. *Molecular Biology Reports*, *37*(3), 1211–1219.

Tisdale, M. J. (1987). Antitumour Imidazotetrazines-XV Role of guanine O6 alkylation in the mechanism of cytotoxicity of imidazotetraziones. *Biochemical Pharmacology*, *36*(4), 457–462.

Tolstikov, V., Nikolayev, A., Dong, S., Zhao, G., & Kuo, M.-S. (2014). Metabolomics Analysis of Metabolic Effects of Nicotinamide Phosphoribosyltransferase (NAMPT) Inhibition on Human Cancer Cells. *PLOS One*, *9*(12), 1–24.

Tomlinson, B. K., Thomson, J. A., Bomalaski, J. S., Diaz, M., Akande, T., Mahaffey, N., ... Lara, P. N. (2015). Phase i trial of arginine deprivation therapy with ADI-PEG 20 plus docetaxel in patients with advanced malignant solid tumors. *Clinical Cancer Research*, *21*(11), 2480–2486.

Touat, M., Sourisseau, T., Dorvault, N., Chabanon, R. M., Morel, D., Krastev, D. B., ... Postel-Vinay, S. (2018). DNA repair deficiency sensitizes lung cancer cells to NAD+ biosynthesis blockade. *Journal of Clinical Investigation*, *128*(4), 1671–1687.

Trammell, S. A. J., Schmidt, M. S., Weidemann, B. J., Redpath, P., Jaksch, F., Dellinger, R. W., ... Lau, D. T. (2016). Nicotinamide riboside is uniquely and orally bioavailable in mice and humans. *Nature Communications*, *7*(12948), 1–14.

Travelli, C., Drago, V., Maldi, E., Kaludercic, N., Galli, U., Boldorini, R., ... Genazzani, A. a. (2011). Reciprocal Potentiation of the Antitumoral Activities of FK866, an Inhibitor of Nicotinamide Phosphoribosyltransferase, and Etoposide or Cisplatin in Neuroblastoma Cells. *The Journal of Pharmacology and Experimental Therapeutics*, *338*(3), 829–840.

Tsai, I. T., Wang, C. P., Yu, T. H., Lu, Y. C., Lin, C. W., Lu, L. F., ... Hsu, C. C. (2017). Circulating visfatin level is associated with hepatocellular carcinoma in chronic hepatitis B or C virus infection. *Cytokine*, *90*, 54–59.

Tu, Y. K., Hong, Y. Y., & Chen, Y. C. (2009). Finite element modeling of kirschner pin and bone thermal contact during drilling. *Life Science Journal*, *6*(4), 23–27.

Tucci, R., Campos, M. S., Matizonkas-Antonio, L. F., Durazzo, M., Pinto Junior, D. d. S., & Nunes, F. D. (2011). HOXB5 expression in oral squamous cell carcinoma. *Journal of Applied Oral Science*, *19*(2), 125–129.

Urbanska, K., Sokolowska, J., Szmidt, M., & Sysa, P. (2014). Glioblastoma multiforme - An overview. *Contemporary Oncology*, *18*(5), 307–312.

Valente, V., Serafim, R. B., de Oliveira, L. C., Adorni, F. S., Torrieri, R., da Cunha Tirapelli, D. P., ... Carlotti, C. G. (2013). Modulation of HJURP (Holliday Junction-Recognizing Protein) Levels Is Correlated with Glioblastoma Cells Survival. *PLOS One*, *8*(4), 1–10.

Valtorta, S., Dico, A., Raccagni, I., Gaglio, D., Belloli, S., Politi, L., ... Moresco, R. (2017). Metformin and temozolomide, a synergic option to overcome resistance in glioblastoma multiforme models. *Oncotarget*, *8*(68), 113090–113104.

Van Brocklyn, J. R., Wojton, J., Meisen, W. H., Kellough, D. A., Ecsedy, J. A., Kaur, B., & Lehman, N. L. (2014). Aurora-A inhibition offers a novel therapy effective against intracranial glioblastoma. *Cancer Research*, *74*(19), 5364–5370.

Van Horssen, R., Willemse, M., Haeger, A., Attanasio, F., Güneri, T., Schwab, A., ... Wieringa, B. (2013). Intracellular NAD(H) levels control motility and invasion of glioma cells. *Cellular and Molecular Life Sciences*, *70*(12), 2175–2190.

Van Meter, M., Simon, M., Tombline, G., May, A., Morello, T. D., Hubbard, B. P., ... Seluanov, A. (2016). JNK Phosphorylates SIRT6 to Stimulate DNA Double-Strand Break Repair in Response to Oxidative Stress by Recruiting PARP1 to DNA Breaks. *Cell Reports*, *16*(10), 2641–2650.

VanBrocklin, M. W., Verhaegen, M., Soengas, M. S., & Holmen, S. L. (2009). Mitogen-activated protein kinase inhibition induces translocation of bmf to promote apoptosis in melanoma. *Cancer Research*, *69*(5), 1985–1994.

Vaquero, A., Scher, M. B., Dong, H. L., Sutton, A., Cheng, H. L., Alt, F. W., ... Reinberg, D. (2006). SirT2 is a histone deacetylase with preference for histone H4 Lys 16 during mitosis. *Genes & Development*, *20*(10), 1256–1261.

Vareki, S. M., Chen, D., Di Cresce, C., Ferguson, P. J., Figueredo, R., Pampillo, M., ... Koropatnick, J. (2015). IDO downregulation induces sensitivity to pemetrexed, gemcitabine, FK866, and methoxyamine in human cancer cells. *PLOS One*, *10*(11), 1–22.

Vartanian, A., Agnihotri, S., Wilson, M. R., Burrell, K. E., Tonge, P. D., Alamsahebpour, A., ... Zadeh, G. (2016). Targeting Hexokinase 2 enhances response to radio-chemotherapy in Glioblastoma. *Oncotarget*, *7*(43), 69518–69535.

Vaziri, H., Dessain, S. K., Ng Eaton, E., Imai, S. I., Frye, R. A., Pandita, T. K., ... Weinberg, R. A. (2001). hSIR2(SIRT1) functions as an NAD-dependent p53 deacetylase. *Cell*, *107*(2), 149–59.

Velpula, K. K., Bhasin, A., Asuthkar, S., & Tsung, A. J. (2013). Combined targeting of PDK1 and EGFR triggers regression of glioblastoma by reversing the warburg effect. *Cancer Research*, *73*(24), 7277–7289.

Verhaak, R. G. W., Hoadley, K. a., Purdom, E., Wang, V., Qi, Y., Wilkerson, M. D., ... Hayes, D. N. (2010). Integrated Genomic Analysis Identifies Clinically Relevant Subtypes of Glioblastoma Characterized by Abnormalities in PDGFRA, IDH1, EGFR, and NF1. *Cancer Cell*, *17*(1), 98–110.

Villa, G. R., Hulce, J. J., Zanca, C., Bi, J., Ikegami, S., Cahill, G. L., ... Mischel, P. S. (2016). An LXR-Cholesterol Axis Creates a Metabolic Co-Dependency for Brain Cancers. *Cancer Cell*, *30*(5), 683–693.

Von Heideman, A., Berglund, Å., Larsson, R., Nygren, P., & Larsson, R. (2010). Safety and efficacy of NAD depleting cancer drugs: Results of a phase i clinical trial of CHS 828 and overview of published data. *Cancer Chemotherapy and Pharmacology*, *65*(6), 1165–1172.

Wakil, S. J., Stoops, J. K., & Joshi, V. C. (1983). Fatty acid synthesis and its regulation. *Annual review of biochemistry*, *52*(1), 537–79.

Walczak, K., Deneka-Hannemann, S., Jarosz, B., Zgrajka, W., Stoma, F., Trojanowski, T., ... Rzeski, W. (2014). Kynurenic acid inhibits proliferation and migration of human glioblastoma T98G cells. *Pharmacological Reports*, *66*(1), 130–136.

Wamelink, M. M. C., Struys, E. A., & Jakobs, C. (2008). The biochemistry, metabolism and inherited defects of the pentose phosphate pathway: A review. *Journal of Inherited Metabolic Disease*, *31*(6), 703–717.

Wang, B., Hasan, M. K., Alvarado, E., Yuan, H., Wu, H., & Chen, W. Y. (2011). NAMPT overexpression in prostate cancer and its contribution to tumor cell survival and stress response. *Oncogene*, *30*(8), 907–921.

Wang, B., Wang, D., Zhu, Z. Z., Wang, W., Zhang, X. B., Tang, F., ... Yan, X. L. (2016a). The role of extracellular-5-nucleotidase/CD73 in glioma peritumoural brain edema. *Neurological Sciences*, *37*(4), 603–611.

Wang, C., Ma, J., Zhang, N., Yang, Q., Jin, Y., & Wang, Y. (2015a). The acetyl-CoA carboxylase enzyme: A target for cancer therapy? *Expert Review of Anticancer Therapy*, *15*(6), 667–676.

Wang, C., Chen, L., Hou, X., Li, Z., Kabra, N., Ma, Y., ... Chen, J. (2006a). Interactions between E2F1 and SirT1 regulate apoptotic response to DNA damage. *Nature Cell Biology*, *8*(9), 1025–1031.

Wang, H., Lee, S., Lo Nigro, C., Lattanzio, L., Merlano, M., Monteverde, M., ... Crook, T. (2012). NT5E (CD73) is epigenetically regulated in malignant melanoma and associated with metastatic site specificity. *British Journal of Cancer*, *106*(8), 1446–52.

Wang, H., Zhang, K., Qin, H., Yang, L., Zhang, L., & Cao, Y. (2016b). Association Between PARP1 Single Nucleotide Polymorphism and Brain Tumors. *Molecular Neurobiology*, *53*(4), 2083–2089.

Wang, J., Yang, T., Xu, G., Liu, H., Ren, C., Xie, W., & Wang, M. (2016c). Cyclin-dependent kinase 2 promotes tumor proliferation and induces radio resistance in glioblastoma. *Translational Oncology*, *9*(6), 548–556.

Wang, P., Wu, J., Ma, S., Zhang, L., Yao, J., Hoadley, K. A., ... Xiong, Y. (2015b). Oncometabolite D-2-Hydroxyglutarate Inhibits ALKBH DNA Repair Enzymes and Sensitizes IDH Mutant Cells to Alkylating Agents. *Cell Reports*, *13*(11), 2353–2361.

Wang, T., Zhang, X., Bheda, P., Revollo, J. R., Imai, S.-i., & Wolberger, C. (2006b). Structure of Nampt/PBEF/visfatin, a mammalian NAD+ biosynthetic enzyme. *Nature Structural & Molecular Biology*, *13*(7), 661–662.

Wang, X., Chen, J.-x., Liu, J.-p., You, C., Liu, Y.-h., & Mao, Q. (2014). Gain of Function of Mutant TP53 in Glioblastoma: Prognosis and Response to Temozolomide. *Annals of Surgical Oncology*, *21*(4), 1337–1344.

Wang, Y., Gao, C., Zhang, Y., Gao, J., Teng, F., Tian, W., ... Xue, F. (2016d). Visfatin stimulates endometrial cancer cell proliferation via activation of PI3K/Akt and MAPK/ERK1/2 signalling pathways. *Gynecologic Oncology*, *143*(1), 168–178.

Wanka, C., Brucker, D. P., Bähr, O., Ronellenfitsch, M., Weller, M., Steinbach, J. P., & Rieger, J. (2012a). Synthesis of cytochrome c oxidase 2: A p53-dependent metabolic regulator that promotes respiratory function and protects glioma and colon cancer cells from hypoxia-induced cell death. *Oncogene*, *31*(33), 3764–3776.

Wanka, C., Steinbach, J. P., & Rieger, J. (2012b). Tp53-induced glycolysis and apoptosis regulator (TIGAR) protects glioma cells from starvation-induced cell death by up-regulating respiration and improving cellular redox homeostasis. *Journal of Biological Chemistry*, *287*(40), 33436–33446.

Warburg, O. (1956). On the Origin of Cancer Cells. *Science*, *123*(3191), 309–314.

Warburg, O., Wind, F., & Negelein, E. (1927). The Metabolism of Tumors in the Body. *The Journal of General Physiology*, *8*(6), 519–530.

Wątroba, M., Dudek, I., Skoda, M., Stangret, A., Rzodkiewicz, P., & Szukiewicz, D. (2017). Sirtuins, epigenetics and longevity. *Ageing Research Reviews*, *40*(1), 11–19.

Watson, A. J., Sabharwal, A., Thorncroft, M., McGown, G., Kerr, R., Bojanic, S., ... Middleton, M. R. (2010). Tumor O6-methylguanine-DNA methyltransferase inactivation by oral lomeguatrib. *Clinical Cancer Research*, *16*(2), 743–749.

Watson, M., Roulston, A., Bélec, L., Billot, X., Marcellus, R., Bédard, D., ... Beauparlant, P. (2009). The small molecule GMX1778 is a potent inhibitor of NAD+ biosynthesis: strategy for enhanced therapy in nicotinic acid phosphoribosyltransferase 1-deficient tumors. *Molecular and Cellular Biology*, *29*(21), 5872–88.

Weisz, L., Oren, M., & Rotter, V. (2007). Transcription regulation by mutant p53. *Oncogene*, *26*(15), 2202–2211.

Weller, M., Cloughesy, T., Perry, J. R., & Wick, W. (2012). Standards of care for treatment of recurrent. *Neuro-Oncology*, *15*(1), 4–27.

Wesseling, P., van den Bent, M., & Perry, A. (2015). Glioblastoma: pathology, molecular mechanisms and markers. *Acta Neuropathologica*, *129*(6), 809–827.

Williams Parsons, D., Jones, S., Zhang, X., Lin, J. C.-H., Leary, R., Angenendt, P., ... Kinzler, K. (2008). An integrated genomic analysis of human glioblastoma multiforme. *Science*, *321*(5897), 1807–1812.

Wise-Draper, T. M., Moorthy, G., Salkeni, M. A., Karim, N. A., Thomas, H. E., Mercer, C. A., ... Morris, J. C. (2017). A Phase Ib Study of the Dual PI3K/mTOR Inhibitor Dactolisib (BEZ235) Combined with Everolimus in Patients with Advanced Solid Malignancies. *Targeted Oncology*, *12*(3), 323–332.

Wise, D. R., DeBerardinis, R. J., Mancuso, A., Sayed, N., Zhang, X.-Y., Pfeiffer, H. K., ... Thompson, C. B. (2008). Myc regulates a transcriptional program that stimulates mitochondrial glutaminolysis and leads to glutamine addiction. *Proceedings of the National Academy of Sciences of the United States of America*, *105*(48), 18782–18787.

Wolf, A., Agnihotri, S., Micallef, J., Mukherjee, J., Sabha, N., Cairns, R., ... Guha, A. (2011). Hexokinase 2 is a key mediator of aerobic glycolysis and promotes tumor growth in human glioblastoma multiforme. *Journal of Experimental Medicine*, *208*(2), 313–326.

Wong, S. & Weber, J. D. (2007). Deacetylation of the retinoblastoma tumour suppressor protein by SIRT1. *Biochemical Journal*, *407*(3), 451–460.

Woods, A., Johnstone, S. R., Dickerson, K., Leiper, F. C., Fryer, L. G., Neumann, D., ... Carling, D. (2003). LKB1 Is the Upstream Kinase in the AMP-Activated Protein Kinase Cascade. *Current Biology*, *13*(22), 2004–2008.

Wu, Q., Lothe, R. A., Ahlquist, T., Silins, I., Tropé, C. G., Micci, F., ... Lind, G. E. (2007). DNA methylation profiling of ovarian carcinomas and their in vitro models identifies HOXA9, HOXB5, SCGB3A1, and CRABP1 as novel targets. *Molecular Cancer*, *6*(45), 1–11.

Wu, Y., Qi, Y., Liu, H., Wang, X., Zhu, H., & Wang, Z. (2016). AMPK activator AICAR promotes 5-FU-induced apoptosis in gastric cancer cells. *Molecular and Cellular Biochemistry*, *411*(1-2), 299–305.

Xi, H., Kurtoglu, M., Liu, H., Wangpaichitr, M., You, M., Liu, X., ... Lampidis, T. J. (2011). 2-Deoxy-d-glucose activates autophagy via endoplasmic reticulum stress rather than ATP depletion. *Cancer Chemotherapy and Pharmacology*, *67*(4), 899–910.

Xia, Z., Wei, P., Zhang, H., Ding, Z., Yang, L., Huang, Z., & Zhang, N. (2013). AURKA Governs Self-Renewal Capacity in Glioma-Initiating Cells via Stabilization/Activation of B-catenin/Wnt Signaling. *Molecular Cancer Research*, *11*(9), 1101–1111.

Xiao, Y., Elkins, K., Durieux, J. K., Lee, L., Oeh, J., Yang, L. X., ... O'Brien, T. (2013). Dependence of tumor cell lines and patient-derived tumors on the NAD salvage pathway renders them sensitive to NAMPT inhibition with GNE-618. *Neoplasia*, *15*(10), 1151–60.

Xiao, Y., Kwong, M., Daemen, A., Belvin, M., Liang, X., Hatzivassiliou, G., & O'Brien, T. (2016). Metabolic Response to NAD Depletion across Cell Lines Is Highly Variable. *PLOS One*, *11*(10), 1–17.

Xing, F., Luan, Y., Cai, J., Wu, S., Mai, J., Gu, J., ... Yan, G. (2017). The Anti-Warburg Effect Elicited by the cAMP-PGC1α Pathway Drives Differentiation of Glioblastoma Cells into Astrocytes. *Cell Reports*, *18*(2), 468–481.

Xu, R., Yuan, Z., Lijuan, Y., Li, L., Li, D., & Lv, C. (2017). Inhibition of NAMPT decreases cell growth and enhances susceptibility to oxidative stress. *Oncology Reports*, *38*(3), 1767–1773.

Xu, S., Shao, Q.-q., Sun, J.-t., Yang, N., Xie, Q., & Wang, D.-h. (2013). Synergy between the ectoenzymes CD39 and CD73 contributes to adenosinergic malignant gliomas. *Neuro-Oncology*, *15*(9), 1160–1172.

Xue, J., Zhou, A., Tan, C., Wu, Y., Lee, H. T., Li, W., ... Huang, S. (2015). Forkhead box M1 is essential for nuclear localization of glioma-associated oncogene homolog 1 in glioblastoma multiforme cells by promoting importin-7 expression. *Journal of Biological Chemistry*, *290*(30), 18662–18670.

Yamaguchi, F., Ohshima, T., & Sakuraba, H. (2007). An enzymatic cycling assay for nicotinic acid adenine dinucleotide phosphate using NAD synthetase. *Analytical Biochemistry*, *364*(2), 97–103.

Yamamoto, H., Schoonjans, K., & Auwerx, J. (2007). Sirtuin Functions in Health and Disease. *Molecular Endocrinology*, *21*(8), 1745–1755.

Yamamoto, Y., Tomiyama, A., Sasaki, N., Yamaguchi, H., Shirakihara, T., Nakashima, K., ... Mori, K. (2018). Intracellular cholesterol level regulates sensitivity of glioblastoma cells against temozolomide-induced cell death by modulation of caspase-8 activation via death receptor 5-accumulation and activation in the plasma membrane lipid raft. *Biochemical and Biophysical Research Communications*, *495*(1), 1292–1299.

Yan, X., Zhao, J., & Zhang, R. (2017). Visfatin mediates doxorubicin resistance in human colorectal cancer cells via up regulation of multidrug resistance 1 (MDR1). *Cancer Chemotherapy and Pharmacology*, *80*(2), 395–403.

Yang, G., Murashige, D. S., Humphrey, S. J., & James, D. E. (2015a). A Positive Feedback Loop between Akt and mTORC2 via SIN1 Phosphorylation. *Cell Reports*, *12*(6), 937–943.

Yang, H., Yan, B., Liao, D., Huang, S., & Qiu, Y. (2015b). Acetylation of HDAC1 and degradation of SIRT1 form a positive feedback loop to regulate p53 acetylation during heat-shock stress. *Cell Death and Disease*, *6*(e1747).

Yang, J., Zhang, K., Song, H., Wu, M., Li, J., Yong, Z., ... Zhang, T. (2016). Visfatin is involved in promotion of colorectal carcinoma malignancy through an inducing EMT mechanism. *Oncotarget*, *7*(22), 32306–32317.

Yang, P., Zhang, L., Shi, Q. J., Lu, Y. B., Wu, M., Wei, E. Q., & Zhang, W. P. (2015c). Nicotinamide phosphoribosyltransferase inhibitor APO866 induces C6 glioblastoma cell death via autophagy. *Pharmazie*, *70*(10), 650–655.

Yang, S., Ryu, J. H., Oh, H., Jeon, J., Kwak, J. S., Kim, J. H., ... Chun, J. S. (2015d). NAMPT (visfatin), a direct target of hypoxiainducible factor-2α, is an essential catabolic regulator of osteoarthritis. *Annals of the Rheumatic Diseases*, *74*(3), 595–602.

Yap, T. A., Yan, L., Patnaik, A., Fearen, I., Olmos, D., Papadopoulos, K., ... Tolcher, A. W. (2011). First-in-man clinical trial of the oral pan-AKT inhibitor MK-206 in patients with advanced solid tumors. *Journal of Clinical Oncology*, *29*(35), 4688–4695.

Yasumoto, Y., Miyazaki, H., Vaidyan, L. K., Kagawa, Y., Ebrahimi, M., Yamamoto, Y., ... Owada, Y. (2016). Inhibition of fatty acid synthase decreases expression of stemness markers in glioma stem cells. *PLOS One*, *11*(1), 1–14.

Yin, W. W., Wang, B., Ding, M. H., Huo, Y., Hu, H., Cai, R. N., ... Chen, D. Z. (2016). Elevated E2F7 expression predicts poor prognosis in human patients with gliomas. *Journal of Clinical Neuroscience*, *33*, 187–193.

Ying, W. (2008). NAD+/NADH and NADP+/NADPH in Cellular Functions and Cell Death: Regulation and Biological Consequences. *Antioxidants & Redox Signaling*, *10*(2), 179–206.

Yip, S., Miao, J., Cahill, D. P., Iafrate, A. J., Aldape, K., Nutt, C. L., & Louis, D. N. (2009). MSH6 mutations arise in glioblastomas during temozolomide therapy and mediate temozolomide resistance. *Clinical Cancer Research*, *15*(14), 4622–4629.

Yosunkaya, E., Kucukyuruk, B., Onaran, I., Gurel, C. B., Uzan, M., & Kanigur-Sultuybek, G. (2010). Glioma risk associates with polymorphisms of DNA repair genes, XRCC1 and PARP1. *British Journal of Neurosurgery*, *24*(5), 561–565.

Yu, Z., Xie, G., Zhou, G., Cheng, Y., Zhang, G., Yao, G., ... Zhao, G. (2015a). NVP-BEZ235, a novel dual PI3K-mTOR inhibitor displays anti-glioma activity and reduces chemoresistance to temozolomide in human glioma cells. *Cancer Letters*, *367*(1), 58–68.

Yu, Z., Zhao, G., Xie, G., Zhao, L., Chen, Y., Yu, H., ... Li, Y. (2015b). Metformin and temozolomide act synergistically to inhibit growth of glioma cells and glioma stem cells in vitro and in vivo. *Oncotarget*, *6*(32), 32930–32943.

Zabka, T. S., Singh, J., Dhawan, P., Liederer, B. M., Oeh, J., Kauss, M. A., ... Misner, D. L. (2015). Retinal toxicity, in vivo and in vitro, associated with inhibition of nicotinamide phosphoribosyltransferase. *Toxicological Sciences*, *144*(1), 163–172.

Zadra, G., Batista, J. L., & Loda, M. (2015). Dissecting the Dual Role of AMPK in Cancer: From Experimental to Human Studies. *Molecular Cancer Research*, *13*(7), 1059–1072.

Zagorodna, O., Martin, S. M., Rutkowski, D. T., Kuwana, T., Spitz, D. R., & Knudson, C. M. (2012). 2-Deoxyglucose-induced toxicity is regulated by Bcl-2 family members and is enhanced by antagonizing Bcl-2 in lymphoma cell lines. *Oncogene*, *31*(22), 2738–2749.

Zalmas, L. P., Coutts, A. S., Helleday, T., & Thangue, N. B. L. (2013). E2F-7 couples DNA damage-dependent transcription with the DNA repair process. *Cell Cycle*, *12*(18), 3037–3051.

Zamecnik, P. C., Loftfield, R. B., Stephenson, M. L., & Steele, J. M. (1951). Studies on the carbohydrate and protein metabolism of the rat hepatoma. *Cancer Research*, *11*(8), 592–602.

Zanardi, E., Verzoni, E., Grassi, P., Necchi, A., Giannatempo, P., Raggi, D., ... Procopio, G. (2015). Clinical experience with temsirolimus in the treatment of advanced renal cell carcinoma. *Therapeutic Advances in Urology*, *7*(3), 152–161.

Zeng, W. F., Navaratne, K., Prayson, R. A., & Weil, R. J. (2007). Aurora B expression correlates with aggressive behaviour in glioblastoma multiforme. *Journal of Clinical Pathology*, *60*(2), 218–221.

Zerp, S. F., Vens, C., Floot, B., Verheij, M., & Van Triest, B. (2014). NAD+ depletion by APO866 in combination with radiation in a prostate cancer model, results from an in vitro and in vivo study. *Radiotherapy and Oncology*, *110*(2), 348–354.

Zhang, B. (2012). Opportunities and challenges for anti-CD73 cancer therapy. *Immunotherapy*, *4*(9), 861–5.

Zhang, B., Li, N., & Zhang, H. (2018). Knockdown of Homeobox B5 (HOXB5) Inhibits Cell Proliferation, Migration, and Invasion in Non-Small Cell Lung Cancer Cells Through Inactivation of the Wnt/β-Catenin Pathway. *Oncology Research*, *26*(1), 37–44.

Zhang, C., Tong, J., & Huang, G. (2013). Nicotinamide Phosphoribosyl Transferase (Nampt) Is a Target of MicroRNA-26b in Colorectal Cancer Cells. *PLOS One*, *8*(7), 1–9.

Zhang, C., Yan, D., Wang, S., Xu, C., Du, W., Ning, T., ... Chen, Z. (2015). Genetic polymorphisms of NAMPT related with susceptibility to esophageal Squamous cell carcinoma. *BMC Gastroenterology*, *15*(49), 1–5.

Zhang, D., Li, J., Wang, F., Hu, J., Wang, S., & Sun, Y. (2014a). 2-Deoxy-D-glucose targeting of glucose metabolism in cancer cells as a potential therapy. *Cancer Letters*, *355*(2), 176–183.

Zhang, H., Bosch-Marce, M., Shimoda, L. A., Yee, S. T., Jin, H. B., Wesley, J. B., ... Semenza, G. L. (2008). Mitochondrial autophagy is an HIF-1-dependent adaptive metabolic response to hypoxia. *Journal of Biological Chemistry*, *283*(16), 10892–10903.

Zhang, J., F.G. Stevens, M., & D. Bradshaw, T. (2012a). Temozolomide: Mechanisms of Action, Repair and Resistance. *Current Molecular Pharmacology*, *5*(1), 102–114.

Zhang, J., Stevens, M. F., Laughton, C. A., Madhusudan, S., & Bradshaw, T. D. (2010a). Acquired resistance to temozolomide in glioma cell lines: Molecular mechanisms and potential translational applications. *Oncology*, *78*(2), 103–114.

Zhang, K., Zhou, B., Zhang, P., Zhang, Z., Chen, P., Pu, Y., ... Zhang, L. (2014b). Genetic variants in NAMPT predict bladder cancer risk and prognosis in individuals from southwest Chinese Han group. *Tumor Biology*, *35*(5), 4031–4040.

Zhang, L. Y., Liu, L. Y., Qie, L. L., Ling, K. N., Xu, L. H., Wang, F., ... Zhang, W. P. (2012b). Anti-proliferation effect of APO866 on C6 glioblastoma cells by inhibiting nicotinamide phosphoribosyltransferase. *European Journal of Pharmacology*, *674*(2-3), 163–170.

Zhang, L. H., Yang, X. L., Zhang, X., Cheng, J. X., & Zhang, W. (2011a). Association of elevated GRP78 expression with increased astrocytoma malignancy via Akt and ERK pathways. *Brain Research*, *1371*(1), 23–31.

Zhang, N., Wei, P., Gong, A., Chiu, W. T., Lee, H. T., Colman, H., ... Huang, S. (2011b). FoxM1 Promotes β-Catenin Nuclear Localization and Controls Wnt Target-Gene Expression and Glioma Tumorigenesis. *Cancer Cell*, *20*(4), 427–442.

Zhang, T., Berrocal, J. G., Frizzell, K. M., Gamble, M. J., DuMond, M. E., Krishnakumar, R., ... Lee Kraus, W. (2009). Enzymes in the NAD+ salvage pathway regulate SIRT1 activity at target gene promoters. *Journal of Biological Chemistry*, *284*(30), 20408–20417.

Zhang, W. B., Wang, Z., Shu, F., Jin, Y. H., Liu, H. Y., Wang, Q. J., & Yang, Y. (2010b). Activation of AMP-activated protein kinase by temozolomide contributes to apoptosis in glioblastoma cells via p53 activation and mTORC1 inhibition. *Journal of Biological Chemistry*, *285*(52), 40461–40471.

Zhang, X., Kurnasov, O. V., Karthikeyan, S., Grishin, N. V., Osterman, A. L., & Zhang, H. (2003). Structural characterization of a human cytosolic NMN/NaMN adenylyltransferase and implication in human NAD biosynthesis. *Journal of Biological Chemistry*, *278*(15), 13503–13511.

Zhang, Y., Adachi, M., Kawamura, R., & Imai, K. (2006). Bmf is a possible mediator in histone deacetylase inhibitors FK228 and CBHA-induced apoptosis. *Cell Death and Differentiation*, *13*(1), 129–140.

Zhao, G., Green, C. F., Hui, Y.-H., Prieto, L., Shepard, R., Dong, S., ... Burkholder, T. P. (2017a). Discovery of a Highly Selective NAMPT Inhibitor That Demonstrates Robust Efficacy and Improved Retinal Toxicity with Nicotinic Acid Co-administration. *Molecular Cancer Therapeutics*, *16*(12), 2677–2688.

Zhao, H., Tang, W., Chen, X., Wang, S., Wang, X., Xu, H., & Li, L. (2017b). The NAMPT/E2F2/SIRT1 axis promotes proliferation and inhibits p53-dependent apoptosis in human melanoma cells. *Biochemical and Biophysical Research Communications*, *493*(1), 77–84.

Zheng, H., Ying, H., Yan, H., Kimmelman, A. C., Hiller, D. J., Chen, A. J., ... DePinho, R. A. (2008). Pten and p53 converge on c-Myc to control differentiation, self-renewal, and transformation of normal and neoplastic stem cells in glioblastoma. *Cold Spring Harbor Symposia on Quantitative Biology*, *73*, 427–437.

Zhou, T., Wang, T., & Garcia, J. G. N. (2014). Expression of Nicotinamide Phosphoribosyltransferase-Influenced Genes Predicts Recurrence-Free Survival in Lung and Breast Cancers. *Scientific Reports*, *4*(6107), 1–8.

Zhou, Y., Zhou, Y., Shingu, T., Feng, L., Chen, Z., Ogasawara, M., ... Huang, P. (2011). Metabolic alterations in highly tumorigenic glioblastoma cells: Preference for hypoxia and high dependency on glycolysis. *Journal of Biological Chemistry*, *286*(37), 32843–32853.

Zhu, G. Y., Shi, B. Z., & Li, Y. (2014). FoxM1 regulates Sirt1 expression in glioma cells. *European Review for Medical and Pharmacological Sciences*, *18*(2), 205–211.

Zhu, Y., Guo, M., Zhang, L., Xu, T., Wang, L., & Xu, G. (2016). Biomarker triplet NAMPT/VEGF/HER as a de novo detection panel for the diagnosis and prognosis of human breast cancer. *Oncology Reports*, *35*(1), 454–462.

Zhuo, B., Li, Y., Li, Z., Qin, H., Sun, Q., Zhang, F., ... Wang, R. (2015). PI3K/Akt signaling mediated Hexokinase-2 expression inhibits cell apoptosis and promotes tumor growth in pediatric osteosarcoma. *Biochemical and Biophysical Research Communications*, *464*(2), 401–406.

Zoppoli, G., Cea, M., Soncini, D., Fruscione, F., Rudner, J., Moran, E., ... Nencioni, A. (2010). Potent synergistic interaction between the Nampt inhibitor APO866 and the apoptosis activator TRAIL in human leukemia cells. *Experimental Hematology*, *38*(11), 979–988.

Zucal, C., D'Agostino, V. G., Casini, A., Mantelli, B., Thongon, N., Soncini, D., ... Provenzani, A. (2015). EIF2A-dependent translational arrest protects leukemia cells from the energetic stress induced by NAMPT inhibition. *BMC Cancer*, *15*(855), 1–14.

Zundel, W., Schindler, C., Haas-Kogan, D., Koong, A., Kaper, F., Chen, E., ... Giaccia, A. J. (2000). Loss of PTEN facilitates HIF-1-mediated gene expression. *Genes & Development*, *14*(4), 391–396.

Appendix A

Supplementary methods

A.1 qPCR primers

Gene	Primer	Sequence (5′-3′)	Product Size (bp)
HPRT1	Forward	CTCCGTTATGGCGACCC	112
	Reverse	CACCCTTTCCAAATCCTCAG	
NAMPT	Forward	TCACGGCATTCAAAGTAGGA	101
	Reverse	GAGTTCAACATCCTCCTGGC	
NAPRT	Forward	TCCCTGGGTGGCGTCTATAA	256
	Reverse	GCAGTAGTGGCTCCACCTG	
NT5E	Forward	TTGGAAATTTGGCCTCTTTG	108
	Reverse	ACTTCATGAACGCCCTGC	
QPRT	Forward	GTAGTTGAGCCCTGGGCAGT	102
	Reverse	GTCACCATGGACGCTGAAG	
IDO1	Forward	CAGGCAGATGTTTAGCAATGA	91
	Reverse	GATGAAGAAGTGGGCTTTGC	
KYNU	Forward	TTCTAGAAGCCAAAGCCTTCCC	117
	Reverse	TTTCTTCCCCCTCTCTTGGCT	
NMNAT1	Forward	GGAAAACTGTGACACCTCCC	103
	Reverse	GAGATGTTCCACTCGCTGG	
NMNAT2	Forward	ACCACCACAATCCCAAAGTC	108
	Reverse	GATCCTGCTGCTGTGTGGTA	

NMRK1	Forward	GAGTGTCTTGCGCTTTCCAT	92
	Reverse	AATGGATTTTTGCAGTACGATG	
NADSYN1	Forward	TCCGAGGCAGAAAGTACTCC	110
	Reverse	GCTCATCAGACCCAAGATGG	
PARP1	Forward	TCTGCCTTGCTACCAATTCC	107
	Reverse	GATGGGTTCTCTGAGCTTCG	
PARP2	Forward	TGTTGTTGTTGAACTGGAGATTG	107
	Reverse	GGACCCAGAGTGTACAGCCA	
SIRT1	Forward	AGAGATGGCTGGAATTGTCC	104
	Reverse	CCAGATCCTCAAGCGATGTT	
SIRT2	Forward	ATGTCTGCTTCTCCACCAGC	103
	Reverse	GGTCGGTGACAGCCTCAAG	
SIRT3	Forward	AACACAATGTCGGGCTTCAC	109
	Reverse	CAGTCTGCCAAAGACCCTTC	
SIRT4	Forward	AGTCTGTTCCCCACAATCCA	99
	Reverse	AATGTGGATGCTTTGCACAC	
SIRT5	Forward	ATCGACTTGGGACAATCTGG	107
	Reverse	CGTGGAGACAACCATCTTCA	
SIRT6	Forward	CTTGGCACATTCTTCCACAA	107
	Reverse	GCTTCCTGGTCAGCCAGA	
SIRT7	Forward	GCTTCTCCCTTTCTGAAGCA	109
	Reverse	CGCCAAATACTTGGTCGTCT	
PPARGC1A	Forward	CTGCTAGCAAGTTTGCCTCA	105
	Reverse	AGTGGTGCAGTGACCAATCA	
PPARGC1B	Forward	GAGTCAAAGTCGCTGGCATC	104
	Reverse	AACTATCTCGCTGACACGCA	
PRKAA1	Forward	CACATCAAGGCTCCGAATCT	96
	Reverse	ACCTTCGGCAAAGTGAAGG	
PRKAA2	Forward	AACTGCCACTTTATGGCCTG	105
	Reverse	CGGGTGAAGATCGGACACTA	
MGMT	Forward	CTCCGGACCTCCGAGAAC	94

	Reverse	GGGTCTGCACGAAATAAAGC	

Table A.1: **Primer sequences used for qPCR.** Forward and reverse primer sequences and their corresponding product sizes used to target genes for qPCR. Primer sequences were obtained from qPrimerDepot.

A.2 ENRICHR databases

Database name	**Data type**	**Description**	**Year**
BioPlex	PPI	The BioPlex (biophysical interactions of ORFeome-based complexes) network contains the results from immunopurification and mass spectrometry applied to cell lines expressing tagged versions of specific proteins from the ORFeome collection.	2017
ChEA	TF	The Chip Enrichment Analysis (ChEA) database contains results from transcription factor ChIP-seq studies from publications, with associated genes showing a peak at their promoter	2016
ENCODE TF Chip-Seq	TF	The Encyclopedia of DNA Elements (ENCODE) database contains ChIP-seq data, with associated genes showing a peak near the gene	2015
GO Biological Process	Ontologies	Gene Ontology (GO) Biological Processes from ontology trees cut at level 4 to generate gene sets	2017
GO Cellular Component	Ontologies	GO Cellular Components from ontology trees cut at level 4 to generate gene sets	2017
GO Molecular Function	Ontologies	GO Molecular Functions from ontology trees cut at level 4 to generate gene sets	2017
HMDB Metabolites	Metabolites	The Human Metabolome Database (HMDB) containing information on the relationship between genes and metabolites	2012
KEA	PPI	The Kinase Enrichment Pathways (KEA) database contains information on kinase-substrate interactions extracted from literature	2015
KEGG	Pathways	The Kyoto Encyclopedia of Genes and Genomes (KEGG) database contains information on genes and their roles in different cellular pathways	2016

NCI-Nature	Pathways	The National Cancer Institute-Nature Pathway Interaction Database contains information on genes and their roles in different cellular pathways	2016
PANTHER	Pathways	The Protein ANalysis THrough Evolutionary Relationships (PANTHER) database contains information on genes and their roles in different metabolic and cell signalling pathways	2016
PPI Hub Proteins	PPI	The PPI hub proteins database contains information on proteins with more than 50 known partners extracted from several literature-based sources	2017
Reactome	Pathways	The Reactome database contains information on genes and their roles in different cell signalling pathways	2016
Transcription Factor PPI's	TF/PPI	The Trasncription Factor PPI database contains information on the protein-protein interactions of major transcription factors	2017
TRANSFAC and JASPAR PWM's	TF	The TRANScription FACtor (TRANSFAC) and JASPAR databases contain position weight matrix (PWM) data for transcription factors detected at the promoters of genes	2017
WikiPathways	Pathways	The WikiPathways database contains information on genes and their roles in different cell signalling pathways	2016

Table A.2: **Summary of the datasets used from the Enrichr analysis.** Datasets include those on cell signalling, gene ontologies, transcription factor networks, protein-protein interactions and metabolism. Version (year) taken from Enrichr.

A.3 Reagents

A.3.1 Composition of buffers and gels used in western blotting

6X protein loading buffer

To make 10 ml of loading buffer:

- 1.2 ml 0.5 M Tris pH 6.8
- 1.2 g SDS
- 4.7 ml glycerol
- 6 mg bromophenol blue
- 0.93 g DTT
- 4.7 ml dH_2O

10% gel composition

To make 10 ml of gel:

- 3.8 ml dH_2O
- 3.4 ml 30% acrylamide/bis-acrylamide
- 2.6 ml 1.5 M Tris (pH 8.8)
- 100 µl SDS
- 100 µl ammonium persulfate (APS)
- 10 µl tetramethylethylenediamine (TEMED)

10X running buffer

- 30.3 g Tris (250 mM)
- 144 g glycine (1.92 M)
- 10 g SDS (35 mM)
- 1 l dH_2O
- Dilute 1:10 in dH_2O to get 1X buffer of 25 mM Tris, 192 mM glycine and 3.5 mM SDS

10X transfer buffer

- 30.3 g Tris (250 mM)
- 144 g glycine (1.92 M)
- 1 l dH_2O
- Dilute 1:8 in dH_2O and add 200 ml methanol to get 1X buffer of 25 mM Tris and 192 mM glycine

Stripping buffer

- 1.25 ml 1 M Tris pH 6.8
- 2 ml 20% SDS
- 140 µl β-mercaptoethanol
- 16.61 ml dH_2O

A.4 Antibodies used in western blotting

A.4.1 Primary antibodies

Target	Antibody class	Description	Company	Catalogue number
NAMPT	Rabbit, pAb, IgG	Polyclonal rabbit immunoglobulin G targeting nicotinamide phosphoribosyltransferase	Proteintech	11776-1-AP
NAPRT	Rabbit, mAb, IgG	Monoclonal rabbit immunoglobulin G targeting nicotinate phosphoribosyltransferase	Abcam	CL0665 (ab211529)
NT5E	Rabbit, mAb, IgG	Monoclonal rabbit antibody targeting amino acids 50-100 of ecto-5'-nucleotidase	Abcam	EPR6114 (ab133582)
QPRT	Rabbit, mAb, IgG	Monoclonal rabbit antibody targeting quinolinate phosphoribosyltransferase	Proteintech	25174-1-AP
β-actin	Mouse, mAb, IgG	Monoclonal mouse antibody targeting β-actin	Sigma Aldrich	A2228

Table A.3: **Primary antibodies used in western blotting.** Primary antibodies targeting genes in the nicotinamide pathway, including their class, source and catalogue number.

A.4.2 Secondary antibodies

Target	Antibody class	Description	Company	Catalogue number
Rabbit	pAb, IgG, HRP	Polyclonal goat immunoglobulin linked to horseradish peroxidase, targeting rabbit antigens	Dako	P0448
Mouse	pAb, IgG, HRP	Polyclonal goat immunoglobulin linked to horseradish peroxidase, targeting mouse antigens	Dako	P0447

Table A.4: **Secondary antibodies used in western blotting.** Secondary antibodies against rabbit and mouse antigens, raised in goat, conjugated to HRP.

A.5 Staining reagents used in histology

Target	Molecule type	Description	Company	Catalogue number
Ki-67	Rabbit pAb, IgG	Polyclonal rabbit immunoglobulin targeting Ki-67	Abcam	ab15580
Rabbit	Goat pAb, IgG	Alex Fluor 568 labelled polyclonal goat immunoglobulin targeting rabbit antigens	Thermo Fisher Scientific	A-11011
Blood vessels	Lectin	DyLight 649 labelled Lycopersicon Esculentum (Tomato) Lectin	Vector Laboratories	DL-1178

Table A.5: **Table showing staining reagents used in FASTClear**. Brain slides were subject to FASTClear with the staining compounds listed, followed by imaging on a confocal microscope.

Appendix B

Supplementary results

B.1 RNAseq

Differentially expressed genes between 42MG vehicle control and 42MG FK866 treated samples:

HSPA5, HJURP, HSP90B1, ATG16L2, TIPARP, CHAC1, MANF, TAF7, SYNGR1, ERMN, VEGFA, SPOCD1, ADAMTS10, CDC6, GINS3, KPNA2, TMSB4XP8, RPL22L1, PDIA6, LOC101928188, AURKA, STRA6, F2R, SYNM, PARPBP, HMGN2, KIF23, TNFRSF10B, USP21, BUB1, CCDC102B, CETN2, RDH10, ACSS1, BUB1B, CALR, DNAJB11, NDC80, NRBP2, SEC11C, HMGCS1, DHRS2, HOXB5, TMPO-AS1, LSM3, DNAH10OS, SMARCA1, ATF6B, ATP1B1, DNAJC3, ERCC6L, MOV10, NICN1, PTMA, HSPA8, CCNA2, HOMER3, NPM1, SCG5, RRM2, ANLN, H2AFZ, SAMD14, ACAT2, RNF20, SEC61B, SLC35E2B, CENPE, SUMO2, COX6C, MAFB, CEP128, CNIH3, DHRS3, PARP3, ROR1, KNSTRN, RBM3, ELN, RAD51AP1, RNF44, MTMR4, PLEKHA6, CCDC18, SPRY1, COL11A1, NUSAP1, RASGRP3, STMN1, CENPF, CACNA1A, AKAP6, DBI, GGCT, GPR68, HMGB2, NUCB2, PDIA3, RGS4, TPX2, BCL6, DYNC1LI1, RHBDF1, RSRC2, CBX1, IRS2, LAMB2, SH2B1, KIF4A, EGLN2, HERC2P3, MEF2A, HMGB1P6.

Differentially expressed genes between DBTRG vehicle control and DBTRG FK866 treated samples:

DHRS3, UNC5B, HK2, BMF, MLXIP, IL11, ADAMTS14, TSHZ1, HOXB3, VEGFA, DKK1, DDIT4, CTGF, B4GALNT3, HOXB9, HOXB5, OAF, HOXA-AS2, PTPRB, HOXB8, TGM2, TNFSF10, DOCK4, NARF, AK4, COL14A1, RERE, SALL1, HOXB4, GFRA1, MXRA5, XBP1, TCEB1, ACAT2, COL4A1, MTHFD2, CDC6, PSMG1, VLDLR, EGLN3, RBP1, C12orf75, RRM2, LZTS1, HNRNPAB, IFT140, ITIH5, MRPS18C, SLC6A6, MRPL39, ATF6B, HSPA8, TPP1, NDP, PFKFB3, HOXB6, BOC, BUD13, HSPA5, NRIP1, STRA6, RARA, ZMYM3, NFIX, SEMA5B, HSP90AA1, MMP14, ETV6, HSPB11, PDK1, HOXA3, SLC2A1, THBS3, DCUN1D5, FAXDC2, RPF1, GTF3C6, HIPK2, MCM6, GLI3, HOXA5, LSM3, BCL9, NRP2, SNX30, SRGAP3, PSMC6, SRGAP1, CCND1, FAM214B, SH3PXD2A, CCNB1, FIGNL1, KDM3A, ANOS1, GBP5, SOCS2, UBA7, CSF1, CNTNAP1, HMGN2, NTRK2, HSPH1, PTCH1, ALPK2, ELMSAN1, FGF12, MAGOHB, NAV2, PCK1, SLC2A12, ST5, COPS3, CCT4, PHF12, ALDH1L2, CYR61, MRPL3, PUS3, SNRPG, YWHAH, LAMA4, TMEM97, SIAH3, ARHGAP18, AFAP1L2, TRIP13, CLN8, SNRPD1, PBXIP1, BNIP3, ACTR3B, GINS2, CHST15, INTS7, MCTS1, MSH6, SCG2, BAMBI, CBFA2T2, CCT8, MYO18A, SFRP2,

SLC35B1, ZNF608, SULF2, ZNF395, MPI, ASNS, C1RL, RFC4, BST2, MCM4, EPHA4, ERH, CCNE2, CDKN3, STK32A, LINC00963, ATAD2, MCM10, CKS1B, EIF2S2, SLC1A4, GBP4, VPS29, SOX4, RNF150, FARSB, HNRNPD, P4HA1, GINS3, IARS, SHF, UNG, FLNB, TNFRSF12A, BHLHE40, JARID2, EGLN1, GLRX3, MMADHC, NAGLU, WDR76, KDM6B, FGFR2, MT-RNR1, MT-RNR2, SHROOM3, ENO3, H2AFZ, COL4A5, PDCD5

ENSEMBL ID	**Gene**	**Gene name**	**Fold change**	**Adjusted P value**	**Poor survival group**
ENSG00000112715	VEGFA	Vascular endothelial growth factor A	1.161	0.011	High expression ($P = 2.70E-04$)
ENSG00000102580	DNAJC3	DnaJ heat shock protein family (Hsp40) member C3	-1.218	0.065	High expression ($P = 0.022$)
ENSG00000143786	CNIH3	Cornichon family AMPA receptor auxiliary protein 3	1.269	0.086	High expression ($P = 0.016$)
ENSG00000151320	AKAP6	A-kinase anchoring protein 6	-1.244	0.098	Low expression ($P = 0.053$)
ENSG00000167004	PDIA3	Protein disulfide isomerase family A member 3	-1.155	0.098	High expression ($P = 0.044$)
ENSG00000068305	MEF2A	Myocyte enhancer factor 2A	-1.173	0.100	High expression ($P = 0.058$)

Table B.1: **Table showing other differentially expressed genes in 42MG cells treated with FK866 that also have an effect on survival in GBM.** Survival analysis was carried out as described previously, with tertile expression groups analysed by two-way ANOVA with Tukey's HSD post-hoc test on TCGA data.

ENSEMBL ID	**Gene**	**Gene name**	**Fold change**	**Adjusted P value**	**Poor survival group**
ENSG00000127329	PTPRB	Protein tyrosine phosphatase, receptor type B	1.252	2.03E-04	Low expression ($P = 0.05$)
ENSG00000121858	TNFSF10	Tumor necrosis factor superfamily member 10	1.316	2.79E-04	High expression ($P = 0.082$)
ENSG00000162433	AK4	Adenylate kinase 4	1.438	4.35E-04	High expression ($P = 0.002$)
ENSG00000182742	HOXB4	Homeobox B4	1.276	7.75E-04	High expression ($P = 0.095$)
ENSG00000151892	GFRA1	GDNF family receptor alpha 1	1.326	1.70E-03	Low expression ($P = 0.015$)
ENSG00000101825	MXRA5	Matrix remodeling associated 5	1.213	1.70E-03	High expression ($P = 0.0097$)
ENSG00000061337	LZTS1	Leucine zipper tumor suppressor 1	1.191	6.33E-03	High expression ($P = 0.034$)
ENSG00000166340	TPP1	Tripeptidyl peptidase 1	1.140	9.16E-03	High expression ($P = 0.014$)
ENSG00000044574	HSPA5	Heat shock protein family A (Hsp70) member 5	-1.177	0.015	High expression ($P = 0.0081$)
ENSG00000008441	NFIX	Nuclear factor I X	1.183	0.018	Low expression ($P = 0.004$)
ENSG00000080824	HSP90AA1	Heat shock protein 90 alpha family class A member 1	-1.192	0.019	High expression ($P = 0.091$)

ENSG00000105997	HOXA3	Homeobox A3	1.293	0.021	Low expression ($P = 0.012$)
ENSG00000106004	HOXA5	Homeobox A5	1.382	0.029	High expression ($P = 0.049$)
ENSG00000182179	UBA7	Ubiquitin like modifier activating enzyme 7	1.207	0.043	High expression ($P = 0.032$)
ENSG00000108797	CNTNAP1	Contactin associated protein 1	1.173	0.044	High expression ($P = 0.026$)
ENSG00000182372	CLN8	Ceroid-lipofuscinosis, neuronal 8	1.146	0.062	High expression ($P = 0.055$)
ENSG00000171951	SCG2	Secretogranin II	-1.203	0.069	High expression ($P = 0.064$)
ENSG00000139178	C1RL	Complement C1r subcomponent like	1.185	0.073	High expression ($P = 0.0001$)
ENSG00000130303	BST2	Bone marrow stromal cell antigen 2	1.194	0.073	High expression ($P = 0.012$)
ENSG00000124766	SOX4	SRY-box 4	1.143	0.086	Low expression ($P = 0.021$)
ENSG00000006327	TNFRSF12A	TNF receptor superfamily member 12A	-1.159	0.094	High expression ($P = 0.027$)
ENSG00000134107	BHLHE40	Basic helix-loop-helix family member e40	1.166	0.095	High expression ($P = 0.091$)

Table B.2: **Table showing other differentially expressed genes in DBTRG cells treated with FK866 that also have an effect on survival in GBM.** Survival analysis was carried out as described previously, with tertile expression groups analysed by two-way ANOVA with Tukey's HSD post-hoc test on TCGA data.

B.2 *In vivo* data

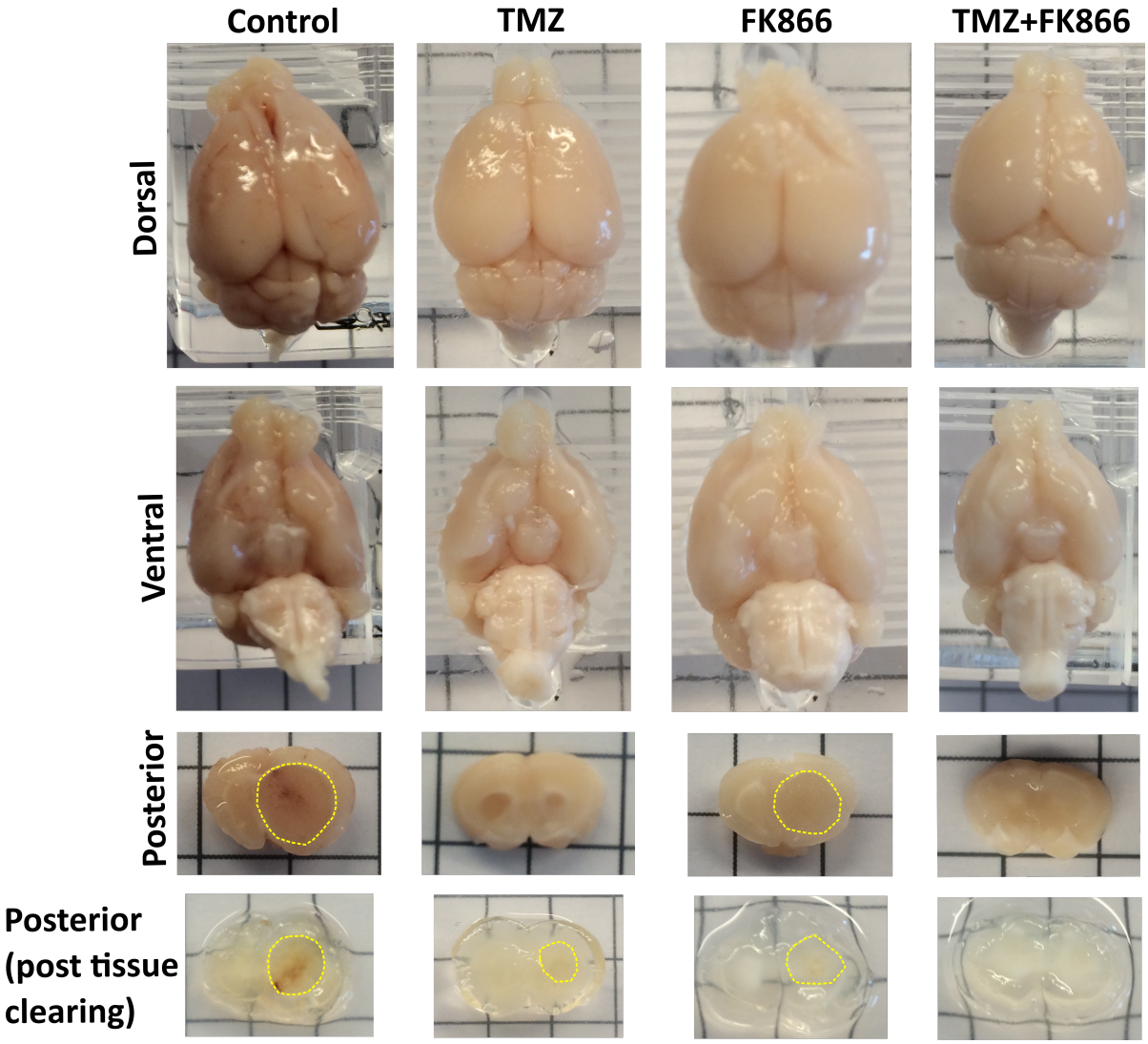


Figure B.1: **Images of the mouse brains used for FASTClear**. Dorsal and ventral images of whole mouse brains, one from each group, as well as posterior images of sections used both before and after the application of FASTClear.